AD_____

Award Number: DAMD17-01-1-0781

TITLE: Mechanisms of α-synuclein aggregation and toxicity

PRINCIPAL INVESTIGATOR: Benjamin Wolozin, Ph.D.

CONTRACTING ORGANIZATION: Boston University School of Medicine
Boston, MA 02118-2526

REPORT DATE: September 2004

TYPE OF REPORT: Annual

PREPARED FOR: U.S. Army Medical Research and Materiel Command
Fort Detrick, Maryland 21702-5012

REPORT DOCUMENTATION PAGE

Form Approved
OMB No. 0704-0188

1. REPORT DATE *(DD-MM-YYYY)*	**2. REPORT TYPE**	**3. DATES COVERED** *(From - To)*
01-09-2004	Annual	1 Sep 2003 – 31 Aug 2004

4. TITLE AND SUBTITLE

Mechanisms of α-synuclein aggregation and toxicity

5a. CONTRACT NUMBER

5b. GRANT NUMBER
DAMD17-01-1-0781

5c. PROGRAM ELEMENT NUMBER

6. AUTHOR(S)

Benjamin Wolozin, Ph.D.

E-Mail: bwolozi@lumc.edu

5d. PROJECT NUMBER

5e. TASK NUMBER

5f. WORK UNIT NUMBER

7. PERFORMING ORGANIZATION NAME(S) AND ADDRESS(ES)

Boston University School of Medicine
Boston, MA 02118-2526

8. PERFORMING ORGANIZATION REPORT NUMBER

9. SPONSORING / MONITORING AGENCY NAME(S) AND ADDRESS(ES)
U.S. Army Medical Research and Materiel Command
Fort Detrick, Maryland 21702-5012

10. SPONSOR/MONITOR'S ACRONYM(S)

11. SPONSOR/MONITOR'S REPORT NUMBER(S)

12. DISTRIBUTION / AVAILABILITY STATEMENT
Approved for Public Release; Distribution Unlimited

13. SUPPLEMENTARY NOTES - original document contains color

14. ABSTRACT
Alpha-synuclein is a protein implicated in the pathophysiology of Parkinson's disease. The purpose of this proposal is to study the regulation of synuclein aggregation by metals, the interaction of synuclein with other proteins associated with its pathophysiology and the effects of aggregated alpha-synuclein on the function of neuronal mitochondria. During the current year, we have identified several novel interactions of Alpha-synuclein, including binding to the proteasome and selective inhibition of Mitochondrial complex I. We have also identified a number of novel pathological changes associated with alpha-synuclein aggregation, including phosphorylation of tau protein and up-regulation of DJ-1 protein. Finally, our studies identify novel chemical and molecular strategies for inhibiting toxicity induced by aggregated alpha-synuclein.

15. SUBJECT TERMS
Protein aggregation, Lewy body, mitochondria, metals

16. SECURITY CLASSIFICATION OF:			**17. LIMITATION OF ABSTRACT**	**18. NUMBER OF PAGES**	**19a. NAME OF RESPONSIBLE PERSON**
a. REPORT	**b. ABSTRACT**	**c. THIS PAGE**			USAMRMC
U	U	U	UU	126	**19b. TELEPHONE NUMBER** *(include area code)*

Table of Contents

Introduction

The goal of this grant proposal is to investigate the interaction of α-synuclein with metals. Our preliminary studies suggested that metals, such as iron, might promote synuclein aggregation. In this proposal, we sought to understand which metals interact with α-synuclein, how these metals might modulate α-synuclein aggregation, and how they might affect the interaction with other proteins relevant to Parkinson's disease. The work in the third year focused on examining how aggregation of α-synuclein, which is induced by iron or aging, affects its interaction with specific targets, such as the proteasome and the mitochondria.

It is important to note that as of July 1, I changed performance sites. I now work at Boston University School of Medicine, Boston, MA 02118-2526

Body:

Work from Aim 1 that was Accomplished

As mentioned in the progress report from 2003, we accomplished the work specified in Aim 1 during the 2002 – 2003 year. The articles related to this work were described in the last progress report, and will not be described in this report.

Work relevant to Aims 2:

In aim 2, we proposed to investigate how different metals might interact to affect α-synuclein aggregation, and how binding of α-synuclein to proteins altered the aggregation. As described in the last progress report, we identified 3 classes of binding states for the interaction of metals with α-synuclein. Class I consists of the redox active metals, Fe(II) and Cu(II), which reduce fluorescence at both 310 and 345 nm. Class II consists of Mg(II), Zn(II) and Ca(II), which increase fluorescence at 345 nm but do not affect fluorescence at 310 nm. Class III consists of Ni(II), Mn(II) and Al(III), which do not affect the fluorescence of α-synuclein.

During the current year, we have made strong advances in our understanding of the mechanism of toxicity of aggregated α-synuclein. We discovered that α-synuclein binds to the proteasomal protein S6', and showed that aggregated α-synuclein inhibits proteasomal function with a potency that is more than 10,000-fold stronger than that of monomeric α-synuclein (1). Recently, we have been examining how β and γ-synuclein, close homologues of α-synuclein, interact with the proteasome. We made two surprising observation. First, we demonstrated the β-synuclein does not affect proteasomal function itself, but can inhibit binding of α-synuclein to the proteasome and prevent aggregated α-synuclein from inhibiting the proteasome. Second, we demonstrated that γ-synuclein also binds to the proteasome, but at a different site that α-synuclein. Both of the findings are described in an article that is under review (7).

Work relevant to Aims 2:

Work on Aim 3 focuses on the affects of α-synuclein on the mitochondria and the effects

of α-synuclein in vivo. We also have supplemented this work with our recent work using C. elegans. We have made numerous findings relevant to this aim. Using C. elegans, we demonstrated that over-expressing α-synuclein causes a selective deficit in complex I of the mitochondria. We also developed a novel therapeutic strategy for reversing inhibition of complex I using a combination of D-β-hydroxybutyrate (which augments the activity of complex II) and TUDCA, which prevents apoptosis. This work demonstrates a strong connection between mitochondrial function and α-synuclein, and is at the revision stage at the journal Neuron (8). We have also examined the effects of α-synuclein on mammalian neurons from the A30P α-synuclein transgenic mice. Using cultured neurons we showed that α-synuclein causes toxicity, but that over-expressing parkin, a protein whose loss of function is associated with PD, protects against this toxicity (1). We demonstrated that aggregation of α-synuclein induces a number of pathological changes including activation of JNK and phosphorylation of microtubule associated protein tau (6). Interestingly, we also observed that the ubiquitin ligase, CHIP, which binds parkin, regulates the turnover of tau (4). We also identified a parkin binding protein, Sept5_v2 (3). Our work has lead to increased understanding of mitochondrial pathology in PD. We identified a number of mitochondrial proteins whose oxidation is strongly increased in response aggregation of α-synuclein (7). Finally, we discovered that aggregation of α-synuclein induces up-regulation of another protein related to Parkinson's disease, DJ-1. This protein is up-regulated in astrocytes but also might be up-regulated in neurons, as shown by its ability to bind to tau protein (9).

Key Research Accomplishments:

- Determined affinity and pH dependence of iron for α-synuclein
- Determined affinity of Cu(II), Mg(II), Zn(II) and Ca(II) for α-synuclein, and determined that Ni(II), Mn(II) and Al(III) do not bind α-synuclein.
- Performed electrospray ionization mass spectroscopy of α-synuclein.
- Demonstrated that iron causes α-synuclein aggregation in neurons, and that α-synuclein increases the vulnerability to iron of neurons.
- Demonstrated that magnesium inhibits α-synuclein aggregation and protects neurons against iron-mediated toxicity.
- Demonstrated that α-synuclein binds the proteasomal protein S6'.
- Demonstrated that β-synuclein inhibits binding of α-synuclein to the proteasome
- Demonstrated that γ-synuclein binds to a different part of the proteasome, the 20S proteasome.
- Demonstrated that aggregation of α-synuclein induces activation of JNK and hyperphosphorylation of tau protein.
- Demonstrated that the parkin binding protein, CHIP binds tau protein.
- Demonstrated that SEPT5_v2 binds parkin.
- Demonstrated that aggregation of α-synuclein induce up-regulation of DJ-1 protein.
- Developed an additional model for α-synuclein toxicity and aggregation using C. Elegans over-expressing α-synuclein, and demonstrated a selective vulnerability of mitochondrial complex I.

- Identified a chemical strategy for reversing the toxicity associated with inhibition of mitochondrial complex I, using DβHB and TUDCA.

Reportable Outcomes:

The research performed this year has resulted in publication of 4 articles relevant to α-synuclein. These articles are listed below, and are provided in the appendices.

Articles relevant to α-synuclein and the DAMD grant award that were published in last year:

1. Petrucelli, L., O'Farrell, C., Kehoe, K., Vink, L., Lockhart, P.J., Baptista, M., **Wolozin, B**. Choi, P., Farrer, M., Hardy, J., Cookson, M.R., Parkin protects against the toxicity associated with over-expression of synuclein: Proteasome dysfunction selectively affects dopaminergic neurons. Neuron 36:1007-19 (2002). Note: This article is more than 1 year old, but is included for referencing purposes.

2. Snyder, H., Mensah, K., Theisler, C., Lee, J. M., Matouschek, A. and **Wolozin, B.**, Aggregated and Monomeric α-Synuclein bind to the S6' Proteasomal Protein and Inhibit Proteasomal Function. J. Biol. Chem. 278:11753-9 2003.

3. Choi P., Snyder, H. ,Petrucelli L., Theisler, C., Chong M., Zhang Y., Lim K. , Chung K. , Kehoe K. , L. D'Adamio, Lee J.M., Cochran E., Bowser R., Dawson T., **Wolozin, B**., S EPT5 v2 is a parkin-binding protein. Mol. Brain Res. 117:179-189 (2003).

4. Petrucelli, L., Dickson, D., Kehoe, K., Taylor, J., Snyder, H., Grover, A., McGowan, E., Lewis, J., Dillman, W., Browne, S.E., Voellmey, R., Tsuboi, Y., Dawson., T.M., **Wolozin, B**., Hardy, J., Hutton, M., CHIP and Hsp70 regulate tau ubiquitination, degradation and aggregation. Human Molecular Genetics 13:703-14 (2004).

5. Frasier, M., **Wolozin, B.**, Following the leader: Fibrillization of α-synuclein and tau. Exp. Neurol. 187:235-9 (2004) (Invited Commentary).

6. Frasier, M., Walzer, M., McCarthy, L., Magnuson, D., Lee, J.M., Haas, C., Kahle, P. and **Wolozin, B**., Tau phosphorylation increases in symptomatic mice over-expressing A30P α-synuclein. (Exp. Neurol, in press).

7. Poon, H.F., Frasier, M., Kahle, P., Haass, C., Sherve, N., Calabrese, V., Wolozin, B., Butterfield, D.A. Mitochondrial associated Metabolic Proteins are Selectively Oxidized in A30P α-Synuclein Transgenic Mice – A Model of Familial Parkinson's Disease. (Neurobio. Dis., in press)

Papers Currently Under Review

8. Snyder, H., Mensah, K., Hashimoto, M., Surgucheva, I.G., Festoff, B., Surguchov, A., Masliah, E., Matouschek, A., **Wolozin, B**. β-Synuclein Reduces Proteasomal

Inhibition by α-Synuclein but not γ-Synuclein. (JBC, submitted).
9. Ved, R., Sluder, A., Westlund, B., Burnam, L., Hoener, M., Przedborsky, S., Alfonso, A., Liu, L., **Wolozin, B**. Similar Patterns of Mitochondrial Vulnerability and Rescue Induced by Genetic Modification of α-Synuclein, Parkin and DJ-1 in *C. Elegans*. (Neuron, submitted).
10. Frasier, M., Frausto, S., Lewicki, D., Golbe, L., Wolozin, B., DJ-1 Expression Increases in Mice Over-Expressing A30P α-Synuclein. (Exp. Neurol, submitted).

Conclusions:

Significance: Our results clearly demonstrate that redox active metals can induce α-synuclein aggregation both in vitro and in cell culture. This is important because it suggests that metals could play an important in stimulating the pathology in PD. Conversely, chelating metal could be protective against PD. A similar strategy has been shown to be effective in preventing formation of Alzheimer type pathology in an animal model of Alzheimer's disease, and is now in clinical trials for treatment of Alzheimer's disease (6).

Our results have also identified a how aggregation of α-synuclein affects the expression and function of a number of other proteins. This work shows that aggregation of α-synuclein strongly impacts on mitochondrial functioning, but also inhibits proteasomal function. The work also points to some potentially new strategies for reversing toxicity associated with the aggregation of α-synuclein or inhibition of mitochondrial function.

Recommended changes: We have recently generated transgenic mice over-expressing parkin protein. Our previous work, described above, indicates that over-expressing parkin might protect against toxicity and neurodegeneration induced by α-synuclein. We would like to cross the transgenic mice over-expressing α-synuclein with the transgenic mice over-expressing parkin to determine whether over-expression of parkin might reverse the mitochondrial pathology induced by α-synuclein in vivo. This work would pave the way for gene therapy that could prevent some of the pathological changes associated with Parkinson's disease.

References:

1. Petrucelli, L., O'Farrell, C., Kehoe, K., Vink, L., Lockhart, P.J., Baptista, M., **Wolozin, B**. Choi, P., Farrer, M., Hardy, J., Cookson, M.R., Parkin protects against the toxicity associated with over-expression of synuclein: Proteasome dysfunction selectively affects dopaminergic neurons. Neuron 36:1007-19 (2002). Note: This article is more than 1 year old, but is included for referencing purposes.

2. Snyder, H., Mensah, K., Theisler, C., Lee, J. M., Matouschek, A. and **Wolozin, B.**, Aggregated and Monomeric α-Synuclein bind to the S6' Proteasomal Protein and Inhibit Proteasomal Function. J. Biol. Chem. 278:11753-9 2003.

3. Choi P., Snyder, H. ,Petrucelli L., Theisler, C., Chong M., Zhang Y., Lim K. , Chung K. , Kehoe K. , L. D'Adamio, Lee J.M., Cochran E., Bowser R., Dawson T., **Wolozin, B**., S EPT5 v2 is a parkin-binding protein. Mol. Brain Res. 117:179-189 (2003).

4. Petrucelli, L., Dickson, D., Kehoe, K., Taylor, J., Snyder, H., Grover, A., McGowan, E., Lewis, J., Dillman, W., Browne, S.E., Voellmey, R., Tsuboi, Y., Dawson., T.M., **Wolozin, B**., Hardy, J., Hutton, M., CHIP and Hsp70 regulate tau ubiquitination, degradation and aggregation. Human Molecular Genetics 13:703-14 (2004).

5. Frasier, M., **Wolozin, B.**, Following the leader: Fibrillization of α-synuclein and tau. Exp. Neurol. 187:235-9 (2004) (Invited Commentary).

6. Frasier, M., Walzer, M., McCarthy, L., Magnuson, D., Lee, J.M., Haas, C., Kahle, P. and **Wolozin, B**., Tau phosphorylation increases in symptomatic mice over-expressing A30P α-synuclein. (Exp. Neurol, in press).

7. Poon, H.F., Frasier, M., Kahle, P., Haass, C., Sherve, N., Calabrese, V., Wolozin, B., Butterfield, D.A. Mitochondrial associated Metabolic Proteins are Selectively Oxidized in A30P α-Synuclein Transgenic Mice – A Model of Familial Parkinson's Disease. (Neurobio. Dis., in press)

Papers Currently Under Review

8. Snyder, H., Mensah, K., Hashimoto, M., Surgucheva, I.G., Festoff, B., Surguchov, A., Masliah, E., Matouschek, A., **Wolozin, B**. β-Synuclein Reduces Proteasomal Inhibition by α-Synuclein but not γ-Synuclein. (JBC, submitted).
9. Ved, R., Sluder, A., Westlund, B., Burnam, L., Hoener, M., Przedborsky, S., Alfonso, A., Liu, L., **Wolozin, B**. Similar Patterns of Mitochondrial Vulnerability and Rescue Induced by Genetic Modification of α-Synuclein, Parkin and DJ-1 in *C. Elegans*. (Neuron, submitted).
10. Frasier, M., Frausto, S., Lewicki, D., Golbe, L., Wolozin, B., DJ-1 Expression Increases in Mice Over-Expressing A30P α-Synuclein. (Exp. Neurol, submitted).

Appendices:

Snyder, H., Mensah, K., Theisler, C., Lee, J. M., Matouschek, A. and **Wolozin, B.**, Aggregated and Monomeric α-Synuclein bind to the S6' Proteasomal Protein and Inhibit Proteasomal Function. J. Biol. Chem. 278:11753-9 2003.

Choi P., Snyder, H. ,Petrucelli L., Theisler, C., Chong M., Zhang Y., Lim K. , Chung K. , Kehoe K. , L. D'Adamio, Lee J.M., Cochran E., Bowser R., Dawson T., **Wolozin, B**., S EPT5 v2 is a parkin-binding protein. Mol. Brain Res. 117:179-189 (2003).

Petrucelli, L., Dickson, D., Kehoe, K., Taylor, J., Snyder, H., Grover, A., McGowan, E., Lewis, J., Dillman, W., Browne, S.E., Voellmey, R., Tsuboi, Y., Dawson., T.M., **Wolozin, B**., Hardy, J., Hutton, M., CHIP and Hsp70 regulate tau ubiquitination, degradation and aggregation. Human Molecular Genetics 13:703-14 (2004).

Frasier, M., Walzer, M., McCarthy, L., Magnuson, D., Lee, J.M., Haas, C., Kahle, P. and **Wolozin, B**., Tau phosphorylation increases in symptomatic mice over-expressing A30P α-synuclein. (Exp. Neurol, in press).

Poon, H.F., Frasier, M., Kahle, P., Haass, C., Sherve, N., Calabrese, V., Wolozin, B., Butterfield, D.A. Mitochondrial associated Metabolic Proteins are Selectively Oxidized in A30P α-Synuclein Transgenic Mice – A Model of Familial Parkinson's Disease. (Neurobio. Dis., in press)

Ved, R., Sluder, A., Westlund, B., Burnam, L., Hoener, M., Przedborsky, S., Alfonso, A., Liu, L., **Wolozin, B**. Similar Patterns of Mitochondrial Vulnerability and Rescue Induced by Genetic Modification of α-Synuclein, Parkin and DJ-1 in *C. Elegans*. (Neuron, in review).

THE JOURNAL OF BIOLOGICAL CHEMISTRY
Vol. 278, No. 14, Issue of April 4, pp. 11753–11759, 2003
Printed in U.S.A.

Aggregated and Monomeric α-Synuclein Bind to the S6′ Proteasomal Protein and Inhibit Proteasomal Function*

Received for publication, August 22, 2002, and in revised form, January 13, 2003
Published, JBC Papers in Press, January 24, 2003, DOI 10.1074/jbc.M208641200

Heather Snyder‡, Kwame Mensah§, Catherine Theisler‡, Jack Lee‡¶, Andreas Matouschek§, and Benjamin Wolozin‡‖

From the ‡Department of Pharmacology and ¶Pathology, Loyola University Medical Center, Maywood, Illinois 60153 and the §Department of Biochemistry and Molecular Biology, Northwestern University, Evanston, Illinois 60208

The accumulation of aggregated α-synuclein is thought to contribute to the pathophysiology of Parkinson's disease, but the mechanism of toxicity is poorly understood. Recent studies suggest that aggregated proteins cause toxicity by inhibiting the ubiquitin-dependent proteasomal system. In the present study, we explore how α-synuclein interacts with the proteasome. The proteasome exists as a 26 S and a 20 S species. The 26 S proteasome is composed of the 19 S cap and the 20 S core. Aggregated α-synuclein strongly inhibited the function of the 26 S proteasome. The IC_{50} of aggregated α-synuclein for ubiquitin-independent 26 S proteasomal activity was 1 nM. Aggregated α-synuclein also inhibited 26 S ubiquitin-dependent proteasomal activity at a dose of 500 nM. In contrast, the IC_{50} of aggregated α-synuclein for 20 S proteasomal activity was > 1 μM. This suggests that aggregated α-synuclein selectively interacts with the 19 S cap. Monomeric α-synuclein also inhibited proteasomal activity but with lower affinity and less potency. Recombinant monomeric α-synuclein inhibited the activity of the 20 S proteasomal core with an IC_{50} > 10 μM, exhibited no inhibition of 26 S ubiquitin-dependent proteasomal activity at doses up to 5 μM, and exhibited only partial inhibition (50%) of the 26 S ubiquitin-independent proteasomal activity at doses up to 10 mM. Binding studies demonstrate that both aggregated and monomeric α-synuclein selectively bind to the proteasomal protein S6′, a subunit of the 19 S cap. These studies suggest that proteasomal inhibition by aggregated α-synuclein could be mediated by interaction with S6′.

A multisubunit complex, termed the proteasome, manages protein turnover in the body. Proteins can be either degraded directly by the proteasome, or they can be tagged with an 8-K_D protein, termed ubiquitin. Three different forms of the proteasome exist in a cell: the 20 S ubiquitin-independent proteasome, the 26 S ubiquitin-independent proteasome, and the 26 S ubiquitin-dependent proteasome. The 20 S particle forms the core of each form of proteasome (1, 2). Both the 26 S ubiquitin-dependent and -independent proteasomes contain the 20 S particle plus an additional smaller cap, which has a sedimentation coefficient of 19 S. Although smaller than the 20 S particle, the 19 S particle is also a multisubunit structure. The protein subunits that compose the 19 and 20 S particles are all known. The 19 S cap contains at least 18 different subunits, whereas the 20 S particle contains 28 subunits (1, 2). The protein S6′ (also known as tat binding protein 1 and Rpt5) is in the 19 S cap and is of particular interest because it was recently shown to directly bind ubiquitinated proteins, which suggests that it is required for ubiquitin-dependent proteasomal function (3).

Although the 26 S proteasome is responsible in both ubiquitin-dependent and -independent protein degradation (4, 5), the 20 S proteasome functions only in ubiquitin-independent protein degradation and is involved in 70–80% of the selective recognition and degradation of mildly oxidized proteins in the cytosol (4, 5). The 26 S proteasomal ubiquitin-dependent pathway degrades all ubiquitinated proteins within the cell and is the primary degradation pathway of the cell. The E1 ubiquitin-activating enzyme forms a thiodiester bond with mono-ubiquitin. The E2 ubiquitin-conjugating enzyme displaces the E1 enzyme and allows for conjugation of multiple ubiquitin moieties with one another. The E3 ubiquitin ligase enzyme binds both to the substrate targeted for degradation and to the E2 enzyme. The E2 and E3 enzymes are displaced, leaving a multichained ubiquitinated substrate protein that is targeted to the 26 S proteasome. This is both an ATP- and ubiquitin-dependent pathway (6–13).

Recent studies suggest that protein aggregates cause toxicity by inhibiting proteasomal function. Extended polyglutamine repeats, such as occur in mutant forms of huntingtin associated with Huntington's disease, aggregate readily (14–16). Polyglutamine aggregates inhibit ubiquitin-dependent proteasomal function (17). Aggregates of other proteins, such as the cystic fibrosis transmembrane receptor, also inhibit ubiquitin-dependent proteasomal function in cell culture (17). Many other proteins with hydrophobic domains also aggregate, and overexpressing the aggregation-prone domains of these proteins is toxic (18). The mechanism of toxicity for most aggregates is unknown.

Blockade of proteasome activity is toxic to many cell types and appears to be potentially important to many neurodegenerative diseases. Proteasomal inhibition causes apoptosis in many cell lines and is being tested as a potential chemotherapy (19). Although proteasomal inhibition causes rapid toxicity in cell culture, the slow accumulation of protein aggregates in neurodegenerative diseases might produce a correspondingly slow inhibition of the proteasome.

α-Synuclein is the major component of Lewy bodies, which are intracellular inclusions that form in Parkinson's disease

* This work was supported by National Institutes of Health Grant NS41786, United States Army Medical Research Command Grant DAMD17–01-1–0781, and the Retirement Research Foundation. The costs of publication of this article were defrayed in part by the payment of page charges. This article must therefore be hereby marked "*advertisement*" in accordance with 18 U.S.C. Section 1734 solely to indicate this fact.

‖ To whom correspondence should be addressed: Dept. of, Pharmacology, Loyola University Medical Center, Bldg. 102, Rm. 3634, 2160 S. First Ave., Maywood, IL 60153. Tel.: 708-216-6195; Fax: 708-216-6596; E-mail: bwolozi@lumc.edu.

(PD)[1] (20, 21). The association of α-synuclein with Lewy bodies suggests that protein aggregation represents an important aspect of the pathophysiology of α-synuclein and of PD. The link between α-synuclein and protein aggregation has been strengthened by the discovery of mutant forms of α-synuclein, A53T and A30P, that are associated with rare cases of familial PD (22, 23). Both mutations accelerate aggregation of α-synuclein (24–27). The link between α-synuclein and aggregation suggests that understanding the mechanism of toxicity induced by protein aggregates could provide important insights into the mechanism of cell death in PD.

Native α-synuclein has been shown to bind both fatty acids and many different proteins, including phospholipase D, G proteins, synphilin-1, protein kinase C, 14–3-3 protein, parkin, and the dopamine transporter (28–34). In addition, rat α-synuclein has been shown to bind to rat S6′ (35). Of these proteins, only synphilin-1 and parkin have been identified in Lewy bodies (33, 36, 37). Perhaps because of the pleiotropic binding properties of native α-synuclein, overexpressing it in cells produces multiple cellular effects. α-Synuclein inhibits protein kinase C activity, phospholipase D activity, and the activity of the dopamine transporter, and α-synuclein has chaperone activity (28, 29, 34, 38). Overexpressing α-synuclein also inhibits proteasomal function (39). The link between α-synuclein and the proteasome is intriguing but is not directly related to the pathophysiology of Parkinson's disease, because overexpressed α-synuclein retains a native structure until the cell is subjected to a stress, such as incubation with rotenone or ferrous chloride (40–44). Thus, whether aggregated α-synuclein inhibits proteasomal function is unknown, and the mechanism by which it might inhibit the proteasome is also unknown.

In this study we examine the interaction of α-synuclein with the three different types of proteasome and demonstrate that aggregated α-synuclein binds to S6′ and inhibits ubiquitin-dependent proteasomal function.

MATERIALS AND METHODS

Cell Lines, Transfections, Chemicals, and Antibodies—The human cell line HEK 293 and the human neuroblastoma cell line BE-M17 were grown in OPTIMEM (Cell Grow) plus 10% fetal bovine serum supplemented with 200 μg/ml G418 (Sigma), as needed. G418 was used for selection. Transfections utilized FuGENE at a 3:1 ratio to DNA, 4 μg per 10-cm dish. Recombinant α-synuclein was generated using wild-type α-synuclein inserted into a ProEX-His_6 plasmid (Invitrogen) as described previously (41). Antibodies used include monoclonal anti-α-synuclein (1:1000 IB, Transduction Labs); polyclonal anti-S6′ (1:1000, Affiniti); monoclonal anti-S6′ (1:1000, Affiniti); polyclonal anti-PA700 (1:1000, Affiniti); monoclonal anti-10b (1:1000, Affiniti); polyclonal anti-α subunit 20 S (1:1000, Affiniti); and polyclonal anti-α-synuclein (against amino acids 116–131, 1:1000).

Pull-down Assay—Brain samples were precleared with nickel-agarose for one hour at 4 °C to eliminate proteins that directly bind to nickel-agarose (Invitrogen). These samples were incubated overnight with 5 μg of recombinant α-synuclein (His-tagged), either aggregated or monomeric. Samples were incubated with nickel-agarose for one hour to allow binding of the His-tagged α-synuclein (monomeric or aggregated), and then they were centrifuged at 1000 rpm for 1 min. Samples were washed three times with immunoprecipitation buffer (50 mM Tris-HCl, 10 mM EGTA, 100 mM NaCl, 0.5% Triton-X, 1 mM dithiothreitol, 1 mM protease inhibitor mixture (Sigma), pH 7.4) and run on 8–16% SDS gradient polyacrylamide gels (BioWhitaker).

Immunoprecipitations—Protein concentration was determined using BCA protein assay (Pierce), and 500 μg of each sample was used per immunoprecipitation in immunoprecipitation buffer (50 mM Tris-HCl, 10 mM EGTA, 100 mM NaCl, 0.5% Triton-X, 1 mM dithiothreitol, 1 mM proteasome inhibitor mixture (Sigma), pH7.4). Samples were precleared using protein G-Sepharose beads (Seize X, Pierce) for 1 h at 4 °C and incubated with antibody overnight at 4 °C while rocking. Samples were washed three times with immunoprecipitation buffer, resuspended in 2× dithiothreitol protein loading buffer, boiled for 5 min at 90 °C, and run on 8–16% SDS gradient polyacrylamide gels (BioWhitaker).

Aggregation of α-Synuclein—Recombinant α-synuclein incubated for 2 months at 37 °C in phosphate-buffered saline while shaking at 800 rpm; aggregation was confirmed by performing immunoblot analysis.

Immunoblot Analysis—Transfers to polyvinylidene difluoride (Bio-Rad) were done overnight at 4 °C at 0.1 A/gel in transfer buffer. The immunoblot was blocked in 0.2% I-block (Tropix) in Tris-buffered saline with 0.1% Tween 20 for one hour at room temperature while shaking. We then incubated blots overnight at 4 °C in primary antibody at appropriate concentration in 5% bovine serum albumin in Tris-buffered saline/0.1% Triton X-100. Blots were washed three times, 10 min each, and incubated three hours in secondary antibody (1:5000, Jackson Laboratories) in I-block at room temperature. Blots were washed three times and developed using a chemiluminescent reaction (PerkinElmer Life Sciences).

Sucrose Gradients—10–30% linear sucrose gradients were prepared using Hoefer SG 15 gradient maker (Amersham Biosciences) following the manufacturer's recommendations. Approximately 10 mg of monomeric or aggregated α-synuclein, as determined by BCA protein assay (Pierce), was added to the top of the gradient; they were centrifuged using a SW41 rotor for 16 ½ hours at 40,000 rpm at 20 °C. After centrifugation, 0.5-ml fractions were collected; 20 μl of each fraction was run on an 8–16% gradient gel, and immunoblotted.

In Vitro 20 S Ubiquitin-independent Chymotryptic Proteasomal Activity Assay—We incubated aggregated or monomeric α-synuclein at various concentrations with purified 20 S proteasome (human erythrocytes, BioMol) for 30 min and then added a fluorogenic substrate (Suc-LLVY-AMC, BioMol). Ten minutes later, the samples were analyzed with a GeminiXS SpectraMax fluorescent spectrophotometer (Amersham Biosciences) using an excitation wavelength of 360 nm and an emission wavelength of 460 nm.

In Vitro 20/26 S Ubiquitin-independent Chymotryptic Proteasomal Activity Assay—Aggregated or monomeric α-synuclein at various concentrations was incubated with 250 μg of HEK 293 cell lysates, as determined by BCA protein assay (Pierce) in assay buffer (10 mM Tris-HCl, pH 7.8, 0.5 mM dithiothreitol, 5 mM $MgCl_2$, and 5 mM ATP) for 30 or 60 min at 37 °C while shaking at 800 rpm. We then added a fluorogenic substrate (Suc-LLVY-AMC, BioMol) and incubated samples an additional 30 min at 37 °C while shaking at 800 rpm. Solutions were analyzed using an excitation wavelength of 360 nm and an emission wavelength of 460 nm with the GeminiXS SpectraMax spectrophotometer (Amersham Biosciences).

In Vitro 26 S Ubiquitin-dependent Proteasomal Activity Assay—Substrates were generated with an *in vitro* transcription and translation of substrate proteins using a T7 promoter in *Escherichia coli* lysate (Promega), supplemented with [^{35}S]methionine, and then partially purified by high-speed centrifugation and ammonium sulfate precipitation as described (45). The protease substrate for ClP assays was derived from barnase, which is a ribonuclease from *Bacillus amyloliquefaciens*; the protease substrate for proteasomal assays was derived from *E. coli* dihydrofolate reductase (DHFR) (45, 46). A ubiquitin moiety was added to the N terminus of the substrate proteins via a 4-amino acid linker from the *E. coli* lac repressor (45). Substrate proteins were constructed in pGEM-3Zf (+) vectors (Promega) and were verified by sequencing. The reaction was resuspended in 40 μl of buffer (25% (v/v) glycerol, 25 mM $MgCl_2$, 0.25 mM Tris/HCl, pH7.4) to which 5 μl of the *in vitro* reaction containing the radiolabeled ubiquitinated substrate protein was added with 35 μl of rabbit reticulocyte lysate (Green Hectares, containing 1 mM dithiothreitol) that is ATP-depleted as described (45). We incubated the reactions with and without monomeric or aggregated α-synuclein. Concentration of α-synuclein was determined by BCA protein assay (Pierce). We incubated at 37 °C for 7 min to allow initial cleavage of substrate proteins. Ubiquitination and degradation was initiated by the addition of ATP and an ATP-regenerating system (0.5 mM ATP, 10 mM creatine phosphate, 0.1 mg/ml creatine phosphokinase, final concentrations). Reactions were incubated at 37 °C. At designated time points (15, 30, 45, 60, 90, 120, 150, and 180 min), small aliquots were removed and transferred to ice-cold 5% trichloroacetic acid. The trichloroacetic acid-insoluble fractions were analyzed by 10% SDS-PAGE and quantified by electronic autoradiography.

Statistics—All statistics were performed using a multifactorial analysis of variance analysis using the Statview statistical package.

[1] The abbreviations used are: PD, Parkinson's disease; DHFR, dihydrofolate reductase; DHFR-U, dihidrofolate reductase with a degradation tag; UPS, ubiquitin proteasomal system.

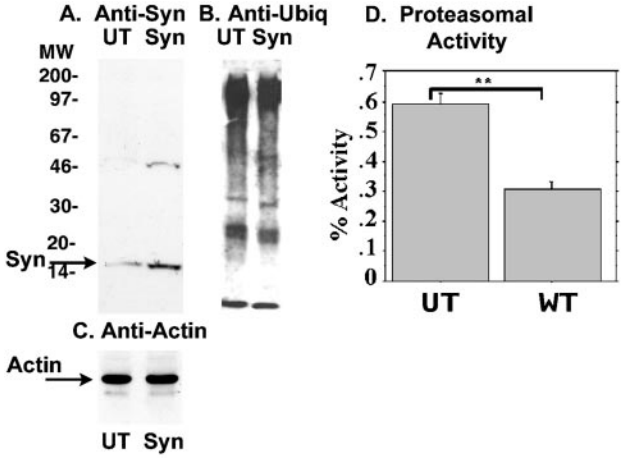

FIG. 1. **Effects of α-synuclein overexpression on the proteasomal system.** *A* and *B*, BE-M17 neuroblastoma cells were transfected with vector or wild-type α-synuclein and immunoblotted with antibodies to α-synuclein (*A*), ubiquitin (*B*), and actin (*C*). No differences in levels of ubiquitin-conjugated proteins were observed among cells transfected with vector or wild-type α-synuclein. This is a representative immunoblot from experiments that have been repeated at least three times. *D*, activity of the ubiquitin-independent proteasomal system in cell lines expressing wild-type α-synuclein compared with untransfected cells (**, $p < 0.0005$). These data represent the combined data from five experiments each containing 5 data points for each sample.

RESULTS

Overexpressing α-Synuclein Inhibits Proteasomal Degradation—To begin analyzing how α-synuclein might interact with the proteasome, wild-type α-synuclein was stably expressed in human neuroblastoma BE-M17 cells by transient transfection, and ubiquitin-dependent and -independent proteasomal activity was quantified. Because α-synuclein does not form aggregates spontaneously under these conditions, this experiment addresses whether increased concentration of cellular α-synuclein inhibits proteasomal activity. Immunoblotting of the cellular lysates demonstrated a significant increase in the α-synuclein levels in the transfected cells (Fig. 1*A*). Next, we investigated whether overexpressing α-synuclein affects the steady state levels of ubiquitin-conjugated proteins, which provides a measure of the ubiquitin-dependent proteasomal system. The BE-M17 cells expressing vector or wild-type α-synuclein were immunoblotted with anti-ubiquitin antibody. The amount of ubiquitin-conjugated proteins did not differ among the groups of transfected cells (Fig. 1, *B* and *C*).

We also investigated how overexpressing α-synuclein affects ubiquitin-independent proteasomal degradation. Previous studies report that cell lines overexpressing α-synuclein exhibit lower ubiquitin-independent proteasomal activity (39). To investigate ubiquitin-independent proteasomal activity, we measured hydrolysis rates of fluorogenic peptide analogues in cells transiently or stably overexpressing α-synuclein (Fig. 1*D*). No difference in activity was observed in cells transiently transfected with α-synuclein (data not shown). However, cell lines stably expressing wild-type α-synuclein showed an approximately 50% reduction in ubiquitin-independent proteasomal degradation, depending on the transgene (39) (Fig. 1*D*). These data suggest that α-synuclein does affect ubiquitin-independent proteasomal function.

α-Synuclein Inhibits the 20 S Proteasome—An increasing number of studies suggest that the state of α-synuclein aggregation plays a key role in the pathophysiology of PD. To better understand how α-synuclein affects the proteasome, we generated recombinant monomeric α-synuclein and aggregated α-synuclein. The aggregated α-synuclein was generated by aging recombinant α-synuclein at 37 °C for 2 months. Aggregation of α-synuclein was verified by immunoblot analysis (Fig. 2*A*). The aggregated protein ran as a smear with an average molecular weight of ~160,000 (Fig. 2*A*). The immunoblot of the aged, aggregated α-synuclein also exhibited some reactivity at 16,000. This could reflect either that the sample had some non-aggregated, monomeric α-synuclein remaining or that some of the α-synuclein could be dissociated from the aggregate by SDS. To examine this question, we fractionated monomeric or aged α-synuclein (37 °C for 2 months) by centrifugation in a sucrose gradient and immunoblotted each of the 25 fractions with anti-synuclein antibody. The initial sample used before the fractionation is shown in the first lane (Fig. 2*B*, labeled *In*). Monomeric α-synuclein had a low density and was most abundant in fractions 1–6 (Fig. 2*B*, *top*). In contrast, the aggregated α-synuclein sample showed nothing in the early fractions (corresponding to a low density) and migrated exclusively in the last fraction, suggesting a high density (Fig. 2*B*, *fraction 25*, *bottom*). Immunoblots of fraction 25 for the aggregated sample showed a small amount of SDS-sensitive α-synuclein that migrated as a monomer following exposure to SDS during the immunoblotting. This SDS-dissociable α-synuclein was particularly evident following longer exposures (Fig. 2*B*, *fraction 25B*, *bottom*). This suggests that aggregated α-synuclein contains SDS-sensitive and SDS-resistant aggregated protein.

Next, we examined the activity of purified 20 S proteasome particles in the presence of varying amounts of monomeric or aggregated α-synuclein using synthetic fluorescent peptides to monitor proteasomal activity. Increasing doses of monomeric α-synuclein progressively inhibited proteasomal activity (Fig. 3*A*). The IC_{50} for inhibition of the proteasome by monomeric α-synuclein was ~16 μM, assuming α-synuclein could achieve complete inhibition. Aggregated α-synuclein also inhibited the 20 S ubiquitin-independent proteasomal activity, exhibiting a maximal inhibition similar to that of monomeric α-synuclein (Fig. 3*B*).

To determine whether the inhibition was at the level of the proteasome or due to binding of the peptide substrate, we examined whether varying the level of substrate affected the α-synuclein-dependent proteasomal inhibition. Inhibition of the 20 S proteasome by monomeric α-synuclein increased with increasing substrate concentration (Fig. 3*C*). Increased proteasomal inhibition by α-synuclein might occur because larger effects are possible at higher rates of substrate degradation. These data indicate that the proteasomal inhibition that was observed did not result from substrate binding and substrate sequestration by α-synuclein. Thus, α-synuclein appears to inhibit the proteasomal activity via an interaction with the proteasome, rather than by binding substrate peptide.

Aggregated α-Synuclein Inhibits the 26 S Proteasome—Next, we examined the effects of monomeric and aggregated α-synuclein on a mixture of the 20 and 26 S proteasomes in HEK 293 cell lysates. Monomeric α-synuclein inhibited the 20 S/26 S proteasome mixture only partially, which could reflect greater inhibition of the 20 S proteasome complex and less inhibition of the 26 S proteasome complex (Fig. 4*B*). The concentration producing maximal inhibition of the 20 S/26 S proteasome complex was similar to that seen for the 20 S proteasome complex (> 10 μM), based on 50% maximal inhibition (Fig. 4*B*). Aggregated α-synuclein also inhibited the 20 S/26 S ubiquitin-independent proteasomal mixture. Based on an estimated molecular weight for aggregated α-synuclein of 160,000, we calculated that the IC_{50} of aggregated α-synuclein for the 20 S/26 S proteasome was 1 nM (Fig. 4*A*). The ability of aggregated α-synuclein to inhibit a mixture of the 26 S and 20 S proteasomes, but not the 20 S proteasome, suggests that aggregated

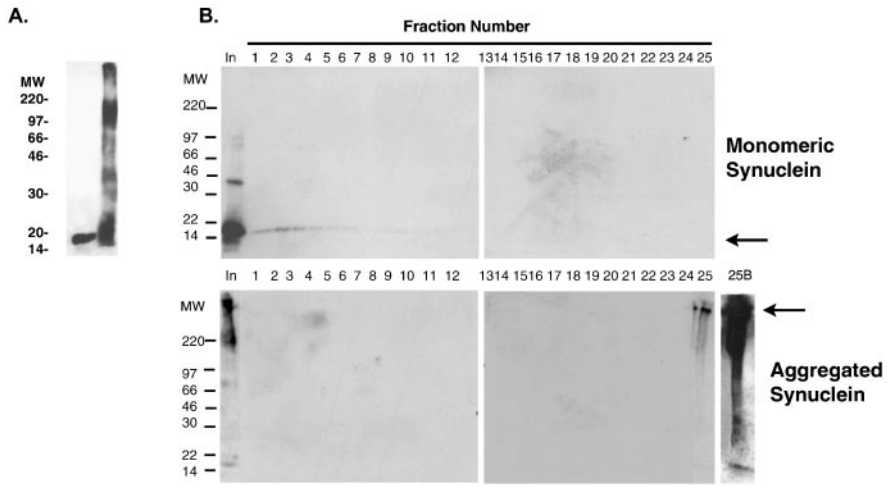

FIG. 2. **Analysis of monomeric and aggregated α-synuclein.** *A*, fresh α-synuclein (*lane 1*) migrated at about 16,000, which is consistent with a monomeric size. Aggregated α-synuclein (*lane 2*) exhibited both low and high molecular weight species following the process of immunoblotting, which involved heating in 2% SDS for 5 min, running on PAGE, and immunoblotting. This is a representative immunoblot from an experiment that had been repeated three times. *B*, samples of fresh (*top*) and aged (*bottom*) α-synuclein were fractionated on a 5–30% sucrose gradient, and each fraction was immunoblotted. An immunoblot of the non-fractionated starting material is shown in the first lane, *IN′*. The monomeric α-synuclein was present predominantly in the early fractions, suggesting a low molecular weight; the aged α-synuclein was present in the last fraction, suggesting a high molecular weight and little if any free monomeric α-synuclein. Because some SDS-sensitive aggregated α-synuclein appeared to be present in the aged Input sample, we overexposed the aged fractionated sample to determine whether it also contained any SDS-sensitive aged α-synuclein. A long exposure of fraction 25 (*lane 25B*) demonstrates the presence of 16,000 α-synuclein, suggesting that some of the aged, aggregated α-synuclein can be dissociated by SDS. This is a representative immunoblot from an experiment that had been repeated three times.

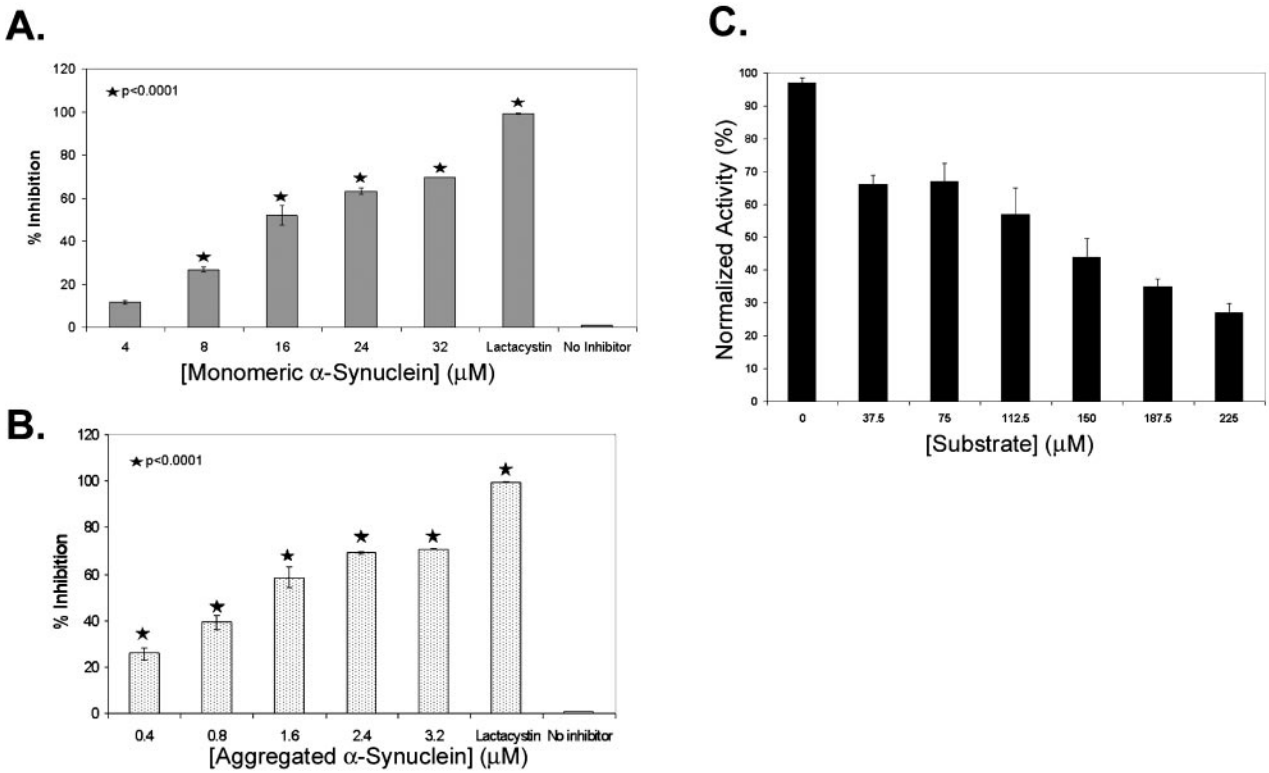

FIG. 3. **Effects of monomeric and aggregated α-synuclein on the 20 S proteasome.** *A*, inhibition of the 20 S proteasome by monomeric α-synuclein dose response. Five data points were used for each sample. *B*, inhibition of the 20 S proteasome by aggregated α-synuclein dose response. Five data points were used for each sample. *C*, substrate dependence of proteasomal inhibition by α-synuclein. Five data points were used for each sample.

α-synuclein selectively inhibits the 26 S proteasome.

Aggregated Synuclein, but Not Monomeric Synuclein, Inhibits Protein Degradation by the 26 S Proteasome—The greater ability of aggregated α-synuclein compared with monomeric α-synuclein in inhibiting 26 S ubiquitin-independent proteasomal activity raises the possibility that 26 S ubiquitin-dependent proteasomal function might also be selectively inhibited by aggregated α-synuclein. To investigate this, we examined ubiquitin-mediated degradation of a fusion protein made up of barnase and *E. coli* dihydrofolate reductase that had been fused with an N-terminal degradation tag (DHFR-U) (45). Prior studies show that degradation of ubiquitinated DHFR-U by reticulocyte lysates is mediated by the 26 S proteasome (45). We used this system to investigate how monomeric and aggregated α-synuclein affect ubiquitin-mediated proteasomal degradation. Degradation of ubiquitinated DHFR-U was examined

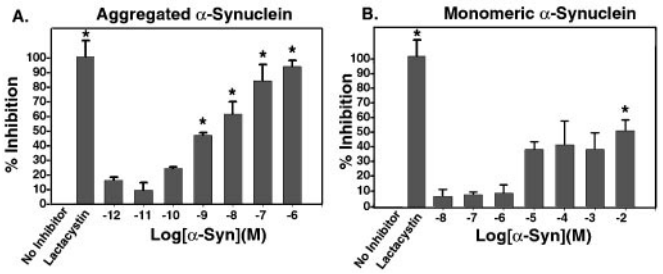

FIG. 4. **Inhibition of ubiquitin-independent proteasomal degradation by the 20 S/26 S proteasome with aggregated (*A*) and monomeric (*B*) α-synuclein using HEK 293 lysates.** The percent inhibition was normalized to the inhibition produced by the proteasomal inhibitor lactacystin (25 μM). *, $p < 0.002$ compared with no inhibitor.

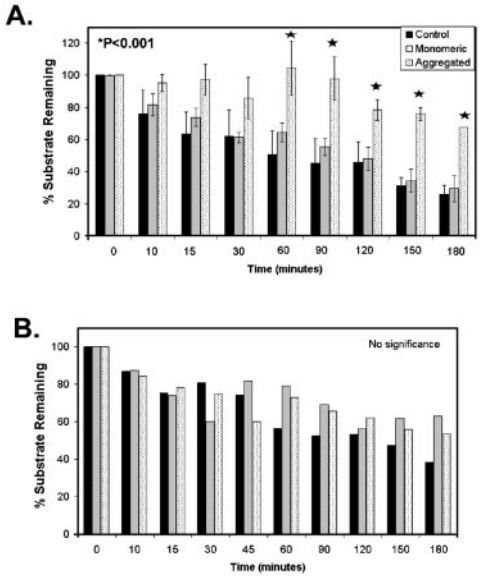

FIG. 5. **Inhibition of ubiquitin-dependent proteasomal degradation by aggregated α-synuclein.** *A*, aggregated α-synuclein (0.5 μM) inhibits ubiquitin-dependent degradation of DHFR-U by reticulocyte lysates by the 26 S proteasome, whereas monomeric α-synuclein (5 μM) does not inhibit degradation of DHFR-U by reticulocyte lysates by the 26 S proteasome. The overall analysis of variance was significant at $p < 0.001$. *Stars* show significance relative to DHFR-U in the absence of added α-synuclein. Each sample point was performed in triplicate. *B*, lack of inhibition of Clp1 by monomeric or aggregated α-synuclein. Degradation of DHFR-U was not significantly different between degradation of DHFR-U alone or in the presence of aggregated (0.5 μM) or monomeric (5 μM) α-synuclein. Each sample point was performed in triplicate.

in the presence of monomeric or aggregated α-synuclein (Fig. 5*A*). The half-life of DHFR-U was 125 min both under basal conditions and in the presence of 5 μM monomeric α-synuclein (Fig. 5*A*, *gray bars*). However, the half-life of DHFR-U greatly increased in the presence of 500 nM aggregated α-synuclein (Fig. 5*A*, *dotted bars*). No inhibition was seen with 50 nM aggregated α-synuclein (data not shown). These data indicate that 26 S ubiquitin-dependent proteasomal degradation is selectively inhibited by aggregated α-synuclein.

To determine whether inhibition of ubiquitin-dependent proteasomal degradation was specific to the 26 S proteasome, we also examined degradation of barnase that had been fused with a 65-amino acid N-terminal tag (DHFR-65) that allows the protein to be recognized and degraded by the bacterial proteasomal analog ClpAP (45). DHFR-65 was incubated with ClpAP alone or in the presence of 5 μM monomeric α-synuclein or in the presence of 500 nM aggregated α-synuclein, and the rate of degradation was monitored. Neither monomeric nor aggregated α-synuclein inhibited degradation of DHFR-65 by ClpAP (Fig. 5*B*). This indicates that proteasomal inhibition by aggregated α-synuclein is specific for the ubiquitin-dependent 26 S proteasomal system.

Native and Aggregated α-Synuclein Bind S6′—The ability of aggregated α-synuclein to inhibit degradation mediated by the 26 S proteasome could be explained by interaction between aggregated α-synuclein and a protein in the 19 S cap that is present in the 26 S proteasome but not the 20 S proteasome. Studies with rat α-synuclein suggest that α-synuclein binds the rodent 19 S proteasomal component S6′ (35). Based on this work, we investigated whether human α-synuclein interacts with S6′. His-tagged recombinant native or aggregated α-synuclein was incubated overnight with substantia nigra or cingulated cortex from normal human brain and then precipitated with nickel-agarose. The precipitates were immunoblotted with antibodies to S6′. A representative immunoblot with native α-synuclein is shown in Fig. 6*A*, and a pull-down with native or aggregated α-synuclein is shown in Fig. 6*B*. Both aggregated and monomeric α-synuclein associated with S6′. The term 'native' is used in this discussion because the overnight incubation of recombinant α-synuclein with the lysates appeared to promote formation of some recombinant α-synuclein dimer, in addition to the more abundant α-synuclein monomer (Fig. 6*B*, *lower panel*). Co-association of α-synuclein with S6′ was also observed by immunoprecipitating endogenous α-synuclein and immunoblotting for S6′ (Fig. 6*C*). To test the selectivity of the association, we examined whether α-synuclein binds other components of the 19 S proteasomal cap, such as Rpn12 and subunit 10b. Neither Rpn12 nor subunit 10b was observed to co-precipitate with α-synuclein (Fig. 6*D*, immunoblot for *10b* shown). It was not possible to test the association of S6′ with α-synuclein by immunoprecipitating S6′, because none of the antibodies to S6′ that we tested were successfully able to precipitate S6′ (data not shown). Together, these data suggest that both monomeric and aggregated α-synuclein bind S6′.

DISCUSSION

Proteasomal inhibition is known to be toxic to many cell types and is thought to contribute to the pathophysiology of neurodegenerative diseases (17, 18, 47). Our data demonstrate that overexpressing α-synuclein inhibits 20 and 26 S proteasomal activity. The relationship between overexpressed α-synuclein and the pathophysiology of PD, though, is unclear. Overexpressing α-synuclein in mammalian neurons does not lead to its spontaneous aggregation, except after delays of 6–12 months (48–51). Because protein aggregation is thought to play a critical role in the pathophysiology of neurodegenerative diseases and aggregation of α-synuclein appears to be important to the pathophysiology of PD, we sought to design experiments that would allow analysis of the actions of aggregated α-synuclein. To investigate whether aggregated α-synuclein interacts with the proteasome, we examined the behavior of α-synuclein that had been aggregated *in vitro*. We observed that aggregated α-synuclein inhibits both ubiquitin-dependent and -independent 26 S proteasomal activity. The IC_{50} of aggregated α-synuclein for ubiquitin-independent 26 S proteasomal activity was 1 nM, which was over 1000-fold higher than the IC_{50} for 20 S proteasomal activity. In contrast, monomeric α-synuclein inhibited 20 and 26 S proteasomal activity with an $IC_{50} > 10$ μM.

The high affinity of aggregated α-synuclein for inhibiting 26 S proteasomal activity could be explained by binding of aggregated α-synuclein to a protein in the 19 S cap, which is the proteasomal complex that binds to the 20 S proteasome and confers ubiquitin-dependence, as discussed below (3). Consist-

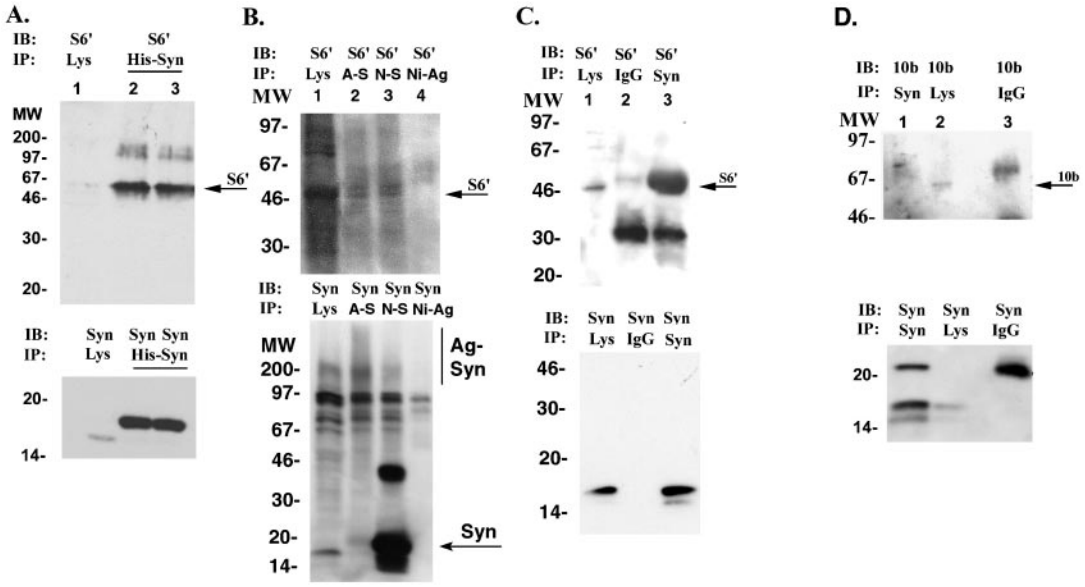

FIG. 6. **α-Synuclein binds S6′.** *A*, *upper panel*, immunoblot showing S6′ in brain lysate (*lane 1*, 10 μg) and precipitation of S6′ by monomeric His-tagged recombinant α-synuclein (*lanes 2* and *3*). *Lower panel*, reprobe of the same immunoblot with anti-α-synuclein antibody. The *arrow* points to the band corresponding to the S6′ protein. The α-synuclein band in lane 1 is lower than that in lanes 2 and 3 in the lower panel because the protein in lane 1 is endogenous α-synuclein, whereas the protein in lane 2 and 3 is His-tagged protein. *B*, *upper panel*, immunoblot showing S6′ in brain lysate (*lane 1*, 30 μg), precipitation of S6′ by aggregated (*lane 2*, *A-S*) or native His-tagged recombinant α-synuclein (*lane 3*, *N-S*), and lack of precipitation of S6′ using Ni-agarose pull-down without recombinant α-synuclein (*lane 4*). The *arrow* points to the band corresponding to the S6′ protein. *Lower panel*, reprobe of the same immunoblot with anti-α-synuclein antibody. The *arrow* points to monomeric α-synuclein, and the *bar* demonstrates the position of aggregated α-synuclein. The band at 36 kDa in lane 3 likely represents an α-synuclein dimer that might have been promoted by incubation of a large amount of recombinant α-synuclein with lysate but was not present in most other experiments (for example, see *panel C*). *C*, *upper panel*, immunoblot of S6′ showing the association of S6′ with α-synuclein following an immunoprecipitation of endogenous α-synuclein by anti-synuclein antibody. The *arrow* points to the band corresponding to the S6′ protein. *Lane 1* (*Lys*), crude brain lysates that had not been subject to immunoprecipitation. *Lane 2* (*IgG*), immunoprecipitation with nonspecific preimmune IgG antibody. *Lane 3* (*Syn*), immunoprecipitation with anti-α-synuclein antibody. *Lower panel*, reprobe with anti-α-synuclein antibody. *D*, no association was observed between α-synuclein and other proteasomal components, such as the 19 S subunit 10b. The *arrow* points to the band corresponding to the 10b protein, which is present in the lysates (*lane 2*) but not immunoprecipitated with α-synuclein (*lane 1*) or nonspecific IgG (*lane 3*). The abbreviations for this panel are the same as for panel B. All immunoblots in this figure are representative immunoblots from experiments that had been repeated at least three times.

ent with this hypothesis, we observed that α-synuclein binds to S6′, which is a subunit of the 19 S cap that was recently shown to bind polyubiquitinated proteins (3). Both aggregated and monomeric α-synuclein bind the S6′ protein. The interaction appears to be selective for S6′ because no association was observed with other 19 S proteasomal proteins, such as Rpn12 or subunit 10b.

Binding of α-synuclein to S6′ is consistent with prior publications. Ghee *et al*. (35) demonstrated that rat S6′ (also termed Tat binding protein-1, TBP1) binds α-synuclein using the yeast two-hybrid method. The association was confirmed by showing that an epitope-tagged S6′ could pull down α-synuclein following transfection of both proteins into HEK 293 cells. However, this study did not demonstrate interaction using the endogenous proteins and also did not investigate whether human α-synuclein binds to human S6′. In addition, Ii *et al.* (52) have documented the presence of proteasomal proteins in Lewy bodies, which supports our observation that aggregated α-synuclein binds S6′. The information presented in this study provides the functional relevance for these observations by showing that binding of α-synuclein to the proteasome inhibits proteasomal function.

The function of S6′ was recently identified and suggests a mechanism explaining why aggregated α-synuclein might inhibit the activity of the 26 S proteasome. The S6′ protein appears to function in the 19 S proteasomal cap as the docking protein for ubiquitin-conjugated proteins and is essential for binding of ubiquitin-conjugated proteins by the proteasome (3). Because aggregated α-synuclein is much larger than monomeric α-synuclein and often contains covalent cross-links, binding to S6′ might inhibit the function of the 19 S protein by competing with binding of other ubiquitin-conjugated proteins. Bound aggregated α-synuclein might occupy the unfolding proteins associated with proteasomal degradation, and the aggregate might also physically block the pore of the 19 S cap. This model provides an explanation for the ability of aggregated α-synuclein to interfere with both the ubiquitin-dependent and -independent 26 S proteasomal function.

Many other protein aggregates have been shown to be toxic to cells (18). Both aggregated cystic fibrosis transmembrane receptor and polyglutamine repeat exhibit toxicity that correlates with proteasomal inhibition (17, 18, 47). This study focuses attention on the interaction between S6′ and protein aggregates. Whether S6′ has a particular affinity for α-synuclein or is a general target for all protein aggregates remains to be determined. Inhibiting the ubiquitin-dependent proteasomal system (UPS) is known to be toxic, perhaps because it induces apoptosis (19). Inhibiting the UPS causes the accumulation of many toxic proteins, such as Pael-R, which was recently identified as a parkin substrate (53). Inhibiting the UPS is also known to cause the accumulation of protein aggregates in the endoplasmic reticulum (17, 47). Inhibiting the UPS could alter the regulation of cell cycle proteins (54). Reduced degradation of cell cycle proteins could account for the apparent abnormal activation of the cell cycle proteins observed in many neurodegenerative processes (55, 56).

Proteasomal inhibitors have recently been shown to induce degeneration of the dopaminergic neurons of the substantia nigra and induce α-synuclein aggregation (57). The tendency of α-synuclein to accumulate under conditions of proteasomal in-

hibition raises the possibility that the accumulation of aggregated α-synuclein adds to the proteasomal inhibition and increases the toxicity associated with proteasomal inhibition.

The discordance between the rapid kinetics of cell death associated with UPS inhibition in cell culture and the slow nature of degeneration in PD is notable. This discordance might be explained by the slow appearance of aggregated α-synuclein. α-Synuclein does not form aggregates under basal conditions when transiently overexpressed, but studies in transgenic mice show that overexpressing α-synuclein does lead to a delayed accumulation of aggregated α-synuclein (48–51). The slow rate of accumulation of aggregated α-synuclein could also lead to a correspondingly gradual inhibition of the UPS during the course of PD. Hence, progressive inhibition of the UPS by aggregated α-synuclein might be a gradual process in PD. Together these data suggest a model in which the gradual accumulation of aggregated α-synuclein progressively inhibits S6′ function, which leads to a gradual but progressive inhibition of the UPS and the progressive neurodegeneration that occurs in PD.

Acknowledgments—We thank John Hardy (National Institutes of Health) for providing the α-synuclein cDNA, Philipp Kahle (University of Munich) for useful comments, and Thomas Gallagher (Loyola University Medical Center) for insight into sucrose gradient methodology.

REFERENCES

1. Glickman, M. H., Rubin, D. M., Fried, V. A., and Finley, D. (1998) *Mol. Cell. Biol.* **18,** 3149–3162
2. Voges, D., Zwickl, P., and Baumeister, W. (1999) *Annu. Rev. Biochem.* **68,** 1015–1068
3. Lam, Y. A., Lawson, T. G., Velayutham, M., Zweier, J. L., and Pickart, C. M. (2002) *Nature* **416,** 763–767
4. Davies, K. J. (2001) *Biochimie (Paris)* **83,** 301–310
5. Shringarpure, R., Grune, T., and Davies, K. J. (2001) *Cell. Mol. Life Sci.* **58,** 1442–1450
6. Rechsteiner, M. (1991) *Cell* **66,** 615–618
7. Rechsteiner, M., Hoffman, L., and Dubiel, W. (1993) *J. Biol. Chem.* **268,** 6065–6068
8. Goldberg, A. L. (1992) *Eur. J. Biochem.* **203,** 9–23
9. Hershko, A., and Ciechanover, A. (1998) *Annu. Rev. Biochem.* **67,** 425–479
10. Coux, O., Tanaka, K., and Goldberg, A. L. (1996) *Annu. Rev. Biochem.* **65,** 801–847
11. Baumeister, W., Walz, J., Zuhl, F., and Seemuller, E. (1998) *Cell* **92,** 367–380
12. Tanaka, K. (1998) *J. Biochem. (Tokyo)* **123,** 195–204
13. Tanaka, K. (1998) *Biochem. Biophys. Res. Commun.* **247,** 537–541
14. Satyal, S. H., Schmidt, E., Kitagawa, K., Sondheimer, N., Lindquist, S., Kramer, J. M., and Morimoto, R. I. (2000) *Proc. Natl. Acad. Sci. U. S. A.* **97,** 5750–5755
15. Paulson, H. L., Perez, M. K., Trottier, Y., Trojanowski, J. Q., Subramony, S. H., Das, S. S., Vig, P., Mandel, J. L., Fischbeck, K. H., and Pittman, R. N. (1997) *Neuron* **19,** 333–344
16. Martindale, D., Hackam, A., Wieczorek, A., Ellerby, L., Wellington, C., McCutcheon, K., Singaraja, R., Kazemi-Esfarjani, P., Devon, R., Kim, S. U., Bredesen, D. E., Tufaro, F., and Hayden, M. R. (1998) *Nat. Genet.* **18,** 150–154
17. Bence, N. F., Sampat, R. M., and Kopito, R. R. (2001) *Science* **292,** 1552–1555
18. Bucciantini, M., Giannoni, E., Chiti, F., Baroni, F., Formigli, L., Zurdo, J., Taddei, N., Ramponi, G., Dobson, C. M., and Stefani, M. (2002) *Nature* **416,** 507–511
19. Jesenberger, V., and Jentsch, S. (2002) *Nat. Rev. Mol. Cell. Biol.* **3,** 112–121
20. Spillantini, M., Schmidt, M., Lee, VM-Y, Trojanowski, J., Jakes, R., and Goedert, M. (1997) *Nature* **388,** 839–840
21. Spillantini, M. G., Crowther, R. A., Jakes, R., Hasegawa, M., and Goedert, M. (1998) *Proc. Natl. Acad. Sci. U. S. A.* **95,** 6469–6473
22. Polymeropoulos, M. H., Lavedan, C., Leroy, E., Ide, S. E., Dehejia, A., Dutra, A., Pike, B., Root, H., Rubenstein, J., Boyer, R., Stenroos, E. S., Chandrasekharappa, S., Athanassiadou, A., Papapetropoulos, T., Johnson, W. G., Lazzarini, A. M., Duvoisin, R. C., Di Iorio, G., Golbe, L. I., and Nussbaum, R. L. (1997) *Science* **276,** 2045–2047
23. Kruger, R., Kuhn, W., Muller, T., Woitalla, D., Graeber, M., Kosel, S., Przuntek, H., Epplen, J., Schols, L., and Riess, O. (1998) *Nature Gen.* **18,** 106–108
24. Conway, K., Harper, J., and Lansbury, P. (1998) *Nature Med.* **4,** 1318–1320
25. Conway, K. A., Lee, S. J., Rochet, J. C., Ding, T. T., Williamson, R. E., and Lansbury, P. T., Jr. (2000) *Proc. Natl. Acad. Sci. U. S. A.* **97,** 571–576
26. Wood, S., Wypych, J., Steavenson, S., Louis, J., Citron, M., and Biere, A. (1999) *J. Biol. Chem.* **274,** 19509–19512
27. Biere, A. L., Wood, S. J., Wypych, J., Steavenson, S., Jiang, Y., Anafi, D., Jacobsen, F. W., Jarosinski, M. A., Wu, G. M., Louis, J. C., Martin, F., Narhi, L. O., and Citron, M. (2000) *J. Biol. Chem.* **275,** 34574–34579
28. Ostrerova, N., Petrucelli, L., Farrer, M., Mehta, N., Alexander, P., Choi, P., Palacino, J., Hardy, J., and Wolozin, B. (1999) *J. Neurosci.* **19,** 5782–5791
29. Jenco, J., Rawlingson, A., Daniels, B., and Morris, A. (1998) *Biochemistry* **37,** 4901–4909
30. Pronin, A. N., Morris, A. J., Surguchov, A., and Benovic, J. L. (2000) *J. Biol. Chem.*
31. Engelender, S., Kaminsky, Z., Guo, X., Sharp, A., Amaravi, R., Kleiderlein, J., Margolis, R., Troncoso, J., Lanahan, A., Worley, P., Dawson, V., Dawson, T., and Ross, C. (1999) *Nature Gen.* **22,** 110–114
32. Sharon, R., Goldberg, M. S., Bar-Josef, I., Betensky, R. A., Shen, J., and Selkoe, D. J. (2001) *Proc. Natl. Acad. Sci. U. S. A.* **98,** 9110–9115
33. Choi, P., Golts, N., Snyder, H., Petrucelli, L., Chong, M., Hardy, J., Sparkman, D., Cochran, E., Lee, J., and Wolozin, B. (2001) *NeuroReport* **12,** 2839–2844
34. Lee, F. J., Liu, F., Pristupa, Z. B., and Niznik, H. B. (2001) *FASEB J.* **15,** 916–926
35. Ghee, M., Fournier, A., and Mallet, J. (2000) *J. Neurochem.* **75,** 2221–2224
36. Wakabayashi, K., Engelender, S., Yoshimoto, M., Tsuji, S., Ross, C. A., and Takahashi, H. (2000) *Ann. Neurol.* **47,** 521–523
37. Schlossmacher, M. G., Frosch, M. P., Gai, W. P., Medina, M., Sharma, N., Forno, L., Ochiishi, T., Shimura, H., Sharon, R., Hattori, N., Langston, J. W., Mizuno, Y., Hyman, B. T., Selkoe, D. J., and Kosik, K. S. (2002) *Am. J. Pathol.* **160,** 1655–1667
38. Souza, J. M., Giasson, B. I., Lee, V. M., and Ischiropoulos, H. (2000) *FEBS Lett.* **474,** 116–119
39. Tanaka, Y., Engelender, S., Igarashi, S., Rao, R. K., Wanner, T., Tanzi, R. E., Sawa, A., Dawson, V. L., Dawson, T. M., and Ross, C. A. (2001) *Hum. Mol. Genet.* **10,** 919–926
40. Ostrerova-Golts, N., Petrucelli, L., Hardy, J., Lee, J., Farrer, M., and Wolozin, B. (2000) *J. Neurosci.* **20,** 6048–6054
41. Golts, N., Snyder, H., Frasier, M., Theisler, C., Choi, P., and Wolozin, B. (2002) *J. Biol. Chem.* **277,** 16116–16123
42. Lee, H. J., Choi, C., and Lee, S. J. (2001) *J. Biol. Chem.* **25,** 25
43. Betarbet, R., Sherer, T. B., MacKenzie, G., Garcia-Osuna, M., Panov, A. V., and Greenamyre, J. T. (2000) *Nat. Neurosci.* **3,** 1301–1306
44. Uversky, V. N., Li, J., and Fink, A. L. (2001) *FEBS Lett.* **500,** 105–108
45. Lee, C., Schwartz, M. P., Prakash, S., Iwakura, M., and Matouschek, A. (2001) *Mol. Cell* **7,** 627–637
46. Matouschek, A., Azem, A., Ratliff, K., Glick, B. S., Schmid, K., and Schatz, G. (1997) *EMBO J.* **16,** 6727–6736
47. Johnston, J., Ward, C., and Kopito, R. (1998) *J. Cell Biol.* **143,** 1883–1898
48. Lee, M. K., Stirling, W., Xu, Y., Xu, X., Qui, D., Mandir, A. S., Dawson, T. M., Copeland, N. G., Jenkins, N. A., and Price, D. L. (2002) *Proc. Natl. Acad. Sci. U. S. A.* **99**
49. Giasson, B. I., Duda, J. E., Quinn, S. M., Zhang, B., Trojanowski, J. Q., and Lee, V. M. (2002) *Neuron* **34,** 521–533
50. Kahle, P. J., Neumann, M., Ozmen, L., Muller, V., Odoy, S., Okamoto, N., Jacobsen, H., Iwatsubo, T., Trojanowski, J. Q., Takahashi, H., Wakabayashi, K., Bogdanovic, N., Riederer, P., Kretzschmar, H. A., and Haass, C. (2001) *Am. J. Pathol.* **159,** 2215–2225
51. Masliah, E., Rockenstein, E., Veinbergs, I., Mallory, M., Hashimoto, M., Takeda, A., Sagara, Y., Sisk, A., and Mucke, L. (2000) *Science* **287,** 1265–1269
52. Ii, K., Ito, H., Tanaka, K., and Hirano, A. (1997) *J. Neuropathol. Exp. Neurol.* **56,** 125–131
53. Imai, Y., Soda, M., Inoue, H., Hattori, N., Mizuno, Y., and Takahashi, Y. (2001) *Cell* **105,** 891–902
54. Yew, P. R. (2001) *J. Cell. Physiol.* **187,** 1–10
55. Husseman, J. W., Nochlin, D., and Vincent, I. (2000) *Neurobiol. Aging* **21,** 815–828
56. Chang, B. D., Watanabe, K., Broude, E. V., Fang, J., Poole, J. C., Kalinichenko, T. V., and Roninson, I. B. (2000) *Proc. Natl. Acad. Sci. U. S. A.* **97,** 4291–4296
57. McNaught, K. S., Bjorklund, L. M., Belizaire, R., Isacson, O., Jenner, P., and Olanow, C. W. (2002) *Neuroreport* **13,** 1437–1441

Available online at www.sciencedirect.com
SCIENCE DIRECT
Molecular Brain Research 117 (2003) 179–189
MOLECULAR BRAIN RESEARCH
www.elsevier.com/locate/molbrainres

Research report

SEPT5_v2 is a parkin-binding protein

P. Choi[a,1], H. Snyder[a,1], L. Petrucelli[b], C. Theisler[a], M. Chong[a], Y. Zhang[c], K. Lim[c], K.K.K. Chung[c], K. Kehoe[c], L. D'Adamio[d], J.M. Lee[a], E. Cochran[e], R. Bowser[f], T.M. Dawson[c], B. Wolozin[a,*]

[a]*Department of Pharmacology, Loyola University Medical Center, Bldg. 102/3634, 2160 S. 1st Ave., Maywood, IL 60153, USA*
[b]*Department of Pharmacology, Mayo Clinic, Jacksonville, FL, USA*
[c]*Department of Neurology and Neuroscience, Johns Hopkins Medical Center, Baltimore, MD, USA*
[d]*Department of Microbiology and Immunology, Albert Einstein College of Medicine, The Bronx, NY, USA*
[e]*Department of Pathology, St. Lukes-Rush-Presbyterian Medical Center, Chicago, IL, USA*
[f]*Department of Pathology, University of Pittsburgh, Pittsburgh, PA, USA*

Accepted 24 June 2003

Abstract

Mutations in parkin are associated with various inherited forms of Parkinson's disease (PD). Parkin is a ubiquitin ligase enzyme that catalyzes the covalent attachment of ubiquitin moieties onto substrate proteins destined for proteasomal degradation. The substrates of parkin-mediated ubiquitination have yet to be completely identified. Using a yeast two-hybrid screen, we isolated the septin, human SEPT5_v2 (also known as cell division control-related protein 2), as a putative parkin-binding protein. SEPT5_v2 is highly homologous to another septin, SEPT5, which was recently identified as a target for parkin-mediated ubiquitination. SEPT5_v2 binds to parkin at the amino terminus and in the ring finger domains. Several lines of evidence have validated the putative link between parkin and SEPT5_v2. Parkin co-precipitates with SEPT5_v2 from human substantia nigra lysates. Parkin ubiquitinates SEPT5_v2 in vitro, and both SEPT5_v1 and SEPT5_v2 accumulate in brains of patients with ARJP, suggesting that parkin is essential for the normal metabolism of these proteins. These findings suggest that an important relationship exists between parkin and septins.

Theme: Disorders of the nervous system

Topic: Degenerative disease: Parkinson's

Keywords: Ubiquitination; Parkinson's disease; Lewy body; Ubiquitin proteasomal system; Autosomal recessive juvenile Parkinsonism; Substantia nigra; Dopamine; Dopaminergic neuron

1. Introduction

Parkinson's disease (PD) is the most common neurodegenerative movement disorder [21]. It is characterized by a classic group of symptoms: rigidity, resting state tremor, bradykinesia, and postural instability. Death of dopaminergic neurons in the substantia nigra with resultant severe dopamine depletion in the neostriatum is believed to underlie the motor symptoms of PD [21]. The cause of this neuronal degeneration is unknown. Recently, several genes have been identified to be associated with familial parkinsonism: α-synuclein, ubiquitin carboxy-terminal hydrolase L1 (UCH-L1), DJ-1, Nurr1 and parkin [3,10,18,20,22,25,29]. Mutations in α-synuclein (A53T and A30P) are associated with rare cases of autosomal dominant parkinsonism [20,29]. An I93M missense mutation in the ubiquitin C-terminal hydrolase, UCH-L1, a thiol protease deubiquitinating enzyme, has been identified in a German family with a history of familial PD [23]. Mutations in

Abbreviations: ARJP, autosomal recessive Juvenile Parkinsonism; PD, Parkinson's disease; SEPT5, cdc-rel1, cell division control-related protein 1; SEPT5_v2, SEPT5_v2, cell division control-related protein 2; UbcH, ubiquitin conjugating enzyme

*Corresponding author. Tel.: +1-708-216-6195; fax: +1-708-216-6596.
E-mail address: bwolozi@lumc.edu (B. Wolozin).
[1]Co-equal authors.

0169-328X/03/$ – see front matter
doi:10.1016/S0169-328X(03)00318-8

DJ-1 are associated with an early onset, autosomal recessive form of PD, while parkin is associated with autosomal recessive juvenile parkinsonism (ARJP) [3,18]. Mutations in Nurr1, an orphan nuclear receptor that is essential for the development of dopamine neurons, are associated with familial PD [22]. The most common mutations associated with Parkinsonism are mutations in *parkin*, including deletion and point mutations, which occur in many families affected by ARJP. The association of mutations in *parkin* with ARJP implicates *parkin* mutations in the etiology of familial parkinsonism [1,24,25]. In the most comprehensive genetic study to date by Lücking et al., 36 of 73 (49%) families with histories of early onset PD all had mutations in *parkin* that segregated with the disease [25]. In addition, mutations in parkin have also been recently linked to forms of adult-onset parkinsonism clinically indistinguishable from sporadic, non-inherited PD [8,19]. Thus, mutations in *parkin* are by far the most prevalent cause of inherited PD discovered to date.

The parkin structure contains a C-terminal RING-IBR-RING construct and an N-terminal region with homology to ubiquitin [18,31]. Recently, parkin was shown to possess ubiquitin ligase (E3) activity that catalyzes the covalent attachment of ubiquitin onto proteins targeted for degradation by the 26S proteasome [14,31,35]. Ubiquitination of proteins is thought to occur by action of a complex that includes E3 ligases, such as parkin, and ubiquitin conjugating enzymes (termed either UbcH or E2). Nine human UbcH enzymes have been identified to date, and parkin has been shown to associate with UbcH7 and UbcH8, via the RING-IBR-RING domain of parkin. Intense research has focused on identifying proteins that bind parkin and are ubiquitinated by parkin. Several parkin-binding proteins have been identified to date: cell division control-related protein 1, α-synuclein, Pael-R, Synphilin-1 and CHIP [6,13,14,32,36]. SEPT5 is a member of the septin family of proteins, which have roles in exocytosis and cell division [2]. Other septins include Nedd5, H5, Diff6, and SEPT5_v2 [2,17]. Wild-type parkin, but not mutant or truncated forms of parkin, increases SEPT5_v1 turnover in vitro, suggesting a central role of parkin in SEPT5_v1 regulation [36]. Parkin has also been shown to control the turnover of SEPT5_v1 and the Pael receptor (Pael-R) [14,36]. The interaction of parkin with CHIP suggests that it operates in the endoplasmic reticulum as part of the unfolded protein response [13,15]. We now report the identification of another parkin-binding protein, SEPT5_v2. Parkin ubiquitinates SEPT5_v2, and SEPT5_v2 steady state levels are increased in brains of patients with ARJP or in cells lacking parkin.

2. Materials and methods

2.1. Human brain samples

Post-mortem brain tissues were obtained from the Loyola University Chicago Brain Bank and from the Rush University Brain Bank. Paraffin-embedded tissues used for immunohistochemical analyses were treated with 10% buffered formalin. Human substantia nigra sections from PD cases and age-matched, neurologically normal controls were examined in this study. The ages and post-mortem interval of all the brains used are shown in Table 1. The mean ages and PMI of the control brains were 73.5±5.7 years and 7.6±1.8 h, while the means ages and post-mortem interval of the PD brains were 68.4±1.4 years and 7.0±1.1 h.

Paraffin-embedded brain sections were deparaffinized by incubation at 65 °C for 45 min. Sections were subsequently treated with three changes in xylene, 10 min each, then 3 min each in 100% ethanol, 95% ethanol, and 70% ethanol. Sections were then washed for 5 min in ddH_2O, placed in fresh ddH_2O, and autoclaved for 15 min at 121 °C. After slides cooled to room temperature, they were washed in 0.05 M PBS, pH 7.4, for 20 min, blocked in 10% FBS/PBS for 20 min, and incubated at 4 °C overnight in primary antibodies. This was followed by three 10-min washes in PBS, incubation with Cy2- and Cy3-tagged fluorescent antibodies (Jackson Immuno.) for 3 h at room temperature, and three 10-min washes in PBS. Slides were then dehydrated through ethanol, mounted with Depex, and cover-slipped.

2.2. Immunoblotting

For immunoblot analyses, protein gel loading buffer was added to 30 μg of total protein lysate per lane and resolved by 12% polyacrylamide gel electrophoresis. Protein bands were transferred to nitrocellulose matrix (Gibco/BRL) at 4 °C, 250 mA, for 10 h. Following blocking in 5% milk/tris-buffered saline plus 0.01% triton X-100 for 1 h at room temperature, blots were incubated with primary antibody overnight at 4 °C. Blots were then washed three times, 10 min each in tris-buffered saline plus 0.01% triton X-100, and incubated in biotinylated secondary antibody for 3 h at room temperature, washed again, and developed by chemiluminescence (DuPont).

Table 1
Brain samples

Case	PMI	Age	Sex	Diagnosis
1	5	64	M	Control
2	10.5	64	F	Control
3	11	79	F	Control
4	4	87	M	Control
5	5	64	F	PD
6	6	68	M	PD
7	4.5	72	M	PD
8	10	67	F	PD
9	9.5	71	M	PD
10	10	65 (17)		ARJP exon 3 deletion
11	18	62 (24)		ARJP exon 4 deletion
12	9	52 (14)		ARJP exon 4 deletion
13	10	68 (33)		ARJP exon 3 deletion

2.3. Antibodies

Park-1 polyclonal antibody (Southwest Immunology) was raised in goat, against an immunogen that corresponds to amino acids 83–97 of the N-terminus of the human parkin protein. Park-2 polyclonal antibody (Chemicon) was raised in rabbit, against an immunogen that corresponds to amino acids 305–323 of the human parkin protein. Park-3 polyclonal antibody was also raised in rabbit, against an immunogen corresponding to amino acids 391–405 of the parkin protein. Park-4 polyclonal antibody was raised against an epitope around amino acid 400 of parkin (Cell Signaling, no epitope sequence supplied). SP20 is a monoclonal antibody that recognizes SEPT5. Anti-α-actin monoclonal antibody (ICN) was used as an internal loading control in Western blot analyses. The anti-c-Myc antibody 9E10 was from Roche. Dilutions were done in tris-buffered saline plus 0.01% triton X-100+5% bovine serum albumin (Sigma). Dilutions: Park-1—1:300 for immunohistochemistry, and 1:5000 for immunoblotting; Park-2—1:1000 for immunohistochemistry; Park-3—1:500 for immunoblotting, and 1:200 for immunoprecipitation; Park-4—1:1500 for immunoblotting; SP20—1:10 for immunohistochemistry, and 1:100 for immunoblotting; anti-α-actin—1:2000 for immunoblotting; 9E10—1:1000 for immunoblotting, 1:200 for immunoprecipitation.

2.4. Plasmids

Wild-type and mutant parkin were cloned into pcDNA3 at the EcoRI/XbaI sites. Myc-parkin was generated by adding a myc epitope by PCR, and inserted into pcDNA3 at the EcoRI/NotI sites. SEPT5_v2a and myc-SEPT5_v2a were cloned into pcDNA3 at the XhoI/NotI sites. For production of recombinant SEPT5_v2a, the cDNA was also cloned into the proEX vector at the BamHI/SpeI sites, and purified with nickel agarose chromatography. UbcH7 and 8 were cloned into the pET3a vector. HA-Ubiquitin was obtained from Cecile Pickart (Johns Hopkins, Baltimore, MD, USA) and was cloned into the pMT123 vector. The parkin deletion constructs were in pRK5 and designed as described previously [36].

2.5. Cell culture

BE-M17 human neuroblastoma cells were maintained in Optimem (Gibco/BRL)+10% fetal bovine serum. SH-SY5Y human neuroblastoma cells were maintained in a 1:1 mixture of Ham's F12:EMEM (Gibco/BRL)+10% fetal bovine serum. Transfections were performed with Fugene (Roche) with 1 μg DNA+6 μl Fugene per ml in Optimem.

2.6. Immunoprecipitation

For immunoprecipitation experiments, approximately 2×10^6 cells were plated into sterile 10-cm Falcon dishes and grown to ≈80% confluence. Cells were harvested by trituration followed by low-speed centrifugation. Pellets were resuspended in lysis solution consisting of ice-cold 1% Triton-X in Tris-buffered saline, pH 7.4, with protease inhibitors (Sigma) and dismembranated via sonication. Protein concentration was determined by the BCA assay (Pierce). 500 μg of protein from each sample was diluted to a final volume of 1 ml in lysis solution. 25 μl protein A (Sigma) was added to pre-clear non-specific binding proteins, 1 h, 4 °C. Samples were centrifuged and supernatants were transferred to new sterile microcentrifuge tubes. 4 μg of primary antibody were added to each sample, followed by a 3-h shaking incubation at 4 °C. 30 μl protein A were then added to each sample and binding to immune complexes was performed by 2 h incubation at 4 °C with gentle agitation. Negative control consisted of 4 μg non-specific IgG plus control brain lysate and protein A. Samples were washed/centrifuged four times in ice-cold lysis solution. After final washing and centrifugation, samples were resuspended in protein loading buffer, heat denatured at 90 °C for 5 min, centrifuged again, and resolved by 12% polyacrylamide gel electrophoresis, 85 V, 90 min. Immunoblots were performed as detailed above.

2.7. Yeast two-hybrid

Assays were performed according to the manufacturer's protocol, using the Matchmaker (Clontech) LexA system. The cDNA library used for screening bait/prey interactions was derived from human brain, and consisted of 3.5×10^6 independent clones. We performed an interaction trap assay using parkin as the bait. Full-length parkin (465 amino acids; bait A), the amino-terminal 133 amino acids (bait B), the carboxy-terminal 332 amino acids (bait C), and the amino-terminal 257 amino acids (bait D) were cloned into plasmid pEG202 in-frame with the LexA DNA-binding domain. Two different reporter genes were used in the LexA system: one was a yeast Leu2 derivative and the other was the bacterial lacZ gene that encodes β-galactosidase and offers a quantitative method of measuring interactions. The LEU2 reporter is stably incorporated into the yeast strain, and has its normal regulatory sequences replaced by six LexA operator sequences. The lacZ reporter was introduced into the yeast strain on a plasmid (pSH18-34) and is also regulated by multiple upstream LexA operators.

2.8. In vitro ubiquitination

Constructs coding for myc-Parkin or myc-SEPT5_v2a were transfected into 293 cells, and immunoprecipitated from 4 mg of lysates with 4 μl 9E10 antibody and 50 μl of agarose coupled protein G. 7 μl of each immunoprecipitate was mixed with 100 ng E1 (Sigma), 200 ng Ubch7 (Affinity), and 5 μg ubiquitin (Sigma) in 50 μl buffer (50 mM Tris HCl pH 7.5, 10 mM DTT, 2 mM $MgCl_2$ and 4

mM ATP). The mixture was incubated for 1 h and then immunoblotted.

3. Results

3.1. Parkin binds to SEPT5_v2

We utilized the LexA yeast two-hybrid system to screen a human brain cDNA library for binding partners of parkin. We isolated positive clones coding for the septin, SEPT5_v2, in both splice variants, rel2a and rel2b (Fig. 1A, SEPT5_v2A shown). These clones collectively encoded sequences at the N-terminus of rel2a from amino acid 1 to 304, and the N-terminus of rel2b from amino acid 1 to 295, in multiple, in-frame overlapping prey cDNA hybrids, indicating that these amino acids mediate the parkin–SEPT5_v2 association. The amino terminus of

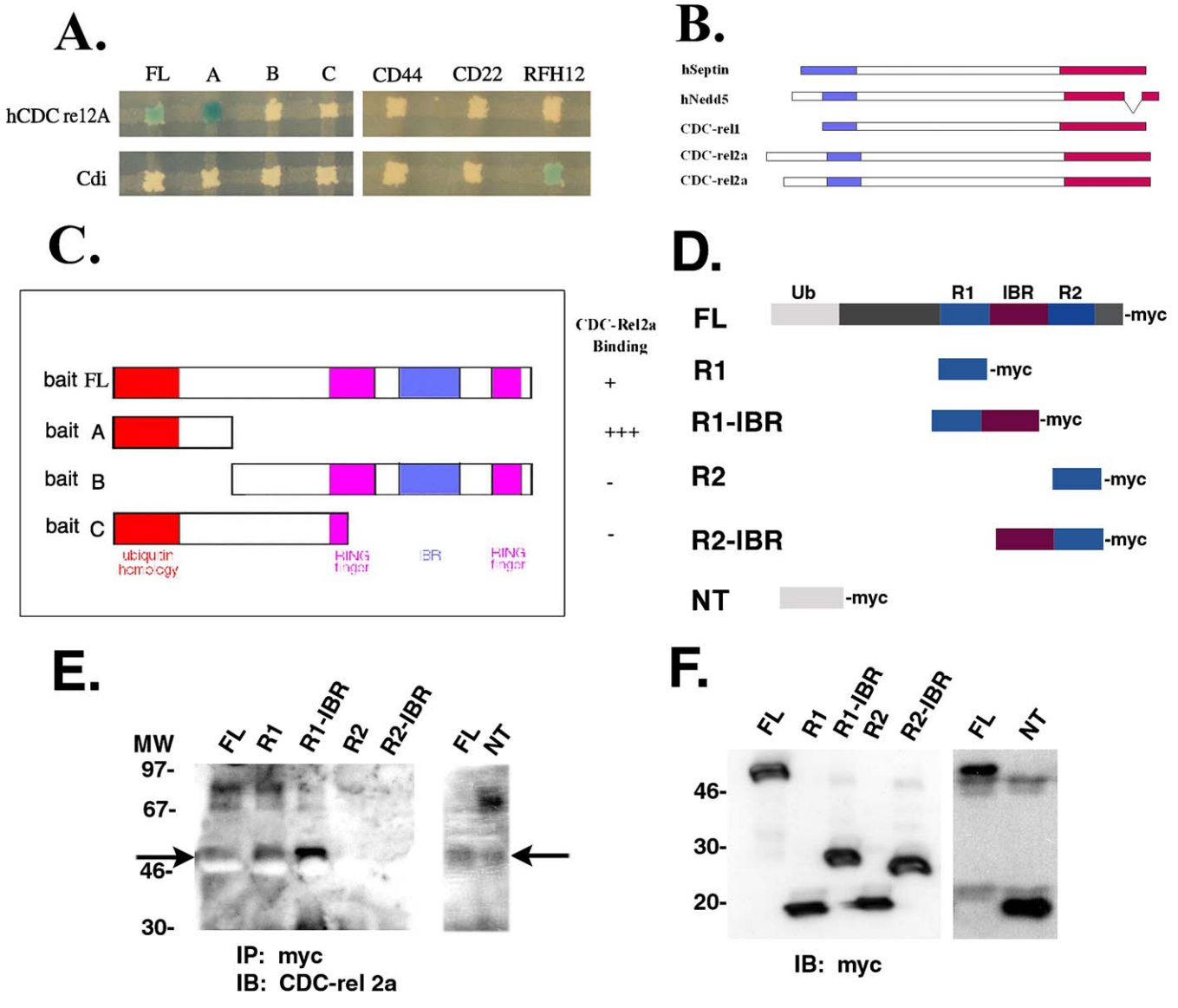

Fig. 1. (A) Yeast mating assay showing interaction between parkin and SEPT5_v2a. Blue represents a positive interaction. CDI is a control that should only interact with the RFH12 protein, thus demonstrating specificity for the assay. FL, full length parkin. (A, B, C) Parkin constructs shown below. CD44, CD22, and RFH12 are constructs that are not expected to interact with parkin, and act as negative controls. (B) Structure of septins. The structures of SEPT5_v2a, SEPT5_v2b, and SEPT5, are shown in relation to some other well-known septins, such as Septin, and Nedd5. Homologous regions are represented by the same color. Adapted from Kartmann and Roth [16]. (C) Structure of yeast parkin-binding constructs, and amount of binding to SEPT5_v2 on the right. (D) Structure of mammalian parkin deletion constructs. Myc-tagged constructs containing full-length parkin (FL), the R1 RING finger domain (R1), the R1 RING finger domain plus the 'In Between RING' finger domain (R1-IBR), the R2 RING finger domain (R2), the R2 RING finger domain plus the 'In Between RING' finger domain (R2-IBR), and the N-terminal ubiquitin homology domain (NT). (E) Co-immunoprecipitation of SEPT5_v2a with myc-tagged parkin deletion constructs. Left panel: SEPT5_v2a (arrow) co-immunoprecipitated with full-length parkin, the R1 RING finger domain and the R1 RING finger domain plus the 'In Between RING' finger domain (R1-IBR). Right panel: SEPT5_v2a (arrow) co-immunoprecipitated with full-length parkin (FL), the N-terminal ubiquitin domain (NT). (F) Immunoblots validating expression of the parkin deletion constructs in the HEK 293 cell lysates used for the immunoprecipitation in (E).

SEPT5_v2 shows minimal homology to other septins, including SEPT5_v1 (Fig. 1B). SEPT5_v2a and b are splice variants, with SEPT5_v2b lacking the first 19 amino acids of SEPT5_v2a (Fig. 1B). Interestingly, in the case of SEPT5, it is the carboxy terminal of parkin that associates with the carboxy terminal of SEPT5_v1 [36]. All further experiments were performed using the LexA yeast two-hybrid system and SEPT5_v2a as the interacting protein.

To understand better the nature of the interaction between parkin and SEPT5_v2, we generated a construct containing full-length parkin, and constructs of parkin truncated at either the amino or carboxy terminal (Fig. 1C). Yeast two-hybrid mating assays were subsequently performed to map the area of parkin responsible for SEPT5_v2a binding. SEPT5_v2a bound to full-length parkin and an amino terminal construct, but not a construct lacking the amino terminus (Fig. 1A and C). This suggests that the ubiquitin homology portion of parkin interacts with SEPT5_v2. Interestingly, no binding was seen to construct C that contained the amino two-thirds of parkin, possibly because of the altered conformation of this construct or inhibition of binding by downstream domains of parkin (Fig. 1C).

3.2. SEPT5_v2a binds to parkin at two sites in mammalian cells

Previous studies with SEPT5, a close homologue of SEPT5_v2a, showed binding to the carboxy region of parkin [36]. Because of the close homology between the two proteins, we examined the association of SEPT5_v2a with domains of parkin previously shown to bind SEPT5_v1, including the RING-IBR domains (Fig. 1C). Based on the yeast two-hybrid data suggesting binding of SEPT5_v2a to a domain near the amino terminus of parkin, we also designed a construct containing only the amino-terminal ubiquitin homology domain, and examined binding of SEPT5_v2a to this domain (Fig. 1C). HEK 293 cells were co-transfected with constructs coding for SEPT5_v2a and myc-tagged parkin deletion constructs corresponding to the amino or carboxy domains of parkin (Fig. 1D and E) [36]. We observed that SEPT5_v2a bound to full-length parkin, as well as parkin deletion constructs containing either the amino domain of parkin or the R1 RING finger (Fig. 1D and E). Binding of SEPT5_v2a to the R1 RING finger domain is consistent with prior studies showing that SEPT5_v1 binds to the R2 RING finger domain [36]. In addition, we observed that SEPT5_v2a binds to the amino domain of parkin, which contains the ubiquitin homology domain. Binding of SEPT5_v2a to the amino region of parkin concurs with the yeast two-hybrid studies, which also showed binding of this region. This indicates that both SEPT5_v1 and SEPT5_v2a associate with the RING finger domains, with SEPT5_v1 binding to the R2 domain and SEPT5_v2a binding to the R1 domain [36].

Although binding to the amino domain and the R1-IBR-R2 domain of parkin show binding to SEPT5_v2 in both the yeast two-hybrid assay and in mammalian cell immunoprecipitation assay, the two assays differ quantitatively in the amount of binding observed (Fig. 1C and E). One reason for the difference might result from the use of different parkin domains in the yeast two-hybrid study and the immunoprecipitation study. One discrepancy lies in the parkin R1-IBR-R2 domain. A construct containing the parkin R1-IBR-R2 domain showed no association with SEPT5_v2a in the yeast two-hybrid study, while a construct containing only the R1-IBR domain showed strong binding in the immunoprecipitation assay (Fig. 1C and E). The absence of an association in the yeast two-hybrid assay might derive from inhibition of SEPT5_v2 binding to parkin by the R2 domain when it is present. This hypothesis could explain why the immunoprecipitation assay showed no binding to a construct containing only the IBR-R2 domain and weak binding to full-length parkin (Fig. 1C and E). Binding to the parkin amino domain also showed a quantitative difference between the yeast two-hybrid assay and the immunoprecipitation assay. This difference could be due to differences in the size of the two constructs (Fig. 1D and F). The parkin amino domain construct used for the yeast two-hybrid studies was longer than that used for the immunoprecipitation studies (Fig. 1D and F). Binding of SEPT5_v2 close to the junction region between the ubiquitin homology domain and the rest of parkin could render it sensitive to interference from the anti-myc antibody used for the immunoprecipitation assay (Fig. 1C and E). Conversely, the increased length of the amino domain yeast two-hybrid construct might prevent interference with SEPT5_v2 binding.

3.3. SEPT5_v2a binds to parkin in human brain lysates

To validate our yeast two-hybrid analysis results, we investigated whether parkin interacts with SEPT5_v2 in human brain. SEPT5_v2a co-precipitated with parkin from human substantia nigra lysates (Fig. 2). Sepharose-coupled anti-parkin antibody P391 was used to immunoprecipitate parkin, and the immunoprecipitate was then immunoblotted with anti-SEPT5_v2a (Fig. 2, upper panel). As a negative control, the lysates were immunoprecipitated with sepharose coupled to non-specific IgG (Fig. 2, upper panel, lane 7). Nigral lysates from both control (Fig. 2, lanes 1–3) and PD (Fig. 2, lanes 4–6) cases were used in the immunoprecipitations to examine whether disease-associated differences in parkin-SEPT5_v2 binding exist. Immunoprecipitation revealed a single band migrating at the expected molecular weight of 52 kDa (Fig. 2). Although significant enrichment of SEPT5_v2a was observed by immunoprecipitation of parkin, indicative of high-affinity binding, there was no significant difference in the amount of co-precipitated rel2a between PD and control brains (Fig. 2). The amount of SEPT5_v2a in the lysates was also immunoblotted (Fig. 2, lower panel). The PD nigral lysates showed a trend toward greater SEPT5_v2a levels in PD than control lysates, but this difference did not reach

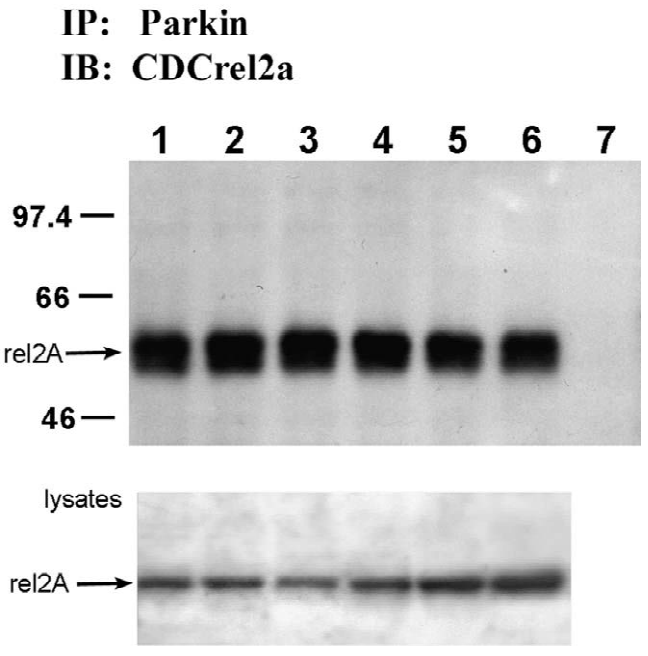

Fig. 2. Co-precipitation of SEPT5_v2a along with parkin from substantia nigra lysates. Sepharose-coupled anti-parkin antibody P391 was used to immunoprecipitate parkin. Immunoblotting the precipitate with the anti-SEPT5_v2a antibody revealed one band at 52 kDa, which is the expected molecular weight of SEPT5_v2a. The top panel shows the immunoprecipitate, while the bottom panel shows an immunoblot of the lysates with anti-SEPT5_v2a. Lanes 1–3 correspond to substantia nigra from three different control donors. Lanes 4–6 correspond to substantia nigra from three different PD donors. Lane 7 is an immunoprecipitation using non-specific rabbit IgG.

statistical significance ($P<0.1$, $N=9$ PD, 10 Control). Immunocytochemical experiments failed to detect any SEPT5_v2a in Lewy bodies (data not shown). The co-immunoprecipitation of parkin and SEPT5_v2a indicates that parkin associates with SEPT5_v2a in human brain tissue, and validates the yeast two-hybrid results.

3.4. Parkin levels affect levels of SEPT5_v2a

The association of SEPT5_v2a with parkin raises the possibility that the degradation of SEPT5_v2a is mediated by parkin. To investigate this, HEK 293 cells were transfected with plasmids coding for sense or anti-sense parkin plus SEPT5_v2a, HA-tagged ubiquitin and UbcH8. Three days following transfection, the cells were incubated with MG132 for 4 h to block proteasomal degradation. The cells were lysed, and centrifuged to separate soluble and insoluble material. Levels of SEPT5_v2a in both the pellet and supernatant were observed to vary with parkin levels. Cell pellets were immunoblotted with antibodies against HA (identifying ubiquitin), SEPT5_v2a, parkin or actin (Fig. 3A and B). Parkin expression was high in cells transfected with parkin cDNA and low in cells transfected with parkin anti-sense cDNA (Fig. 3A, bottom left panel). HA-ubiquitin immunoreactivity paralleled parkin expression (Fig. 3A, top left panel). The level of SEPT5_v2a was inversely related to parkin expression, and was low in cells transfected with parkin cDNA and high in cells transfected with parkin anti-sense cDNA (Fig. 3B, left panel). Finally, immunoblotting with anti-actin antibody showed that protein expression was similar in each lane (Fig. 3B, right panel).

3.5. Parkin ubiquitinates SEPT5_v2a

Next we examined whether SEPT5_v2a was ubiquitinated by parkin. To determine whether parkin was able to ubiquitinate SEPT5_v2a, we used an in vitro ubiquitination assay, similar to that used for the analysis of ubiquitination of Pael-R [14]. For the in vitro ubiquitination assay, HEK 293 cells were transfected cells with either myc-SEPT5_v2a or myc-parkin. After 48 h, the cells were harvested, and the myc-tagged proteins (SEPT5_v2a or parkin) were immunoprecipitated from the lysates. The parkin and SEPT5_v2a were then combined together along with recombinant UbcH8 and HA-ubiquitin, as well as ATP and buffer. Following 1 h of incubation, the mixture was immunoblotted with either anti-ubiquitin to detect ubiquitinated proteins or anti-SEPT5_v2a. SEPT5_v2a that had been incubated with parkin showed the presence of higher molecular weight bands, suggesting that it had been ubiquitinated. The anti-ubiquitin immunoblot showed increased levels of high molecular weight ubiquitin conjugates in lanes containing the SEPT5_v2a (Fig. 4A). Omission of parkin eliminated the high molecular weight bands seen with the SEPT5_v2a or ubiquitin antibodies, and omission of SEPT5_v2a eliminated all reactivity seen with anti-SEPT5_v2a and reduced the high molecular weight ubiquitin conjugated proteins. Omission of SEPT5_v2a would not have been expected to eliminate the high molecular weight ubiquitin proteins because parkin auto-ubiquitinates. In a parallel experiment, we performed in vitro ubiquitination and immunoblotted with antibody to SEPT5_v2a. High molecular weight bands were apparent only in the lanes containing SEPT5_v2a, parkin and other requisite reagents (Fig. 4B). Omission of SEPT5_v2a, parkin, Ubch8, or ubiquitin+E1 eliminated the bands. Quantification of the in vitro ubiquitination reactions is shown in Fig. 4C and D. These data suggest that parkin can ubiquitinate SEPT5_v2a.

3.6. Levels of SEPT5_v1 and SEPT5_v2a are increased in brains from patients with ARJP

The ability of parkin to modulate the ubiquitination and turnover of SEPT5_v2a in cell culture suggests that parkin might also regulate turnover of SEPT5_v2a in the brain. To investigate this question, we examined the levels of SEPT5_v2a in brains of patients who died with ARJP. Lysates were obtained from frontal cortex of ARJP brains ($N=4$), and age-matched control brains ($N=5$). Frontal

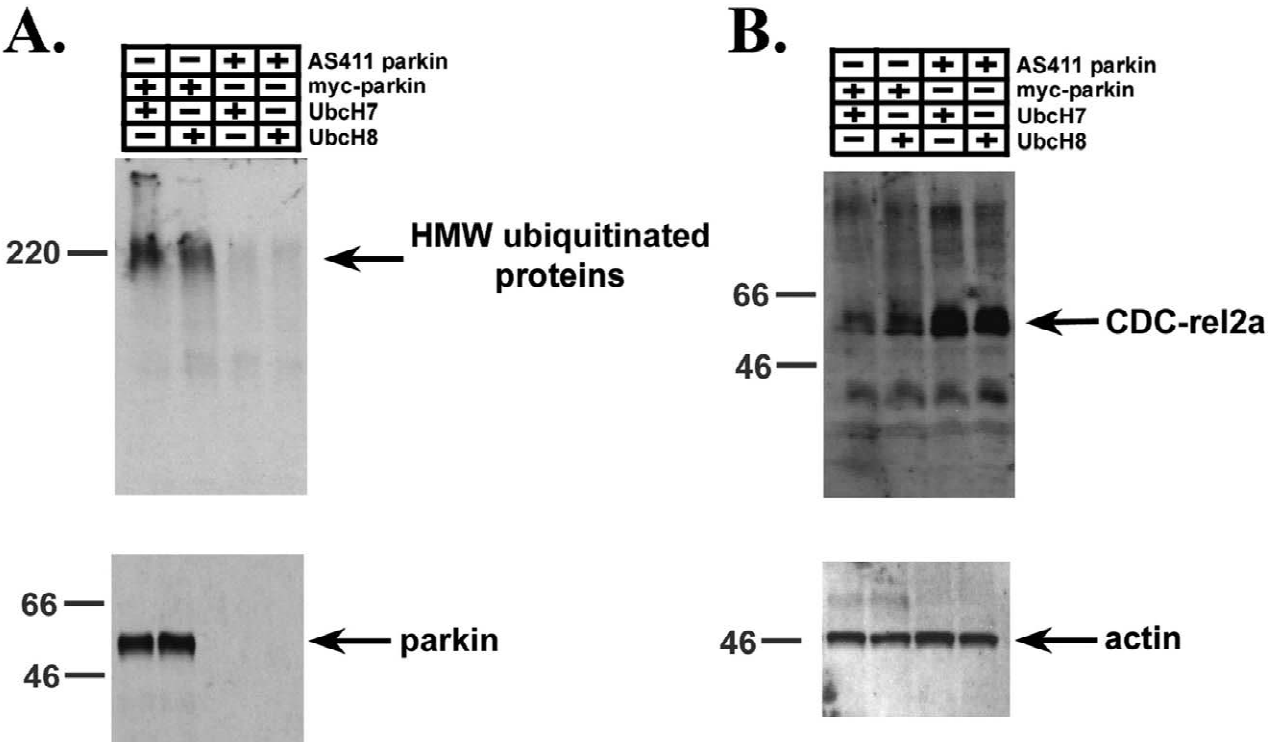

Fig. 3. (A, B) HEK 293 cells were transfected with SEPT5_v2a, parkin (sense or antisense), HA-ubiquitin and UbcH8. Two days after transfection, the cells were harvested and the lysates immunoblotted. (A) The top panel shows immunoblotting with anti-HA (recognizing ubiquitin), and the bottom panel shows immunoblotting with anti-parkin. Ubiquitination paralleled parkin expression. (B) In the same samples, immunoblots were performed with anti-SEPT5_v2a (top panel) and actin (bottom panel). Although the amount of protein did not vary, decreased parkin expression corresponded to increased SEPT5_v2a expression.

cortex was used because of the limited availability of substantia nigra from ARJP. We felt that analysis of cortical tissue in ARJP might be informative because parkin is expressed throughout the brain. Based on this distribution, loss of parkin might be expected to affect areas other than the substantia nigra, even though pathology (in the form of cell loss) is most severe in the substantia nigra. Consistent with this hypothesis, we observed that the levels of SEPT5_v2a were increased in brains from ARJP donors, although no change was seen in levels of actin (Fig. 5, top panel). Because SEPT5_v1 has also been shown to associate with parkin, we examined whether levels of SEPT5_v1 protein were increased in ARJP brain. We observed that SEPT5_v1 was also increased in three out of four cases of ARJP brain that were examined (Fig. 5, middle panel). No significant differences in actin were observed among the samples (Fig. 5, lower panel). These data suggest that parkin regulates the turnover of both SEPT5_v1 and SEPT5_v2a in vivo.

4. Discussion

Parkin is an E3 ligase, but its substrates are only beginning to be identified. Recently, SEPT5_v1 was shown to bind parkin and have its catabolism regulated by parkin [36]. The protein SEPT5_v2a is a member of the septin family of proteins, and is a close homologue of SEPT5_v1 [9]. We have now shown that parkin also binds SEPT5_v2a, ubiquitinates SEPT5_v2a, and can modulate the levels of SEPT5_v2a in cells. We also observe that levels of both SEPT5_v1 and SEPT5_v2a are increased in the brains of patients with ARJP. Septins are small proteins that can have GTPase activity and appear to function in membrane transport and exocytosis [2,9,26]. The ability of parkin to bind both SEPT5_v1 and SEPT5_v2 suggests a biochemical link between septins and parkin, although the functional consequences of the putative interaction between parkin and SEPT5_v1 proteins remain to be determined.

4.1. Parkin binds to specific domains on SEPT5_v2

Parkin appears to bind SEPT5_v2a at two different regions within the protein, the N-terminal ubiquitin-homology domain and the R1 RING finger domain. The RING finger domains appear to be important for binding and ubiquitination of ligase substrates. For instance, SEPT5, Synphilin-1 and Pael-R bind the R2 RING finger domain, and Tau all bind the R2-IBR domain [6,14,27,36]. In our experiments, we observed different binding patterns depending on whether we examined binding by yeast two-

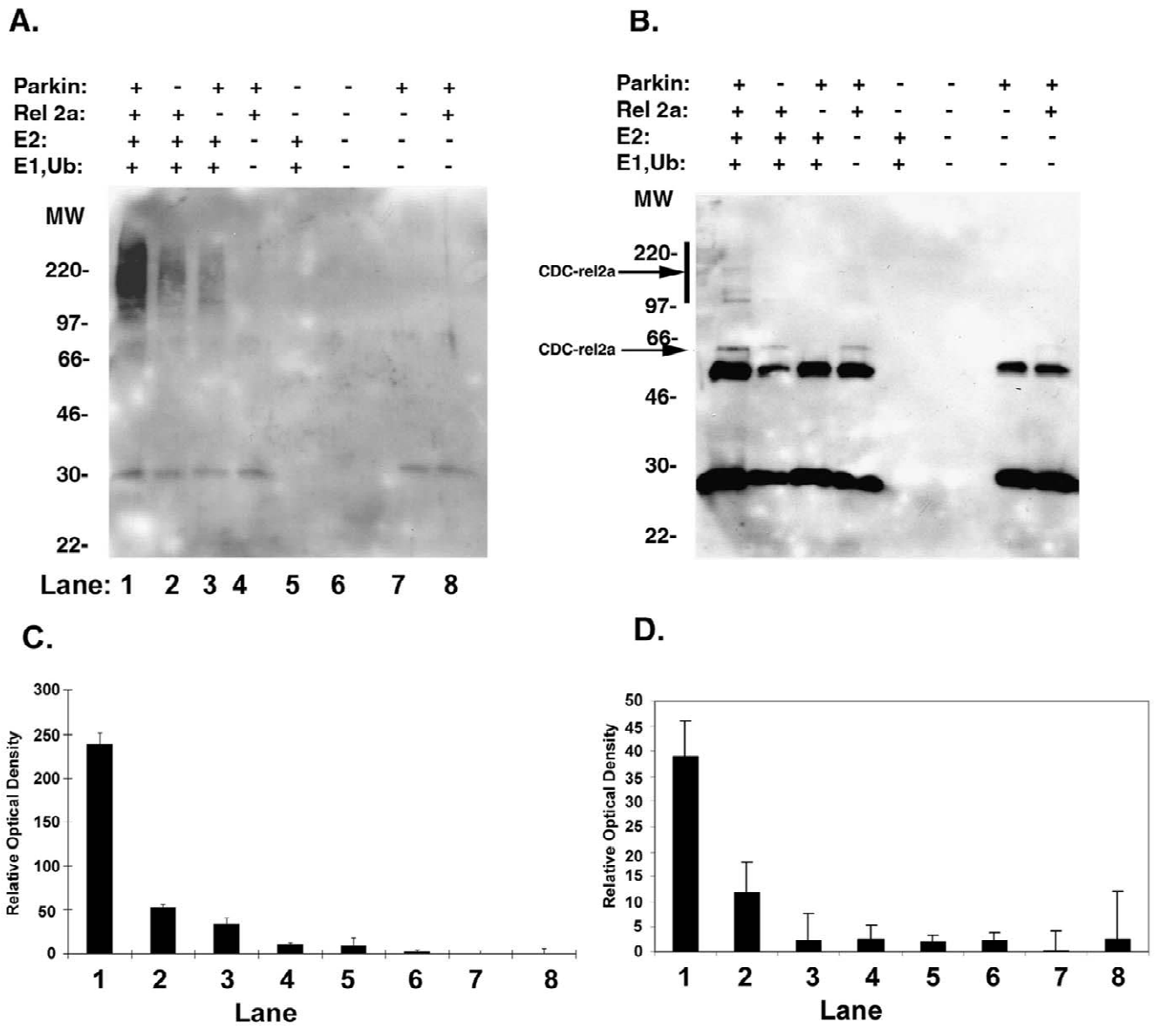

Fig. 4. In vitro ubiquitination of SEPT5_v2a by parkin. HEK cells were transfected with either myc-tagged SEPT5_v2a or myc-tagged parkin. The SEPT5_v2a and parkin were immunoprecipitated, combined, an in vitro ubiquitination was performed and the product was immunoblotted for anti-ubiquitin (A) or anti-SEPT5_v2a (B). High molecular weight bands positive for both ubiquitin and SEPT5_v2a were present in samples of SEPT5_v2a that had been co-transfected with parkin, suggesting that parkin lead to ubiquitination of SEPT5_v2a. Omission of any of the reaction components eliminated the ubiquitination. The prominent bands at 25 and 50 kDa represent the heavy and light chains of the anti-myc antibody used to immunoprecipitate the parkin and SEPT5_v2a proteins. Quantification of the in vitro ubiquitination for both ubiquitin reactivity and high molecular weight SEPT5_v2a reactivity is shown in panels (C) and (D), respectively ($n=3$).

hybrid analysis or by immunoprecipitation from mammalian cells. Binding in the yeast occurs only with the full-length construct or a construct containing only the N-terminal ubiquitin binding domain. Binding in mammalian cells is detected with constructs coding for either the N-terminal ubiquitin binding domain or constructs containing the RING1-IBR domain. Because other parkin substrates bind to the RING-IBR domains, the immunoprecipitation experiments appear more likely to reflect the true association that occurs in mammals. Several studies show that the RING-IBR-RING domain is required for ubiquitin ligase activity, which suggests that binding of SEPT5_v2 to this region is important for the ability of parkin to ubiquitinate the protein [36].

The N-terminal ubiquitin homology domains of ligases are important for the binding of ligases to other proteins in the ubiquitin proteasomal cascade. For instance, the ubiquitin homology domain is important for binding of ligases to proteasomal proteins [33]. The N-terminal ubiquitin homology domain of parkin also appears to be required for parkin function because mutations in this domain block the ubiquitin ligase activity of parkin, and

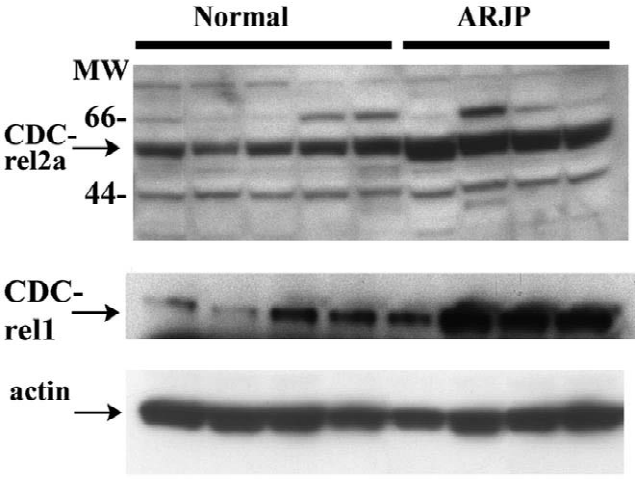

Fig. 5. Levels of SEPT5_v1 and SEPT5_v2 are increased in brains of patients with ARJP. Samples of cortex from cases of ARJP and age-matched controls were immunoblotted with anti-SEPT5_v2a (top panel), SP20 (middle panel), or anti-actin (bottom panel). Although the levels of actin were constant among the samples, the levels of SEPT5_v1 and 2a were increased in the ARJP brains.

are associated with ARJP [1,31,36]. By binding to the ubiquitin homology domain of parkin, SEPT5_v2a could modulate the association of parkin with other proteins or cellular organelles, such as the proteasome.

4.2. Parkin and disease

One of the critical tests of whether a protein is a substrate of parkin is determining whether loss of parkin function increases the steady state level of the protein. The levels of several parkin substrates, including glycosylated α-synuclein, synphilin-1 and Pael-R, are all increased in brains from ARJP donors [6,14,32]. We observed a similar phenomenon for both SEPT5_v1 and SEPT5_v2. Brains from subjects with ARJP show increased levels of SEPT5_v1 and SEPT5_v2 compared to controls, although SEPT5_v1 was increased in only three out of four ARJP brains examined. Unfortunately, insufficient knowledge is available to determine how elevated levels of SEPT5_v1 and SEPT5_v2 might contribute to the pathophysiology of ARJP.

Although mutations in parkin are associated with ARJP, parkin also appears to contribute to the pathophysiology of PD. Some parkin mutations are also associated with familial forms of PD that are indistinguishable from sporadic PD [1]. In addition, parkin accumulates in Lewy bodies [4,5,30]. The mechanism by which parkin accumulates in Lewy bodies is unknown, but could derive from the association of parkin with other proteins that accumulate in Lewy bodies. Shimura and colleagues observed that parkin associates with α-synuclein, but they observed that parkin only binds and ubiquitinates a glycosylated form of α-synuclein that represents only about 1% of the total α-synuclein pool [32]. Parkin also binds to other proteins that are present in LB, such as synphilin and cytochrome *c* [7,11]. Synphilin was recently shown to also bind and be a substrate for parkin [6]. Binding of parkin to α-synuclein and synphilin raises the possibility that parkin might appear in Lewy bodies due to its binding to synuclein and synphilin. In this context, it is interesting that we did not detect SEPT5_v2a in Lewy bodies (data not shown). The reason for the absence of SEPT5_v2a in Lewy bodies could simply result from antibodies that are not sufficiently sensitive to detect the protein in Lewy bodies. A recent study by Ihara and colleagues did identify septins in Lewy bodies [12]. This observation is consistent with a previous study showing the association of septins with inclusions in neurodegenerative diseases, because prior studies have identified the septins Nedd5, diff6 and H5 in neurofibrillary tangles in Alzheimer's disease [17]. These observations add septins to the list of proteins affected by the pathophysiology of PD.

Increasing evidence suggests that parkin might serve a neuroprotective function in the brain. As an ubiquitin ligase, parkin could promote the degradation of proteins that have been damaged by oxidation or other events that might denature the proteins. Studies show that parkin associates with a multi-protein complex that handles such denatured proteins [15]. Other studies show that over-expressing parkin protects against toxicity induced by α-synuclein in cell culture or in Drosophila [28,34]. Parkin also suppresses the toxicity of the Pael receptor, which is toxic when over-expressed and is present in elevated levels in subjects with ARJP [14,34]. The ability of septins to associate with particular vesicles suggests that they could function to target parkin to particular organelles, which could be important for controlling the proteins with which parkin associates [2]. Although we do not know whether SEPT5_v2 modulates parkin-mediated neuroprotection, the importance of parkin in neuroprotection suggests that this is an important line for further investigation.

References

[1] N. Abbas, C. Lücking, S. Ricard, A. Dürr, V. Bonifati, G. De Michele, S. Bouley, J. Vaughan, T. Gasser, R. Marconi, E. Broussolle, C. Brefel-Courbon, B. Harhangi, B. Oostra, E. Fabrizio, G. Böhme, L. Pradier, N. Wood, A. Filla, G. Meco, P. Denefle, Y. Agid, A. Brice, A wide variety of mutations in the parkin gene are responsible for autosomal recessive parkinsonism in Europe, Hum. Mol. Genet. 8 (1999) 567–574.

[2] C.L. Beites, H. Xie, R. Bowser, W.S. Trimble, The septin CDCrel-1 binds syntaxin and inhibits exocytosis, Nat. Neurosci. 2 (1999) 434–439.

[3] V. Bonifati, P. Rizzu, M.J. van Baren, O. Schaap, G.J. Breedveld, E. Krieger, M.C. Dekker, F. Squitieri, P. Ibanez, M. Joosse, J.W. van Dongen, N. Vanacore, J.C. van Swieten, A. Brice, G. Meco, C.M. van Duijn, B.A. Oostra, P. Heutink, Mutations in the DJ-1 gene associated with autosomal recessive early-onset parkinsonism, Science 299 (2003) 256–259.

[4] P. Choi, N. Golts, H. Snyder, L. Petrucelli, M. Chong, J. Hardy, D.

Sparkman, E. Cochran, J. Lee, B. Wolozin, Co-association of parkin and α-synuclein, NeuroReport 12 (2001) 2839–2844.
[5] P. Choi, N. Ostrerova-Golts, D. Sparkman, E. Cochran, J. Lee, B. Wolozin, Parkin is metabolized by the ubiquitin/proteosomal system, NeuroReport 11 (2000) 2635–2638.
[6] K. Chung, Y. Zhang, K. Lim, Y. Tanaka, H. Huang, J. Gao, C. Ross, V. Dawson, T. Dawson, Parkin ubiquitinates the α-synuclein-interacting protein, Synphilin-1: implications for Lewy body formation in Parkinson's disease, Nature Med. 7 (2001) 1144–1150.
[7] S. Engelender, Z. Kaminsky, X. Guo, A. Sharp, R. Amaravi, J. Kleiderlein, R. Margolis, J. Troncoso, A. Lanahan, P. Worley, V. Dawson, T. Dawson, C. Ross, Synphilin-1 associates with alpha-synuclein and promotes the formation of cytosolic inclusions, Nat. Genet. 22 (1999) 110–114.
[8] M. Farrer, P. Chan, R. Chen, L. Tan, S. Lincoln, D. Hernandez, L. Forno, K. Gwinn-Hardy, L. Petrucelli, J. Hussey, A. Singleton, C. Tanner, J. Hardy, J.W. Langston, Lewy bodies and parkinsonism in families with parkin mutations, Ann. Neurol. 50 (2001) 293–300.
[9] C.M. Field, D. Kellogg, Septins: cytoskeletal polymers or signalling GTPases?, Trends Cell Biol. 9 (1999) 387–394.
[10] B.S. Harhangi, M.J. Farrer, S. Lincoln, V. Bonifati, G. Meco, G. De Michele, A. Brice, A. Durr, M. Martinez, T. Gasser, B. Bereznai, J.R. Vaughan, N.W. Wood, J. Hardy, B.A. Oostra, M.M. Breteler, The Ile93Met mutation in the ubiquitin carboxy-terminal-hydrolase-L1 gene is not observed in European cases with familial Parkinson's disease, Neurosci. Lett. 270 (1999) 1–4.
[11] M. Hashimoto, A. Takeda, L. Hsu, T. Takenouchi, E. Masliah, Role of cytochrome *c* as a stimulator of α-synuclein aggregation in Lewy body disease, J. Biol. Chem. 274 (1999) 28849–28852.
[12] M. Ihara, H. Tomimoto, H. Kitayama, Y. Morioka, I. Akiguchi, H. Shibasaki, M. Noda, M. Kinoshita, Association of the cytoskeletal GTP-binding protein Sept4/H5 with cytoplasmic inclusions found in Parkinson's disease and other synucleinopathies, J. Biol. Chem. (2003).
[13] Y. Imai, M. Soda, S. Hatakeyama, T. Akagi, T. Hashikawa, K.I. Nakayama, R. Takahashi, CHIP is associated with Parkin, a gene responsible for familial Parkinson's disease, and enhances its ubiquitin ligase activity, Mol. Cell 10 (2002) 55–67.
[14] Y. Imai, M. Soda, H. Inoue, N. Hattori, Y. Mizuno, Y. Takahashi, An unfolded putative transmembrane polypeptide, which can lead to endoplasmic reticulum stress, is a substrate of parkin, Cell 105 (2001) 891–902.
[15] Y. Imai, M. Soda, R. Takahashi, Parkin suppresses unfolded protein stress-induced cell death through its E3 ubiquitin-protein ligase activity, J. Biol. Chem. 275 (2000) 35661–35664.
[16] B. Kartmann, D. Roth, Novel roles for mammalian septins: from vesicle trafficking to oncogenesis, J. Cell Sci. 114 (2001) 839–844.
[17] A. Kinoshita, M. Kinoshita, H. Akiyama, H. Tomimoto, I. Akiguchi, S. Kumar, M. Noda, J. Kimura, Identification of septins in neurofibrillary tangles in Alzheimer's disease, Am. J. Pathol. 153 (1998) 1551–1560.
[18] T. Kitada, S. Asakawa, N. Hattori, H. Matsumine, Y. Yamamura, S. Minoshima, M. Yokochi, Y. Mizuno, N. Shimizu, Mutations in the parkin gene cause autosomal recessive juvenile parkinsonism, Nature 392 (1998) 605–608.
[19] C. Klein, P.P. Pramstaller, B. Kis, C.C. Page, M. Kann, J. Leung, H. Woodward, C.C. Castellan, M. Scherer, P. Vieregge, X.O. Breakefield, P.L. Kramer, L.J. Ozelius, Parkin deletions in a family with adult-onset, tremor-dominant parkinsonism: expanding the phenotype, Ann. Neurol. 48 (2000) 65–71.
[20] R. Kruger, W. Kuhn, T. Muller, D. Woitalla, M. Graeber, S. Kosel, H. Przuntek, J. Epplen, L. Schols, O. Riess, Ala30Pro mutation in the gene encoding α-synuclein in Parkinson's disease, Nat. Genet. 18 (1998) 106–108.
[21] A. Lang, A. Lozano, Parkinson's disease, New Engl. J. Med. 339 (1998) 1044–1053.
[22] W.D. Le, P. Xu, J. Jankovic, H. Jiang, S.H. Appel, R.G. Smith, D.K. Vassilatis, Mutations in NR4A2 associated with familial Parkinson disease, Nat. Genet. 33 (2003) 85–89.
[23] E. Leroy, R. Boyer, G. Auburger, B. Leube, G. Ulm, E. Mezey, G. Harta, M. Brownstein, S. Jonnalagada, T. Chernova, A. Dehejia, C. Lavedan, T. Gasser, P. Steinbach, K. Wilkinson, M. Polymeropoulos, The ubiquitin pathway in Parkinson's disease, Nature 395 (1998) 451–452.
[24] C.B. Lucking, N. Abbas, A. Durr, V. Bonifati, A. Bonnet, T. de Broucker, G. De Michele, N.W. Wood, Y. Agid, A. Brice, Homozygous deletions in parkin gene in European and North African families with autosomal recessive juvenile parkinsonism, Lancet 352 (1999) 1355–1356.
[25] C.B. Lucking, A. Durr, V. Bonifati, J. Vaughan, G. De Michele, T. Gasser, B.S. Harhangi, P. Pollak, A.M. Bonnet, D. Nichol, M. DeMari, R. Marconi, E. Broussolle, O. Rascol, M. Rosier, I. Arnould, B.A. Oostr, M. Breteler, A. Filla, G. Meco, P. Denefle, N.W. Wood, Y. Agid, A. Brice, Association between early-onset parkinson's disease and mutations in the parkin gene, New Engl. J. Med. 342 (2000) 1560–1567.
[26] I.G. Macara, R. Baldarelli, C.M. Field, M. Glotzer, Y. Hayashi, S.C. Hsu, M.B. Kennedy, M. Kinoshita, M. Longtine, C. Low, L.J. Maltais, L. McKenzie, T.J. Mitchison, T. Nishikawa, M. Noda, E.M. Petty, M. Peifer, J.R. Pringle, P.J. Robinson, D. Roth, S.E. Russell, H. Stuhlmann, M. Tanaka, T. Tanaka, W.S. Trimble, J. Ware, N.J. Zeleznik-Le, B. Zieger, Mammalian septins nomenclature, Mol. Biol. Cell 13 (2002) 4111–4113.
[27] L. Petrucelli, K. Kehoe, Y. Tsuboi, T. Ishizawa, D. Dickson, R. Ved, J. Lewis, E. McGowan, G. Gonzalez-de-Chavez, P. Lockhart, C. O'Farrell, D. Hernandez, M. Van Slegtenhorst, M. Cookson, J. Lee, E. Cochran, P. Choi, M. Farrer, N. Hattori, Y. Mizuno, K. Chung, K. Lim, Y. Zhang, T. Dawson, J. Hardy, M. Hutton, B. Wolozin, Tau is a target for the E3 ligase activity of CHIP and parkin (submitted for publication).
[28] L. Petrucelli, C. O'Farrell, P.J. Lockhart, M. Baptista, K. Kehoe, L. Vink, P. Choi, B. Wolozin, M. Farrer, J. Hardy, M.R. Cookson, Parkin protects against the toxicity associated with mutant alpha-synuclein: proteasome dysfunction selectively affects catecholaminergic neurons, Neuron 36 (2002) 1007–1019.
[29] M.H. Polymeropoulos, C. Lavedan, E. Leroy, S.E. Ide, A. Dehejia, A. Dutra, B. Pike, H. Root, J. Rubenstein, R. Boyer, E.S. Stenroos, S. Chandrasekharappa, A. Athanassiadou, T. Papapetropoulos, W.G. Johnson, A.M. Lazzarini, R.C. Duvoisin, G. Di Iorio, L.I. Golbe, R.L. Nussbaum, Mutation in the alpha-synuclein gene identified in families with Parkinson's disease, Science 276 (1997) 2045–2047.
[30] M.G. Schlossmacher, M.P. Frosch, W.P. Gai, M. Medina, N. Sharma, L. Forno, T. Ochiishi, H. Shimura, R. Sharon, N. Hattori, J.W. Langston, Y. Mizuno, B.T. Hyman, D.J. Selkoe, K.S. Kosik, Parkin localizes to the lewy bodies of Parkinson disease and dementia with lewy bodies, Am. J. Pathol. 160 (2002) 1655–1667.
[31] H. Shimura, N. Hattori, S. Kubo, Y. Mizuno, S. Asakawa, S. Minoshima, N. Shimizu, K. Iwai, T. Chiba, K. Tanaka, T. Suzuki, Familial parkinson disease gene product, parkin, is a ubiquitin-protein ligase, Nat. Genet. 25 (2000) 302–305.
[32] H. Shimura, M.G. Schlossmacher, N. Hattori, M.P. Frosch, A. Trockenbacher, R. Schneider, Y. Mizuno, K.S. Kosik, D.J. Selkoe, Ubiquitination of a new form of alpha-synuclein by parkin from human brain: implications for Parkinson's disease, Science 293 (2001) 263–269.
[33] K.J. Walters, M.F. Kleijnen, A.M. Goh, G. Wagner, P.M. Howley, Structural studies of the interaction between ubiquitin family proteins and proteasome subunit S5a, Biochemistry 41 (2002) 1767–1777.
[34] Y. Yang, I. Nishimura, Y. Imai, R. Takahashi, B. Lu, Parkin suppresses dopaminergic neuron-selective neurotoxicity induced by Pael-R in Drosophila, Neuron 37 (2003) 911–924.
[35] D.M. Zhang, D. Levitan, G. Yu, M. Nishimura, F. Chen, A. Tandon, T. Kawarai, S. Arawaka, A. Supala, Y.Q. Song, E. Rogaeva, Y.

Liang, E. Holmes, P. Milman, C. Sato, L. Zhang, P. St George-Hyslop, Mutation of the conserved N-terminal cysteine (Cys92) of human presenilin 1 causes increased A beta42 secretion in mammalian cells but impaired Notch/lin-12 signalling in *C. elegans*, Neuroreport 11 (2000) 3227–3230.

[36] Y. Zhang, J. Gao, K.K. Chung, H. Huang, V.L. Dawson, T.M. Dawson, Parkin functions as an E2-dependent ubiquitin-protein ligase and promotes the degradation of the synaptic vesicle-associated protein, CDCrel-1, Proc. Natl. Acad. Sci. USA 97 (2000) 13354–13359.

Human Molecular Genetics, 2004, Vol. 13, No. 7 ***703–714***
DOI: 10.1093/hmg/ddh083
Advance Access published on February 12, 2004

CHIP and Hsp70 regulate tau ubiquitination, degradation and aggregation

Leonard Petrucelli[1], Dennis Dickson[1], Kathryn Kehoe[1], Julie Taylor[1], Heather Snyder[2], Andrew Grover[1], Michael De Lucia[1], Eileen McGowan[1], Jada Lewis[1], Guy Prihar[1], Jungsu Kim[1], Wolfgang H. Dillmann[3], Susan E. Browne[4], Alexis Hall[5], Richard Voellmy[5], Yoshio Tsuboi[6], Ted M. Dawson[7,8,9], Benjamin Wolozin[2], John Hardy[10] and Mike Hutton[1,*]

[1]Mayo Clinic, Jacksonville, FL 32224, USA, [2]Loyola University School of Medicine, Department of Pharmacology, Maywood, IL 60153, USA, [3]University of California, Department of Medicine, La Jolla, CA, USA, [4]Weill Medical College of Cornell University, New York, NY 10021, USA, [5]University of Miami School of Medicine, Miami, FL 33136, USA, [6]Fukuoka University, Department of Internal Medicine, Japan, [7]Institute for Cell Engineering, [8]Department of Neurology, [9]Department of Neuroscience, Johns Hopkins University School of Medicine, Baltimore, MD 21205, USA and [10]National Institutes of Health, Department of Neurogenetics, Bethseda, MD 20892, USA

Received November 17, 2003; Revised and Accepted January 30, 2004

Molecular chaperones, ubiquitin ligases and proteasome impairment have been implicated in several neurodegenerative diseases, including Alzheimer's and Parkinson's disease, which are characterized by accumulation of abnormal protein aggregates (e.g. tau and α-synuclein respectively). Here we report that CHIP, an ubiquitin ligase that interacts directly with Hsp70/90, induces ubiquitination of the microtubule associated protein, tau. CHIP also increases tau aggregation. Consistent with this observation, diverse of tau lesions in human postmortem tissue were found to be immunopositive for CHIP. Conversely, induction of Hsp70 through treatment with either geldanamycin or heat shock factor 1 leads to a decrease in tau steady-state levels and a selective reduction in detergent insoluble tau. Furthermore, 30-month-old mice overexpressing inducible Hsp70 show a significant reduction in tau levels. Together these data demonstrate that the Hsp70/CHIP chaperone system plays an important role in the regulation of tau turnover and the selective elimination of abnormal tau species. Hsp70/CHIP may therefore play an important role in the pathogenesis of tauopathies and also represents a potential therapeutic target.

INTRODUCTION

Neurodegenerative diseases as diverse as Alzheimer's disease (AD) and Parkinson's disease (PD) share an obvious common feature—aggregation and accumulation of abnormal proteins. A large group of these diseases, known as the tauopathies, are characterized by filamentous lesions in neurons and sometimes in glia that are composed of aggregates of hyperphosphorylated microtubule-associated protein tau (tau).

Tau promotes microtubule (MT) assembly, reduces MT instability and plays a role in maintaining neuronal integrity and axonal transport (1,2). Human tau protein is encoded by a single gene on chromosome 17q21 that consists of 16 exons, and central nervous system isoforms are generated by alternative splicing involving 11 of these exons (3–7). Tau is a phosphoprotein, predominantly expressed in neurons, where it is largely localized in axons (8). During the development of tau pathology, tau becomes hyperphosphorylated, detaches from the axonal microtubules and aggregates. The abnormal tau eventually accumulates in filamentous inclusions within neuronal cell bodies and processes. The precise sequence of events and the mechanisms involved in this process are not fully understood, but it is clear that abnormal tau accumulation and aggregation are sufficient to cause neurodegeneration. This in turn leads progressively to the onset of clinical symptoms. The primary tauopathies include Pick's disease (PiD), corticobasal degeneration (CBD), progressive supranuclear palsy (PSP) and frontotemporal dementia and parkinsonism linked to chromosome 17 (FTDP-17). Tau also accumulates in AD, where where the tau neurofibrillary pathology (e.g. tangles and

*To whom correspondence should be addressed at: Department of Neuroscience, 4500 San Pablo Road, Jacksonville, FL 32224, USA. Email: hutton.michael@mayo.edu

neuropil threads) occurs with a second protein aggregate, the amyloid plaque. The identification of exonic and intronic tau gene mutations associated with FTDP-17 established that tau dysfunction can cause neurodegeneration (9–11).

Unfolded or misfolded protein generated under diverse conditions must be either refolded by molecular chaperones, for instance Hsc/Hsp70 and Hsp40, or eliminated by the ubiquitin proteasomal system (UPS) through an energy-dependent process and concerted action of a number of molecules, including specific ubiquitin ligases. CHIP (carboxyl terminus of the Hsc70-interacting protein) is a molecule with dual function: (i) a co-chaperone of Hsp70 linked through the tetratricopeptide repeat (TPR) domain of CHIP; and (ii) possessing intrinsic E3 ubiquitin ligase activity (U-box domain) which promotes ligation/chain elongation for substrates (12–16). It is structurally similar to RING finger motifs typical of E3 ligases, like parkin. CHIP interacts functionally and physically with the stress-responsive ubiquitin-conjugating (E2 conjugase) enzyme family UBCH5. Thus CHIP is a bona fide ubiquitin ligase which provides a direct link between the chaperone and UPS and has been suggested to contribute in regulating the cellular balance between folding and degradation (17).

Recently, Imai *et al.* (18,19) showed that CHIP, Hsp70, parkin and PAELR formed a complex *in vitro* and *in vivo*. Unfolded PAELR is a substrate of the E3 ubiquitin ligase parkin and accumulation of non-ubiquitinated PAELR in the endoplasmic reticulum (ER) of dopaminergic neurons induces ER stress, leading to neurodegeneration (19). CHIP promotes the dissociation of Hsp70 from parkin and PAELR, thus facilitating parkin-mediated PAELR ubiquitination. Moreover, CHIP enhances parkin-mediated *in vitro* ubiquitination of PAELR in the absence of Hsp70. CHIP also enhances the ability of parkin to inhibit cell death induced by PAELR (18).

The role of the chaperones Hsp70/90 in tau biology has previously been examined by Dou *et al.* (20), who found an inverse relationship between tau aggregation and chaperone levels. Specifically, transgenic mice harboring the V337M tau mutation, which develop hippocampal tau aggregates, had lower levels of Hsp90 than control mice, suggesting that Hsp90 might be degraded along with aggregated tau. In addition, a small number of neurons in the hippocampus that were devoid of aggregated tau were observed to have significantly higher levels of Hsp90. The same relationship between Hsp90 and Hsp70 and tau aggregates in post-mortem samples from a single human AD brain were also reported (20).

In cell cultures transfected with tau constructs increased levels of both Hsp70 and 90, induced by treatment with geldanamycin, led to an ~80% reduction in levels of aggregated, detergent-insoluble tau. This reduction, however, was not accompanied by a decrease in total tau levels, but rather by a redistribution of tau from the insoluble fraction to the soluble fraction. The increased levels of soluble tau were accompanied by an increase in microtubule-bound tau. Reduction of Hsp70 or Hsp90 by RNAi caused the levels of the microtubule-bound tau to decrease (20).

Overall, these studies suggest that abnormal tau accumulation might be associated with perturbation of the major components of the cellular protein quality control machinery—molecular chaperones and the UPS. Hsp70/90 and other chaperones identify proteins that require proper folding, whereas aberrant unfolded proteins are directed to the UPS. CHIP is a ubiquitin E3 ligase that is involved in ubiquitination of Hsp70-bound proteins; this generally results in their targeting to the proteasome. This is a tandem event (chaperone and UPS activity) such that perturbation in either of these systems might play a role in tau accumulation. Moreover, evidence suggests that the Hsp70/90 chaperones and ubiquitin ligases are neuroprotective and can suppress the toxicity associated with abnormal protein accumulation in *Drosophila* and mouse models of disease (21–24).

In the present study we examined the relationship between CHIP/Hsp70 and tau and the role of this chaperone system in tau degradation, ubiquitination and aggregation. We show that CHIP associates with tau through the microtubule-binding domain, is able to ubiquitinate tau and increases the level of insoluble aggregated tau. In addition, a diversity of neuronal and glial tau-related lesions in several neurodegenerative disorders have CHIP immunoreactivity. This suggests that CHIP may play a role in the formation of, or cellular response to, fibrillary tau lesions. Hsp70 also binds to tau, but has opposing effects. Hsp70 decreases tau steady-state levels and selectively reduces insoluble and hyperphosphorylated tau species. Together, these data suggest that the Hsp70–CHIP chaperone system plays an important role in tau biology and in the pathogenesis of tauopathies.

RESULTS

CHIP interacts with tau

Because Hsp70 is known to interact with tau, the major protein species in neurofibrillary pathology, we investigated whether the Hsp70 co-chaperone CHIP, an E3 ubiquitin ligase, was able to interact with and ubiquitinate tau. Although CHIP has several known substrates, none of these have been associated with neurodegenerative disease.

To determine if CHIP and tau interact we first conducted co-immunoprecipitation experiments. Myc-tagged CHIP, parkin and Hsp70 were separately co-transfected with V5-tagged tau into HEK293 cells and then immunoprecipitation was performed with the V5 antibody. Detection of co-immunoprecipitating species was performed by western blotting with the Myc-tag antibody. Tau was found to co-immunoprecipitate with CHIP and Hsp70 (Fig. 1A). Tau also co-immunoprecipitated with parkin, an E3 ligase associated with autosomal recessive juvenile parkinsonism (25). This was not surprising given that parkin has previously been shown to interact with CHIP and that there is considerable structural homology between these two E3 ligases. To determine whether CHIP and tau interact *in vivo*, we performed co-immunoprecipitation using an antibody against CHIP in brain homogenates from transgenic mice (JNPL3 line) expressing mutant (P301L) tau (26). Western blot analysis was then performed with an antibody against tau (Fig. 1B). Tau co-immunoprecipitated with CHIP (Fig. 1B). These data clearly support the physiological and potential pathological relevance of the observed CHIP–tau interaction.

Using co-immunoprecipitation and *in vitro* binding assays, we next examined which regions of CHIP are necessary for the

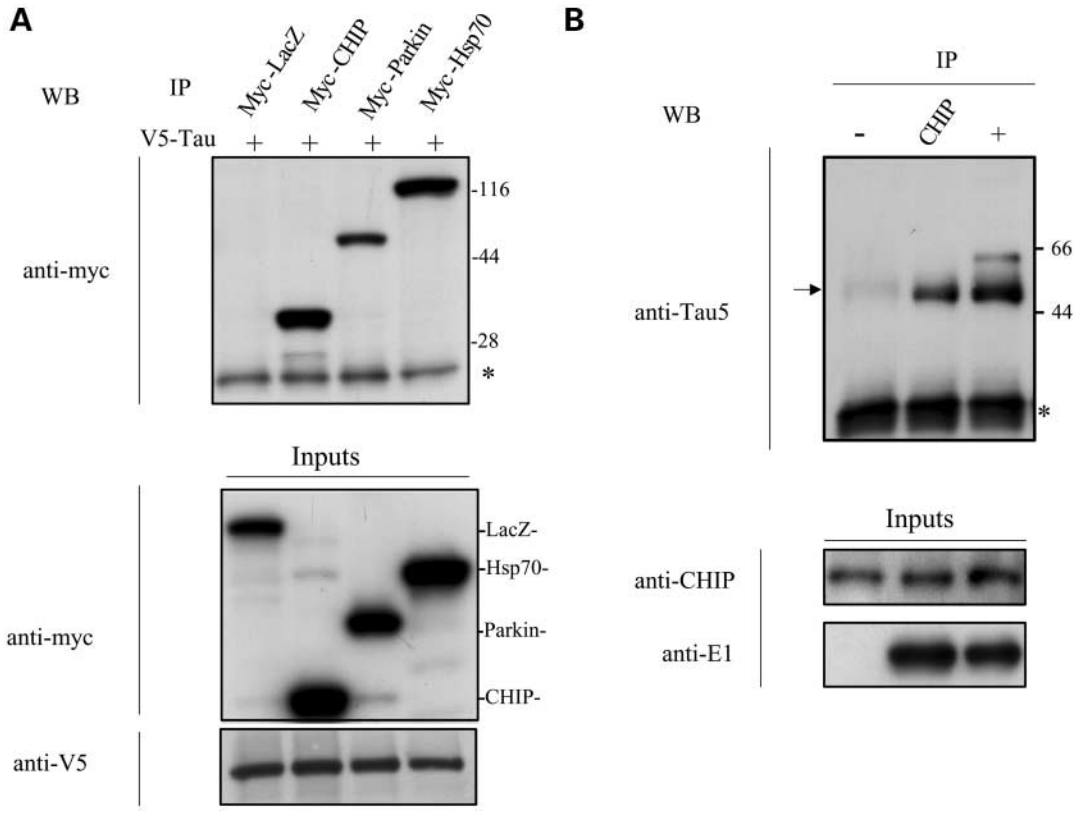

Figure 1. Tau associates with CHIP. (**A**) Interaction of Tau with CHIP, Hsp70 and parkin. Lysates from HEK293 cells transfected with an LacZ vector (Control), myc-tagged CHIP, myc-tagged Hsp70 or myc-tagged parkin and V5-tagged tau were immunoprecipitated with anti-V5 antibody. Immunoprecipitates (IP) and total soluble lysates (total lysate) were analyzed by western blotting (WB). (**B**) *In vivo* interaction of tau with CHIP in brain tissue. Mouse brain tissue from P301L transgenic mice (JNPL3) was homogenized as described in Experimental Procedures. The supernatant fractions were immunoprecipitated with anti-CHIP (CHIP), anti-E1 (+) or an irrelevant (−) polyclonal antibody. The co-precipitated tau was detected by western blotting using Tau5. An asterisk indicates the IgG light chain. The arrow indicates native tau species.

interaction with tau. CHIP contains two major structural motifs—a TPR motif and a U-box domain. The TPR motif is required for interaction with Hsc70 and Hsp90, while the U-box domain has ubiquitin ligase activity (Fig. 2A). To determine the site of interaction of CHIP with tau, we monitored the interaction of tau with these two domains of CHIP. The TPR mutant (C1; 1–189 amino acids) and U-box mutant (C2; 145-303 amino acids) both failed to bind to tau; in contrast, full-length CHIP bound strongly to tau (Fig. 2C). Although these results did not reveal a specific binding domain of CHIP with tau, it is conceivable that the interaction with tau requires both domains, as might be expected if complex formation with Hsp70 is required for the tau–CHIP interaction, or one of these domains and a third undefined region of CHIP. A series of truncated tau constructs were also generated to determine the domain of tau that interacted with CHIP (Fig. 2B). These experiments demonstrated that residues 187–311 contain the region of the tau protein necessary for interaction with CHIP. This includes the microtubule binding domains and the region immediately N-terminal (Fig. 2C).

CHIP ubiquitinates tau

To ascertain whether CHIP or parkin ubiquitinates tau, HEK293 cells were transfected with myc-tagged parkin or myc-tagged CHIP, V5-tagged tau and HA-tagged ubiquitin (Fig. 3A). Two days later, immunoprecipitation was performed with an antibody against V5 and probed with an antibody against HA to assess the degree of tau ubiquitination. Immunoprecipitated tau showed prominent anti-HA (ubiquitin) immunoreactivity in CHIP-transfected cells, with ubiquitin positive species appearing as mulitple higher molecular weight species, possibly representing oligomeric and multimeric ligations (Fig. 3A). To characterize the effect of Hsp70 on CHIP-mediated tau ubiquitination, cells were transfected as described above; however, they were also transfected with myc-tagged Hsp70 in the presence of CHIP. As shown in Figure 3B, Hsp70 attenuates CHIP activity, suggesting that Hsp70 antagonizes CHIP ubiquitination of tau. We further explored which ubiquitin lysine linkage (K48 or K68) was primarily responsible for ubiquitination of tau. Ubiquitin linkage through K48 is associated with proteasome targeting, while K68 ubiquitin linkage appears to be involved in cellular signaling/DNA repair (27). HEK293 cells were transfected with myc-tagged CHIP, V5-tagged tau and HA-tagged wild-type ubiquitin, K48 or K63 constructs. K48 and K63 refer to the particular lysine amino acid used to link the ubiquitins to each other. CHIP-mediated ubiquitination of tau did not discriminate between K48 or K63 type ubiquitin linkage suggesting that both types of linkage occur in tau (Fig. 3C). This has potential functional implications for the role of ubiquitination in tau biology. A further study showed that

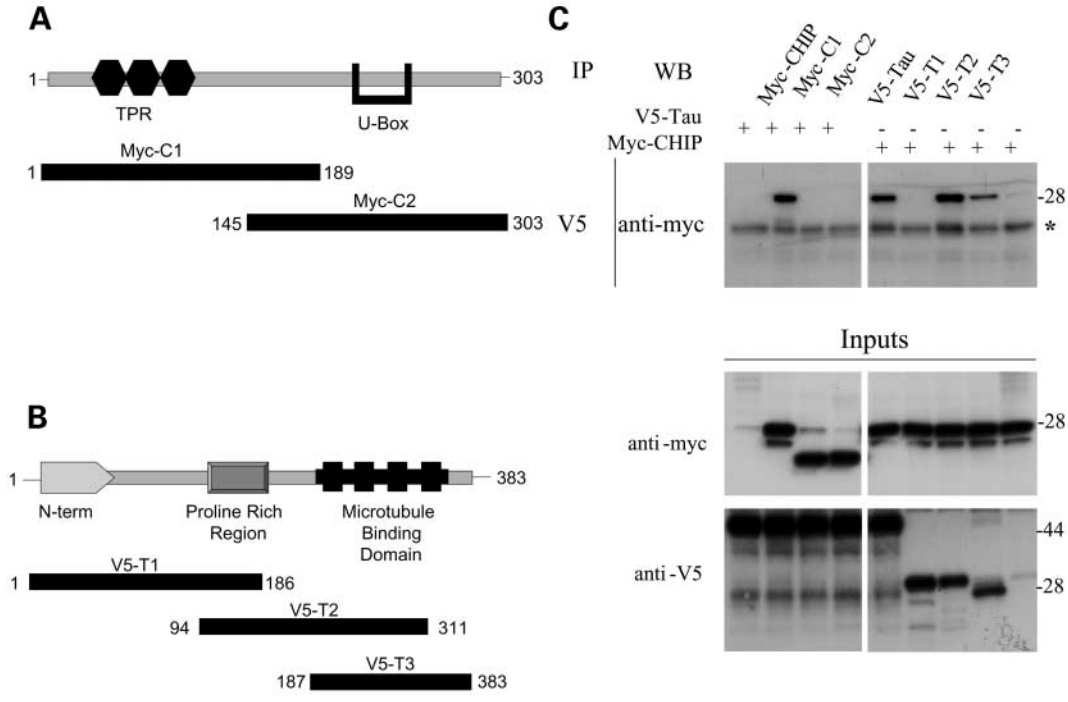

Figure 2. CHIP preferentially interacts with the microtubule-binding domain of tau and tau binding requires full-length CHIP. (**A**) Diagrammatically representation of full-length CHIP and the two structural domains (C1 and C2) used to determine the Tau binding. (**B**) Diagrammatically representation of tau and the three domains (T1, T2 and T3) used to determine the CHIP binding domain. (**C**) Lysates prepared from HEK293 cells transfected with V5-tagged tau and various myc-tagged CHIP domain constructs and various V5-tagged tau domains constructs and myc-CHIP and subjected to IP with anti-V5 followed by anti-myc immunoblotting. Lysates (inputs) were immunoblotted with either anti-V5 or anti-myc antibodies. The asterisk indicates IgG light chain. A representative result from three experiments is shown.

the amount of multimeric ubiquitinated tau (>200 kDa) increased dramatically after the cells were treated with the proteasome inhibitor MG-132, suggesting that a proportion of tau is degraded through the proteasome (Fig. 3D). In particular, it would appear that tau carrying long ubiquitin chains in the soluble fraction is degraded by the proteasome.

To verify the functional interaction between CHIP and tau, we reconstituted the ubiquitination reaction *in vitro*. In this experiment, immunoprecipitated CHIP or parkin and recombinant His-tagged tau were combined with other essential components for *in vitro* ubiquitination, including ATP and E2 conjugases. Again, immunoprecipitated CHIP, but not parkin, ubiquitinated tau (Fig. 4), demonstrating that tau is a substrate of CHIP. Further, when the western blot was re-probed with an antibody against the His-tag on tau, a ladder of species was observed, confirming that tau was directly ubiquitinated by CHIP. Finally, we observed that, in the absence of additional cellular components, Hsp70 had no impact on tau ubiquitination by CHIP; this is in contrast to the attenuation associated with increased Hsp70 activity observed in the *in vivo* ubiquitination studies. This suggests that *in vivo* an additional component of the complex or a particular Hsp70 conformation is required to down regulate tau ubiquitination by CHIP.

CHIP immunoreactivity in human neurodegenerative tauopathies

To evaluate the potential pathological significance of the interaction between tau and CHIP, we examined the immunolocalization of CHIP in postmortem brain sections of different human tauopathies, including AD, PSP, CBD, FTDP-17 and PiD, as well as JNPL3 transgenic mice that express mutant (P301L) tau. CHIP immunoreactivity was detected in a wide range of tau-positive lesions in both neurons and glia, including neurofibrillary tangles (NFTs; Fig. 5A) and dystrophic neurites in neuritic plaques (Fig. 5B) of AD, Pick bodies in PiD (Fig. 5C), globose NFTs (Fig. 5D) and tufted astrocytes (Fig. 5E) in PSP, and oligodendroglial coiled bodies and thread-like processes in CBD (Fig. 5F).

To confirm CHIP co-localization with tau lesions, serial sections from PiD, were immunostained with anti-phospho-tau (CP13; Fig. 5G) and with antibodies anti-CHIP (Fig. 5H), and to ubiquitin 3–39 (Fig. 5I).

The degree of CHIP immunoreactivity correlated to the predominant isoform of tau in the lesions, with 3R tauopathies showing more immunoreactivity than 3R+4R tauopathies or 4R tauopathies. Specifically, there was more robust CHIP immunoreactivity in Pick bodies (3R) than in NFTs in AD (3R+4R). Almost all Pick bodies were also ubiquitin-immunoreactive on adjacent sections stained for ubiquitin. In adjacent sections of AD stained for ubiquitin, most of the CHIP-positive NFTs were also ubiquitin-immunoreactive. The major exception was extracellular NFT, which had no CHIP-immunoreactivity yet variable ubiquitin immunoreactivity. Pre-tangles, neurons with non-fibrillar abnormal phospho-tau immunoreactivity, were negative for CHIP (data not shown). There were only a few NFTs stained in PSP, CBD and FTDP-17. These were all 4R tauopathies and neurofibrillary lesions in these disorders had

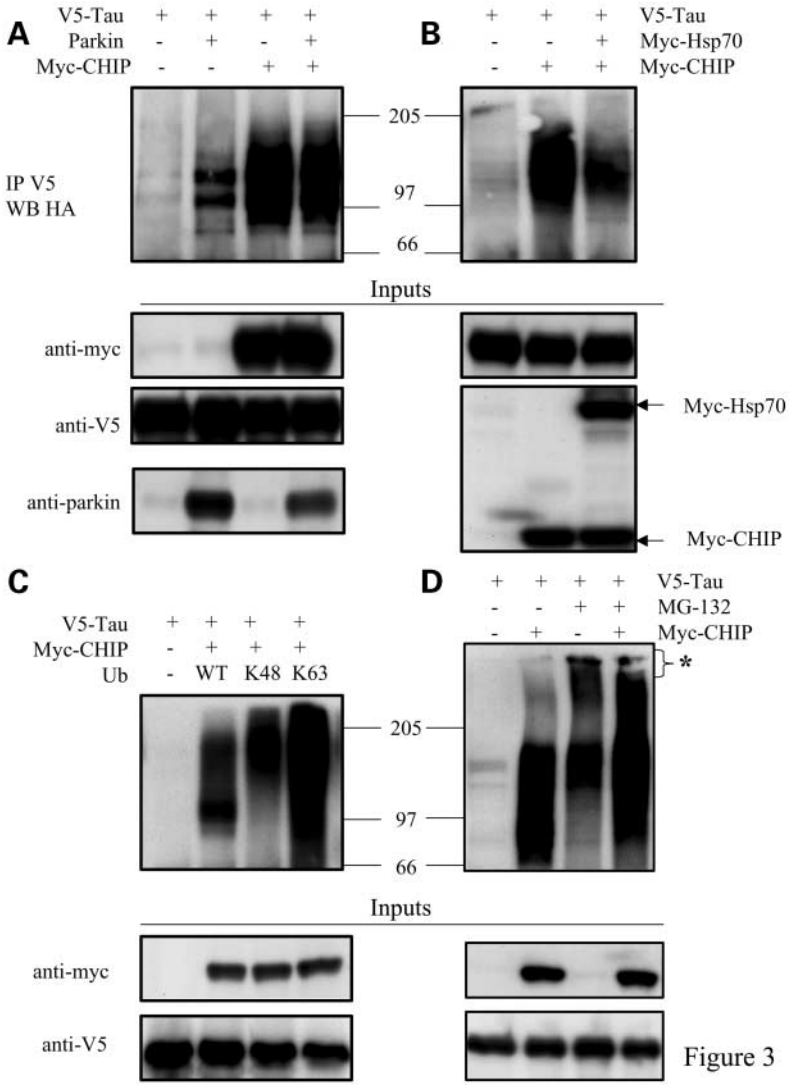

Figure 3. Tau tends to be ubiquitinated *in vivo.* (**A**) CHIP, not parkin, mediates tau ubiquitination. V5-tagged Tau cDNA combined with empty vector, untagged parkin or myc-tagged CHIP and HA-Ub construct were transfected into HEK293 cells. Immunoprecipitates with anti-V5 mAb (V5-IP) immunoblotted with HA mAb to assess the amount of ubiquitination. Total soluble lysates (inputs) were analyzed by western blotting using anti-myc, anti-V5 or anti-parkin. (**B**) Hsp70 attenuates CHIP activity. V5-tagged Tau cDNA combined with empty vector, myc-tagged CHIP and myc-tagged Hsp70 and HA-Ub construct were transfected into HEK293 cells. Immunoprecipitates with anti-V5 mAb immunoblotted with HA mAb to assess the amount of ubiquitination. Total soluble lysates (inputs) were analyzed by western blotting using anti-myc, anti-V5 or anti-parkin. (**C**) CHIP ubiquitinates tau through K48 and K63 ubiquitin linkages. V5-tagged Tau cDNA combined with myc-tagged CHIP (or vector as a control) and HA-tagged wild type or K48 or K63 ubiquitin mutants were transfected into HEK293 cells. Immunoprecipitates with anti-V5 mAb immunoblotted with HA mAb to assess the amount of ubiquitination. Total soluble lysates (inputs) were analyzed by western blotting using anti-myc or anti-V5. (**D**) Proteasome inhibition increases CHIP-mediated ubiquitination of tau. V5-tagged Tau cDNA combined with either empty vector or myc-tagged CHIP and HA-tagged ubiquitin were transfected into HEK293 cells. Thirty-six hours post-transfection cells were exposed to MG132 (5 μM, 12 h). Immunoprecipitates with anti-V5 and immunoblotted with HA mAb to access the amount of ubiquitination. Total soluble lysates (inputs) were analyzed by western blotting using anti-myc or anti-V5.

almost no ubiquitin immunoreactivity. Only a few glial lesions in the latter 4R tauopathies were CHIP-immunoreactive. Overall, the number of CHIP immunoreactive lesions was 50–70% for PiD, 5–10% for AD and 1–5% for both PSP and CBD. These data suggest a role for CHIP in pathologies involving tauopathies in humans. Similar to humans, neurofibrillary lesions in spinal cord sections of JNPL3 mice, which contain mutant 4R tau, were weakly immunoreactive for CHIP and ubiquitin, yet strongly positive for phospho-tau (data not shown).

Controls for specificity of CHIP included omission of primary antibody and absorption with CHIP synthetic peptide. These sections showed no immunoreactivity in Pick bodies (Fig. 5K) or NFTs (data not shown).

Effects of CHIP and Hsp70 on accumulation of detergent-insoluble tau

To examine the impact of CHIP-mediated ubiquitination on tau aggregation, COS-7 cells were transfected with a mutant

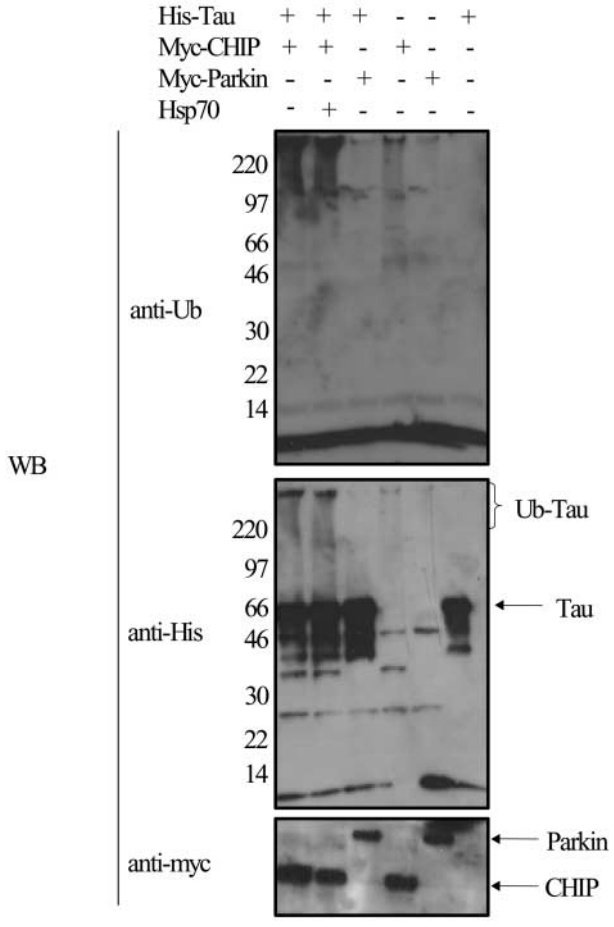

Figure 4. *In vitro* ubiquitination of tau by CHIP. The ubiquitination of Tau by CHIP (or parkin) was reconstituted by using immunoprecipitated myc-tagged parkin and myc-tagged CHIP from transfected HEK293 cells with the addition of purified UBCH7 or UBCH5b and the additional essential components for *in vitro* ubiquitination (see Materials and Methods). The reaction products were analyzed by western blot analysis with both anti-ubiquitin and anti-His antibodies. Inputs were immunoblotted with anti-myc antibodies. Brackets and molecular marker at 220 kDa indicate both Tau and ubiquitin-positive high molecular species. All experiments were replicated twice with similar results.

(P301L) tau expression construct in the absence or presence of either CHIP or Hsp70. Total tau was extracted and then fractionated into triton-soluble and insoluble pools. Transfection of CHIP dramatically increased the accumulation of high molecular weight aggregated tau species in the detergent (triton) insoluble fraction (Fig. 6), detected by western blot analysis with the Tau5 and E1 antibodies. The apparent molecular weight of these aggregated tau species ranged from ~90 kDa to large enough to be retained in the stacking gel. In contrast, expression of Hsp70 selectively reduced the amount of detergent insoluble tau to the point where little or no tau partitioned into the detergent-insoluble fraction. Although the level of insoluble tau was selectively reduced by Hsp70 transfection, there was no corresponding increase in detergent-soluble tau levels, which were also reduced relative to non-transfected cells (Fig. 6).

Induction of Hsp70 reduces tau levels *in vitro* and *in vivo*

To further explore the relationship between Hsp70 and tau steady-state levels *in vitro* we upregulated Hsp70 through geldanamycin (GA) treatment and activated heat shock factor 1 [(HSF-1 (+)] transfection (28). GA is a naturally occurring benzoquinone ansamycin that specifically binds to and interferes with the activity of the molecular chaperone Hsp90 (29), a negative regulator of heat-shock factor 1 (HSF-1), which regulates the transcription of several molecular chaperones, including Hsp70 (28,30). M17 human neuroblastoma cells, which express significant levels of endogenous tau, were either treated with GA or transfected with a mutant (constitutive active) form of HSF-1 (mHSF-1). As shown in Figure 7, treatment with GA reduced tau levels in a dose-dependent manner. Similar results were observed in cells transfected with mHSF-1. Both GA and mHSF-1 increased Hsp70 levels, with mHSF-1 causing the greater induction of the molecular chaperones (Fig. 7). HSF-1 (+), but not GA, also caused an increase in Hsp40 levels, suggesting that Hsp40 is unlikely to be necessary for the reduction of steady-state tau levels produced by these two treatments.

Based on the results described above, Hsp70 appears likely to be involved in regulating tau metabolism, especially the turnover of triton-insoluble species. To obtain additional evidence supporting this idea, we assessed the amount of endogenous tau in the brains of old mice overexpressing the inducible form of Hsp70 (31). There was no significant difference in age between transgenic and control littermates (30.6 ± 5.1 and 28.3 ± 2.1 months of age for non-transgenic and TgHsp70i mice, respectively). Whole brain homogenates from three non-transgenic and three tgHsp70 mice were homogenized and separated into 1% Triton X-100-soluble or -insoluble fractions. The fractions were then immunoblotted using Tau46, a polyclonal antibody to a carboxyl terminal epitope in tau that detects all forms of human and mouse tau (Fig. 8A). The amount of tau was normalized to β-actin levels in the brain of each mouse. Tau levels in TgHsp70 mice in both the soluble and insoluble fractions were significantly lower (~50% lower in both fractions) compared with NT mice (Fig. 8A and B). Moreover, high molecular weight triton-insoluble tau species present in the stacking gel that were observed in the very old NT mice were absent in the age-matched TgHsp70 mice (Fig. 8B). Tau levels were normalized to β-actin from the same gel from either the soluble or insoluble fractions with all the mice in the study. Statistical significance was estimated using Student's *t*-test for difference between NT and tgHsp70i mice in both fractions ($*P < 0.01$, $**P < 0.001$).

DISCUSSION

In the current study, we identified tau as a substrate for the ubiquitin ligase–chaperone protein CHIP. We concluded that tau is an authentic substrate of CHIP from the following evidence: first, CHIP interacts with tau and is specifically ubiquitinated by CHIP *in vivo* and *in vitro* in the presence of the E2 conjugase, UbcH5b. Second, proteasome inhibition augmented CHIP-mediated tau ubiquitination and promoted the insolubility of tau in triton-X-100 detergent. Finally, CHIP

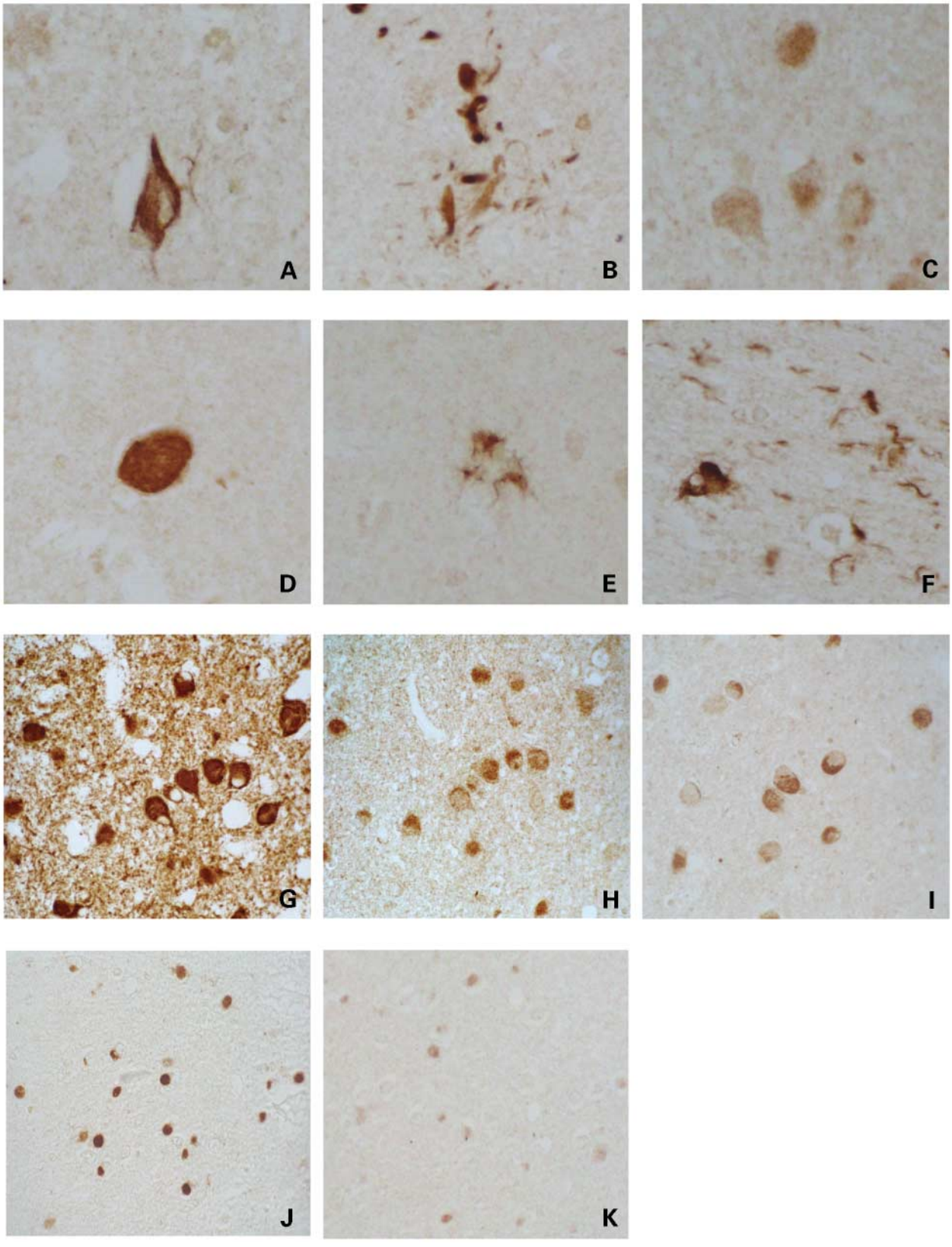

Figure 5. CHIP immunoreactivity is present in a diversity of neurodegenerative tauopathies. Immunostaining of CHIP in several tauopathies. (**A**) NFT in AD, (**B**) dystrophic neurites in senile plaques in AD, (**C**) Pick bodies in PiD, (**D**) globose NFT in PSP, (**E**) tufted astrocyte in PSP and (**F**) oligodendroglial coiled bodies and threads in CBD. CHIP co-localization with tau and ubiquitin was visualized using serial sections immunostained for phospho-tau with CP13 (**G**), CHIP (**H**) and anti-ubiquitin 3–39 (**I**). CHIP staining in PiD case (**J**) and preabsorption with CHIP synthetic peptide (**K**).

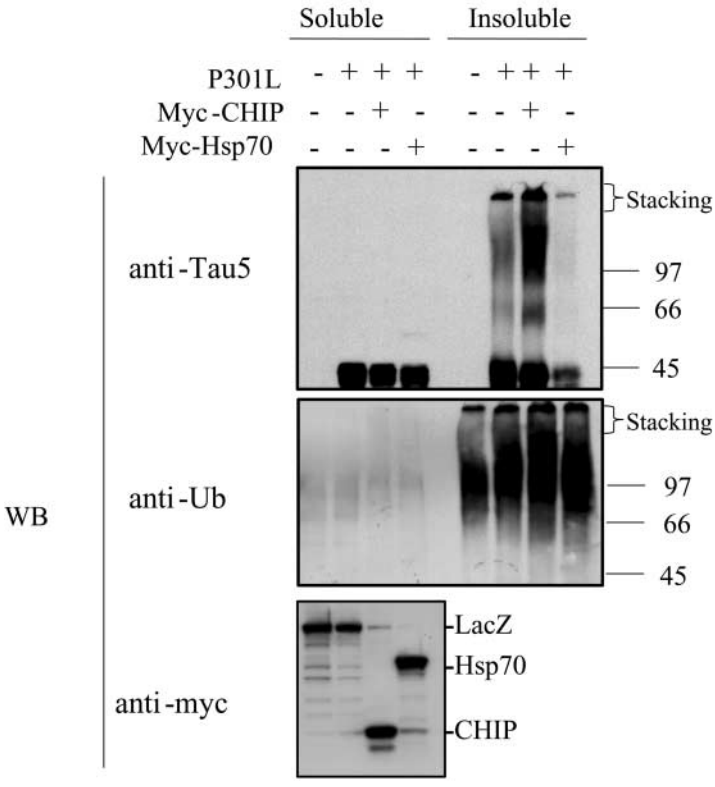

Figure 6. CHIP increases, Hsp70 suppresses tau aggregation. CHIP increases and Hsp70 decreases the accumulation of insoluble Tau in the COS7 cells. Cells transfected with vector plasmid (lacZ) or construct for mutant tau (P301L) combined with construct for mock (Control), myc-tagged CHIP or myc-Hsp70, were lysed and separated into 1% Triton X-100-soluble (S) or -insoluble (I) fractions, then immunoblotted with Tau5. Membrane was stripped and re-probed with anti-ubiquitin. Soluble fraction was used to demonstrate expression of respective constructs.

immunoreactivity was present in a range of tau lesions in several neurodegenerative tauopathies, especially those in which 3R tau is present in pathologic lesions, such as PiD and AD. The tauopathies with CHIP immunoreactivity were also those that have been shown in other studies to have ubiquitin-positive lesions (32). In contrast, disorders such as PSP or CBD in which lesions show almost no ubiquitin immunoreactivity were also negative for CHIP (35–38).

In this study, we found that CHIP mediated ubiquitination of tau. Moreover, both CHIP and Hsp70 interact with tau, suggesting that these two proteins act in concert to control tau metabolism. In fact, overexpression of Hsp70, in cells, attentuated the ubiquitination of tau induced by CHIP (Fig. 3B). These results suggest that Hsp70 and CHIP interact at the functional and/or cellular level. Interestingly the negative effect of Hsp70 on tau ubiquitination was not observed with *in vitro* assays, suggesting that additional chaperones that interact with the Hsp70/CHIP complex might play a role *in vivo*. Furthermore, it appears that a proportion of the tau ubiquitinated by CHIP via K48 ubiquitin linkage is consistent with the observed evidence of proteasome degradation of poly-ubiquitinated tau; however, tau was also ubiquitinated via K63 ubiquitin linkage, suggesting an alternative cellular fate for these species possibly including altered distribution and aggregation.

Although Dou *et al.* (20) reported that increased levels of Hsp70 reduce tau aggregation, which is in accord with results of the present study, they did not determine if this was a result of a reduction in tau levels (Figs 7 and 8), as our data indicate, rather than a redistribution of tau. Our data would further suggest that the CHIP and Hsp70 levels are critical to tau physiology such that excess CHIP would promote tau aggregation whereas Hsp70 would suppress it. In our model systems, insoluble tau aggregates represented a small fraction of total tau protein, which is a consistent observation in several tauopathies, including AD. Hsp/Hsc70 may protect against tau aggregation, neurofibrillary degeneration and neurotoxicity. Our data argue that Hsp70 (with CHIP) may be a critical determinant of normal tau degradation and may possibly be involved in the pathogenesis of human tauopathy. In this scheme, molecular chaperones would mediate tau degradation and directly or indirectly prevent tau aggregation and the toxicity associated with this protein. The balance between CHIP and Hsp70 levels may well be critical. Dai *et al.* (33) have recently shown that CHIP regulates activation of Hsp70 through induced trimerization and transcriptional activation of HSF-1. The activation of HSF-1 by CHIP emphasizes that a single protein (i.e. CHIP) within the complex can regulate major and often diametrically opposed chaperone activities (Hsp70) to alter the metabolism of substrate, in this case tau (33).

Although CHIP has been implicated in the ubiquitination of several substrates, including unfolded CFTR, glucocorticoid receptor and androgen receptor (14–16), tau is the first CHIP substrate that has been implicated in a number of

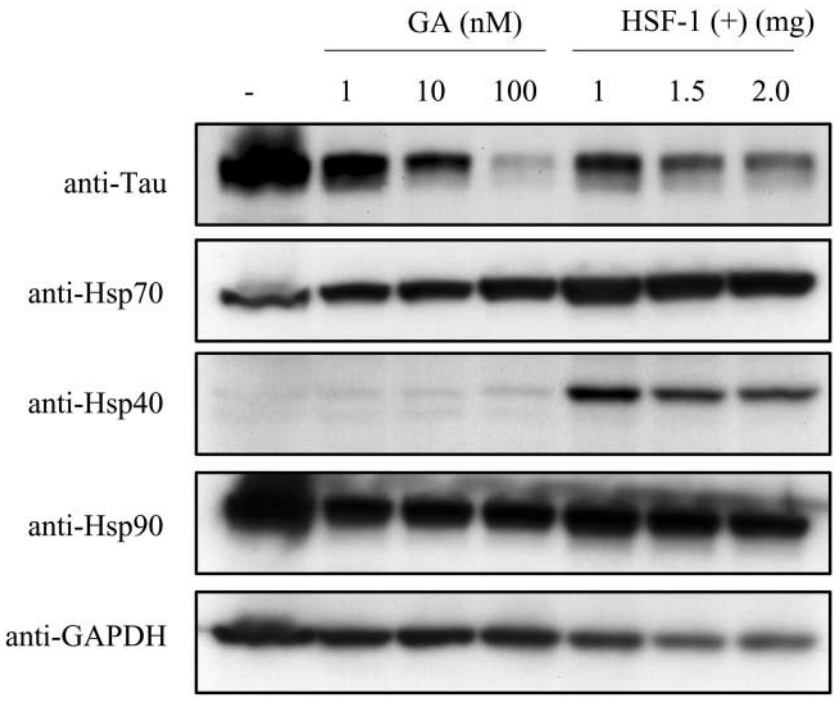

Figure 7. Induction of molecular chaperones decreases tau steady-state levels. M17 human neuroblastoma cell lines expressing endogenous tau were treated with geldanamycin (GA) at 1, 10 and 100 nM or transfected with activated heat shock factor 1 at 1, 1.5 and 2 μg DNA for 48 h. Cells were lysed and immunoblotted with Tau5 mAb. Membranes were stripped and sequentially re-probed with monoclonal antibodies to Hsp70, Hsp40, Hsp90 and GADPH (for protein loading).

neurodegenerative diseases. It is also clear that the another member of this chaperone complex, Hsp70, is involved in tau metabolism. Although many questions remain, the multiple effects of the Hsp70/CHIP chaperone system on tau biology make it of interest as a potential therapeutic target for the human tauopathies including AD.

MATERIALS AND METHODS

Expression vectors, cell culture and antibodies

cDNAs for parkin, tau (4R0N ± P301L), Hsp70 and CHIP were cloned into the mammalian expression vector pcDNA31.1 (Myc- or V5-tagged). Deletion constructs targeted for the respective domains were cloned into similar expression vectors. Ubiquitin constructs were obtained from Dr Ted Dawson (Johns Hopkins). A mutated cDNA sequence encoding an HSF1 lacking residues 203–315 was inserted into vector pcDNA3.1 to prepare expression construct HSF1(+). The integrity of all constructs was confirmed by automated sequencing.

COS-7 and HEK-293 cells were maintained in Optimem (Life Technologies) supplemented with 10% fetal bovine serum (Life Technologies), heat inactivated. Cells were transfected using Lipofectamine 2000 (Life Technologies) or FuGene6 (Roche) incubated for 48 h and treated as previously described. Human M17 Neuroblastoma cell lines stably overexpressing vector, wild-type tau (4R0N) and P301L cell lines were maintained in DMEM (Life Technologies) supplemented with 10% fetal bovine serum heat inactivated, glutamine, and 500 μg ml^{-1} G418.

CHIP polyclonal antibody was obtained from Abcam; HA and Myc antibodies was obtained from Roche; parkin antibody was obtained from Cell Signaling; Tau5 was generously provided by Dr Binder (Northwestern University); Hsp70 antibody was obtained from Stressgen abs; E1, human specific tau and Tau46 antibody were obtained from Dr Shu-Hui Yen (Mayo Clinic); CP13 (phospho-tau ser202) was obtained from Peter Davies (Albert Einstein College of Medicine) and ubiquitin 3–39 from Signet. HRP-coupled anti-mouse and anti-rabbit secondary antibodies were obtained from Jackson Immunoresearch. Ubiquitin polyclonal antibodies were obtained from Dako. His monoclonal antibody was obtained from Calbiochem. LB509 to α-synuclein (Zymed, San Francisco, CA, USA). Hsp40 and Hsp90 were obtained from BD Transduction laboratories. Hsp70 was obtained from Stressgen.

Ubiquitination assays

In vitro. Reactions were performed in 50 μl mixture containing 50 mM Tris–HCl, pH 7.5, 2.5 mM MgCl, 10 mM DTT, 4 mM ATP, 10 μg ubiquitin (Sigma), 500 ng of E1 (Calbiochem, San Diego, CA, USA), 200 ng of UbcH7 or UbcH5b (Affinti-Research, Exeter, UK), immunoprecipitated myc-tagged parkin or myc-tagged CHIP and 2 μg recombinant monomeric his-tagged tau (Dr Binder). Reactions were carried out for 2 h at 37°C before terminating with an equal volume of 2× SDS sample buffer. The reaction products were then subjected to western blot analysis with anti-ubiquitin (Dako, Carpinteria, CA, USA), Tau5 or anti-His antibodies.

In vivo. HEK293 cells were transfected with 4 μg of V5-tagged tau or 4 μg Myc-tagged parkin, Myc-tagged CHIP or Myc-tagged CHIP and Myc-tagged Hsp70 and 4 μg of

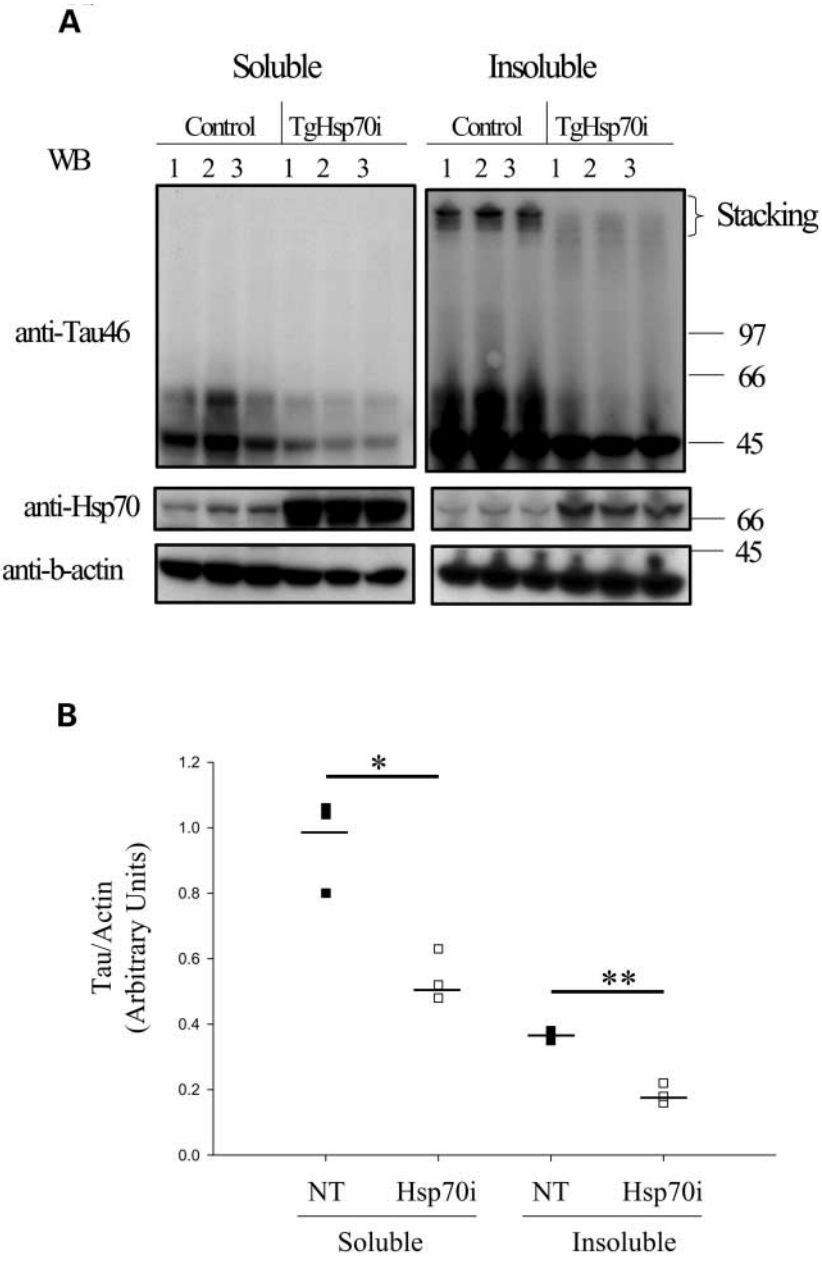

Figure 8. Tau levels in brains of mice overexpressing inducible form of Hsp70. (**A**, **B**) Whole brain tissues from 30-month-old normal (NT) or transgenic mice expressing the Hsp70 transgene were separated into 1% Triton X-100-soluble or -insoluble fractions, then immunoblotted with Tau46. Membrane was stripped and re-probed with anti-Hsp70 and anti-β-actin (control for protein loading). There was no significant difference between mice (30.6 ± 5.1 and 28.3 ± 2.1 months of age for NT and TgHsp70i, respectively). Tau normalized to β-actin from the same gel from either the soluble or insoluble fractions on all mice examined. Statistical significance was estimated using Student's *t*-test for difference between NT and tgHsp70i mice in both fractions. $*P < 0.01$; $**P < 0.001$.

pRK5–HA–wild-type ubiquitin, pRK5–HA–K48–ubiquitin, or pRK5–HA–K63–ubiquitin plasmids. After 48 h, immunoprecipitation was performed with an antibody against V5. The precipitates were submitted to western blotting with an antibody against HA.

Co-immunoprecipitation

For co-immunoprecipitation from cell cultures, HEK293 cells were transfected with 4 μg of each plasmid. After 48 h, cells were washed with cold PBS and harvested in immunoprecipitation buffer (0.1% Triton X-100, 2 μg/ml aprotinin, 100 μg/ml PMSF, 100 mM NaCl in 50 mM Tris–HCl, pH 7.2). The lysate was sonicated, pre-cleared for 1 h at 4°C with 25 μl of protein G (Pierce) and centrifuged at 14 000 rpm. The supernatants were incubated with 2 μg of an antibody against V5 (Life Technologies) and 60 μl of protein G and rocked at 4°C overnight. The protein G beads were pelleted and washed three times with immunoprecipitation buffer. The precipitates were resolved on SDS–PAGE gel and subjected to western blot

analysis. Bands were visualized with chemiluminescence (Pierce, Rockford, IL, USA).

For co-immunoprecipitation of proteins from mice, whole brains from adult mice expressing the P301L transgene brain (or non-transgenic mice as controls) were homogenized in 4 vols of ice-cold PBS containing 320 mM sucrose and 0.1% Triton X-100 with protease inhibitor cocktail (Sigma). The tissue homogenate was centrifuged at 37 000*g* at 4°C for 20 min. The supernatant was collected and 500 µg of protein was used for immunoprecipitation with one of the following antibodies: anti-CHIP, anti-E1 or anti-GFP (irrelevant antibody). The precipitates were subjected to western blot analysis and immunoblotted with Tau5.

M17 human neuroblastoma cells were either treated with GA (100 nM) or transfected with mHSF-1 (1, 1.5 and 2 µg DNA) for 48 h. Cells lysates were 1% Triton–PBS plus protease inhibitors. The precipitates were subjected to western blot analysis and immunoblotted with Tau5 and HSPs 70, 40 and 90.

Immunohistochemistry

Pre-absorption and specificity testing of polyclonal anti-CHIP antibody. CHIP peptide was re-suspended in 1% BSA in PBS to a concentration of 1 mg mL^{-1}. The peptide solution was added to diluted CHIP antibody in TBST to obtain a final dilution of 1 : 500. The mixture was rocked for 1 h at room temperature. The mixture was centrifuged at 13 500*g* for 2 min. The supernatant was separated from the pellet. Serial sections (5 µm thick) from a PiD case were deparaffinized and rehydrated in xylene and graded series of alcohol (100, 100, 95 and 70%). Antigen retrieval was performed in dH_2O in steam bath for 30 min. The sections were allowed to cool. The supernatant and diluted CHIP antibody (1 : 500 in TBST) were used for immunohistochemistry on the DAKO Autostainer (DakoCytomation, Carpinteria, CA, USA) using the DAKO EnVision HRP system on the serial sections. DAKO Liquid DAB Substrate–Chromogen system was the chromogen. The slides were then dehydrated and coverslipped.

Single antibody staining. Paraffin serial sections (5 µm thick) were used for immunohistochemistry from, diffuse Lewy body disease ($n = 6$), multiple system atrophy ($n = 2$) JNPL3 and littermate control mice (one each), AD ($n = 2$), PiD ($n = 4$), PSP ($n = 2$), CBD ($n = 2$), and FTDP_17 ($n = 2$). The sections were then processed the same as above. Primary antibodies used in the serial sections were: CHIP (1 : 250), CP13 (1 : 500) and 3–39 (1 : 200 000). In Lewy body disease and multiple system atrophy cases anti-synuclein (LB509, 1 : 100) replaced CP13. All antibodies were diluted in DAKO Antibody Diluent with background reducing components.

Fractionation experiments

For triton soluble/insoluble fractionation experiments, cells or tissue were lysed in a buffer containing PBS with 1% Triton X-100 and a cocktail of protease inhibitors. After sonication, cells were centrifuged at 100 000 *g* at 4°C for 30 min. Triton X-100 insoluble pellets were dissolved in a buffer containing 1% Triton X-100/1% SDS. The soluble and insoluble fractions were used in western blot analysis using the antibodies described in the figure legend.

ACKNOWLEDGEMENTS

This work was supported by NINDS grant RO1-NS41816-01.

NOTE ADDED IN PROOF

Very recently Shimura *et al.* (34) reported that tau binds to Hsc70 and phosphorylation is a requirement for ubiquitination by CHIP. In addition, CHIP was able to rescue phosphorylated tau-induced toxicity. Our data, while generally consistent with the findings of Shimura *et al.*, extends our understanding of the interaction between the Hsp70/CHIP chaperone system and tau by demonstrating the *in vivo* co-localization of CHIP with tau lesions in human patients with tauopathy and further by exploring the antagonistic action of Hsp70 and CHIP on tau ubiquitination and aggregation. In addition, while Shimura *et al.* report that CHIP ubiquitination is dramatically enhanced by GSK-3β driven phosphorylation of tau, our data show that GSK-3β phosphorylation is not absolutely required for CHIP to ubiquitinate tau.

REFERENCES

1. Ebneth, A., Godemann, R., Stamer, K., Illenberger, S., Trinczek, B. and Mandelkow, E. (1998) Overexpression of tau protein inhibits kinesin-dependent trafficking of vesicles, mitochondria, and endoplasmic reticulum: implications for Alzheimer's disease. *J. Cell Biol.*, **143**, 777–794.
2. Hirokawa, N. (1994) Microtubule organization and dynamics dependent on microtubule-associated proteins. *Curr. Opin. Cell. Biol.*, **6**, 74–81.
3. Andreadis, A., Brown, W.M. and Kosik, K.S. (1992) Structure and novel exons of the human tau gene. *Biochemistry*, **31**, 10626–10633.
4. Neve, R.L., Harris, P., Kosik, K.S., Kurnit, D.M. and Donlon, T.A. (1986) Identification of cDNA clones for the human microtubule-associated protein tau and chromosomal localization of the genes for tau and microtubule-associated protein 2. *Brain Res.*, **387**, 271–280.
5. Goedert, M., Wischik, C.M., Crowther, R.A., Walker, J.E. and Klug, A. (1988) Cloning and sequencing of the cDNA encoding a core protein of the paired helical filament of Alzheimer disease: identification as the microtubule-associated protein tau. *Proc. Natl Acad. Sci. USA*, **85**, 4051–4055.
6. Goedert, M., Spillantini, M.G., Potier, M.C., Ulrich, J. and Crowther, R.A. (1989) Cloning and sequencing of the cDNA encoding an isoform of microtubule-associated protein tau containing four tandem repeats: differential expression of tau protein mRNAs in human brain. *EMBO J.*, **8**, 393–399.
7. Goedert, M., Spillantini, M.G., Jakes, R., Rutherford, D. and Crowther, R.A. (1989) Multiple isoforms of human microtubule-associated protein tau: sequences and localization in neurofibrillary tangles of Alzheimer's disease. *Neuron*, **3**, 519–526.
8. Kanemaru, K., Takio, K., Miura, R., Titani, K. and Ihara, Y. (1992) Fetal-type phosphorylation of the tau in paired helical filaments. *J. Neurochem.*, **58**, 1667–1675.
9. Poorkaj, P., Bird, T.D., Wijsman, E., Nemens, E., Garruto, R.M., Anderson, L., Andreadis, A., Wiederholt, W.C., Raskind, M. and Schellenberg, G.D. (1998) Tau is a candidate gene for chromosome 17 frontotemporal dementia. *Ann. Neurol.*, **43**, 815–825.
10. Spillantini, M.G., Murrell, J.R., Goedert, M., Farlow, M.R., Klug, A. and Ghetti, B. (1998) Mutation in the tau gene in familial multiple system tauopathy with presenile dementia. *Proc. Natl Acad. Sci. USA*, **95**, 7737–7741.
11. Hutton, M., Lendon, C.L., Rizzu, P., Baker, M., Froelich, S., Houlden, H., Pickering-Brown, S., Chakraverty, S., Isaacs, A., Grover, A.*et al.* (1998) Association of missense and 5′-splice-site mutations in tau with the inherited dementia FTDP-17. *Nature*, **393**, 702–705.

12. Ballinger, C.A., Connell, P., Wu, Y., Hu, Z., Thompson, L.J., Yin, L.Y. and Patterson, C. (1999) Identification of CHIP, a novel tetratricopeptide repeat-containing protein that interacts with heat shock proteins and negatively regulates chaperone functions. *Mol. Cell. Biol.*, **19**, 4535–4545.
13. Jiang, J., Ballinger, C.A., Wu, Y., Dai, Q., Cyr, D.M., Hohfeld, J. and Patterson, C. (2001) CHIP is a U-box-dependent E3 ubiquitin ligase: identification of Hsc70 as a target for ubiquitylation. *J. Biol. Chem.*, **276**, 42938–42944.
14. Cardozo, C.P., Michaud, C., Ost, M.C., Fliss, A.E., Yang, E., Patterson, C., Hall, S.J. and Caplan, A.J. (2003) C-terminal Hsp-interacting protein slows androgen receptor synthesis and reduces its rate of degradation. *Arch. Biochem. Biophys.*, **410**, 134–140.
15. Connell, P., Ballinger, C.A., Jiang, J., Wu, Y., Thompson, L.J., Hohfeld, J. and Patterson, C. (2001) The co-chaperone CHIP regulates protein triage decisions mediated by heat-shock proteins. *Nat. Cell. Biol.*, **3**, 93–96.
16. Meacham, G.C., Patterson, C., Zhang, W., Younger, J.M. and Cyr, D.M. (2001) The Hsc70 co-chaperone CHIP targets immature CFTR for proteasomal degradation. *Nat. Cell. Biol.*, **3**, 100–105.
17. McClellan, A.J. and Frydman, J. (2001) Molecular chaperones and the art of recognizing a lost cause. *Nat. Cell. Biol.*, **3**, E51–53.
18. Imai, Y., Soda, M., Hatakeyama, S., Akagi, T., Hashikawa, T., Nakayama, K.I. and Takahashi, R. (2002) CHIP is associated with Parkin, a gene responsible for familial Parkinson's disease, and enhances its ubiquitin ligase activity. *Mol. Cell.*, **10**, 55–67.
19. Imai, Y., Soda, M. and Takahashi, R. (2000) Parkin suppresses unfolded protein stress-induced cell death through its E3 ubiquitin-protein ligase activity. *J. Biol. Chem.*, **275**, 35661–35664.
20. Dou, F., Netzer, W.J., Tanemura, K., Li, F., Hartl, F.U., Takashima, A., Gouras, G.K., Greengard, P. and Xu, H. (2003) Chaperones increase association of tau protein with microtubules. *Proc. Natl Acad. Sci. USA*, **100**, 721–726.
21. Cummings, C.J., Mancini, M.A., Antalffy, B., DeFranco, D.B., Orr, H.T. and Zoghbi, H.Y. (1998) Chaperone suppression of aggregation and altered subcellular proteasome localization imply protein misfolding in SCA1. *Nat. Genet.*, **19**, 148–154.
22. Auluck, P.K. and Bonini, N.M. (2002) Pharmacological prevention of Parkinson disease in Drosophila. *Nat. Med.*, **8**, 1185–1186.
23. Auluck, P.K., Chan, H.Y., Trojanowski, J.Q., Lee, V.M. and Bonini, N.M. (2002) Chaperone suppression of alpha-synuclein toxicity in a *Drosophila* model for Parkinson's disease. *Science*, **295**, 865–868.
24. Yang, Y., Nishimura, I., Imai, Y., Takahashi, R. and Lu, B. (2003) Parkin suppresses dopaminergic neuron-selective neurotoxicity induced by Pael-R in *Drosophila*. *Neuron*, **37**, 911–924.
25. Kitada, T., Asakawa, S., Hattori, N., Matsumine, H., Yamamura, Y., Minoshima, S., Yokochi, M., Mizuno, Y. and Shimizu, N. (1998) Mutations in the parkin gene cause autosomal recessive juvenile parkinsonism. *Nature*, **392**, 605–608.
26. Lewis, J., McGowan, E., Rockwood, J., Melrose, H., Nacharaju, P., Van Slegtenhorst, M., Gwinn-Hardy, K., Paul Murphy, M., Baker, M., Yu, X. *et al.* (2000) Neurofibrillary tangles, amyotrophy and progressive motor disturbance in mice expressing mutant (P301L) tau protein. *Nat. Genet.*, **25**, 402–405.
27. Marx, J. (2002) Cell biology. Ubiquitin lives up to its name. *Science*, **297**, 1792–1794.
28. Xia, W., Vilaboa, N., Martin, J.L., Mestril, R., Guo, Y. and Voellmy, R. (1999) Modulation of tolerance by mutant heat shock transcription factors. *Cell Stress Chaperones*, **4**, 8–18.
29. Whitesell, L., Mimnaugh, E.G., De Costa, B., Myers, C.E. and Neckers, L.M. (1994) Inhibition of heat shock protein HSP90-pp60v-src heteroprotein complex formation by benzoquinone ansamycins: essential role for stress proteins in oncogenic transformation. *Proc. Natl Acad. Sci. USA*, **91**, 8324–8328.
30. Zou, J., Guo, Y., Guettouche, T., Smith, D.F. and Voellmy, R. (1998) Repression of heat shock transcription factor HSF1 activation by HSP90 (HSP90 complex) that forms a stress-sensitive complex with HSF1. *Cell*, **94**, 471–480.
31. Marber, M.S., Mestril, R., Chi, S.H., Sayen, M.R., Yellon, D.M. and Dillmann, W.H. (1995) Overexpression of the rat inducible 70-kD heat stress protein in a transgenic mouse increases the resistance of the heart to ischemic injury. *J. Clin. Invest.*, **95**, 1446–1456.
32. Love, S., Saitoh, T., Quijada, S., Cole, G.M. and Terry, R.D. (1988) Alz-50, ubiquitin and tau immunoreactivity of neurofibrillary tangles, Pick bodies and Lewy bodies. *J. Neuropathol. Exp. Neurol.*, **47**, 393–405.
33. Dai, Q., Zhang, C., Wu, Y., McDonough, H., Whaley, R.A., Godfrey, V., Li, H.H., Madamanchi, N., Xu, W., Neckers, L.*et al.* (2003) CHIP activates HSF1 and confers protection against apoptosis and cellular stress. *EMBO J.*, **22**, 5446–5458.
34. Shimura, H., Schwartz, D., Gygi, S.P. and Kosik, K.S. (2004) CHIP-Hsc70 complex ubiquitinates phosphorylated Tau and enhances cell survival. *J. Biol. Chem.*, in press.
35. Wakabayashi, K., Oyanagi, K., Makifuchi, T., Ikuta, F., Homma, A., Homma, Y., Horikawa, Y. and Tokiguchi, S. (1994) Corticobasal degeneration: etiopathological significance of the cytoskeletal alterations. *Acta. Neuropathol. (Berl.)*, **87**, 545–553.
36. Yamada, T., McGeer, P.L. and McGeer, E.G. (1992) Appearance of paired nucleated, Tau-positive glia in patients with progressive supranuclear palsy brain tissue. *Neurosci. Lett.*, **135**, 99–102.
37. Verny, M., Duyckaerts, C., Delaere, P., He, Y. and Hauw, J.J. (1994) Cortical tangles in progressive supranuclear palsy. *J. Neural. Transm. Suppl.*, **42**, 179–188.
38. Yang, L. and Ksiezak-Reding, H. (1998) Ubiquitin immunoreactivity of paired helical filaments differs in Alzheimer's disease and corticobasal degeneration. *Acta. Neuropathol. (Berl.)*, **96**, 520–526.

ARTICLE IN PRESS
YEXNR-08627; No. of pages: 14; 4C: 4, 6, 8

Available online at www.sciencedirect.com

SCIENCE DIRECT®

Experimental Neurology xx (2004) xxx–xxx

Experimental Neurology

www.elsevier.com/locate/yexnr

Tau phosphorylation increases in symptomatic mice overexpressing A30P α-synuclein

M. Frasier[a], M. Walzer[a,b], L. McCarthy[a], D. Magnuson[b], J.M. Lee[b], C. Haas[c], P. Kahle[c], B. Wolozin[a,*]

[a]*Department of Pharmacology, Loyola University Medical Center, Maywood, IL, United States*
[b]*Department of Pathology, Loyola University Medical Center, Maywood, IL, United States*
[c]*University of Munich, Germany*

Received 10 May 2004; revised 2 July 2004; accepted 21 July 2004

Abstract

Mice overexpressing mutant α-synuclein develop a progressive loss of motor function associated with the accumulation of aggregated α-synuclein in neurons of the brainstem. Recent reports suggest that tau pathology might also be associated with Parkinson disease (PD) and aggregation of α-synuclein. We now report that mice overexpressing A30P α-synuclein develop abnormally phosphorylated tau in parallel with the accumulation of aggregated α-synuclein. Enhanced phosphorylation of tau occurs only in symptomatic mice that also harbor abundant aggregated α-synuclein. The increased phosphorylation of tau occurs at S396/404 and S202 as shown by immunoblotting and immunocytochemical studies with the antibodies PHF-1 and AT8. Neurons that accumulated α-synuclein occurred in the dorsal brainstem and did not show strong colocalization with neurons that showed abnormal tau phosphorylation, which largely occurred in the ventral brainstem. Aggregation of α-synuclein and phosphorylation of tau are associated with increased levels of phosphorylated c-jun kinase (JNK), which is a stress kinase known to phosphorylate tau protein. These results suggest that α-synuclein pathology can stimulate early pathological changes in tau.

Keywords: Aggregation; Parkinson disease; Lewy body; JNK; c-jun Kinase; GSK-3β; CDK5; Astrocytosis; Fibrillization

Introduction

The protein α-synuclein appears to play an important role in the pathophysiology of Parkinson disease (PD). Lewy bodies are a pathological hallmark of PD that are composed primarily of α-synuclein (Spillantini et al., 1997; Spillantini et al., 1998b). α-Synuclein is thought to play a critical role in the pathophysiology of PD because it accumulates in Lewy bodies and because genetic studies identified mutations in α-synuclein that are associated with familial PD (Kruger et al., 1998; Polymeropoulos et al., 1997; Singleton et al., 2003; Spillantini et al., 1998b; Zarranz et al., 2004). The A53T and A30P α-synuclein appear to be causative in PD by increasing the tendency of α-synuclein to aggregate. The mutations both increase the tendency of α-synuclein to aggregate spontaneously or in response to exogenous factors, such as metals and oxidative stress (Conway et al., 2000; Hashimoto et al., 1999; Kruger et al., 1998; Ostrerova-Golts et al., 2000; Paik et al., 1999, 2000; Polymeropoulos et al., 1997). The A53T and A30P mutations in α-synuclein also cause age-dependent α-synuclein aggregation and neuronal injury in transgenic mice and *Drosophila* (Giasson et al., 2002; Kahle et al., 2001). These results emphasize the relevance of α-synuclein to the study of neurodegeneration.

α-Synuclein appears to have pleitropic actions. The α-synuclein protein contains regions of homology with the

* Corresponding author. Department of Pharmacology, Loyola University Medical Center, Building 102/3634, 2160 S. 1st Avenue, Maywood, IL 60153. Fax: +1 708 216 6596.
E-mail address: bwolozi@lumc.edu (B. Wolozin).

0014-4886/$ - see front matter © 2004 Elsevier Inc. All rights reserved.
doi:10.1016/j.expneurol.2004.07.016

protein chaperone 14-3-3, displays functions resembling a chaperone, and also binds many proteins recognized by 14-3-3 as well as other proteins (Ostrerova et al., 1999; Souza et al., 2000). The proteins bound by α-synuclein include 14-3-3, protein kinase C, phospholipase C δ, extracellular regulated kinase, synphilin-1, tyrosine hydroxylase, the dopamine transporter, SEPT4, and the S6′ proteasomal protein (Choi et al., 2001; Engelender et al., 1999; Ihara et al., 2003; Jenco et al., 1998; Lee et al., 2001a; Ostrerova et al., 1999; Perez et al., 2002; Pronin et al., 2000; Sharon et al., 2001; Snyder et al., 2003). α-Synuclein shows avid binding to lipids, and functional studies suggest that α-synuclein plays a role in vesicular exocytosis (Murphy et al., 2000; Sharon et al., 2001). However, the relationship between α-synuclein function and its role in neurodegeneration remain unclear.

The microtubule-associated protein tau is another protein implicated in the pathophysiology of many neurodegenerative diseases. Tau aggregation is a prominent feature in many diseases, including Alzheimer disease and frontotemporal dementias (Lee et al., 2001b). Increasing evidence suggests that many disorders exhibit both tau and α-synuclein aggregation. Tau and α-synuclein pathology both occur in Alzheimer disease, PD, Guam–Parkinson–ALS dementia complex, and PD caused by mutations α-synuclein (Duda et al., 2002; Forman et al., 2002; Ishizawa et al., 2003). Abnormal phosphorylated tau is present in Lewy bodies found in sporadic PD patients and occurs in neurons near areas containing α-synuclein pathology (Ishizawa et al., 2003). In vitro evidence also links α-synuclein and tau as α-synuclein binds tau in vitro, and stimulates tau phosphorylation by protein kinase A in vitro (Giasson et al., 2003; Jensen et al., 1999). Recent results indicate that α-synuclein enhances tau fibrillization in vitro and that abnormal tau fibrils are present in the brains of symptomatic transgenic mice overexpressing mutant A53T synuclein (Giasson et al., 2003). However, the mechanism by which tau and α-synuclein fibrillization might occur in the same diseases is poorly understood.

We set out to investigate whether A30P α-synuclein aggregation occurs alongside tau pathology and to explore potential mechanisms by which α-synuclein aggregation might occur in parallel with tau pathology in transgenic mice overexpressing A30P α-synuclein (Kahle et al., 2001). We report that symptomatic A30P α-synuclein transgenic mice exhibit abnormal tau phosphorylation and that the phosphorylation correlates with activation of a c-jun kinase.

Materials and methods

Animals

The human [A30P] α-synuclein transgene had been injected in hybrid B6/DBA oocytes (Kahle et al., 2000). Founders were extensively (7–10 generations) back-crossed into a C57Bl/6 background. Intercrossing of the highest expressing line 31 yielded a stable colony of homozygous 31H mice (Neumann et al., 2002). These were the animals used in the present study. The mice develop symptoms between 6 and 14 months. The symptoms begin with a tremor and progress to an end-stage phenotype characterized by muscular rigidity, postural instability, and ultimately, paralysis. Mice that progressed to end-stage symptoms were sacrificed by cervical dislocation, and their brains were hemisectioned. The right hemisphere was fixed in formalin and subsequently embedded in paraffin for immunohistochemistry. The left hemisphere was flash-frozen in methyl-2-butane and kept at −80°C for immunoblot analysis. Asymptomatic A30P α-synuclein transgenic mice were age-matched littermates (therefore from the same line as the transgenic A30P α-synuclein symptomatic mice) and were sacrificed at the same time. Nontransgenic control mice were C57Bl/6 mice and were also sacrificed at the same time as the symptomatic transgenic mice.

Antibodies and immunohistochemistry

Brains were sagittally sectioned at a thickness of 4 μm and mounted on Superfrost-plus slides (Fisher Scientific). Distinct monoclonal phospho-specific tau antibodies AT8 (Pierce Endogen, 1:200, Ser 199, 202, Thr 205) and PHF-1 (generously provided by P. Davies, 1:200, Ser 396, 404) were used to detect phosphorylated tau epitopes. Antibodies against α-synuclein included a mouse monoclonal anti-α-synuclein antibody directed against the N-terminus (Immunoblot: Transduction Labs: 1:1000, immunohistochemistry: Zymed, 1:100) and a rabbit polyclonal antibody directed against amino acids 116–131 (used for immunohistochemistry, 1:500) (Ostrerova-Golts et al., 2000). Other antibodies used were: anti-glial fibrillary acidic protein (Dako, 1:500), rabbit polyclonal anti-phospho CDK5 antibody (Tyr15) (Santa Cruz Biotechnology, Santa Cruz, CA, 1:50), anti-phospho-GSK-3β (Serine-9) (Santa Cruz Biotechnology, 1:500), anti-phospho-GSK-3α/β (Tyr216) (BioSource, 1:200), anti-phospho-SAPK/JNK (Thr183/Tyr185) G9 monoclonal antibody (Cell Signaling, 1:1000), and rabbit polyclonal anti-ubiquitin antibody (Dako, 1:500). Immunofluorescence was performed using the same antibody concentrations as above. For immunofluorescence, sections were first treated with 70% formic acid at room temperature for 15 min, rinsed in PBS for 10 min, and then blocked for 20 min in 2% fetal bovine serum and 1% normal goat serum in PBS at room temperature. Primary antibody was incubated on the sections overnight at 4°C and followed by two 10-min washes in PBS. Fluorescent cy2 anti-mouse (1:2500) and rhodamine anti-rabbit (1:200) secondary antibodies (Jackson Immunology) were incubated on the sections for 1 h at room temperature in the dark. Following two more 10-min washes in PBS, coverslips were applied using the Fluormount G mounting media (Electron Microscopy Sciences, Washington, PA).

Brain tissue extraction

Brain tissue extraction was performed as previously described by Sahara et al. (2002) with minor modifications. Left hemibrains were weighed and homogenized in three volumes of TBS (TBS, pH 7.4, 1 mM EDTA, 5 mM sodium pyrophosphate, 30 mM glycerol 2-phosphate, 30 mM sodium fluoride, 1 mM EDTA) containing a protease inhibitor cocktail (Sigma-Aldrich). Protein content was determined via the BCA method, and total protein and concentration were adjusted with the homogenization buffer to be equal between samples. Samples were then centrifuged at 150,000 × *g* for 15 min at 4°C in a Beckman TLA 1004 rotor (Beckman, Palo Alto, CA). The resulting pellet was rehomogenized in three volumes of a salt sucrose buffer (10 mM Tris-HCl, pH 7.4, 0.8 M NaCl, 10% sucrose, 1 mM EDTA) with a protease inhibitor cocktail added immediately before use, while the supernatant was labeled as S1 and frozen at −80°C. The resuspended pellet was again centrifuged at 150,000 × *g* for 15 min at 4°C; this time, the pellet was discarded, and the supernatant was brought to a 1% sarkosyl solution and incubated at 37°C for 1 h with gentle shaking. After centrifugation (150,000 × *g* for 30 min at 4°C), the supernatant was kept, labeled as S2, and frozen at −80°C. The pellet was resuspended in Tris/EDTA (10 mM Tris HCl, pH 7.4, 1 mM EDTA), washed once more with 1% sarkosyl solution, and frozen at −80°C.

Immunoblot analysis

Samples were separated on a gradient 8–16% SDS–PAGE, transferred to PVDF membranes, and stained with either a monoclonal α-synuclein antibody (Transduction Labs, 1:1000) or a phospho-dependent tau monoclonal antibody (PHF-1 or AT8, 1:200) followed by anti-mouse HRP-conjugated secondary antibody (Santa Cruz Biotechnology) and detected with SuperSignal™ West Pico Enhanced Chemiluminescence Kit (Pierce), followed by exposure to Kodak film.

Quantification of immunoblots

Densitometry analysis was performed using ImageJ software. Bands were analyzed and normalized to actin levels. Unpaired student *t* tests were used to determine statistical significance between expression levels in the animals (n = 5 for both the transgenic symptomatic and nontransgenic animals).

Results

Symptomatic A30P mice exhibit synuclein and ubiquitin aggregates in the brainstem

As reported previously, mice overexpressing the A30P α-synuclein transgene developed symptoms between 6 and 14 months (Kahle et al., 2001). The clinical phenotype presented with tremor followed by increasing bradykinesia, first manifest as hind limb impairment. As the clinical phenotype progressed, the mice developed postural instability and ultimately paralysis. For most experiments, we sacrificed mice when they developed an end-stage phenotype, which consisted of paralysis, postural instability, and absence of grooming behavior. The clinical phenotype evolved over a time course of 3–4 weeks.

Mice exhibiting an end-stage phenotype were sacrificed, and their brains were analyzed by biochemistry and immunoblotting. For the these studies, whole brain tissue was homogenized, and protein aggregates were partially purified based on insolubility in the presence of the detergent sarkosyl, as described previously (Giasson et al., 2002; Kahle et al., 2001). The samples were separated into three fractions: aqueous-soluble, sarkosyl-soluble, and sarkosyl-insoluble. All fractions showed more monomeric α-synuclein in the transgenic mice compared to the nontransgenic mice. The sarkosyl-insoluble fraction from symptomatic transgenic mice showed extensive higher molecular weight α-synuclein reactivity that was not apparent in sarkosyl-insoluble fractions from either age-matched nontransgenic or asymptomatic transgenic mice (Fig. 1A). These higher molecular weight bands likely represent oligomeric and aggregated α-synuclein as reported previously (Giasson et al., 2002; Kahle et al., 2001).

To determine where aggregated α-synuclein was present in the brain, we performed immunohistochemistry on sagittally cut brain sections. Aggregated α-synuclein accumulated mainly in large neurons in the rostral part of the reticular formation and as punctate inclusions in the neuropil throughout the reticular formation of transgenic symptomatic mice (Fig. 1C, panel a). α-Synuclein staining in age-matched nontransgenic mice was weaker and showed fewer inclusions (Fig. 1C, panel d). α-Synuclein staining in large neurons of symptomatic transgenic mice also showed strong diffuse expression, which was not observed in nontransgenic or asymptomatic mice (Fig. 1C, panel a). These neurons also contained α-synuclein inclusions (Fig. 1C, panels a and c, arrows). Double staining demonstrated that these inclusions also stained positively with anti-ubiquitin antibody indicating that they contain ubiquitin (Fig. 1C, panels b and c, arrows). No reactivity was seen with preimmune serum (Fig. 1C, panel e).

Symptomatic A30P mice exhibit increased pathological phosphorylation of tau

Phosphorylation of tau protein can be detected by the PHF-1 and AT8 antibodies, and is associated with tau pathology (Spillantini et al., 1998a). Brain sections from mice exhibiting end-stage motor impairment (defined as tremor, muscular rigidity, and full paralysis) were analyzed by immunoblot for the presence of abnormally phosphorylated tau with the phospho-specific antibody PHF-1, which

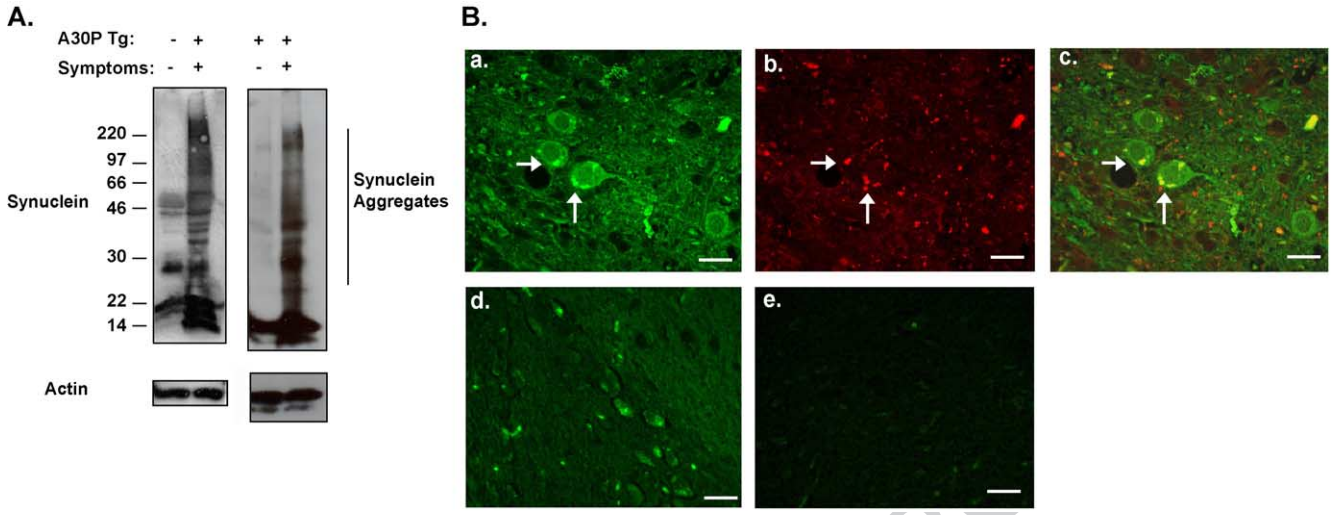

Fig. 1. Accumulation of aggregated α-synuclein. (A) The amount of aggregated α-synuclein observed in the sarkosyl-insoluble fraction from symptomatic A30P transgenic mice (lanes 2 and 4, from a 14-month female mouse shown) is much greater than the amount present in an age-matched nontransgenic female mouse (lane 1) or old asymptomatic transgenic A30P α-synuclein female mouse (lane 3). (B) Immunocytochemical analysis of a symptomatic A30P transgenic mouse shows neurons in the dorsal pons exhibiting both diffuse and punctate accumulation of α-synuclein (a). This region also shows an increase in ubiquitin immunoreactivity (b) that partly colocalizes with the α-synuclein reactivity (c, arrows). Less α-synuclein immunoreactivity is seen in the same region from an age-matched nontransgenic α-synuclein mouse (d), and no α-synuclein immunoreactivity is seen in the same region from a symptomatic A30P transgenic mouse following preadsorption of antibody (e). Bar = 20 μm.

detects phosphorylation of serine at amino acids 396/404. (Lewis et al., 2001) Immunoblots of whole brain homogenates demonstrated over a fourfold increase in PHF-1 reactivity in symptomatic transgenic mice compared to nontransgenic controls (Fig. 2A). In addition, some of the PHF-1-reactive tau migrated at a higher molecular weight, which is characteristic of abnormally phosphorylated tau in diseased brain (Fig. 2A). The total amount of tau as detected by the Tau-5 antibody, however, did not differ among the groups (Figs. 2A and B). Abnormally phosphorylated tau in disease brain often shifts to an insoluble pool as the tau fibrillizes. To determine whether such a shift was apparent in the symptomatic transgenic mice, we performed stepwise solubility fractionation to separate salt-soluble, sarkosyl-soluble, and sarkosyl-insoluble fractions. All brain tissue fractions of symptomatic transgenic mice showed increased PHF-1 signal compared to age-matched nontransgenic mice as analyzed by PHF-1 immunoblot. A representative immunoblot of the sarkosyl-insoluble fraction in Fig. 2C (left panel) shows increased S396 and S404 phosphorylation detected with the PHF-1 antibody in a symptomatic transgenic mouse. A similar pattern of reactivity was observed when the insoluble fraction was probed with the Tau-5 antibody, an antibody that recognizes tau from Arg221 to Leu282 and is independent of phosphorylation state (Fig. 2C, right panel). The increased total tau reactivity observed in the insoluble fraction from symptomatic transgenic mice compared to control mice reflects the tendency of abnormally phosphorylated tau to shift to the sarkosyl-insoluble fraction, which could be due to fibrillization of tau or association with other species that are aggregating. Immunoblotting with anti-actin antibody confirmed equal protein loading among the different samples (Fig. 2C). Immunohistochemical analysis using the MC1 and Alz-50 antibodies that detect a conformational change in tau associated with tangles did not stain positively in the symptomatic transgenic animals (data not shown), suggesting that the phosphorylated tau is in a "pretangle" state. Further washing of the insoluble fraction did not remove either the PHF-1-positive or Tau-5-positive tau, which indicates that the presence of the tau in the insoluble fraction was not due to carryover of sample from the soluble fraction (data not shown).

To further characterize the pathological phosphorylation of tau in these animals, we utilized AT8, another phospho-tau antibody that recognizes tau phosphorylated on amino acids Ser199, Ser202, and Thr205 (Drewes et al., 1992). The results paralleled those seen with the PHF-1 antibody. Immunoblot analysis showed more reactivity in the sarkosyl-insoluble fraction from the symptomatic transgenic mice than in asymptomatic transgenic control mice or nontransgenic mice (Fig. 2D, asymptomatic mouse data shown). In addition, tau from the symptomatic transgenic mice migrated at a slightly higher molecular weight (Fig. 2D, AT8 and Tau-5 panels). The sarkosyl-soluble fractions also showed increased AT8 signal in the symptomatic transgenic mice compared to nontransgenic mice (Fig. 2D). The size of the shift in tau varied among experiments but was often more apparent with Tau-5, perhaps because the PHF-1 and AT8 only detect tau that has already been phosphorylated. No difference in actin reactivity was observed among the lanes demonstrating that there was equal protein among the samples (Fig. 2D).

To determine whether tau phosphorylation is found in the same brain regions as the synuclein pathology, we

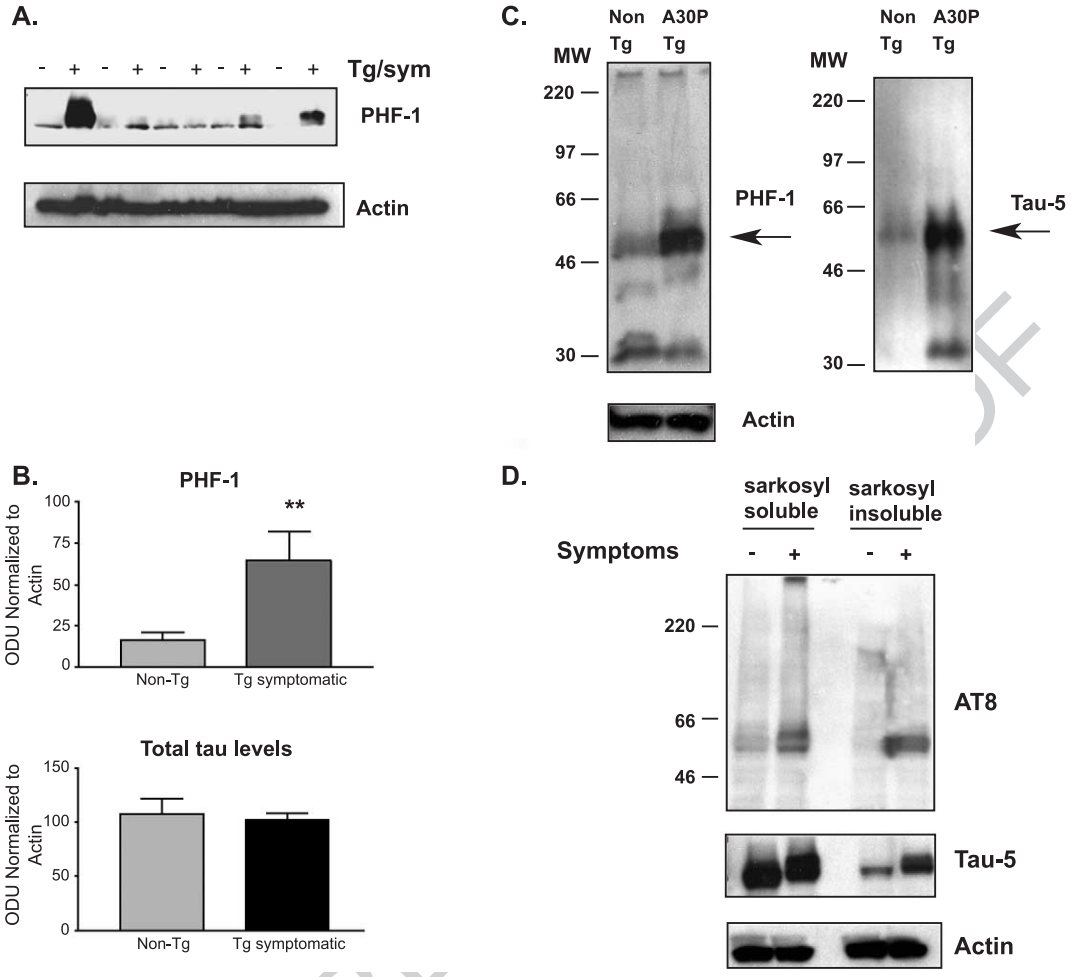

Fig. 2. Induction of phosphorylated PHF-1 and AT8-reactive tau protein. (A) PHF-1 immunoblot of nonfractionated whole brain homogenates from transgenic symptomatic (+) or age-matched nontransgenic mice. The blot was stripped and reprobed with tau-5 antibody which recognizes total tau, indicating similar total tau levels between animals. Actin immunoblot demonstrates equal protein loading. (B) Quantification of differences in PHF-1 and total tau immunoreactivity in the homogenates. ImageJ densitometric analysis of the PHF-1 immunoreactivity normalized to actin levels in each animal (*$P = 0.0035$ in PHF-1, $n = 5$) No significant difference in tau levels detected by Tau-5 existed between transgenic symptomatic and nontransgenic animals. (C) Immunoblot of the sarkosyl-insoluble fraction from a symptomatic A30P transgenic mouse showed increased PHF-1-reactive tau protein compared to the same fraction from an age-matched nontransgenic mouse (arrow). Also, note the electrophoretic shift in the PHF-1 immunoreactive band in the symptomatic transgenic mouse corresponding to increased phosphorylation (triangle). The lower panel shows actin immunoreactivity as a loading control. (D) Immunoblot of fractionated samples in old (12 months, lanes 2 and 4) symptomatic A30P transgenic mouse and young (2 months, lanes 1 and 3) asymptomatic A30P transgenic mouse. Sarkosyl-soluble fractions are lanes 1 and 2, while insoluble fractions are lanes 3 and 4. AT8 antibody demonstrates increased phosphorylation of tau in the symptomatic mouse compared to the asymptomatic mouse. Tau-5 immunoreactivity of the same immunoblot shows a shift in tau mobility in the symptomatic mouse likely due to an increased phosphorylated tau protein which migrates more slowly on SDS–PAGE

performed double-label immunofluorescence analysis. Double-labeling immunofluorescence analysis with antibodies to synuclein and phosphorylated tau (PHF-1, Ser396, and Ser404) demonstrated increased labeling of neurons in the brainstems of symptomatic animals compared to age-matched nontransgenic mice (Fig. 3A). Many neurons in the brainstem exhibited both diffuse cytoplasmic PHF-1 reactivity and punctate PHF-1 labeling within neurons (Fig. 2A, panel e). Much less PHF-1 staining was observed in the same region from nontransgenic mice. The neurons that were diffusely positive for PHF-1 staining showed either no α-synuclein staining or a small amount of punctate α-synuclein staining (Fig. 2A, panels d and f). PHF-1-positive neurons were most abundant in the ventral brainstem. In contrast, the neurons that stained strongly for α-synuclein were large neurons located in the dorsal reticular formation (Fig. 1C). A merge of the pictures showing strong PHF-1 tau inclusions showed only occasional colocalized with punctate α-synuclein inclusions (Fig. 2B, panel f, white arrows). The age-matched nontransgenic mouse displayed weaker staining of synuclein and phosphorylated tau (Fig. 2B, panels a and b). These results suggest that the neurons that develop phosphorylated tau at Ser395/404 do not contain large aggregations or accumulations of α-synuclein protein.

Immunofluorescence analysis with AT8 antibody also showed increased tau pathology in the ventral forebrain. AT8 reactivity associated with phosphorylation on residues

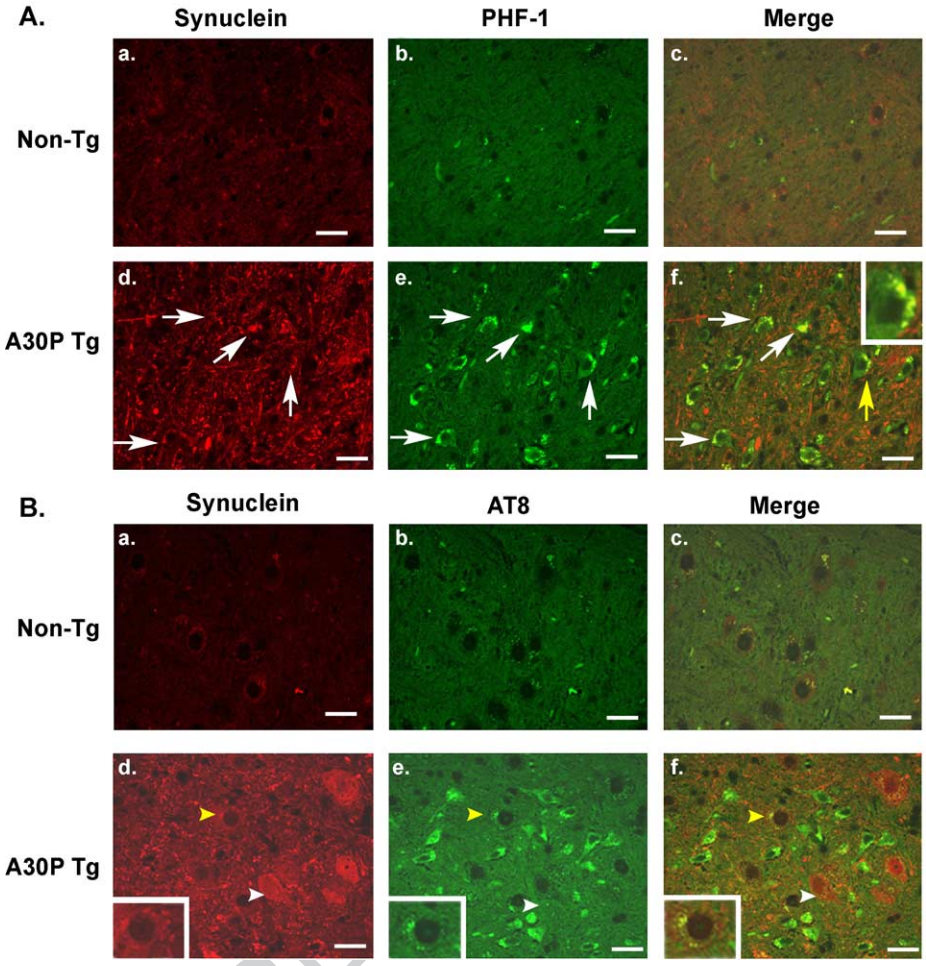

Fig. 3. Phosphorylated tau and α-synuclein aggregates can occur independently. (A) Immunocytochemical analysis of α-synuclein and PHF-1 immunoreactivity in the ventral pons. Staining of ventral pons from an aged nontransgenic mouse showed little α-synuclein (a, c) or PHF-1 (b, c) reactivity. In contrast staining of a symptomatic A30P, transgenic mouse showed an increase in punctate α-synuclein staining (d), and both diffuse and punctate staining for PHF-1 (e). Merging of the pictures shows that some of the α-synuclein staining occurred in neurons containing the PHF-1 reactivity (f, arrows). Inset highlights α-synuclein and PHF-1 colocalization of a single neuron (yellow arrow). Bar = 20 μm. (B) Immunocytochemical analysis of an aged nontransgenic mouse shows little staining of α-synuclein (a, c) or AT8 (b, c). In contrast staining of a symptomatic A30P, transgenic mouse shows an increase in punctate α-synuclein labeling (d), and neurons in the ventral pons with both diffuse and punctate accumulation of AT8 (e). Merging of the pictures shows that some of the α-synuclein staining occurs in neurons containing the AT8 reactivity (f, arrows). Bar = 20 μm.

199, 202, 205 was apparent in small neurons of the pontine reticular formation of symptomatic transgenic mice (Fig. 3B, panel e). Staining with an antibody to α-synuclein showed large neurons in this area that exhibited diffuse anti-α-synuclein reactivity (Fig. 3B, panel d). In addition, there was some punctate α-synuclein staining present both in the large neurons and throughout the neuropil (Fig. 3B, panel d). The neurons that were diffusely positive for AT8 were small neurons that did not colocalize with the neurons showing diffuse α-synuclein accumulation (Fig. 3B, panel f). Some of the large, synuclein-positive neurons also harbored punctate AT8-positive inclusions (Fig. 3B, panel f, arrow heads). The nontransgenic animal exhibited weaker staining with both synuclein and AT8 (Fig. 3B, panels a, b, and c), and colocalization was not evident. These results parallel those observed with PHF-1 and indicate that neurons that develop phosphorylated tau at Ser202/204 do not contain large aggregations or accumulations of α-synuclein protein.

Increased activity of cellular stress kinases in symptomatic transgenic mice

Three kinases are commonly associated with PHF-1 reactivity including cyclin-dependent kinase 5 (CDK5), c-jun kinase (JNK), and glycogen synthase kinase 3β (GSK-3β) (Godemann et al., 1999; Paudel, 1997; Wang et al., 1998). We examined whether any of these kinases are activated as the A30P α-synuclein mice develop motor impairment. We obtained tissue sections from symptomatic and nonsymptomatic A30P α-synuclein mice and age-matched nontransgenic control mice. The tissue was probed with antibodies to the activated c-jun kinase (JNK, phospho-Thr183/Tyr185), tyrosine 216, or Serine 9 of glycogen

synthase kinase 3β, and p25, the cellular activator of cdk5. The antibody recognizing activated JNK exhibited higher reactivity in the symptomatic animals compared to age-matched nontransgenic controls, although no change was observed in the level of total JNK (Figs. 4A and B, phospho-JNK data shown). Reactivity for phospho-GSK-3β Serine 9 was increased (Figs. 4C and D), while reactivity for phospho-GSK-3β tyrosine Y216 was unchanged (Fig. 4E). Phosphorylation of Serine 9 of GSK-3β is associated with inactivation of the protein, while phosphorylation of tyrosine 216 is associated with activation of GSK-3β (Fang et al., 2000; Wang et al., 1994). Immunoblotting with antibody to p25, the activator of CDK5, also failed to show a difference between transgenic and nontransgenic animals (Figs. 4F and G).

We performed immunofluorescence analysis to determine if the activated p-JNK is located in the same neurons of either phosphorylated tau or α-synuclein aggregates. Double labeling revealed p-JNK and α-synuclein colocalization (Fig. 5A) in neurons of the dorsal brainstem area

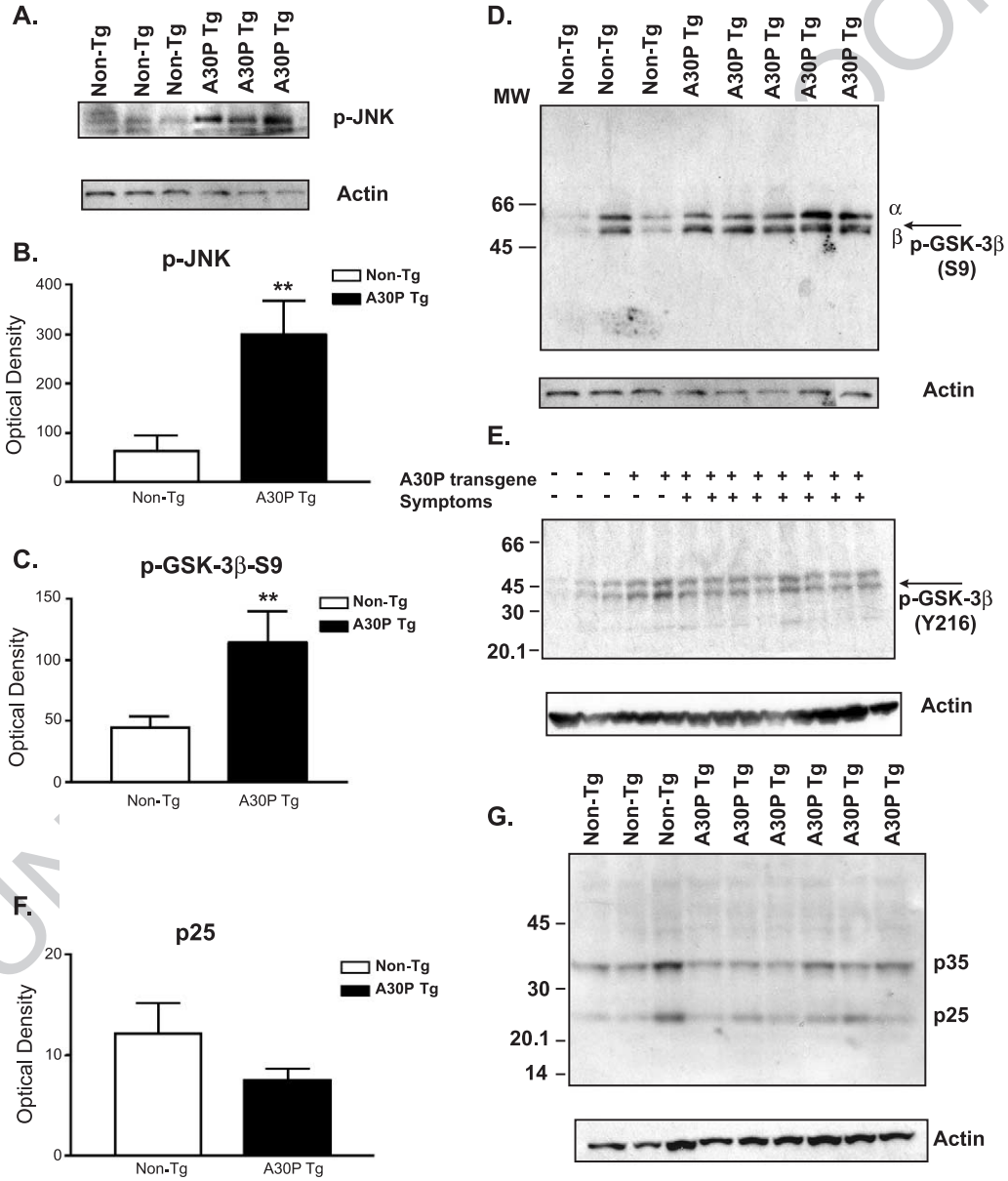

Fig. 4. Levels of activated c-jun kinase increase in symptomatic A30P α-synuclein mice. (A) Immunoblot of brainstem homogenates probed with an antibody recognizing activated JNK. Activated JNK reactivity (upper panel) is increased in motor-impaired animals relative to nontransgenic control animals; actin levels (lower panel) were used to normalize for protein loading. (B) Densitometric analysis demonstrates a significant increase in the levels of activated JNK in symptomatic animals when normalized to actin. (C and D) Levels of GSK-3β phosphorylated at Serine-9 are increased in symptomatic animals when normalized to actin; phosphorylation at Serine-9 is a modification that inhibits GSK-3β activity. (E) Phosphorylation at Y216 of GSK-3β is not changed in symptomatic transgenic animals compared to nontransgenic controls. (F and G) Immunoblot of p25, the activator of cdk5, shows no significant change in p25 levels between symptomatic and asymptomatic animals. Actin is used to demonstrate equal protein loading for all protein analyses. $^{**}P < 0.05$.

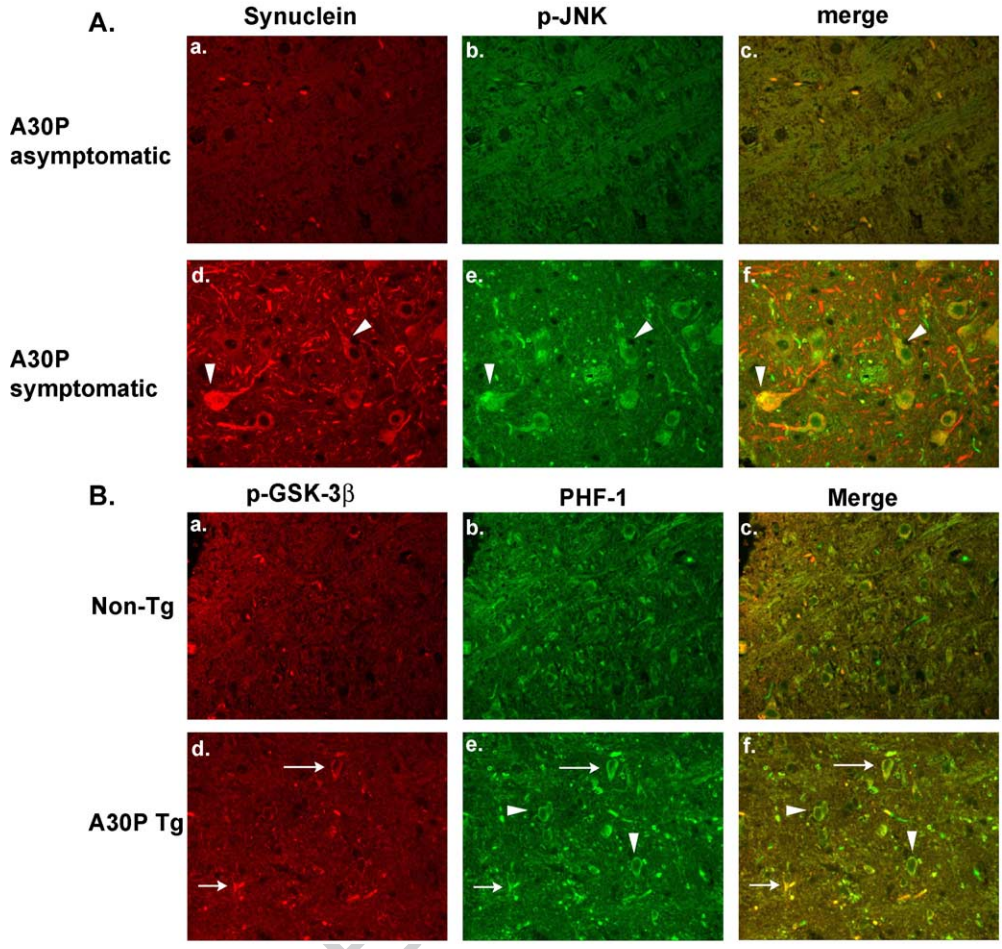

Fig. 5. Phosphorylated-JNK and GSK-3β-S9 are localized in neurons containing α-synuclein or PHF-1 phospho-tau reactivity. (A) Immunocytochemical analysis comparing tissue from an age-matched asymptomatic transgenic animal (top panels) to a motor-impaired transgenic animal (second panel). Staining in the dorsal pons for α-synuclein (a, d) and phospho-JNK (b, e) reveals weak staining in the asymptomatic animal compared to the motor-impaired animal. Merge of the two (c, f) shows moderate co-occurrence. Arrowheads point to colocalization. (B) Immunocytochemical analysis of the dorsal pons region of a nontransgenic mouse (upper panel) and a symptomatic transgenic mouse (lower panel). Antibodies towards phospho-GSK-3β Serine-9 (red, a and d) and PHF-1 (green, b and e) show increased reactivity in the symptomatic animal compared to the age-matched nontransgenic animal. Merging the two (c and f) reveals some colocalization of PHF-1 and GSK-3β S9 reactivity in the symptomatic animals (designated by arrows) and other PHF-1-positive neurons that do not show GSK-3β S9 reactivity (designated by arrowheads). Magnification ×40.

where neurons were diffusely positive for α-synuclein in symptomatic transgenic mice. In areas with fewer α-synuclein-positive neurons, such as the ventral brainstem, anti-phospho-JNK reactivity appeared to colocalize with PHF-1 reactivity rather than anti-α-synuclein reactivity. Serial sections with antibodies towards p-JNK and PHF-1 showed similar patterns of staining in the ventral brainstem in symptomatic transgenic mice (Figs. 6a and b). This suggests that p-JNK reactivity does not always occur in neurons that have overt accumulation of α-synuclein. In contrast, staining for p-JNK and PHF-1 in the asymptomatic transgenic mice (Figs. 6c and d) or nontransgenic mice (Figs. 6e and f) was weak. Studies with antibodies towards phospho-GSK-3β, showed no increase in reactivity (data not shown), although reactivity with antibody identifying phospho-Ser9 of GSK-3β showed some colocalization with PHF-1 in the ventral portion of the brainstem of motor-impaired animals (Fig. 5B, lower panel, arrows), while very little staining is present in age-matched nontransgenic mice (Fig. 5B, upper panel).

Increased reactivity for glial fibrillary acidic protein in symptomatic transgenic mice

Because gliosis has not been reported on in this line of A30P α-synuclein mice, and to assess other signs of injury, we performed immunohistochemistry with an antibody directed against glial fibrillary (GFAP) acidic protein to detect astrocytosis, which is a classic marker for neuronal injury. We observed a massive increase in GFAP reactivity present throughout the brainstem of symptomatic A30P α-synuclein mice (Fig. 7B, c.) compared to nonsymptomatic A30P α-synuclein transgenic mice (Fig. 7B, b.) or nontransgenic mice (Fig. 7B,

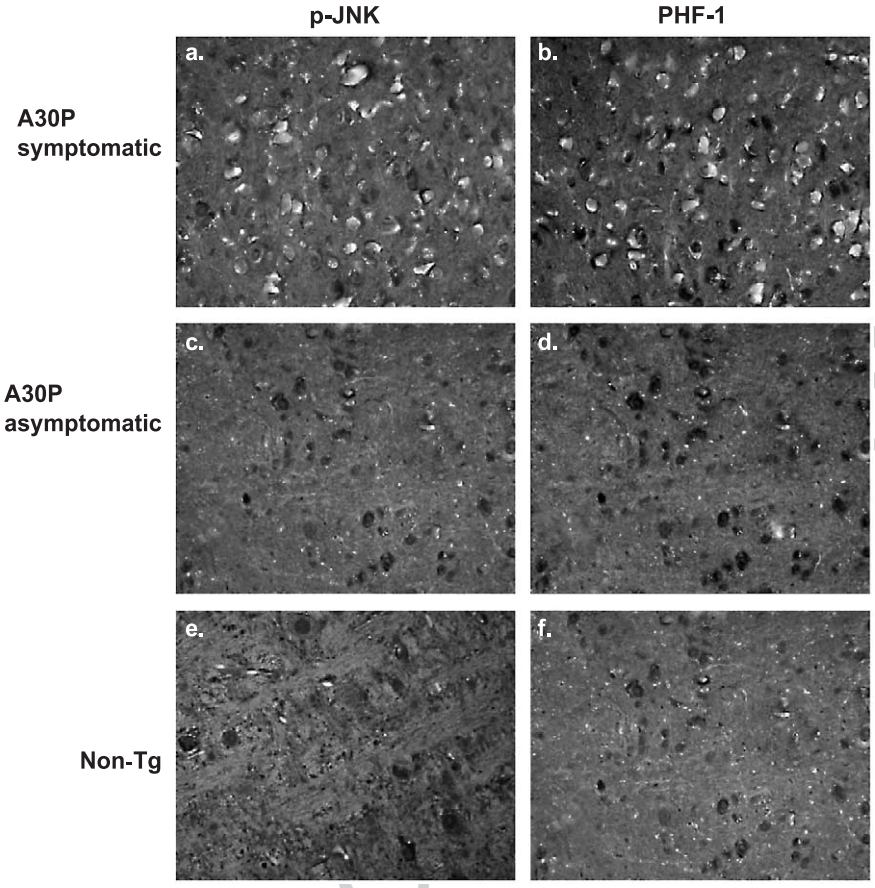

Fig. 6. Phosphorylated-JNK is present in neurons similar to those exhibiting PHF-1 phospho-tau reactivity in the ventral brainstem. Serial sections of brain tissue from symptomatic transgenic A30P α-synuclein transgenic mice showed staining for both phosphorylated-JNK (a) and PHF-1 (b) in similar neurons observed in serial sections. No staining for either antibody was observed in sections from asymptomatic A30P α-synuclein transgenic mice (c and d) or aged, nontransgenic mice (e and f). Magnification ×40.

a). The presence of the GFAP reactivity throughout contrasted sharply with the focal loci of reactivity seen with the phospho-tau or α-synuclein immunoreactivity (Figs. 1B, 2B, and 3B).

Discussion

Transgenic mice overexpressing α-synuclein develop an age-dependent accumulation of α-synuclein in neurons of the brainstem (Giasson et al., 2002; Kahle et al., 2001). Our study confirms the observations of α-synuclein aggregation observed by Kahle et al. (2000, 2001), as well as by other groups studying mice overexpressing A53T or wild-type α-synuclein. We also observed the surprising finding that transgenic α-synuclein mice with impaired motor function accumulate tau that is phosphorylated at Ser202/Thr205 (detected with the AT8 antibody) and Ser396/Ser404 (detected with the PHF-1 antibody).

Phosphorylation of tau at Ser202/Thr205 and Ser396/Ser404 is commonly observed in neurodegenerative diseases that are associated with tau pathology including FTDP-17, AD, and PSP (Godemann et al., 1999; Jicha et al., 1997; Paudel, 1997; Wang et al., 1998). Abnormal tau phosphorylation was readily apparent by both immunohistochemistry and immunoblot. Biochemical analyses of the brain homogenates indicate that hyperphosphorylated tau was present in both sarkosyl-soluble and the sarkosyl-insoluble fractions of whole brain homogenates. The presence of tau in the sarkosyl-insoluble fraction suggests that some of the tau is either self-aggregated or associated with another aggregate, such as aggregated α-synuclein. Indeed, we demonstrated that some of the tau coassociates with α-synuclein in the symptomatic transgenic mice but not in the nontransgenic or asymptomatic transgenic mice. The presence of tau with pathological phosphorylation but lacking conformational epitopes associated with neurofibrillary tangles suggests that the tau exists at a stage characteristic of pretangles or early tangle formation. Incomplete tangle formation has been observed in aged mice expressing the human amyloid precursor protein APP 717 or Swedish mutations (Games et al., 1995; Hsiao et al., 1996). Progression to full tangle formation might not occur in mice because mouse tau does not appear to have the same tendency as human tau to aggregate in vivo (Lewis et al., 2000, 2001; Tatebayashi et al., 2002).

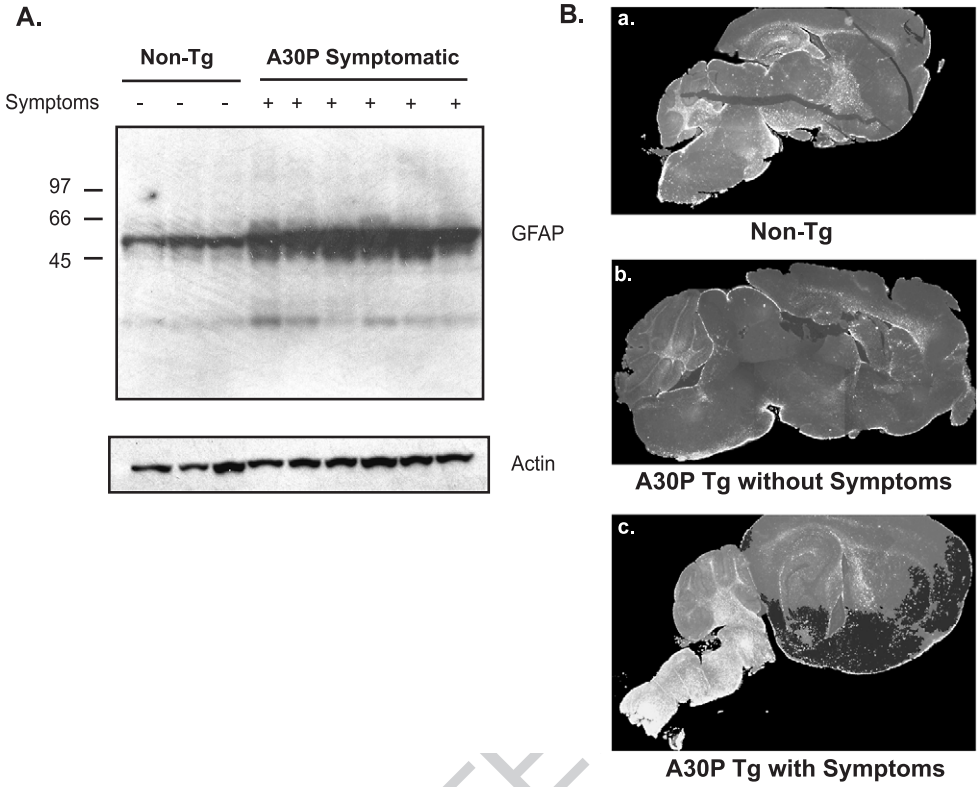

Fig. 7. GFAP activity increases in symptomatic A30P α-synuclein mice. (A) Immunoblot of whole brain homogenates with an antibody against glial fibrillary acidic protein. GFAP reactivity is elevated in symptomatic animals compared to nontransgenic animals. Actin is used as a loading control. (B) Immunocytochemistry of sagittally cut brains from nontransgenic, asymptomatic transgenic, or symptomatic transgenic mice. Abundant immunoreactivity against GFAP was apparent in the brainstem from a 12-month-old symptomatic A30P α-synuclein mouse (c) using an antibody against activated GFAP, while little GFAP reactivity was apparent in tissue sections from a 4-month-old nonsymptomatic A30P α-synuclein mouse (b) and a 12-month-old nontransgenic mouse (a). Magnification ×2.

One surprising aspect of tau pathology in the A30P α-synuclein mice is that the phospho-tau appears to form predominantly in neurons that did not overtly accumulate α-synuclein. This observation is consistent with recent studies of pathological tau and α-synuclein aggregates in human and mouse tissues. Tau can be detected in some Lewy bodies in PD substantia nigra, but many Lewy bodies do not contain pathological tau (Ishizawa et al., 2003). Pathological tau can also be detected in brain tissue from human PD subjects caused by the A53T α-synuclein mutation as well as in transgenic mice coexpressing P301L tau and A53T α-synuclein; however, the tau and α-synuclein are not always colocalized (Duda et al., 2002; Giasson et al., 2003). Duda et al. found tau in a halo shape surrounding α-synuclein inclusions in the brains of patients overexpressing A53T α-synuclein, which indicates that the two proteins can aggregate in close proximity. Giasson et al. reported approximately 25% of α-synuclein inclusions contained tau threads in mice overexpressing A53T α-synuclein. These results are therefore consistent with our observation that only a fraction of pathological tau colocalizes with α-synuclein accumulations. The amount of colocalization might vary depending on extrinsic factors, such as the oxidative stress present in neurons of patients with PD, and on intrinsic factors, such as the type of mutation that is present; the P301L tau mutation, A53T α-synuclein, and A30P α-synuclein mutations might impact colocalization of tau and α-synuclein aggregates differentially. Previous studies examining tau pathology in mice developing amyloid accumulations also observed tau phosphorylation occurring at a distance from the amyloid accumulation. Mice transgenic for both amyloid precursor protein and P301L tau develop tau pathology in some regions that are separate from the amyloid accumulation (Lewis et al., 2001). Following injection of Aβ, tau pathology also develops at some sites distant from the injection site (Gotz et al., 2001; Sigurdsson et al., 1997). The separation of tau and synuclein pathology that we observed in this study might reflect similar processes. The presence of pathological tau in neurons that do not show α-synuclein accumulation could result from the presence of small amounts of fibrillar α-synuclein in these neurons, which might either directly stimulate the stress kinases or might stimulate aggregation of tau. Alternatively, the pathological tau might derive from distant signals. Neurons that have been injured by the accumulation of large amounts of α-synuclein might secrete factors such as cytokines that would stimulate tau phosphorylation, as well as gliosis. Neurons containing large

amounts of α-synuclein accumulation might also generate free radicals and/or might fail to send out trophic signals required by neighboring neurons.

Other proteins known to be involved in the neurodegenerative pathology appear to accumulate along with the α-synuclein. Lewy bodies are composed primarily of the proteins α-synuclein and ubiquitin, but other proteins are present in some Lewy bodies in smaller amounts, such as parkin, Synphilin-1, SEPT4, torsin, and neurofilament (Choi et al., 2001). Interestingly, we did not observe increases in parkin associated with the α-synuclein accumulation (data not shown). Ubiquitin is the protein most commonly associated with Lewy bodies, and we observed that the A30P α-synuclein mice show concomitant accumulation of ubiquitin. The ubiquitin that accumulates appears to occur in only a subset of the neurons that accumulate α-synuclein as shown by double-staining sections from the brainstem of affected mice using antibodies to both α-synuclein and ubiquitin. The lower prevalence of ubiquitin accumulations suggests that ubiquitin accumulation occurs after that of α-synuclein and is consistent with a prior study indicating that the accumulation of α-synuclein precedes the accumulation of ubiquitin in these mice (Kahle et al., 2001). Astrocytosis is another common indicator of neuronal injury, and immunocytochemical staining for GFAP showed a massive increase in GFAP reactivity throughout the brainstem of symptomatic A30P transgenic mice. The pattern of GFAP reactivity is striking because the distribution is much broader than that observed for α-synuclein accumulation or phospho-tau immunoreactivity. Because the Thy1 promoter, which is neuron-specific, drives the human A30P α-synuclein transgene, we hypothesize that the astrocytosis occurs in response to the neuronal injury. The widespread gliosis suggests that the neuronal injury is either more widespread than is apparent by immunocytochemical analysis, determined with antibodies to α-synuclein, or that the injured neurons secrete diffusible signals, such as cytokines. Astrocytosis has been noted in another transgenic α-synuclein mouse model, in MPTP toxicity and in PD with dementia, but is not a prevalent feature of rotenone-induced toxicity or of classic cases of Parkinson disease (Gomez-Isla et al., 2003; Muramatsu et al., 2003; Tsuchiya et al., 2002). The presence of astrocytosis in the α-synuclein transgenic mice distinguishes an important difference between this transgenic mouse model of PD and actual PD in humans.

Our studies suggest that the mechanism of increased phosphorylation of tau may involve selective activation of JNK. The kinases glycogen synthase kinase 3β, CDK5, and c-jun kinase are all activated by oxidative stress (Nemoto et al., 2000; Shaw et al., 1998; Strocchi et al., 2003). JNK, GSK-3β, and CDK5 all phosphorylate tau at S396 and S404 (Godemann et al., 1999; Paudel, 1997; Wang et al., 1998). In our study, the increased tau phosphorylation correlated with increased phosphorylation of JNK but not with phosphorylation of GSK-3β (at Tyr216) or CDK5. Interestingly, we also observed some increase in phosphorylation of GSK-3β at Ser9, which is associated with reduced activity (Wang et al., 1988, 1998). This pattern or reactivity differs somewhat from the pattern of reactivity seen in Alzheimer disease. Hyperphosphorylation of tau is associated with increased activity of both CDK5 and GSK3β in CNS neurons in Alzheimer disease and in Niemann-Pick disease (Bu et al., 2002; Takashima et al., 1996; Vincent et al., 1997). The identification of JNK as a pathway that is selectively associated with α-synuclein pathology in the A30P α-synuclein mice in vivo provides a useful tool for identifying the biochemical pathways associated with α-synuclein pathology. Our results contradict findings by Hashimoto et al. (2002) that show cells overexpressing α-synuclein inactivate JNK in response to oxidative stress. This discrepancy could reflect differences between in vitro and in vivo studies. Hashimoto overexpressed wild-type α-synuclein in cell culture, while we utilized mice overexpressing mutant A30P α-synuclein. The A30P mutation may disrupt the ability of α-synuclein to inactivate JNK, or aggregated α-synuclein may prevent the JNK inactivation in the animals. Activation of JNK by α-synuclein might explain how α-synuclein pathology leads to abnormal phosphorylation of tau in the A30P α-synuclein mice. Because phosphorylation of tau predisposes tau to aggregation, the phosphorylation could provide a mechanism that contributes to the increased fibrillization of tau observed in synucleinopathies (Giasson et al., 2003). In addition, activation of JNK through a transsynaptic mechanism (perhaps due to trophic withdrawal or release of reactive oxygen species) might also explain how abnormal phosphorylation and fibrillization of tau occur in neurons without large amounts of aggregated α-synuclein, such as is observed in this study and other studies (Giasson et al., 2003).

Increasing evidence suggests common mechanisms of neurodegeneration among different diseases. In Alzheimer disease, Parkinson disease, frontotemporal dementias, and polyglutamine disorders such as Huntington disease, protein aggregation appears to drive neurodegeneration. In each case, in vitro studies show that the proteins that accumulate have a inherent tendency to aggregate (Conway et al., 1998; DiFiglia et al., 1997; Hong et al., 1998; Hutton et al., 1998; Lewis et al., 2000). Many of these proteins have also been shown to stimulate concomitant aggregation of proteins prone to aggregate. Human tau aggregates as Aβ accumulates in vivo, Aβ stimulates aggregation of α-synuclein, α-synuclein coaggregates with proteins containing expanded polyglutamine regions, and α-synuclein stimulates tau aggregation (Charles et al., 2000; Furlong et al., 2000; Giasson et al., 2003; Lewis et al., 2001; Masliah et al., 2001). In addition, the formation of protein aggregates appears to stimulate similar pathological reactions, including formation of free radicals, activation of stress kinases, and inhibition of proteasomal activity. In our study, we observed that the tau and synuclein pathology can occur at spatially distinct sites. Because formation of microaggre-

gates (also known as protofibrils) and activation of stress responses often occur in parallel, the exact mechanism of tau pathology in the A30P α-synuclein mice remains to be determined. However, our data provide in vivo support for the hypothesis that accumulation and aggregation of α-synuclein can stimulate pathological changes in tau protein.

Uncited references

Feany and Bender, 2000
Goldman and Yen, 1986
Masliah et al., 2000
Schlossmacher et al., 2002
Sharma et al., 2001
Wakabayashi et al., 2000

Acknowledgments

We would like to thank Nancy Muma (Loyola) for her useful suggestions. This research was supported by grants to BW from NINDS (NS41786-01), NIA (AG17485), and USAMRC (DAMD17-01-1-0781).

References

Bu, B., Klunemann, H., Suzuki, K., Li, J., Bird, T., Jin, L.W., Vincent, I., 2002. Niemann-Pick disease type C yields possible clue for why cerebellar neurons do not form neurofibrillary tangles. Neurobiol. Dis. 11, 285–297.

Charles, V., Mezey, E., Reddy, P.H., Dehejia, A., Young, T.A., Polymeropoulos, M.H., Brownstein, M.J., Tagle, D.A., 2000. alpha-Synuclein immunoreactivity of huntingtin polyglutamine aggregates in striatum and cortex of Huntington's disease patients and transgenic mouse models. Neurosci. Lett. 289, 29–32.

Choi, P., Golts, N., Snyder, H., Petrucelli, L., Chong, M., Hardy, J., Sparkman, D., Cochran, E., Lee, J., Wolozin, B., 2001. Co-association of parkin and α-synuclein. NeuroReport 12, 2839–2844.

Conway, K., Harper, J., Lansbury, P., 1998. Accelerated in vitro fibril formation by a mutant alpha-synuclein linked to early-onset Parkinson disease. Nat. Med. 4, 1318–1320.

Conway, K.A., Lee, S.J., Rochet, J.C., Ding, T.T., Williamson, R.E., Lansbury Jr., P.T., 2000. Acceleration of oligomerization, not fibrillization, is a shared property of both alpha-synuclein mutations linked to early-onset Parkinson's disease: implications for pathogenesis and therapy. Proc. Natl. Acad. Sci.U. S. A. 97, 571–576.

DiFiglia, M., Sapp, E., Chase, K., Davies, S., Bates, G., Vonsattel, J., Aronin, N., 1997. Aggregation of huntingtin in neuronal intranuclear inclusions and dystrophic neurites in brain. Science 277, 1990–1993.

Drewes, G., Lichtenberg-Kraag, B., Doring, F., Mandelkow, E., Biernat, J., Goris, J., Doree, M., Mandelkow, E., 1992. Mitogen activated protein (MAP) kinase transforms tau protein into an Alzheimer-like state. EMBO J. 11, 2131–2138.

Duda, J.E., Giasson, B.I., Mabon, M.E., Miller, D.C., Golbe, L.I., Lee, V.M., Trojanowski, J.Q., 2002. Concurrence of alpha-synuclein and tau brain pathology in the Contursi kindred. Acta Neuropathol. (Berl.) 104, 7–11.

Engelender, S., Kaminsky, Z., Guo, X., Sharp, A., Amaravi, R., Kleiderlein, J., Margolis, R., Troncoso, J., Lanahan, A., Worley, P., Dawson, V., Dawson, T., Ross, C., 1999. Synphilin-1 associates with alpha-synuclein and promotes the formation of cytosolic inclusions. Nat. Genet. 22, 110–114.

Fang, X., Yu, S.X., Lu, Y., Bast Jr., R.C., Woodgett, J.R., Mills, G.B., 2000. Phosphorylation and inactivation of glycogen synthase kinase 3 by protein kinase A. Proc. Natl. Acad. Sci.U. S. A. 97, 11960–11965.

Feany, M.B., Bender, W.W., 2000. A *Drosophila* model of Parkinson's disease. Nature 404, 394–398.

Forman, M.S., Schmidt, M.L., Kasturi, S., Perl, D.P., Lee, V.M., Trojanowski, J.Q., 2002. Tau and alpha-synuclein pathology in amygdala of Parkinsonism–dementia complex patients of Guam. Am. J. Pathol. 160, 1725–1731.

Furlong, R.A., Narain, Y., Rankin, J., Wyttenbach, A., Rubinsztein, D.C., 2000. alpha-Synuclein overexpression promotes aggregation of mutant huntingtin. Biochem. J. 346 (Pt. 3), 577–581.

Games, D., Adams, D., Alessandrini, R., Barbour, R., Berthelette, Blackwell, C., Carr, T., Clemens, J., Donaldson, T., Gillespie, F., Guido, T., Hagopian, S., Johnson, M., Wood, K., Khan, K., Lee, M., Leibowitz, P., Lieberburg, I., Little, S., Masliah, E., McConlogue, L., Montoya-Zavala, M., Mucke, L., Paganini, L., Penniman, E., Power, M., Schenk, D., Seubert, P., Snyder, B., Soriano, F., Tan, H., Vitale, J., Wadsworth, S., Wolozin, B., Zhao, J., 1995. Development of neuropathology similar to Alzheimer's disease in transgenic mice overexpressing the 717V-F β-amyloid precursor protein. Nature 373, 523–527.

Giasson, B.I., Duda, J.E., Quinn, S.M., Zhang, B., Trojanowski, J.Q., Lee, V.M., 2002. Neuronal alpha-synucleinopathy with severe movement disorder in mice expressing A53T human alpha-synuclein. Neuron 34, 521–533.

Giasson, B.I., Forman, M.S., Higuchi, M., Golbe, L.I., Graves, C.L., Kotzbauer, P.T., Trojanowski, J.Q., Lee, V.M., 2003. Initiation and synergistic fibrillization of tau and alpha-synuclein. Science 300, 636–640.

Godemann, R., Biernat, J., Mandelkow, E., Mandelkow, E.M., 1999. Phosphorylation of tau protein by recombinant GSK-3beta: pronounced phosphorylation at select Ser/Thr-Pro motifs but no phosphorylation at Ser262 in the repeat domain. FEBS Lett. 454, 157–164.

Goldman, J.E., Yen, S.H., 1986. Cytoskeletal protein abnormalities in neurodegenerative diseases. Ann. Neurol. 19, 209–223.

Gomez-Isla, T., Irizarry, M.C., Mariash, A., Cheung, B., Soto, O., Schrump, S., Sondel, J., Kotilinek, L., Day, J., Schwarzschild, M.A., Cha, J.H., Newell, K., Miller, D.W., Ueda, K., Young, A.B., Hyman, B.T., Ashe, K.H., 2003. Motor dysfunction and gliosis with preserved dopaminergic markers in human alpha-synuclein A30P transgenic mice. Neurobiol. Aging 24, 245–258.

Gotz, J., Chen, F., van Dorpe, J., Nitsch, R.M., 2001. Formation of neurofibrillary tangles in P301l tau transgenic mice induced by Abeta 42 fibrils. Science 293, 1491–1495.

Hashimoto, M., LJ, H., Xia, Y., Takeda, A., Sisk, A., Sundsmo, M., Masliah, E., 1999. Oxidative stress induces amyloid-like aggregate formation of NACP/α-synuclein in vitro. NeuroReport 10, 717–721.

Hashimoto, M., Hsu, L.J., Rockenstein, E., Takenouchi, T., Mallory, M., Masliah, E., 2002. alpha-Synuclein protects against oxidative stress via inactivation of the c-Jun N-terminal kinase stress-signaling pathway in neuronal cells. J. Biol. Chem. 277, 11465–11472.

Hong, M., Zhukareva, V., Vogelsberg-Ragaglia, V., Wszolek, Z., Reed, L., Miller, B., Geschwind, D., Bird, T., McKeel, D., Goate, A., Morris, J., Wilhelmsen, K., Schellenberg, G., Trojanowski, J., Lee, V., 1998. Mutation-specific functional impairments in distinct tau isoforms of hereditary FTDP-17. Science 282, 1914–1917.

Hsiao, K., Chapman, P., Nilsen, S., Eckman, C., Harigaya, Y., Younkin, S., Yang, F., Cole, G., 1996. Correlative memory deficits, Abeta elevation, and amyloid plaques in transgenic mice. Science 274, 99–102.

Hutton, M., Lendon, C., Rizzu, P., Baker, M., Froelich, S., Houlden, H., Pickering-Brown, S., Chakraverty, S., Isaacs, A., Grover, A., Hackett, J., Adamson, J., Lincoln, S., Dickson, D., Davies, P., Petersen, R., Stevens, M., de Graaff, E., Wauters, E., van Baren, J., Hillebrand, M., Joosse, M., Kwon, J., Nowotny, P., Heutink, P., al, e., 1998. Association

of missense and 5′-splice-site mutations in tau with the inherited dementia FTDP-17. Nature 393, 702–705.

Ihara, M., Tomimoto, H., Kitayama, H., Morioka, Y., Akiguchi, I., Shibasaki, H., Noda, M., Kinoshita, M., 2003. Association of the cytoskeletal GTP-binding protein Sept4/H5 with cytoplasmic inclusions found in Parkinson's disease and other synucleinopathies. J. Biol. Chem. 278, 24095–24102.

Ishizawa, T., Mattila, P., Davies, P., Wang, D., Dickson, D.W., 2003. Colocalization of tau and alpha-synuclein epitopes in Lewy bodies. J. Neuropathol. Exp. Neurol. 62, 389–397.

Jenco, J., Rawlingson, A., Daniels, B., Morris, A., 1998. Regulation of phospholipase D2: selective inhibition of mammalian phospholipase D isoenzymes by a and b synucleins. Biochemistry 37, 4901–4909.

Jensen, P.H., Hager, H., Nielsen, M.S., Hojrup, P., Gliemann, J., Jakes, R., 1999. alpha-Synuclein binds to tau and stimulates the protein kinase A-catalyzed tau phosphorylation of serine residues 262 and 356. J. Biol. Chem. 274, 25481–25489.

Jicha, G.A., Lane, E., Vincent, I., Otvos Jr., L., Hoffmann, R., Davies, P., 1997. A conformation- and phosphorylation-dependent antibody recognizing the paired helical filaments of Alzheimer's disease. J. Neurochem. 69, 2087–2095.

Kahle, P.J., Neumann, M., Ozmen, L., Muller, V., Jacobsen, H., Schindzielorz, A., Okochi, M., Leimer, U., van Der Putten, H., Probst, A., Kremmer, E., Kretzschmar, H.A., Haass, C., 2000. Subcellular localization of wild-type and Parkinson's disease-associated mutant alpha-synuclein in human and transgenic mouse brain. J. Neurosci. 20, 6365–6373.

Kahle, P.J., Neumann, M., Ozmen, L., Muller, V., Odoy, S., Okamoto, N., Jacobsen, H., Iwatsubo, T., Trojanowski, J.Q., Takahashi, H., Wakabayashi, K., Bogdanovic, N., Riederer, P., Kretzschmar, H.A., Haass, C., 2001. Selective insolubility of alpha-synuclein in human Lewy body diseases is recapitulated in a transgenic mouse model. Am. J. Pathol. 159, 2215–2225.

Kruger, R., Kuhn, W., Muller, T., Woitalla, D., Graeber, M., Kosel, S., Przuntek, H., Epplen, J., Schols, L., Riess, O., 1998. Ala30Pro mutation in the gene encoding α-synuclein in Parkinson's disease. Nat. Genet. 18, 106–108.

Lee, F.J., Liu, F., Pristupa, Z.B., Niznik, H.B., 2001a. Direct binding and functional coupling of alpha-synuclein to the dopamine transporters accelerate dopamine-induced apoptosis. FASEB J. 15, 916–926.

Lee, V.M., Goedert, M., Trojanowski, J.Q., 2001b. Neurodegenerative tauopathies. Annu. Rev. Neurosci. 24, 1121–1159.

Lewis, J., McGowan, E., Rockwood, J., Melrose, H., Nacharaju, P., Van Slegtenhorst, M., Gwinn-Hardy, K., Paul Murphy, M., Baker, M., Yu, X., Duff, K., Hardy, J., Corral, A., Lin, W.L., Yen, S.H., Dickson, D.W., Davies, P., Hutton, M., 2000. Neurofibrillary tangles, amyotrophy and progressive motor disturbance in mice expressing mutant (P301L) tau protein. Nat. Genet. 25, 402–405.

Lewis, J., Dickson, D.W., Lin, W.L., Chisholm, L., Corral, A., Jones, G., Yen, S.H., Sahara, N., Skipper, L., Yager, D., Eckman, C., Hardy, J., Hutton, M., McGowan, E., 2001. Enhanced neurofibrillary degeneration in transgenic mice expressing mutant tau and APP. Science 293, 1487–1491.

Masliah, E., Rockenstein, E., Veinbergs, I., Mallory, M., Hashimoto, M., Takeda, A., Sagara, Y., Sisk, A., Mucke, L., 2000. Dopaminergic loss and inclusion body formation in alpha-synuclein mice: implications for neurodegenerative disorders. Science 287, 1265–1269.

Masliah, E., Rockenstein, E., Veinbergs, I., Sagara, Y., Mallory, M., Hashimoto, M., Mucke, L., 2001. beta-Amyloid peptides enhance alpha -synuclein accumulation and neuronal deficits in a transgenic mouse model linking Alzheimer's disease and Parkinson's disease. Proc. Natl. Acad. Sci.U. S. A. 25, 25.

Muramatsu, Y., Kurosaki, R., Watanabe, H., Michimata, M., Matsubara, M., Imai, Y., Araki, T., 2003. Cerebral alterations in a MPTP-mouse model of Parkinson's disease—An immunocytochemical study. J. Neural Transm. 110, 1129–1144.

Murphy, D.D., Rueter, S.M., Trojanowski, J.Q., Lee, V.M., 2000. Synucleins are developmentally expressed, and alpha-synuclein regulates the size of the presynaptic vesicular pool in primary hippocampal neurons. J. Neurosci. 20, 3214–3220.

Nemoto, S., Takeda, K., Yu, Z.X., Ferrans, V.J., Finkel, T., 2000. Role for mitochondrial oxidants as regulators of cellular metabolism. Mol. Cell. Biol. 20, 7311–7318.

Ostrerova, N., Petrucelli, L., Farrer, M., Mehta, N., Alexander, P., Choi, P., Palacino, J., Hardy, J., Wolozin, B., 1999. α-Synuclein shares physical and functional homology with 14-3-3 proteins. J. Neurosci. 19, 5782–5791.

Ostrerova-Golts, N., Petrucelli, L., Hardy, J., Lee, J., Farrer, M., Wolozin, B., 2000. The A53T α-synuclein mutation increases iron-dependent aggregation and toxicity. J. Neurosci. 20, 6048–6054.

Paik, S., Shin, H., Lee, J., Chang, C., Kim, J., 1999. Copper(II)-induced self-oligomerization of α-synuclein. Biochem. J. 340, 821–828.

Paik, S.R., Shin, H.J., Lee, J.H., 2000. Metal-catalyzed oxidation of alpha-synuclein in the presence of copper(II) and hydrogen peroxide. Arch. Biochem. Biophys. 378, 269–277.

Paudel, H.K., 1997. The regulatory Ser262 of microtubule-associated protein tau is phosphorylated by phosphorylase kinase. J. Biol. Chem. 272, 1777–1785.

Perez, R.G., Waymire, J.C., Lin, E., Liu, J.J., Guo, F., Zigmond, M.J., 2002. A role for alpha-synuclein in the regulation of dopamine biosynthesis. J. Neurosci. 22, 3090–3099.

Polymeropoulos, M.H., Lavedan, C., Leroy, E., Ide, S.E., Dehejia, A., Dutra, A., Pike, B., Root, H., Rubenstein, J., Boyer, R., Stenroos, E.S., Chandrasekharappa, S., Athanassiadou, A., Papapetropoulos, T., Johnson, W.G., Lazzarini, A.M., Duvoisin, R.C., Di Iorio, G., Golbe, L.I., Nussbaum, R.L., 1997. Mutation in the alpha-synuclein gene identified in families with Parkinson's disease. Science 276, 2045–2047.

Pronin, A.N., Morris, A.J., Surguchov, A., Benovic, J.L., 2000. Synucleins are a novel class of substrates for G protein-coupled receptor kinases. J. Biol. Chem.

Sahara, N., Lewis, J., DeTure, M., McGowan, E., Dickson, D.W., Hutton, M., Yen, S.H., 2002. Assembly of tau in transgenic animals expressing P301L tau: alteration of phosphorylation and solubility. J. Neurochem. 83, 1498–1508.

Schlossmacher, M.G., Frosch, M.P., Gai, W.P., Medina, M., Sharma, N., Forno, L., Ochiishi, T., Shimura, H., Sharon, R., Hattori, N., Langston, J.W., Mizuno, Y., Hyman, B.T., Selkoe, D.J., Kosik, K.S., 2002. Parkin localizes to the Lewy bodies of Parkinson disease and dementia with Lewy bodies. Am. J. Pathol. 160, 1655–1667.

Sharma, N., Hewett, J., Ozelius, L.J., Ramesh, V., McLean, P.J., Breakefield, X.O., Hyman, B.T., 2001. A close association of torsinA and alpha-synuclein in Lewy bodies: a fluorescence resonance energy transfer study. Am. J. Pathol. 159, 339–344.

Sharon, R., Goldberg, M.S., Bar-Josef, I., Betensky, R.A., Shen, J., Selkoe, D.J., 2001. alpha-Synuclein occurs in lipid-rich high molecular weight complexes, binds fatty acids, and shows homology to the fatty acid-binding proteins. Proc. Natl. Acad. Sci. U. S. A. 98, 9110–9115.

Shaw, M., Cohen, P., Alessi, D.R., 1998. The activation of protein kinase B by H_2O_2 or heat shock is mediated by phosphoinositide 3-kinase and not by mitogen-activated protein kinase-activated protein kinase-2. Biochem. J. 336 (Pt. 1), 241–246.

Sigurdsson, E.M., Lee, J.M., Dong, X.W., Hejna, M.J., Lorens, S.A., 1997. Laterality in the histological effects of injections of amyloid-beta 25–35 into the amygdala of young Fischer rats. J. Neuropathol. Exp. Neurol. 56, 714–725.

Singleton, A.B., Farrer, M., Johnson, J., Singleton, A., Hague, S., Kachergus, J., Hulihan, M., Peuralinna, T., Dutra, A., Nussbaum, R., Lincoln, S., Crawley, A., Hanson, M., Maraganore, D., Adler, C., Cookson, M.R., Muenter, M., Baptista, M., Miller, D., Blancato, J., Hardy, J., Gwinn-Hardy, K., 2003. alpha-Synuclein locus triplication causes Parkinson's disease. Science 302, 841.

Snyder, H., Mensah, K., Theisler, C., Lee, J., Matouschek, A., Wolozin, B., 2003. Aggregated and monomeric alpha-synuclein bind to the S6′

proteasomal protein and inhibit proteasomal function. J. Biol. Chem. 278, 11753–11759.
Souza, J.M., Giasson, B.I., Lee, V.M., Ischiropoulos, H., 2000. Chaperone-like activity of synucleins. FEBS Lett. 474, 116–119.
Spillantini, M., Schmidt, M., VM-Y, L., Trojanowski, J., Jakes, R., Goedert, M., 1997. α-Synuclein in Lewy bodies. Nature 388, 839–840.
Spillantini, M.G., Bird, T.D., Ghetti, B., 1998a. Frontotemporal dementia and parkinsonism linked to chromosome 17: a new group of tauopathies. Brain Pathol. 8, 387–402.
Spillantini, M.G., Crowther, R.A., Jakes, R., Hasegawa, M., Goedert, M., 1998b. α-Synuclein in filamentous inclusions of Lewy bodies from Parkinson's disease and dementia with Lewy bodies. Proc. Natl. Acad. Sci. U. S. A. 95, 6469–6473.
Strocchi, P., Pession, A., Dozza, B., 2003. Up-regulation of cDK5/p35 by oxidative stress in human neuroblastoma IMR-32 cells. J. Cell. Biochem. 88, 758–765.
Takashima, A., Noguchi, K., Michel, G., Mercken, M., Hoshi, M., Ishiguro, K., Imahori, K., 1996. Exposure of rat hippocampal neurons to amyloid beta peptide (25–35) induces the inactivation of phosphatidyl inositol-3 kinase and the activation of tau protein kinase I/glycogen synthase kinase-3 beta. Neurosci. Lett. 203, 33–36.
Tatebayashi, Y., Miyasaka, T., Chui, D.H., Akagi, T., Mishima, K., Iwasaki, K., Fujiwara, M., Tanemura, K., Murayama, M., Ishiguro, K., Planel, E., Sato, S., Hashikawa, T., Takashima, A., 2002. Tau filament formation and associative memory deficit in aged mice expressing mutant (R406W) human tau. Proc. Natl. Acad. Sci. U. S. A. 99, 13896–13901.
Tsuchiya, K., Ikeda, K., Niizato, K., Watabiki, S., Anno, M., Taki, K., Haga, C., Iritani, S., Matsushita, M., 2002. Parkinson's disease mimicking senile dementia of the Alzheimer type: a clinicopathological study of four autopsy cases. Neuropathology 22, 77–84.
Vincent, I., Jicha, G., Rosado, M., Dickson, D.W., 1997. Aberrant expression of mitotic cdc2/cyclin B1 kinase in degenerating neurons of Alzheimer's disease brain. J. Neurosci. 17, 3588–3598.
Wakabayashi, K., Engelender, S., Yoshimoto, M., Tsuji, S., Ross, C.A., Takahashi, H., 2000. Synphilin-1 is present in Lewy bodies in Parkinson's disease. Ann. Neurol. 47, 521–523.
Wang, Y.H., Fiol, C.J., DePaoli-Roach, A.A., Bell, A.W., Hermodson, M.A., Roach, P.J., 1988. Identification of phosphorylation sites in peptides using a gas-phase sequencer. Anal. Biochem. 174, 537–547.
Wang, Q.M., Fiol, C.J., DePaoli-Roach, A.A., Roach, P.J., 1994. Glycogen synthase kinase-3 beta is a dual specificity kinase differentially regulated by tyrosine and serine/threonine phosphorylation. J. Biol. Chem. 269, 14566–14574.
Wang, J.Z., Wu, Q., Smith, A., Grundke-Iqbal, I., Iqbal, K., 1998. Tau is phosphorylated by GSK-3 at several sites found in Alzheimer disease and its biological activity markedly inhibited only after it is prephosphorylated by A-kinase. FEBS Lett. 436, 28–34.
Zarranz, J.J., Alegre, J., Gomez-Esteban, J.C., Lezcano, E., Ros, R., Ampuero, I., Vidal, L., Hoenicka, J., Rodriguez, O., Atares, B., Llorens, V., Tortosa, E.G., Del Ser, T., Munoz, D.G., De Yebenes, J.G., 2004. The new mutation, E46K, of alpha-synuclein causes Parkinson and Lewy body dementia. Ann. Neurol. 55, 164–173.

Mitochondrial associated Metabolic Proteins are Selectively Oxidized in A30P α-Synuclein Transgenic Mice – A Model of Familial Parkinson's Disease

H. Fai Poon[1], Mark Frasier[2], Phillip Kahle[3], Christian Haas[3], Nathan Sherve[1], Vittorio Calabrese[4], Benjamin Wolozin[2A] and D. Allan Butterfield[1,5,6*]

[1] Department of Chemistry, University of Kentucky, Lexington KY 40506-0055

[2] Department of Pharmacology, Loyola University Medical Center, Maywood, IL 60153, USA

[3] Department of Biochemistry, University of Munich, Munich, Germany

[4] Department of Chemistry, Section of Biochemistry, University of Catania, Catania, Italy

[5] Center of Membrane Sciences, University of Kentucky, Lexington, KY 40506-0059, USA

[6] Sanders-Brown Center on Aging, University of Kentucky, Lexington, KY 40536, USA

[A] Current address: Department of Pharmacology, Boston University School of Medicine, Boston, MA 02118

*Address correspondence to: Professor D. Allan Butterfield, Dept. of Chemistry, Center of Membrane Sciences, and Sanders-Brown Center on Aging, University of Kentucky, Lexington KY 40506-0055
Tel: 859 257-3184
Fax 859-257-5876
e-mail:dabcns@uky.edu

Abstract

Parkinson's disease (PD) is the most common neurodegenerative movement disorder, and is characterized by the loss of dopaminergic neurons in the substantia nigra compacta. α-Synuclein is strongly implicated in the pathophysiology of PD because aggregated α-synuclein accumulates in the brains subjects with PD, mutations in α-synuclein cause familial PD and over-expressing mutant α-synuclein (A30P or A53T) causes degenerative disease in mice or drosophila. The pathophysiology of PD is poorly understood, but increasing evidence implicates mitochondrial dysfunction and oxidative stress. To understand how mutations in α-synuclein contribute to the pathophysiology of PD, we undertook a proteomic analysis of transgenic mice over-expressing A30P α-synuclein to investigate which proteins are oxidized. We observed more than two fold selective increases in specific carbonyl levels of three metabolic proteins in brains of symptomatic A30P α-synuclein mice: carbonic anhydrase 2 (Car2), alpha-enolase (Eno1) and lactate dehydrogenase 2 (Ldh2). Our findings suggest that proteins associated with impaired energy metabolism and mitochondria are particularly prone to oxidative stress associated with A30P α-synuclein.

Introduction

Parkinson's disease (PD) is the second most common neurodegenerative disorder, approximately 1% of the population by age 65 is affected with PD, increasing to 4-5% of the population by the age of 85 [1]. Loss of dopaminergic neurons in the substantia nigra compacta results in clinical symptoms of PD, such as bradykinesia, resting tremor, cogwheel rigidity, and postural instability. Although the majority of PD is sporadic, approximately 10% of PD are familial cases [2]. Mutations in α-synuclein, parkin, DJ-1 and PINK1 are all linked to early onset familial PD [3]. In the case of α-synuclein, 4 different mutations have been identified in kindreds associated with familial PD: A53T, A30P, E46A and genomic duplication [4, 5].

Oxidative damage is a prominent pathological change in PD brains [6-8]. Free radicals produced by autoxidation of dopamine, semiquinone formation, and polymerization of protein are all thought to contribute to the oxidative stress, although other stresses might also contribute to the oxidative stress associated with PD [9, 10]. The degradation of dopamine by monoamine oxidases produces hydrogen peroxide (H_2O_2) [11], and the oxidation is scavenged by the anti-oxidant systems, such as oxidation of glutathione (GSH) [12]. Other factors, such as high level of iron, might also contribute to oxidative stress [13]. Toxicity associated with this reaction is exacerbated by over-expression of wild type or mutant α-synuclein [14]. All of these factors might contribute to the oxidative changes observed in brains of subjects with PD. Increasing evidence suggests that oxidative stress in PD might also be linked to mitochondrial dysfunction, excitotoxicity, and the toxic effects of nitric oxide, all of which are believed to be associated with cell death in PD brains [15]. Although the relationships of oxidative

stress to PD are still unknown, basal protein oxidation is high in the substantia nigra of PD patients, and the levels of reactive carbonyls are increased in PD brains [7, 8]. Together, these data suggest that oxidative stress contributes significantly to the pathophysiology of PD.

α-Synuclein is a protein that is normally abundant in the brain, although its physiological functions are poorly understood. Wild-type α-synucleins can bind to lipid membranes, inhibit enzymes such as phospholipase D2, protein kinase C and the dopamine transporter (Reviewed in [16]) as well as induce brain-derived neurotrophic factor (BDNF). The A53T and A30P mutant forms of α-synucleins do not induce BDNF [17]. α-Synuclein share physical and functional homology with chaperone protein 14-3-3 and can has chaperone functions [18, 19]. These studies together suggest that α-synuclein is neuroprotective. However, the effects of α-synuclein depend on the experimental conditions. α-Synuclein has a strong tendency to aggregate, and most studies suggest that the accumulation of aggregated α-synuclein is toxic [20, 21]. The toxicity of α-synuclein aggregation may due to the decrease level of soluble α-synuclein. Expression of mutant α-synuclein cells produces increased levels of 8-hydroxyguanine, protein carbonyls, lipid peroxidation and 3-nitrotyrosine, and markedly accelerated cell death in response to oxidative insult [22]. These studies suggest that accelerated aggregation of mutant α-synucleins stimulate oxidative stress by losing the soluble α-synuclein protective effect because mutant α-synuclein increases the propensity of aggregation [23, 24]. In order to gain insight into the mechanism(s) by which loss of antioxidant ability caused by a mutation on α-synuclein lead to cell death, we used proteomics to identify the brain proteins that are significantly oxidatively modified in

symptomatic mice with a A30P mutation in α-synuclein compared to the brain proteins from wild-type mice.

Methods:

Animals

The human [A30P] α-synuclein transgene had been injected in hybrid B6 / DBA oocytes [25]. Founders were extensively (7-10 generations) back-crossed into a C57Bl/6 background. Intercrossing of the highest expressing line 31 yielded a stable colony of homozygous 31H mice [26]. These were the animals used in the present study. The mice develop symptoms between 6-14 months. The symptoms begin with a tremor and progress to an end-stage phenotype characterized by muscular rigidity, postural instability and ultimately paralysis. Mice that progressed to end stage symptoms were sacrificed by cervical dislocation and their brains hemi-sectioned. Non-transgenic control mice were C57Bl/6 mice, and were also sacrificed at the same time as the symptomatic transgenic mice.

Sample Preparation

Brain tissue extraction was performed as previously described by Sahara et al. [27] with minor modifications. Left hemi-brains were weighed and homogenized in 3 volumes of TBS (TBS, pH 7.4, 1 mM EDTA, 5mM sodium pyrophosphate, 30 mM glycerol 2-phosphate, 30 mM sodium fluoride, 1 mM EDTA) containing a protease inhibitor cocktail (Sigma-Aldrich, St. Louis, MO). Protein content was determined via the BCA method and total protein and concentration was adjusted with the homogenization buffer to be equal between samples.

Two-dimensional gel electrophoresis

Samples of the proteins in the whole brains were prepared as previously described [28]. Briefly, 200μg of protein were applied to a pH 3-10 ReadyStrip™ IPG strip (Bio-Rad, Hercules, Hercules,, CA) for isoelectric focusing. The focused IEF strip was stored at –80^{o}C until second dimension electrophoresis was performed.

For second dimension electrophoresis, Linear Gradient (8-16%) Precast criterion Tris-HCl gels (Bio-Rad, Hercules, CA) were used to separate proteins according to their molecular weight (MrW). Precision Protein^{TM} Standards (Bio-Rad, Hercules, CA) were run along with the samples.

After electrophoresis, the gel was incubated in fixing solution for 20 min. Sypro Ruby stain were used to stain the gel for 2 hours. The gels were placed in deionized water overnight for destaining.

Western Blotting

Western Blotting for 2D gels was performed as previously described [28]. 200μg of the brain protein were incubated with 2,4-dinitrophenyl hydrazine (DNPH) at room temperature (25°C) for 20 min. The gels were prepared in the same manner as for 2D-electrophoresis. The proteins from the second dimension electrophoresis gels were transferred onto nitrocellulose paper (Bio-Rad, Hercules, CA) using a Transblot-Blot® SD semi-Dry Transfer Cell (Bio-Rad, Hercules, CA) at 15V for 2 hrs. The 2,4-dinitrophenyl hydrazone (DNP) adducts of the carbonyls of the brain proteins were detected immunochemically.

Image Analysis

The gels and nitrocellulose blots were scanned and saved in TIF format using a Storm 860 Scanner (Molecular Dynamics) and Scanjet 3300C (Hewlett Packard),

respectively. PDQuest (Bio-Rad, Hercules, CA) was used for matching and analysis of visualized protein spots among differential gels and oxyblots. The principles of measuring intensity values by 2-D analysis software were similar to those of densitometric measurement. The average mode of background subtraction was used to normalize intensity values, which represents the amount of protein (total protein on gel and oxidized protein on oxyblot) per spot. After completion of spot matching, the normalized intensity of each protein spot from individual gels (or oxyblots) was compared between groups using statistical analysis.

Statistics

The data of specific carbonyl level (intensity of carbonyl level divided by the intensity of protein level of an individual spot) of 6 animals per groups (6 in control group and 6 in A30P group) were analyzed by Student's *t* tests. A value of $p < 0.05$ was considered statistically significant. Only the proteins that are considered significantly different by Student's *t*-test were selected for identification.

Trypsin digestion

Samples were digested using the techniques previously described [28]. Briefly, the selected protein spots were excised and washed with ammonium bicarbonate (NH_4HCO_3), then acetonitrile at room temperature. The protein spots were incubated with dithiothreitol, then iodoacetamide solutions. The gel pieces were digested with 20 ng/μl modified trypsin (Promega, WI) in 25 mM NH_4HCO_3 with the minimal volume to cover the gel pieces. The gel pieces were chopped into smaller pieces and incubated at 37°C overnight in a shaking incubator.

Mass Spectrometry

Digests (1 μL) were mixed with 1 μL α-cyano-4-hydroxy-trans-cinnamic acid (10 mg/mL in 0.1% TFA:ACN, 1:1, v/v). The mixture (1 μL) was deposited onto a fast evaporation nitrocellulose matrix surface, washed twice with 2 μL 5% formic acid, and analyzed with a TofSpec 2E (Micromass, UK) MALDI-TOF mass spectrometer in reflectron mode. The mass axis was adjusted with trypsin autohydrolysis peaks (m/z 2239.14, 2211.10, or 842.51) as lock masses. The MALDI spectra used for protein identification from tryptic fragments were searched against the NCBI protein databases using the MASCOT search engine (*http://www.matrixscience.com*). Peptide mass fingerprinting used the assumption that peptides are monoisotopic, oxidized at methionine residues and carbamidomethylated at cysteine residues [29-32]. Up to 1 missed trypsin cleavage was allowed. Mass tolerance of 150 ppm was the window of error allowed for matching the peptide mass values.

Results

We used a parallel approach to investigate the effect of an A30P α-synuclein mutation on specific protein oxidation [28-34]. Fig. 1 shows representative 2D-electrophoresis gels of symptomatic A30P α-synuclein transgenic mice (A30P) and non-transgenic mice after Sypro Ruby staining. Fig.2 shows representative 2D western blots of the brains of symptomatic non-transgenic mouse and A30P-α-synuclein transgenic mice. The specific carbonyl levels indicate the carbonyl level per unit mass of protein (Table I).

In comparison to wild-type mice, three proteins in the brains of A30P α-synuclein transgenic mice were found to have significantly higher specific carbonyl levels. Only the specific carbonyl level of proteins that are different statistically were identified and

reported here. These proteins were identified as carbonic anhydrase 2 (Car2), alpha-enolase (Eno1) and lactate dehydrogenase 2 (Ldh2). The specific carbonyl levels of these proteins are summarized in Table 1. The summary of the mass spectrometry results for the proteins is listed in Table 2.

Discussion

Aggregation of synuclein, increased production of free radicals, low level of reduced glutathione (GSH) and high level of iron lead to oxidative stress in PD brains [9-12, 16, 20, 21]. Processes, such as mitochondrial dysfunction, excitotoxicity, and the toxic effects of nitric oxide, then interact with the free radicals in a reinforcing cycle to produce reactive oxidative species (ROS), which further damage the brains of PD patients [15]. Significant oxidative damage was demonstrated in PD brains [6-8]. This increased production of ROS can oxidatively modify brain proteins and perturb their proper functions and activities [28-35]. A30P mutation accelerates synuclein aggregation [23, 24, 36, 37], suggesting α-synuclein aggregation mediated oxidative stress is increased in the mutant [22]. Consistent with this notion, the aggregation of α-synuclein occurs in parallel with symptoms in A30P α-synuclein transgenic mice [26]. Also, transgenic mice over-expressing α-synuclein develop an age dependent-accumulation of α-synuclein in neurons of the brain stem [38, 39], suggesting the α-synuclein aggregation associated oxidative stress is responsible for the pathology in the A30P α-synuclein transgenic mice.

However, the target of oxidation and mechanism of toxicity is not well understood. In the current study, we identified that Car2, Eno1 and Ldh2 are oxidized significantly (2-fold, 2-fold and 6-fold increase, respectively) in the brains of A30P-α-synuclein transgenic mice, when compared to those brain proteins of wild-type mice.

Car2 is a Zn^{2+} metallo-enzyme that catalyzes reversible hydration of carbon dioxide (CO_2) to bicarbonate (HCO_3^-), a reaction fundamental to many cellular and

systemic processes including glycolysis and fluid secretion. Glia use this process to govern the pH shift associated with normal neuroactivity [40-42]. Since the extracellular pH shift affects normal and pathological brain functions, dysfunction of Car2 usually results in neuronal abnormalities. BLAST alignments of Car2 with proteins from *M. musculus* shows high (68%) similarity in amino acid level to the mitochondrial counterpart carbonic anhydrase 5a (Car5a) and 5b (Car5b). One can speculate that they may couple or interact with each other to function in metabolic process, cellular transport, gluconeogenesis and mitochondrial metabolism [43, 44]. Car2-deficient mice display shrinking and possible degeneration of oligodendrocytes in the gray and white matter, swollen astrocytes in the gray matter and hypertrophied astrocytes in the white matter [45]. The activity decline of Car2 in the forebrain of the C57/B quaking mice, which show rapid tremor, indicates that Car2 plays an important role in normal functions of motor neurons [46]. Our study shows that Car2 is significantly oxidized in A30P α-synuclein mice and since oxidative preteen generally have decreased acitivity [35], this result suggests the activity of this enzyme is possibly decreased. The declined activity of Car2 likely would lead to the loss of the buffering system in brains and result in neurodegeneration. Also, since zinc is the cofactor of Car2 [47], oxidative modification of Car2 may trigger the release of the Zn^{2+} metal to the A30P α-synuclein mice brains. A 18-35% increase of zinc content was demonstrated in the caudate nucleus and lateral putamen of PD brains [48]. The precipitation of α-synuclein is also significantly accelerated in vitro when Zn^{2+} is present [49]. Therefore, oxidative modification of Car2 possibly enhances α-synuclein aggregation, and causes pH shift and mitochondrial dysfunction in the A30P α-synuclein transgenic mice.

Ldh2 is a subunit of lactate dehydrogenase (LDH). LDH is a glycolytic protein that catalyzes the reversible NAD-dependent interconversion of pyruvate to lactate. A single mutation in Ldh2 can decrease the activity of LDH [50, 51], suggesting that the Ldh2 subunit is critical to LDH activity. Unlike in muscle cells where lactate is only formed under anaerobic condition, LDH isoform 5 (LDH-5) in astrocytes favors the formation of lactate [52]. Also, LDH-5 is more abundant in mitochondria than elsewhere in cells [53], indicating that lactate is the predominant monocarboxylate oxidized by mitochondria for intracellular lactate transport. Moreover, production of lactate also serves a purpose of intercellular energy transfer from astrocytes to neurons because lactate is secreted by astrocytes, taken up by neurons, and converted to pyruvate, which enters the Kerb's cycle for ATP production [54]. These studies together suggest that LDH play a significant role in intra- and intercellular lactate shuttling. Lactate appears to be the main energetic compound delivered by astrocytes [55] and is the only oxidizable energy substrate available to support neuronal recovery in CNS [56-58]. Here we show that Ldh2 is significantly modified by oxidative insults in A30P α-synuclein transgenic mice brains, suggesting the possible oxidative inactivation of Ldh2 may decrease the production of lactate, thus decrease ATP availability for cellular processes. Impairment of energy metabolism in PD models was reported [59, 60]. Therefore, the oxidative inactivation of Ldh2 may contribute to the alteration of energy metabolism in PD brain.

Eno1 is a subunit of enolase, the other subunits being β- and γ-enolase. Two of the subunits form the active enolase isoforms (αα, ββ, γγ, αβ and αβ), which interconvert 2-phosphoglycerate and phosphoenolpyruvate during glycolysis. Since αγ and γγ isoforms are predominately in the brain, they are called neuron-specific enolases (NSE)

[61]. A decline of enolase activity results in abnormal growth and reduced metabolism in brains [62]. It was also reported that the expression of NSE coincides with the onset of synaptic connections [63-65]. Also, the loss of the mitochondrial constituent (α-ketoglutarate dehydrogenase complex, KGDHC)-enriched cells is proportional to the total loss of immunoreactivity to NSE. These studies show that enolase not only is involved in metabolism, but also in cell differentiation, normal growth and mitochondrial function. Moreover, enolase and other glycolytic enzymes were identified in an intermembrane space/outer mitochondrial membrane fraction [66], suggesting glycolytic enzymes are associated with proper mitochondrial function. Additionally, increased Eno1 specific carbonyl level in the Alzheimer's disease brain suggests that the loss of activity by oxidative modification of Eno1 possibly leads to neurodegeneration [67]. We show here that the specific carbonyl level of Eno1 also is significantly increased in A30P α-synuclein transgenic mice compared to that of non-transgenic mice, suggesting the activity of Eno1 is possibly declined by oxidative modification. This putative oxidative inactivation may also alter normal glycolysis and mitochondrial function in brain and contribute to the alteration of energy metabolism in PD.

The striking feature of Ldh2, Eno1 (possibly Car2) is that they are all associated with mitochondrial function. Oxidative inactivation of Car2 can cause the accumulation of CO_2 and pH shift in neurons, which possibly leads to alteration of mitochondria potential and mitochondrial deficits. Increasing data implicate mitochondrial decrements and oxidation in PD [68-70]. Also, 1-methyl-4-phenyl-1,2,3,6-tetrahydropyridine (MPTP) and rotenone target the mitochondria with increased oxidative modification of proteins and α-synuclein aggregation [71-74]. Moreover, DJ-1, PINK1 and parkin all

appear to modulate mitochondrial function [75-77]. The observation that each of the proteins significantly oxidized in the A30P synuclein mice is associated with mitochondria, is consistent with the mitochondrial hypothesis and implicates mitochondrial pathology in toxicity associated with aggregated synuclein.

Glucose is transferred from capillaries to astrocytes where it undergoes either glycolysis or gluconeogenesis. Since the LDH in astrocytes favors the formation of lactate [52], lactate is formed even under aerobic conditions. Lactate is then transferred to neurons with a proton by the monocarboxylate transporter (MCT). In neurons, lactate is then converted to pyruvate to enter the Kerb's cycle, ATPs are generated subsequently through the electron transport chain with CO_2 and H_2O as the by-products. CO_2 is diffused from neurons to astrocytes then removed from the CNS. Car2 is responsible for maintaining this CO_2 gradient between astrocytes and neurons by converting CO_2 to HCO_3^-. In our current study, we found the specific carbonyl level of Ldh2, Eno1 and Car2 are significantly increased in A30P α-synuclein transgenic mice compared to that of wild-type mice. Since oxidative inactivation of enzyme is well-established [35], current study suggests that the activity of Ldh2, Car2 and Eno1 are possibly impaired. Since Eno1 and Ldh2 are involved in glycolysis and mitochondria function, the declined activity of these enzymes would not only reduce ATP production directly in astrocytes, but also decrease the production of lactate for further ATP production in neurons. This may result in neuronal starvation and eventually cell death. Also, wide spread astrocytosis observed in A30P α-synuclein transgenic mice not only indicate neuronal injury [78], but also implicate the incapability of astrocytes to produce lactate for neuronal recovery in the brain stem of the A30P α-synuclein transgenic mice.

Aggregations of α-synuclein in neuron may induce oxidative stress in the brain stem of A30P α-synuclein transgenic mice [38, 39]. Since impairment of energy production and mitochondrial dysfunction leads to neurodegeneration PD both *in vitro* and *in vivo* studies [79-86], our current study suggests that the oxidative stress mediated impaired energy metabolism and mitochondrial dysfunction may be responsible, at least partially, for the neurodegeneration in the brains of A30P α-synuclein transgenic mice. Furthermore, this oxidative stress mediated impaired energy metabolism and mitochondrial dysfunction may possibly be brought about through the oxidative inactivation of Eno1, Ldh2 and Car2. Comparison of the enzymes' activities and energy metabolism in the A30P α-synuclein mice with the wild-type mice are in progress. This suggests that the mitochondria dysfunction and impaired metabolism in familial PD may be associated with the oxidative inactivation of Eno1, Ldh2 and Car2.

Acknowledgements

This work was supported in part by grants from NIH to D.A.B. [AG-105119; AG-10836] and to B.W. [NIH grant NS41786 and DAMD grant 17-01-1-0781].

Reference

1. Eriksen, J.L., T.M. Dawson, D.W. Dickson, and L. Petrucelli, *Caught in the act: alpha-synuclein is the culprit in Parkinson's disease.* Neuron, 2003. **40**(3): p. 453-6.
2. Giasson, B.I. and V.M. Lee, *Are ubiquitination pathways central to Parkinson's disease?* Cell, 2003. **114**(1): p. 1-8.
3. Dawson, T.M. and V.L. Dawson, *Molecular pathways of neurodegeneration in Parkinson's disease.* Science, 2003. **302**(5646): p. 819-22.
4. Polymeropoulos, M.H., C. Lavedan, E. Leroy, S.E. Ide, A. Dehejia, A. Dutra, et al., *Mutation in the alpha-synuclein gene identified in families with Parkinson's disease.* Science, 1997. **276**(5321): p. 2045-7.
5. Kruger, R., W. Kuhn, T. Muller, D. Woitalla, M. Graeber, S. Kosel, et al., *Ala30Pro mutation in the gene encoding alpha-synuclein in Parkinson's disease.* Nat Genet, 1998. **18**(2): p. 106-8.
6. Yoritaka, A., N. Hattori, K. Uchida, M. Tanaka, E.R. Stadtman, and Y. Mizuno, *Immunohistochemical detection of 4-hydroxynonenal protein adducts in Parkinson disease.* Proc Natl Acad Sci U S A, 1996. **93**(7): p. 2696-701.
7. Alam, Z.I., S.E. Daniel, A.J. Lees, D.C. Marsden, P. Jenner, and B. Halliwell, *A generalised increase in protein carbonyls in the brain in Parkinson's but not incidental Lewy body disease.* J Neurochem, 1997. **69**(3): p. 1326-9.
8. Floor, E. and M.G. Wetzel, *Increased protein oxidation in human substantia nigra pars compacta in comparison with basal ganglia and prefrontal cortex measured with an improved dinitrophenylhydrazine assay.* J Neurochem, 1998. **70**(1): p. 268-75.
9. Graham, D.G., *Oxidative pathways for catecholamines in the genesis of neuromelanin and cytotoxic quinones.* Mol Pharmacol, 1978. **14**(4): p. 633-43.
10. Tse, D.C., R.L. McCreery, and R.N. Adams, *Potential oxidative pathways of brain catecholamines.* J Med Chem, 1976. **19**(1): p. 37-40.
11. Adams, R.N., E. Murrill, R. McCreery, L. Blank, and M. Karolczak, *6-Hydroxydopamine, a new oxidation mechanism.* Eur J Pharmacol, 1972. **17**(2): p. 287-92.
12. Spina, M.B. and G. Cohen, *Exposure of striatal [corrected] synaptosomes to L-dopa increases levels of oxidized glutathione.* J Pharmacol Exp Ther, 1988. **247**(2): p. 502-7.
13. Youdim, M.B., D. Ben-Shachar, and P. Riederer, *Is Parkinson's disease a progressive siderosis of substantia nigra resulting in iron and melanin induced neurodegeneration?* Acta Neurol Scand Suppl, 1989. **126**: p. 47-54.
14. Ostrerova-Golts, N., L. Petrucelli, J. Hardy, J.M. Lee, M. Farer, and B. Wolozin, *The A53T alpha-synuclein mutation increases iron-dependent aggregation and toxicity.* J Neurosci, 2000. **20**(16): p. 6048-54.
15. Jenner, P., *Oxidative stress in Parkinson's disease.* Ann Neurol, 2003. **53 Suppl 3**: p. S26-36; discussion S36-8.
16. Goedert, M., *Alpha-synuclein and neurodegenerative diseases.* Nat Rev Neurosci, 2001. **2**(7): p. 492-501.

17. Kohno, R., H. Sawada, Y. Kawamoto, K. Uemura, H. Shibasaki, and S. Shimohama, *BDNF is induced by wild-type alpha-synuclein but not by the two mutants, A30P or A53T, in glioma cell line.* Biochem Biophys Res Commun, 2004. **318**(1): p. 113-8.
18. Ostrerova, N., L. Petrucelli, M. Farrer, N. Mehta, P. Choi, J. Hardy, et al., *alpha-Synuclein shares physical and functional homology with 14-3-3 proteins.* J Neurosci, 1999. **19**(14): p. 5782-91.
19. Souza, J.M., B.I. Giasson, V.M. Lee, and H. Ischiropoulos, *Chaperone-like activity of synucleins.* FEBS Lett, 2000. **474**(1): p. 116-9.
20. Lee, S.J., *alpha-synuclein aggregation: a link between mitochondrial defects and Parkinson's disease?* Antioxid Redox Signal, 2003. **5**(3): p. 337-48.
21. Snyder, H., K. Mensah, C. Theisler, J. Lee, A. Matouschek, and B. Wolozin, *Aggregated and monomeric alpha-synuclein bind to the S6' proteasomal protein and inhibit proteasomal function.* J Biol Chem, 2003. **278**(14): p. 11753-9.
22. Lee, M., D. Hyun, B. Halliwell, and P. Jenner, *Effect of the overexpression of wild-type or mutant alpha-synuclein on cell susceptibility to insult.* J Neurochem, 2001. **76**(4): p. 998-1009.
23. Li, J., V.N. Uversky, and A.L. Fink, *Conformational behavior of human alpha-synuclein is modulated by familial Parkinson's disease point mutations A30P and A53T.* Neurotoxicology, 2002. **23**(4-5): p. 553-67.
24. Li, J., V.N. Uversky, and A.L. Fink, *Effect of familial Parkinson's disease point mutations A30P and A53T on the structural properties, aggregation, and fibrillation of human alpha-synuclein.* Biochemistry, 2001. **40**(38): p. 11604-13.
25. Kahle, P.J., M. Neumann, L. Ozmen, V. Muller, H. Jacobsen, A. Schindzielorz, et al., *Subcellular localization of wild-type and Parkinson's disease-associated mutant alpha -synuclein in human and transgenic mouse brain.* J Neurosci, 2000. **20**(17): p. 6365-73.
26. Neumann, M., P.J. Kahle, B.I. Giasson, L. Ozmen, E. Borroni, W. Spooren, et al., *Misfolded proteinase K-resistant hyperphosphorylated alpha-synuclein in aged transgenic mice with locomotor deterioration and in human alpha-synucleinopathies.* J Clin Invest, 2002. **110**(10): p. 1429-39.
27. Sahara, N., J. Lewis, M. DeTure, E. McGowan, D.W. Dickson, M. Hutton, et al., *Assembly of tau in transgenic animals expressing P301L tau: alteration of phosphorylation and solubility.* J Neurochem, 2002. **83**(6): p. 1498-508.
28. Poon, H.F., A. Castegna, S.A. Farr, V. Thongboonkerd, B.C. Lynn, W.A. Banks, et al., *Quantitative proteomics analysis of specific protein expression and oxidative modification in aged senescence-accelerated-prone 8 mice brain.* Neuroscience, 2004. **126**(4): p. 915-26.
29. Castegna, A., M. Aksenov, M. Aksenova, V. Thongboonkerd, J.B. Klein, W.M. Pierce, et al., *Proteomic identification of oxidatively modified proteins in Alzheimer's disease brain. Part I: creatine kinase BB, glutamine synthase, and ubiquitin carboxy-terminal hydrolase L-1.* Free Radic Biol Med, 2002. **33**(4): p. 562-71.
30. Castegna, A., V. Thongboonkerd, J.B. Klein, B. Lynn, W.R. Markesbery, and D.A. Butterfield, *Proteomic identification of nitrated proteins in Alzheimer's disease brain.* J Neurochem, 2003. **85**(6): p. 1394-401.

31. Castegna, A., V. Thongboonkerd, J.B. Klein, B. Lynn, W.R. Markesbery, and D.A. Butterfield, *Proteomic identification of oxidatively modified proteins in gracile axonal dystrophy mice.* J Neurochem, 2004. **88**(6): p. 1540-6.
32. Butterfield, D.A., D. Boyd-Kimbel, and C. A., *Proteomics in Alzheimer's disease; Insights into mechanisms into neurodegeneration.* J. Neurochem., 2003. **86**(1313-1327).
33. Butterfield, D.A., *Proteomics: a new approach to investigate oxidative stress in Alzheimer's disease brain.* Brain Res, 2004. **1000**(1-2): p. 1-7.
34. Butterfield, D.A. and A. Castegna, *Proteomics for the identification of specifically oxidized proteins in brain: technology and application to the study of neurodegenerative disorders.* Amino Acids, 2003. **25**(3-4): p. 419-25.
35. Butterfield , D.A. and E.R. Stadtman, *Protein oxidation processes in aging brain.* Adv. Cell Aging Gerontol, 1997. **2**: p. 161–191.
36. Conway, K.A., J.D. Harper, and P.T. Lansbury, *Accelerated in vitro fibril formation by a mutant alpha-synuclein linked to early-onset Parkinson disease.* Nat Med, 1998. **4**(11): p. 1318-20.
37. Narhi, L., S.J. Wood, S. Steavenson, Y. Jiang, G.M. Wu, D. Anafi, et al., *Both familial Parkinson's disease mutations accelerate alpha-synuclein aggregation.* J Biol Chem, 1999. **274**(14): p. 9843-6.
38. Kahle, P.J., M. Neumann, L. Ozmen, V. Muller, S. Odoy, N. Okamoto, et al., *Selective insolubility of alpha-synuclein in human Lewy body diseases is recapitulated in a transgenic mouse model.* Am J Pathol, 2001. **159**(6): p. 2215-25.
39. Giasson, B.I., J.E. Duda, S.M. Quinn, B. Zhang, J.Q. Trojanowski, and V.M. Lee, *Neuronal alpha-synucleinopathy with severe movement disorder in mice expressing A53T human alpha-synuclein.* Neuron, 2002. **34**(4): p. 521-33.
40. Chesler, M. and K. Kaila, *Modulation of pH by neuronal activity.* Trends Neurosci, 1992. **15**(10): p. 396-402.
41. Deitmer, J.W. and C.R. Rose, *pH regulation and proton signalling by glial cells.* Prog Neurobiol, 1996. **48**(2): p. 73-103.
42. Tong, C.K. and M. Chesler, *Endogenous pH shifts facilitate spreading depression by effect on NMDA receptors.* J Neurophysiol, 1999. **81**(4): p. 1988-91.
43. Heck, R.W., S.M. Tanhauser, R. Manda, C. Tu, P.J. Laipis, and D.N. Silverman, *Catalytic properties of mouse carbonic anhydrase V.* J Biol Chem, 1994. **269**(40): p. 24742-6.
44. Shah, G.N., D. Hewett-Emmett, J.H. Grubb, M.C. Migas, R.E. Fleming, A. Waheed, et al., *Mitochondrial carbonic anhydrase CA VB: differences in tissue distribution and pattern of evolution from those of CA VA suggest distinct physiological roles.* Proc Natl Acad Sci U S A, 2000. **97**(4): p. 1677-82.
45. Cammer, W., H. Zhang, and M. Cammer, *Glial cell abnormalities in the CNS of the carbonic anhydrase II deficient mutant mouse.* J Neurol Sci, 1993. **118**(1): p. 1-9.
46. Sapirstein, V.S., C. Flynn, and M.B. Lees, *Developmental changes in carbonic anhydrase and adenylate cyclase in quaking mice.* Brain Res, 1980. **185**(2): p. 373-83.

47. Kiefer, L.L. and C.A. Fierke, *Functional characterization of human carbonic anhydrase II variants with altered zinc binding sites.* Biochemistry, 1994. **33**(51): p. 15233-40.
48. Dexter, D.T., F.R. Wells, A.J. Lees, F. Agid, Y. Agid, P. Jenner, et al., *Increased nigral iron content and alterations in other metal ions occurring in brain in Parkinson's disease.* J Neurochem, 1989. **52**(6): p. 1830-6.
49. Kim, T.D., S.R. Paik, C.H. Yang, and J. Kim, *Structural changes in alpha-synuclein affect its chaperone-like activity in vitro.* Protein Sci, 2000. **9**(12): p. 2489-96.
50. Maekawa, M., K. Sudo, M. Kitajima, Y. Matsuura, S.S. Li, and T. Kanno, *Analysis of a genetic mutation in an electrophoretic variant of the human lactate dehydrogenase-B(H) subunit.* Hum Genet, 1993. **91**(5): p. 423-6.
51. Sudo, K., M. Maekawa, T. Kanno, S.S. Li, S. Akizuki, and T. Magara, *Premature termination mutations in two patients with deficiency of lactate dehydrogenase H(B) subunit.* Clin Chem, 1994. **40**(8): p. 1567-70.
52. Bittar, P.G., Y. Charnay, L. Pellerin, C. Bouras, and P.J. Magistretti, *Selective distribution of lactate dehydrogenase isoenzymes in neurons and astrocytes of human brain.* J Cereb Blood Flow Metab, 1996. **16**(6): p. 1079-89.
53. Brooks, G.A., H. Dubouchaud, M. Brown, J.P. Sicurello, and C.E. Butz, *Role of mitochondrial lactate dehydrogenase and lactate oxidation in the intracellular lactate shuttle.* Proc Natl Acad Sci U S A, 1999. **96**(3): p. 1129-34.
54. Deitmer, J.W., *Strategies for metabolic exchange between glial cells and neurons.* Respir Physiol, 2001. **129**(1-2): p. 71-81.
55. Dringen, R., R. Gebhardt, and B. Hamprecht, *Glycogen in astrocytes: possible function as lactate supply for neighboring cells.* Brain Res, 1993. **623**(2): p. 208-14.
56. Sahlas, D.J., A. Liberman, and H.M. Schipper, *Role of heme oxygenase-1 in the biogenesis of corpora amylacea.* Biogerontology, 2002. **3**(4): p. 223-31.
57. Schurr, A., R.S. Payne, J.J. Miller, and B.M. Rigor, *Brain lactate is an obligatory aerobic energy substrate for functional recovery after hypoxia: further in vitro validation.* J Neurochem, 1997. **69**(1): p. 423-6.
58. Schurr, A., R.S. Payne, J.J. Miller, and B.M. Rigor, *Brain lactate, not glucose, fuels the recovery of synaptic function from hypoxia upon reoxygenation: an in vitro study.* Brain Res, 1997. **744**(1): p. 105-11.
59. Mytilineou, C., P. Werner, S. Molinari, A. Di Rocco, G. Cohen, and M.D. Yahr, *Impaired oxidative decarboxylation of pyruvate in fibroblasts from patients with Parkinson's disease.* J Neural Transm Park Dis Dement Sect, 1994. **8**(3): p. 223-8.
60. Zeevalk, G.D., L. Manzino, and P.K. Sonsalla, *NMDA receptors modulate dopamine loss due to energy impairment in the substantia nigra but not striatum.* Exp Neurol, 2000. **161**(2): p. 638-46.
61. Keller, A., A. Berod, M. Dussaillant, N. Lamande, F. Gros, and M. Lucas, *Coexpression of alpha and gamma enolase genes in neurons of adult rat brain.* J Neurosci Res, 1994. **38**(5): p. 493-504.
62. Tholey, G., M. Ledig, and P. Mandel, *Modifications in energy metabolism during the development of chick glial cells and neurons in culture.* Neurochem Res, 1982. **7**(1): p. 27-36.

63. Whitehead, M.C., P.J. Marangos, S.M. Connolly, and D.K. Morest, *Synapse formation is related to the onset of neuron-specific enolase immunoreactivity in the avian auditory and vestibular systems.* Dev Neurosci, 1982. **5**(4): p. 298-307.
64. Maxwell, G.D., M.C. Whitehead, S.M. Connolly, and P.J. Marangos, *Development of neuron-specific enolase immunoreactivity in avian nervous tissue in vivo and in vitro.* Brain Res, 1982. **255**(3): p. 401-18.
65. Hedgecock, E.M., J.G. Culotti, J.N. Thomson, and L.A. Perkins, *Axonal guidance mutants of Caenorhabditis elegans identified by filling sensory neurons with fluorescein dyes.* Dev Biol, 1985. **111**(1): p. 158-70.
66. Giege, P., J.L. Heazlewood, U. Roessner-Tunali, A.H. Millar, A.R. Fernie, C.J. Leaver, et al., *Enzymes of glycolysis are functionally associated with the mitochondrion in Arabidopsis cells.* Plant Cell, 2003. **15**(9): p. 2140-51.
67. Castegna, A., M. Aksenov, V. Thongboonkerd, J.B. Klein, W.M. Pierce, R. Booze, et al., *Proteomic identification of oxidatively modified proteins in Alzheimer's disease brain. Part II: dihydropyrimidinase-related protein 2, alpha-enolase and heat shock cognate 71.* J Neurochem, 2002. **82**(6): p. 1524-32.
68. Sherer, T.B., R. Betarbet, and J.T. Greenamyre, *Environment, mitochondria, and Parkinson's disease.* Neuroscientist, 2002. **8**(3): p. 192-7.
69. Schapira, A.H., M. Gu, J.W. Taanman, S.J. Tabrizi, T. Seaton, M. Cleeter, et al., *Mitochondria in the etiology and pathogenesis of Parkinson's disease.* Ann Neurol, 1998. **44**(3 Suppl 1): p. S89-98.
70. Schapira, A.H., *Causes of neuronal death in Parkinson's disease.* Adv Neurol, 2001. **86**: p. 155-62.
71. Pennathur, S., V. Jackson-Lewis, S. Przedborski, and J.W. Heinecke, *Mass spectrometric quantification of 3-nitrotyrosine, ortho-tyrosine, and o,o'-dityrosine in brain tissue of 1-methyl-4-phenyl-1,2,3, 6-tetrahydropyridine-treated mice, a model of oxidative stress in Parkinson's disease.* J Biol Chem, 1999. **274**(49): p. 34621-8.
72. Ferrante, R.J., P. Hantraye, E. Brouillet, and M.F. Beal, *Increased nitrotyrosine immunoreactivity in substantia nigra neurons in MPTP treated baboons is blocked by inhibition of neuronal nitric oxide synthase.* Brain Res, 1999. **823**(1-2): p. 177-82.
73. Sherer, T.B., R. Betarbet, J.H. Kim, and J.T. Greenamyre, *Selective microglial activation in the rat rotenone model of Parkinson's disease.* Neurosci Lett, 2003. **341**(2): p. 87-90.
74. Sherer, T.B., J.H. Kim, R. Betarbet, and J.T. Greenamyre, *Subcutaneous rotenone exposure causes highly selective dopaminergic degeneration and alpha-synuclein aggregation.* Exp Neurol, 2003. **179**(1): p. 9-16.
75. Canet-Aviles, R.M., M.A. Wilson, D.W. Miller, R. Ahmad, C. McLendon, S. Bandyopadhyay, et al., *The Parkinson's disease protein DJ-1 is neuroprotective due to cysteine-sulfinic acid-driven mitochondrial localization.* Proc Natl Acad Sci U S A, 2004. **101**(24): p. 9103-8.
76. Valente, E.M., P.M. Abou-Sleiman, V. Caputo, M.M. Muqit, K. Harvey, S. Gispert, et al., *Hereditary early-onset Parkinson's disease caused by mutations in PINK1.* Science, 2004. **304**(5674): p. 1158-60.

77. Palacino, J.J., D. Sagi, M.S. Goldberg, S. Krauss, C. Motz, M. Wacker, et al., *Mitochondrial dysfunction and oxidative damage in parkin-deficient mice.* J Biol Chem, 2004. **279**(18): p. 18614-22.
78. Frasier, M., M. Walzer, L. McCarthy, D. Magnuson, J.M. Lee, C. Haas, et al., *Tau phosphorylation increases in symptomatic mice over-expressing A30P alpha-synuclein.* Exp. Neuro., 2004. **(In Press)**.
79. Benecke, R., P. Strumper, and H. Weiss, *Electron transfer complexes I and IV of platelets are abnormal in Parkinson's disease but normal in Parkinson-plus syndromes.* Brain, 1993. **116 (Pt 6)**: p. 1451-63.
80. Bouyer, J.J., D.H. Park, T.H. Joh, and V.M. Pickel, *Chemical and structural analysis of the relation between cortical inputs and tyrosine hydroxylase-containing terminals in rat neostriatum.* Brain Res, 1984. **302**(2): p. 267-75.
81. Mizuno, Y., S. Ohta, M. Tanaka, S. Takamiya, K. Suzuki, T. Sato, et al., *Deficiencies in complex I subunits of the respiratory chain in Parkinson's disease.* Biochem Biophys Res Commun, 1989. **163**(3): p. 1450-5.
82. Parker, W.D., Jr., S.J. Boyson, and J.K. Parks, *Abnormalities of the electron transport chain in idiopathic Parkinson's disease.* Ann Neurol, 1989. **26**(6): p. 719-23.
83. Shoffner, J.M., R.L. Watts, J.L. Juncos, A. Torroni, and D.C. Wallace, *Mitochondrial oxidative phosphorylation defects in Parkinson's disease.* Ann Neurol, 1991. **30**(3): p. 332-9.
84. Marey-Semper, I., M. Gelman, and M. Levi-Strauss, *The high sensitivity to rotenone of striatal dopamine uptake suggests the existence of a constitutive metabolic deficiency in dopaminergic neurons from the substantia nigra.* Eur J Neurosci, 1993. **5**(8): p. 1029-34.
85. Zeevalk, G.D., E. Derr-Yellin, and W.J. Nicklas, *Relative vulnerability of dopamine and GABA neurons in mesencephalic culture to inhibition of succinate dehydrogenase by malonate and 3-nitropropionic acid and protection by NMDA receptor blockade.* J Pharmacol Exp Ther, 1995. **275**(3): p. 1124-30.
86. Zeevalk, G.D., L. Manzino, J. Hoppe, and P. Sonsalla, *In vivo vulnerability of dopamine neurons to inhibition of energy metabolism.* Eur J Pharmacol, 1997. **320**(2-3): p. 111-9.

Table 1: Specific carbonyl level of oxidized proteins in A30P-α synuclein mice			
Proteomics Identified Protein	Wild-type Mice (A.U.± S.E.M.) (n=6)	A30P-α synuclein Transgenic Mice (n = 6)	p value
Carbonic anhydrase 2 (Car2)	0.92±0.19	2.22±0.59	< 0.05
alpha-enolase (Eno1)	0.51±0.09	0.93±0.17	< 0.05
Lactate dehydrogenase 2 (Ldh2)	0.29±0.18	1.73±0.63	< 0.05

Table 2: Summary of proteins identified by mass spectrometry						
Identified Protein	gi accession #	# Peptides matched	% Coverage of matched peptides	pI, MrW (kD)	Mowse Score	Probability of a random identification hit
Carbonic anhydrase 2 (Car2)	gi|33243954	9	30	6.52, 29.1	75	3.16×10^{-8}
alpha-enolase (Eno1)	gi|13637776	23	61	6.37, 47.4	208	1.58×10^{-21}
lactate dehydrogenase 2 (Ldh2)	gi|6678674	11	36	5.7, 36.8	103	5.0×10^{-11}

Figure legends

Fig. 1 Representative 2D gel electrophoresis pattern of proteins from mouse brain stem of control (top panel) and symptomatic A30P α-synuclein transgenic mice (bottom panel). Proteins after 2D electrophoresis from the brains of non-transgenic (control, left, top panel) mice and symptomatic A30P α-synuclein transgenic mice (left, bottom panel). Panels on right show expanded of regions of the 2D gel from the mouse brain stems (outlined in the box). The right, top panel shows the expanded region of non-transgenic control brain stem, and the right bottom panel shows the expanded region of symptomatic A30P α-synuclein transgenic mouse brain stem.

Fig. 2 Representative Western blot showing carbonyl-modified proteins from the brains of A30P α-synuclein transgenic mice and non-transgenic mice. Left hand blots show carbonyl western blots of brain stem lysates from A30P α-synuclein transgenic mice (top) and non-transgenic control mice (bottom). Arrows point to proteins showing significant changes. Right hand blots show expansions of the blot outlined in the box. Carbonyl western-blot from the brain stem of non-transgenic mice are shown in the upper panel and A30P α-synuclein transgenic mice in the lower panel. .

Fig. 1

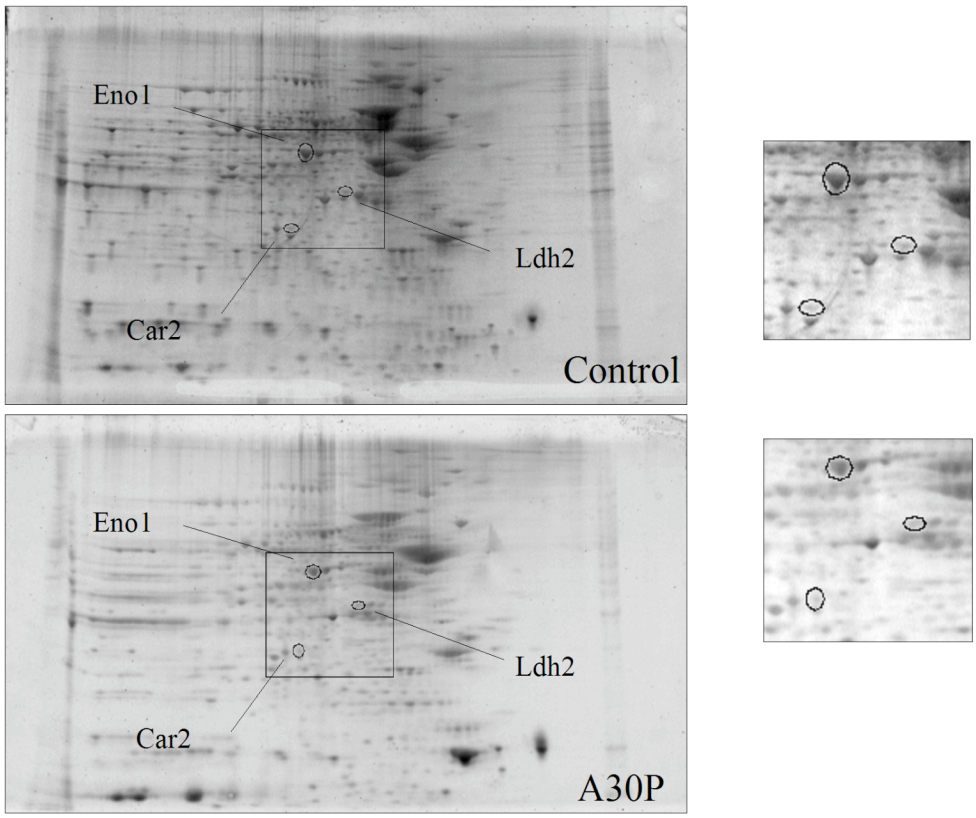

Fig. 2

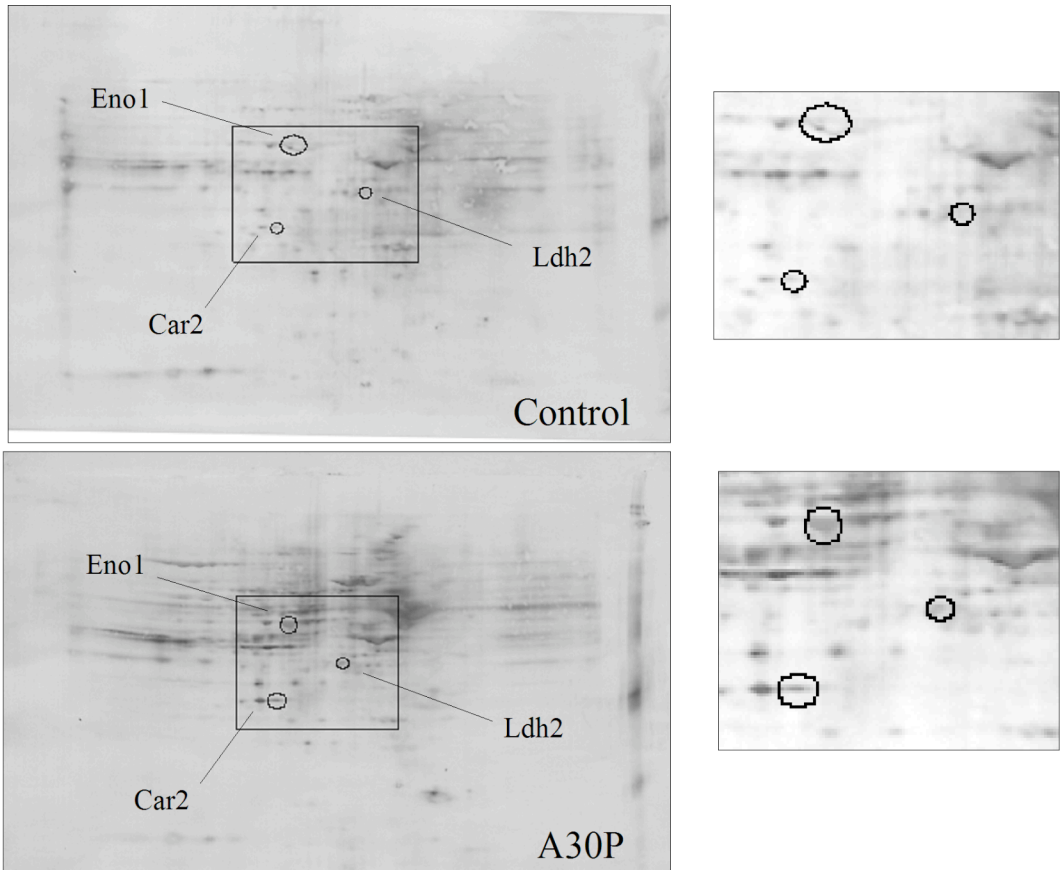

Similar Patterns of Mitochondrial Vulnerability and Rescue Induced by Genetic Modification of α-Synuclein, Parkin and DJ-1 in *C. Elegans*

Rina Ved[1], Anne Sluder[2], Beth Westlund[2], Marius Hoener[3], Serge Przedborsky[4], Clifford Steer, Aixa Alfonso[5], Leo Liu[2] and Benjamin Wolozin[1]

[1]Dept. of Pharmacology, Loyola University Medical Center; [2]Cambria Biosciences; [3]Hoffmann-La Roche [4]Neurology Institute, Columbia University; [5]Dept. of Biological Science, University of Illinois

Abstract

The etiology of Parkinson's disease is thought to have both genetic and environmental factors, but the mechanism by which these factors might intersect remains poorly understood. We have now used a pharmacological screen to compare the patterns of vulnerability and rescue of *C. elegans* with modification of three different genetic factors implicated in PD, α-synuclein, parkin and DJ-1. We report that *C. elegans* with genetic manipulation of α-synuclein, DJ-1 or the C. elegans parkin homologue, KO8E3.7, produces similar patterns of pharmacological vulnerability and rescue. C. elegans lines expressing wild type α-synuclein or A53T α-synuclein, or lacking the C. elegans parkin homologue, KO8E3.7, were more vulnerable than non-transgenic nematodes to mitochondrial complex I inhibitors, including rotenone, fenperoximate, pyridaben or stigmatellin. In contrast, the lines did not show increased sensitivity to paraquat, sodium azide, divalent metal ions (FeII or CuII) or etoposide compared to non-transgenic nematodes. Analysis of rescue from rotenone toxicity also showed similar responses for the nematodes expressing α-synuclein constructs or lacking KO8E3.7. Each of the PD-related lines was partially rescued by the anti-oxidant probucol, the mitochondrial complex II activator, D-β-hydroxybutyrate (DβHB) or the anti-apoptotic bile acid tauro-urso-dexycholic acid (TUDCA). Complete protection in all lines was achieved by combining DβHB with TUDCA but not with probucol. DJ-1 is another gene implicated in PD that has been previously shown to sensitize cells to a variety of toxic insults. We observed that knockdown of the *C. elegans* homologue of DJ-1, B0432.2, sensitized *C. elegans* to rotenone, and that a combination of DβHB and TUDCA fully rescued *C. elegans* from rotenone induced toxicity. These results suggest that mitochondrial

function is an important target of different PD-related genes in *C. elegans*.

INTRODUCTION

The etiology of Parkinson's disease is thought to have both genetic and environmental components (Dauer and Przedborski, 2003). Epidemiological studies show that PD is more common in rural areas, and increased rates of PD are associated with the use of agricultural toxins, such as pesticides and herbicides (Langston, 1998). Attention has focused on inhibitors of the mitochondrial electron transport chain because some of the agricultural toxins implicated in PD are complex I inhibitors (Langston, 1998). In addition, ingestion of complex I inhibitors causes syndromes related to PD. The complex I inhibitor MPTP selectively kills dopaminergic neurons in many types of animals (Dauer and Przedborski, 2003). Rotenone, another complex I inhibitor, also causes a PD-related syndrome in rats (Betarbet et al., 2000). Recent studies suggest that rotenone causes multiple changes in the mitochondria, inhibiting mitochondrial function, reducing ATP generation, increasing free radical production and possibly inducing other changes (Hoglinger et al., 2003; Sherer et al., 2002; Sherer et al., 2003). These factors implicate disruption of mitochondrial function, and particularly complex I inhibition, in the etiology of PD.

Some cases of PD and PD-related disorders show genetic transmission, and an increasing number of the genes associated with these familial cases of PD have been identified. Mutation of α-synuclein (at A53T, A30P or K46E) or duplication of α-synuclein is associated with familial Parkinsonisms in a number of kindreds (Kruger et al., 1998; Polymeropoulos et al., 1997; Singleton et al., 2003; Zarranz et al., 2004). Loss of the ubiquitin ligase, parkin, causes autosomal recessive juvenile Parkinsonism (Kitada et al., 1998). Mutations in the genes coding for UCH-L1, DJ-1 and PINK1 are also all

associated with autosomal recessive PD (Bonifati et al., 2003; Maraganore et al., 1999; Valente et al., 2004). α-Synuclein is a small ubiquitous protein whose function is unclear. It binds lipids, and might regulate vesicular function, proteasomal activity and signal transduction (Ostrerova et al., 1999; Perez et al., 2002; Sharon et al., 2001; Snyder et al., 2003; Souza et al., 2000). α-Synuclein has a tendency to form oligomers and fibrils, particularly after exposure to oxidative stress (Conway et al., 1998; Conway et al., 2001; Conway et al., 2000; Ostrerova-Golts et al., 2000). This property is one shared with other proteins that form inclusions related to neurodegenerative disease. α-Synuclein is most abundant in neurons in the brain, and is present in all mammals, but does not exist in *C. elegans* or Drosophila. Parkin is a putative E3 ubiquitin ligase that has neuroprotective actions (Petrucelli et al., 2002; Shimura et al., 2000; Zhang et al., 2000). Studies of neurons in cell culture and of transgenic Drosophila suggest that the protective properties observed during over-expression of parkin protect against α-synuclein toxicity, which suggests that the two proteins affect intersecting biochemical pathways (Petrucelli et al., 2002; Yang et al., 2003). DJ-1 is an oncogene that modulates oxidative stress possibly by affecting mitochondrial function (Mitsumoto and Nakagawa, 2001; Nagakubo et al., 1997; Yokota et al., 2003). Each of these proteins has very different functions. There is only a limited understanding of how, or even whether, these proteins affect the biochemical pathways related to the environmental toxins implicated in PD. Identifying common mechanisms by which mutations in these genes might contribute to the etiology of PD is an important goal of research into PD.

RESULTS

Characterization of the wild type and A53T α-synuclein nematodes: The presence of wild type or A53T α-synuclein in the *C. elegans* transgenic lines was demonstrated by PCR and immunoblot analysis (Figures 1A and B). PCR of the transgenic *C. elegans* genomes yielded 450 bp bands that corresponded to full-length wild type and A53T α-synuclein cDNA (Figure 1A, Lanes 1 and 2). The plasmid used to generate the wild type α-synuclein transgenic lines was used as a control to verify the size of α-synuclein (Figure 1A, Lane 4). No α-synuclein was detected through PCR analysis in the NON-TG (non-tg) strain, which is consistent with the absence of a homologue for α-synuclein in *C. elegans* (Figure 1A, Lane 3). Immunoblot analysis of the lysates from the wild type and A53T α-synuclein strains yielded a 19 kD band corresponding to monomeric α-synuclein (Figure 1B, Lanes 2 and 3). The non-tg, strain showed no α-synuclein bands in the immunoblot (Figure 1B, Lane 1). A band at 45 kD was present in all lanes of the immunoblot, indicating that the band is non-specific to α-synuclein (Figure 1B).

Characterization of the K08E3.7 knockout: Human parkin shows high homology to the KO8E3.7 gene in *C. elegans* (Figure 1D). Based on this homology, we searched for a strain of nematodes lacking KO8E3.7. Generation of the K08E3.7 knockout nematodes (K08E3.7 KO) was demonstrated by PCR based on the expected region deleted (Fig. 1C and E). A 1131 base pair region including exons 1-4 of the K08E3.7 gene was deleted to yield a non-functional form of K08E3.7 (Fig 1E). The non-tg nematodes yield a 1.37 kb

band that corresponds to full length K08E3.7 (Figure 1C, Lane 1). Knockout of K08E3.7 yields a 0.26 kb band (Figure 1C, Lane 2).

The life spans of the non-transgenic and transgenic strains of *C. elegans* were examined as a simple test to determine whether expression of α-synuclein or lack of K08E3.7 affects the metabolism of the nematodes. Expression of human wild type and A53T α-synuclein in the nematode did not alter the life span of the nematodes (Figure 2A). The mean life span of the non-tg, wild type and A53T α-synuclein expressing strains was 18.5 days. The mutated K08E3.7 strain had a shorter life span (Figure 2A). We began to see differences in survival rates after eight days of monitoring. The mean survival for the non-tg strain and K08E3.7 KO strains was 18.5 ± 0.169 and 15.65 ± 0.211, respectively. Overall, the K08E3.7 KO strain had a 15.4% shorter life span than the non-tg strain. The transgenic and non-transgenic *C. elegans* strains were also examined visually at multiple life stages from larval development through adulthood. No defects were observed in any transgenic strains through development and into adulthood.

KO8E3.7/Parkin knockout leads to reduced ubiquitination in C. elegans: The K08E3.7 KO and non-tg nematodes were examined to explore the function of K08E3.7 in the nematode. The results show that the K08E3.7 KO strain exhibits reduced levels of basal ubiquitination (Fig. 2B-D). Basal ubiquitination in the K08E3.7 KO strain was 55% ± 6.5% ($p<0.01$) than of the non-tg strain. Reduced ubiquitination in the K08E3.7 KO strain lends support to the hypothesis that parkin is involved in the ubiquitin proteasomal system.

PD-Related genetic factors do not increase vulnerability to agents that induce oxidative stress or DNA damage: To test whether PD-related genetic factors affect the vulnerability of nematodes to toxins, the non-tg, K08E3.7 KO, wild type and A53T expressing α-synuclein transgenic lines were exposed to different concentrations of metals, paraquat, rotenone, azide or etoposide. Toxicity of the non-tg nematodes was analyzed using a dose response format for each of the toxins (metals, paraquat, rotenone, azide or etoposide) to determine whether the non-tg strain was vulnerable to these toxins and to determine the optimal concentration of toxin to use in subsequent assays. Dose-dependant mortality was observed for all of the toxins in the non-tg strain (data not shown).

The sensitivity of the wild type and A53T α-synuclein expressing transgenic strains and the K08E3.7 KO strain was tested using the toxins mentioned above. The nematodes tested with agents that induce oxidative stress, such as iron (II), copper (II) and paraquat did not have a higher sensitivity to the toxins compared to the non-tg strain (Figure 3A-B). The α-synuclein expressing strains did not show increased vulnerability to etoposide, a topoisomerase II inhibitor (Figure 3C). Four days of treatment with etoposide showed some vulnerability of the non-tg, K08E3.7 KO, wild type and A53T α-synuclein expressing strains compared to the untreated strains. However, the survival of the non-tg strain was 8% lower than that of the wild type and A53T α-synuclein expressing strains (Figure 3C). The survival of the non-tg strain was significantly different from the α-synuclein expressing strains with $p<0.05$. There was no statistical difference between the survival of the wild type and A53T α-synuclein strains. The data

suggests that α-synuclein can be mildly protective against etoposide toxicity when expressed in the transgenic strains. However, loss of K08E3.7 renders *C. elegans* more vulnerable to etoposide-induced toxicity compared to the non-tg strain. The survival of the K08E3.7 KO strain was 7.5% lower than that of the non-tg strain (Figure 3C). The susceptibility of the K08E3.7 strain indicates that K08E3.7 may act to protect *C. elegans* against DNA damage.

Transgenic lines expressing PD-related genetic factors are selectively vulnerable to mitochondrial complex I inhibitors: The transgenic strains were also tested with compounds that inhibit mitochondrial complexes. The first treatment was with rotenone, a known mitochondrial complex I inhibitor. Rotenone (25 or 50 μM) induced a significant dose dependent mortality in all the strains, which demonstrates that rotenone is toxic to the non-tg, K08E3.7 KO and α-synuclein expressing transgenic strains (Figure 3D). Interestingly, the K08E3.7 KO, wild type and A53T α-synuclein expressing strains showed reduced viability at each concentration of rotenone compared to the non-tg strain at the same dose (Figure 3D). After 25 μM rotenone treatment for 4 days, the K08E3.7, wild type and A53T α-synuclein expressing strains showed 74% ± 1.48%, 60% ± 1.2%, and 56% ± 1.12% survival, respectively. Lower survival rates were also seen following 50 μM rotenone treatment for 4 days. The survival rates for the K08E3.7, wild type and A53T α-synuclein expressing strains were 70% ± 1.39%, 57.5% ± 1.15%, and 39.3% ± 0.79%, respectively. The A53T α-synuclein expressing strain showed greater vulnerability to rotenone as compared to the wild type α-synuclein expressing strain with 50 μM rotenone treatment. A comparison of the wild type and A53T α-synuclein

expressing strains after 4 days of 50 μM rotenone treatment shows that the A53T α-synuclein expressing strain has 68.4% ($p<0.01$) lower survival that the wild type α-synuclein expressing strain. Other known mitochondrial complex I inhibitors were also tested on the non-tg and transgenic strains. Toxicity associated with fenperoximate, pyridaben or stigmatellin treatement was similar to that observed in the strains treated with rotenone (Figure 4). However, 4-phenylpyridine, caspsaicin, and papaverine showed no toxicity in any strain of nematode (data not shown).

The data suggests that PD-related genetic factors increase the vulnerability of *C. elegans* to mitochondrial impairment via rotenone treatment. In contrast, no increase in sensitivity was observed to agents that induce oxidative stress, such as iron (II), copper (II), and paraquat. We also tested the transgenic strains with 500 mM azide, a mitochondrial complex IV inhibitor. Both the non-tg and transgenic strains were equally vulnerable to azide (Figure 3E). We saw 50% survival for the non-tg and transgenic strains at 12.5 hours following azide treatment. Antimycin A, a complex III inhibitor, and 3-nitroproprionic acid (3-NP), a complex II inhibitor, were also tested, but had no effect on the nematodes (data not shown). These data suggest that PD related genetic factors renders *C. elegans* selectively vulnerable to mitochondrial complex I inhibition and not to other toxins that induce DNA damage or oxidative stress.

Pathological changes in rotenone treated nematodes show increased fibrillogenesis in C. elegans lines expressing α-synuclein: Studies performed *in vitro* and *in vivo* indicate that α-synuclein has a strong tendency to fibrillize (Conway et al., 1998; Feany and Bender,

2000; Giasson et al., 2002; Kahle et al., 2002; Lee et al., 2002; Ostrerova-Golts et al., 2000). The PD-related mutations in α-synuclein increase its fibrillization rate. In addition, oxidative stress increases the rate of α-synuclein fibrillization (Hashimoto et al., 1999; Ostrerova-Golts et al., 2000). The tendency of α-synuclein to fibrillize raises the possibility that *C. elegans* lines expressing α-synuclein might show evidence of fibril formation, particularly after rotenone treatment. The non-tg *C. elegans* line and transgenic *C. elegans* line expressing A53T α-synuclein were exposed to rotenone (25 μM) for 4 days. The lysates were then examined by dot blot using an antibody that selectively recognizes aggregated α-synuclein (Syn303) . The anti-aggregated α-synuclein antibody reacted with lysates from the *C. elegans* line expressing A53T α-synuclein that had been exposed to rotenone, but did not react with either the *C. elegans* line expressing A53T α-synuclein grown under basal conditions or the non-tg *C. elegans* line (supplemental Figure 1A & B). Next, the *C. elegans* lines (non-tg and A53T α-synuclein) were grown for two days ± 25 μM rotenone, then fixed, paraffin embedded and analyzed with thioflavine-S a marker of β-sheet formation. The rotenone treated A53T α-synuclein *C. elegans* line showed abundant thioflavine reactivity, while the rotenone treated non-tg nematodes and untreated A53T α-synuclein expressing strain showed no thioflavine reactivity (supplemental fig. 1C). However, the aggregates that formed were not SDS-resistant because immunoblots with α-synuclein antibody failed to detect high molecular weight aggregates either in the total lysates or in a sarkosyl insoluble fraction (data not show). These results show that the presence of α-synuclein in

the nematodes stimulates fibrillization, but suggests that the type of amyloid formed is a SDS-sensitive protofibrils.

Rescue of mitochondrial function protects against rotenone-induced toxicity: Rotenone is known to induce free radical generation, inhibition of complex I, and apoptosis. To test whether preventing these processes protects against rotenone toxicity, the non-tg and transgenic strains (A53T α-synuclein strain and KO8E3.7 KO strain) were co-treated with rotenone and putative protective compounds such as anti-oxidants, mitochondrial complex II activators, or anti-apoptotic compounds. Testing of the α-synuclein strains with these compounds was limited to the A53T α-synuclein strain to limit the complexity of the analysis. We reasoned that examining the A53T α-synuclein line was a more stringent test because it is more vulnerable than the wild type line.

Two known anti-oxidants, N-acetyl cysteine (NAC) and probucol, were tested for protection against rotenone-induced free radical generation (Barnhart et al., 1989). NAC was unable to protect any of the strains against rotenone toxicity (data not shown). In contrast, probucol significantly reduced rotenone toxicity, yielding 12.13%, 13.34%, and 24.45% higher survival rates for the non-tg, K08E3.7 KO and A53T α-synuclein expressing strain than treatment with rotenone alone (Figure 5A). However, probucol was unable to fully protect any of the nematode strains against rotenone-induced toxicity. The ability of probucol to partially protect against rotenone-induced toxicity suggests that the mechanism of toxicity involves generation of free radicals.

Rotenone is known to inhibit mitochondrial complex I. To bypass complex I, and rescue the mitochondrial electron transport chain, we utilized D-β-hydroxybutyrate

(DβHB), which is known to increase cellular succinate. Succinate can be used directly by complex II to bypass the inhibition of complex I by rotenone (Kashiwaya et al., 2000; Tieu et al., 2003). Treatment of the non-tg and transgenic strains provided protection against rotenone-induced toxicity in a dose-dependent manner (Figure 5B). Co-treatment with 50 mM DβHB fully protected the non-transgenic strain while providing partial protection against the K08E3.7 KO and the A53T α-synuclein expressing strains. Treatment with DβHB increased survival of the K08E3.7 KO and α-synuclein expressing strains by 23.3% and 37.8%, respectively. Full protection by DβHB in the non-tg strain indicates that rotenone acts via inhibition of mitochondrial complex I.

The cytoprotective bile acid tauroursodeoxycholic acid (TUDCA) was examined next for protection against rotenone-induced toxicity. TUDCA is a putative anti-apoptotic compound that inhibits Bax activity in eukaryotes, and might affect the apoptotic system in nematodes (Rodrigues et al., 1998a; Rodrigues et al., 2003a; Rodrigues et al., 2003b). Treatment with TUDCA yielded a dose-dependent protection against rotenone-induced toxicity (Figure 5C). The non-tg strain was fully protected against rotenone-induced toxicity following co-treatment of rotenone and 10 mM TUDCA. Treatment with 10 mM TUDCA increased survival of the K08E3.7 KO and α-synuclein expressing strains by 23.8% and 25%, respectively, but was unable to provide full protection (Figure 5C). The ability of TUDCA to partially protect against rotenone-induced toxicity suggests that rotenone also induces apoptosis in *C. elegans*.

DβHB shows additive protection in combination with TUDCA but not probucol: No dose of probucol, DβHB, or TUDCA, provided complete protection against rotenone-induced

toxicity in the K08E3.7 KO or A53T α-synuclein expressing transgenic strains (Figure 5A-C). Our observations of partial protection by these compounds could result from either of two explanations. One possibility is that the concentrations of the compounds used were not high enough to overcome rotenone-induced complex I inhibition, free radical generation or apoptosis. The tendency of the protection graphs to plateau argues against this explanation. An alternate possibility is that the PD-related proteins exacerbate rotenone-induced toxicity through alternate pathways. For instance, one mechanism of toxicity might be rotenone-induced formation fibrils in the α-synuclein lines, and another potential mechanism of toxicity might be the reduced activity of the ubiquitin proteasomal system that occurs with deletion of K08E3.7 (Figure 2 and supplemental figure 1). We hypothesize that the pleiotropic nature of toxicity in the PD-related nematode lines leads to toxicity that cannot be overcome by treatment with one compound alone.

To determine whether two pathways were being activated, the non-tg and transgenic nematode strains were treated with different combinations of probucol, DβHB or TUDCA. Probucol did not supplement the protection against rotenone-induced toxicity provided by either DβHB or TUDCA in the K08E3.7 KO and A53T α-synuclein expressing strains (Figure 6A and B). However, co-treatment with DβHB and TUDCA fully prevented against rotenone-induced toxicity in the non-tg and transgenic strains (Figure 6C). Comparison of the K08E3.7 KO and A53T α-synuclein expressing transgenic strains treated with rotenone plus the combination of DβHB and TUDCA showed no significant difference from the untreated strains. These results indicate that

co-treatment of DβHB and TUDCA provided full protection against rotenone toxicity in both the NON-TG and A53T α-synuclein expressing strains.

The ability of the combination of DβHB and TUDCA to provide full protection in the K08E3.7 KO and A53T α-synuclein expressing transgenic strains suggests that rotenone induced two biochemical pathways in the transgenic strains: complex I inhibition and apoptosis. This work also suggests that activating mitochondrial complex II and inhibiting apoptosis in *C. elegans* can prevent the toxicity induced by rotenone in the presence of α-synuclein or KO8E3.7 KO.

TUDCA acts by a putative anti-apoptotic mechanism in mammalian cells, but the mechanism of action in *C. elegans* is unknown. To test whether TUDCA also inhibits apoptosis in *C. elegans*, we treated *C. elegans* lacking the executioner caspase *ced-3* with 25 μM rotenone ± 10 mM TUDCA (Figure 7A). Following treatment with 25 μM rotenone, TUDCA was unable to provide any additional protection to the Ced-3 knockout nematodes beyond the partial protection provided by the gene knockout (Figure 7A). The inability of TUDCA to add to the protection provided by Ced3 suggests that TUDCA acts via an anti-apoptotic mechanism.

Paraquat's Mechanism of Action is Oxidative Stress in Nature: Treatment of the non-tg and transgenic strains with paraquat indicated that all the strains were equally vulnerable to paraquat treatment (Figure 3B). Because the mechanism of paraquat toxicity is not fully understood, we sought to use the nematodes to explore the mechanism of toxicity. Co-treatment of non-tg nematodes with 25 μM paraquat ± 25 or 50 mM DβHB did not attenuate paraquat toxicity (Figure 7B). However, co-treatment with paraquat and

probucol increased survival of all strains by 30% compared to paraquat treated alone (Figure 7C). The partial protection provided by probucol indicates that free radical generation contributes to paraquat toxicity. The inability of DβHB to protect against paraquat toxicity suggests that the toxicity in *C. elegans* is independent of complex I inhibition. A lack of full protection by probucol suggests either that paraquat has a secondary unknown mechanism of toxicity or that multiple free radical scavengers are required to minimize oxidation.

*Knockdown of DJ-1 (*B0432.2) *increases vulnerability to rotenone, which is rescued by a combination of DβHB and TUDCA*: The results described above show that *C. elegans* lines expressing α-synuclein (wild type or A53T) respond to complex I inhibition in much the same manner as *C. elegans* lines lacking parkin. To investigate whether this might be a trait that generalizes to other PD-related genes, we examined the responses of nematodes following knockdown of the B0432.2, the *C. elegans* homologue of DJ-1. *C. elegans* was grown on *HT115(DE3)* E. Coli containing the L4440 vector coding for RNAi of B0432.2 (DJ-1). Two days later, the nematodes were exposed to 25 μM rotenone, and after four days the viability of the nematodes was scored. The response of the nematodes resembled that of the other PD-related lines because the nematodes with B0432.2 (DJ-1) knockdown were observed to be significantly more sensitive to rotenone treatment than control nematodes (fig. 8A). Rescue by DβHB and TUDCA was also examined. Nematodes with B0432.2 (DJ-1) knockdown were exposed to rotenone and either 25 mM DβHB, 10 mM TUDCA or both. Treatment with either DβHB or TUDCA alone induced a partial rescue of the B0432.2 (DJ-1) knockdown nematodes, but

treatment with DβHB and TUDCA together elicited full protection (fig. 8B). These results provide evidence that PD-related lines of *C. elegans* carrying three different PD-related genetic factors exhibit similar responses to complex I inhibition.

DISCUSSION

Studies implicate a diverse array of environmental and genetic factors in the pathophysiology of PD. Increasing lines of evidence suggest that mitochondrial toxicity represents a common target of each of these agents. The research described above demonstrates that genetic manipulation of α-synuclein, parkin or DJ-1 in *C. elegans* all increase vulnerability to rotenone, an inhibitor of the mitochondrial complex I. This points to the mitochondria as potentially a central target of injury in PD. The involvement of complex I is further supported by a similar increase in vulnerability observed with three other complex I inhibitors, fenperoximate, pyridaben or stigmatellin. The defect cause by over-expressing wild type α-synuclein, A53T α-synuclein or deleting the *C. elegans* parkin homologue KO8E3.7 appears to be selective for complex I inhibition because the nematodes are not more sensitive than non-transgenic *C. elegans* to other types of toxins, including divalent metal ions, paraquat, etoposide or azide. The selectivity of the deficit for complex I is supported by the full protection afforded by DβHB in non-transgenic lines and partial protection afforded by DβHB in genetically modified lines. DβHB enhances the activity of complex II by increasing the levels of the complex II substrate, succinate. The enhanced activity compensates for the decreased mitochondrial function caused by complex I inhibition. Interestingly, nematodes carrying PD-related genetic changes were more vulnerable to complex I inhibition than non-

transgenic nematodes, and full protection from the complex I inhibition occurred only when DβHB was used in combination with TUDCA, an inhibitor of apoptosis. These results suggest that rotenone and other complex I inhibitors might be causing toxicity through a mechanism that is more complicated than a simple loss of energy production.

The stable *C. elegans* lines that we describe in this manuscript have not been described previously in the literature. A previous study has described a similar line of *C. elegans*, which over time developed dopaminergic loss, which is analogous to that seen in PD and in Drosophila over-expressing α-synuclein (Auluck et al., 2002; Feany and Bender, 2000; Lakso et al., 2003). The similarities between the characteristics of *C. elegans* lines expressing A53T and wild type α-synuclein and the characteristics of transgenic mice, transgenic Drosophila or cell lines expressing α-synuclein suggests that the information obtained with the PD-related *C. elegans* lines has relevance beyond *C. elegans*. Stable over-expression of α-synuclein is tolerated well by the mice and Drosophila in that both animals develop normally, eat normally, and reproduce normally. This is also true for the *C. elegans* α-synuclein cell lines. The studies described above also show that expressing α-synuclein in *C. elegans* also does not weaken the animals to toxins non-specifically. The *C. elegans* lines expressing α-synuclein showed vulnerability to divalent metal cations, paraquat and etoposide that is similar to or less than that of non-transgenic nematodes. This suggests that the α-synuclein constructs are not rendering the nematodes generally sick and more vulnerable to chemical insults.

Increasing levels of α-synuclein or expressing α-synuclein constructs with PD-related mutations increases α-synuclein aggregation in mammalian cell lines and in vitro. This is also true for the *C. elegans* α-synuclein strains because nematodes expressing the A53T

α-synuclein are slightly more vulnerable than those expressing wild type α-synuclein. Aggregation of α-synuclein occurs in parallel with neurotoxicity in transgenic Drosophila, transgenic mice and mammalian neuronal cell lines, which is consistent with a mechanism derived from toxic aggregates. Aggregation of α-synuclein also occurs in the *C. elegans* lines expressing α-synuclein. Following exposure to rotenone, the nematodes expressing α-synuclein showed reactivity to antibodies against amyloid (either antibodies against amyloid-like α-synuclein or general amyloid structures) or by thioflavine after rotenone treatment, which suggests that amyloid fibrils or proto-fibrils form after rotenone treatment . The aggregates that form are likely to be protofibrils that are SDS-sensitive because they do not form high molecular weight smears evident by immunoblot. Restriction of the pathology to protofibrils is not surprising because the short life span of *C. elegans* and the short duration of rotenone treatment might not provide adequate time for mature amyloid fibrils to form. In vivo, SDS resistant α-synuclein aggregates only appear in Drosophila after 3 weeks of aging, in rat after 6 weeks of rotenone treatment and in transgenic mice after 6 – 11 months of aging. In this study we were most interested in studying the mechanisms of cell death. Comparison to the mammalian models suggests that prolonged treatment of the *C. elegans* lines, such as by growing the nematodes in sub-lethal doses of rotenone, might increase the amount of α-synuclein aggregation the observed and also produce more stable aggregates.

The *C. elegans* line with the KO8E3.7/parkin deletion is particularly interesting because the levels of high molecular weight ubiquitin conjugates are reduced. This represents the first in vivo evidence that loss of a parkin homologue affects the ubiquitin proteasomal system. The studies reporting knockout of parkin in mice and knockout of

parkin in Drosophila did not report any changes in ubiquitination (Goldberg et al., 2003; Palacino et al., 2004). Once antibodies to the nematode homologues of parkin substrates are available it will be of great interest to study the turnover of these proteins. The toxicology profile of KO8E3.7/parkin knockout in the nematode contrasts somewhat with the toxicology profile of parkin knockout in Drosophila, which shows selective extensive damage and particular vulnerability to some divalent cations, such as manganese and cobalt (Greene et al., 2003). KO8E3.7/parkin knockout in the nematode does not appear to selectively affect muscle because the nematodes continue to move normally until just prior to death. However, KO8E3.7/parkin knockout in the nematode and fruit fly share a similar characteristic in that both exhibit mitochondrial vulnerability.

The selective vulnerability to mitochondrial complex I inhibition of each of the nematode models that we investigated represents one of the striking features of this study. The pharmacological profile of the α-synuclein expressing and parkin deletion lines were investigated in detail, and both showed toxicity and protection profiles that were strikingly similar. In particular, α-synuclein expression and parkin deletion both selectively sensitized the nematodes to rotenone and three other complex I inhibitors. Knockdown of DJ-1 also sensitized *C. elegans* to complex I inhibition. This is somewhat less surprising because knockdown of DJ-1 has been shown to sensitize cells to a variety of toxic stimuli (Yokota et al., 2003). However, the ability of DJ-1 knockdown to sensitize *C. elegans* to rotenone strengthens the linkage between complex I inhibition and proteins associated with PD. The comparable patterns of protection among the three PD-related nematode models provide further evidence suggesting that the mechanisms of toxicity among the three gene models are similar. DβHB increases succinate levels,

which enhances the activity of complex II (Kashiwaya et al., 2000). By increasing complex II activity, DβHB partially protects against rotenone toxicity in cells and in rat (Kashiwaya et al., 2000). DβHB appears to be even more effective in the nematode than in mammalian cells. However, DβHB was unable to fully protect against rotenone toxicity once the PD-related genetic changes were introduced, which indicates that these genetic changes increased the amount of toxicity. TUDCA but not probucol was able to add to the protection provided by DβHB, although both TUDCA and probucol were partially protective on their own. The ability of TUDCA to add to protective response observed for DβHB suggests that it acts via a mechanism that differs from that of DβHB or probucol, which is an anti-oxidant.

Studies of rotenone induced toxicity show a pleiotropic mechanism. Acute rotenone toxicity causes loss of ATP production, which interferes with many physiological systems, including the proteasome (Hoglinger et al., 2003). Chronic rotenone toxicity is also associated with production of free radicals and aggregation of α-synuclein (Betarbet et al., 2000; Sherer et al., 2002; Sherer et al., 2003). The mechanism for free radical production is incompletely understood, but might result from impaired electron transfer from NADH-ubiquinone oxidoreductase to ubiquinone (Ramsay et al., 1991). Our studies are consistent with these prior studies. The ability of DβHB to compensate for rotenone toxicity suggests that some of the toxicity observed in the *C. elegans* derives from loss of energy production, because DβHB increases substrate supply to complex II observed increased oxidation in *C. elegans* exposed to rotenone (Tieu et al., 2003). The increased protein oxidation that present in the rotenone-treated C. elegans lines also indicates that rotenone causes free radical production, which is

consistent with the studies observed by Sherer et al (Sherer et al., 2002; Sherer et al., 2003). The ability of the anti-oxidant probucol to partially protect against rotenone toxicity provides further evidence of a mechanism of toxicity that involves oxidative stress. Probucol is an anti-oxidant that was developed by cardiologists and is particularly useful because it is more potent than typical anti-oxidants, such as vitamin C or E (Barnhart et al., 1989). However, the protection afforded by probucol in the C. elegans lines was not additive with that of DβHB, which suggests that both agents effectively reduce oxidative stress and further reduction of oxidative stress does not benefit the nematode. The fact that the PD-related C. elegans lines showed vulnerability to paraquat similar to that of non-transgenic nematodes provides further evidence that oxidative stress alone does not account for the increased vulnerability associated with PD-related genetic changes. The mechanism of action of paraquat in C. elegans appears to involve a significant oxidative component because probucol partially protects against paraquat toxicity. The inability of the combination of DβHB and probucol to fully protect the C. elegans lines with PD-related genetic changes (α-synuclein expression, KO8E3.7/parkin deletion or B0432.2/DJ-1 knockdown) suggests that the mechanism of toxicity in these nematodes involves an additional component beyond energy loss and free radical production. One last point related to the mechanism of action of paraquat that is worth noting is that the inability of DβHB to protect against paraquat toxicity indicates that paraquat is unlikely to act in C. elegans by reducing the activity of mitochondrial complex I.

Several lines of evidence from our studies suggest that apoptosis is the additional component associated with rotenone toxicity in the PD-related C. elegans lines.

Nematodes exposed to rotenone show increased caspase activity, which is a classic sign of apoptosis. The ability of TUDCA to partially protect against rotenone toxicity provides further support that apoptosis is occurring because TUDCA inhibits apoptosis (Keene et al., 2002; Rodrigues et al., 2003a; Rodrigues et al., 2003b). TUDCA has not been studied in C. elegans previously, but our studies with C. elegans lacking Ced 3 demonstrate that TUDCA does act in C. elegans by inhibiting apoptosis because TUDCA does not provide any protection against rotenone toxicity in nematodes lacking Ced 3. Finally, the ability of TUDCA to add to the protection provided by DβHB contrasts with the results observed for probucol and suggests that it acts through a mechanism different than that of DβHB, and further suggests that the additional mechanism is the activation of apoptosis. Prior studies implicate apoptosis in the pathophysiology of PD. The complex I inhibitor MPTP induces apoptosis in vivo, and mice lacking the pro-apoptotic protein Bax are less vulnerable to MPTP (Chun et al., 2001; Vila et al., 2001). Studies in humans also implicate apoptosis in PD because post-mortem studies of patients who died from PD show histochemical evidence of apoptosis (Dragunow et al., 1995; Mochizuki et al., 1996). Our studies now provide additional evidence implicating apoptosis in PD. The ability of combination therapy involving complex II compensation and apoptotic inhibition to prevent rotenone toxicity in PD-related C. elegans lines could have important implication for therapy of PD.

METHODS

Generation of the wild type α-synuclein transgenic strain: Human wild type α-synuclein cDNA was inserted into the vector pPD95.75 downstream of a synaptobrevin promoter. The Bristol NON-TG (Non-Tg) strain was co-injected with the wild type α-synuclein construct and a pDPSU006-GFP vector to produce extrachromosomal arrays. Both constructs were injected at a concentration of 50 ng/μl. The pDPSU006-GFP vector was used as a marker for gene transmission. Transgenes were integrated by exposing animals to 1,800 rads of γ irradiation, and animals were out-crossed five times.

Generation of the A53T α-synuclein transgenic strain: A53T α-synuclein expression is driven by an *unc-119* neuronal promoter. GFP driven by the dopamine transporter promoter was used as a marker to identify those nematodes expressing the extrachromosomal array. The methods used to create this transgenic strain are the same as described above.

Detection of the wild type and A53T α-synuclein transgene: Polymerase chain reaction (PCR) was performed to detect the transgene. The following primers were used to detect the transgene: sense primer 5'-ATTAATTCATAGCC-3' and antisense primer 5'-CTGGGAGCAAAGATA-3' (IDTDNA, Coralville, IA).

Generation of the K08E3.7 knockout: The following protocol was used to derive the knockout. A deletion library of nematodes derived from 460,000 trimethlypsoralen/UV mutagenized non-tg animals was used to generate the knockout. Previously described methods were used for library construction and screening (Dong et al., 2000). PCR with the primers listed below was used to verify a K08E3.7 deletion within the mutagenized

animals. Animals verified as K08E3.7 knockouts were outcrossed five times to the wild type strain to produce a clean genetic background. The K08E3.7 knockout is a deletion of 1132 bp whose limits are GGACATTTCAAACTTTGAAT …AAAATAACTTCAGGAGTGGT. The following primers were used to detect the deletion: sense primer 5'-ATACAAGATAGAAAAACAGGTC-3' and antisense primer 5'- GCAAAACGAAAAAAAAC A-3' (IDTDNA, Coralville, IA).

Ced-3 Knockout - The *ced-3* knockout strain used in this thesis was kindly given to us by Dr. Horvitz at Massachusetts Institute of Technology (Cambridge, MA)

Lifespan Analysis: The life spans of the non-tg, strains expressing wild type and A53T α-synuclein, and the K08E3.7 KO strains were determined using previous described techniques {Tissenbaum, 2001 #1675}. Three NGM plates (2.5 g bacto-peptone (Beckton Dickinson, Sparks, MD), 3 g NaCl, 20 g agar, 1 mM $CaCl_2$, 1 mM $MgSO_4$, 5 mg cholesterol, 25 mM KH_2PO_4, (Sigma, St. Louis, MO) ddH_2O) seeded with OP50-1 *E. coli*] of 40 nematodes were monitored throughout the lifecycle for each strain.

Culturing of Nematodes and Isolation of Nematode Lysates: The Bristol NON-TG strain was used as the wild-type strain. Growth and culture of nematodes were performed using standard techniques {Wood, 1988 #1619; Brenner, 1974 #1697}. Previously described methods were used to isolate mixed stage nematode lysates {Slice, 1990 #1698}. In addition to previously described methods, the isolated pellet of nematodes was washed with 5 ml cold 1X PBS + Protease Inhibitor Cocktail (Sigma, St. Louis, MO). The nematodes were then spun down, extra supernatant removed, and sonicated for lysis.

Immunoblot Analysis: Protein concentration of nematode lysates was determined using BCA protein assay (Pierce, Rockford, IL). 30 µg of protein were used for immunoblot assays. 2× dithiothreitol protein loading buffer was added to each sample. The samples were then heated for 5 min at 90 °C, and run on 8-16% sodium dodecyl sulfate (SDS) gradient polyacrylamide gels (BioWhitaker, Walkersville, MD).

Proteins on the polyacrylamide gels were then transferred to polyvinylidene difluoride (BioRad, Hercules, CA) overnight at 4 °C at 0.1 A/gel in transfer buffer. The immunoblot was blocked in 5% milk in 100 mM Tris-buffered saline/0.1% Tween 20 (TBST) for one hour at room temperature while shaking. The blots were then incubated overnight at 4 °C in primary antibody at appropriate concentration in 5% bovine serum albumin in TBST. The blots were washed three times, 10 min each, and incubated three hours in secondary antibody (1:5000) (Jackson Laboratories, West Grove, PA) in 5% milk in TBST at room temperature. Blots were washed three times and developed using a chemiluminescent reaction (PerkinElmer Life Sciences, Boston, MA).

Immunoblot analysis was performed using a monoclonal anti-α-synuclein antibody (1:1000) (Zymed, San Francisco, CA) and monoclonal anti-ubiquitin antibody (1:1000) (Zymed, San Francisco, CA) and secondary donkey anti-mouse (1:5000) (Jackson Laboratories, West Grove, PA). Resulting bands were analyzed using Image J (NIH).

Chemical Treatments: Non-tg, wild type α-synuclein, A53T α-synuclein and K08E3.7 KO nematodes were treated with rotenone (0, 25, 50, 75 or 100 -50 μM), paraquat (0, 100, 200, 300, 400 or -500 μM), etoposide (0 and 500 uM), or metals ($FeCl_3$: 0 and 7.5 mM and $CuCl_2$: 0, 0.3, and 0.75 mM). 35 mm plates were poured with the indicated concentrations of rotenone, paraquat, etoposide or metal (Sigma, St. Louis, MO) diluted in NGM agar. The plates were seeded with bacteria medium containing rotenone, paraquat or metal. 40 nematodes of the appropriate strain were placed on each plate. Every other day surviving nematodes were transferred onto a new plate with the same concentrations of rotenone, paraquat, etoposide or metal. The number of surviving nematodes was counted on days 2 and 4. The number of live nematodes was determined by counting nematodes that were either moving or those that responded to light touch with a platinum wire. Toxicity was measured as a function of percent survival of the nematodes following treatment.

Non-tg, A53T α-synuclein, K08E3.7 KO, and ced-3 knockout nematodes were treated with D-β-hydroxybutyrate (DβHB), a mitochondrial complex II activator, (0-50 mM); tauroursodeoxycholic acid (TUDCA) that inhibits Bax and cytochrome C release (0-10 mM); or probucol, an antioxidant, (0-10 mM) (Sigma, St. Louis, MO) in

conjunction with 25 μM rotenone (Rodrigues et al., 1998b; Tieu et al., 2003). The assay was performed as described above.

Non-tg, transgene expressing A53T α-synuclein and K08E3.7 KO nematodes were also treated with 500 mM azide, a complex IV inhibitor. A previously described protocol was used to test for azide toxicity (Scott et al., 2002). The number of live nematodes was determined by counting nematodes that were moving or those that responded to light touch with a platinum wire. Toxicity was measured as a function of % survival of the nematodes following treatment.

Treatment with siRNA: Generation of the B0432.2 Knockdown - E. coli containing a B0432.2 genomic fragment cloned into L4440 was used to generate the C. elegans knockdown (Fraser et al., 2000). The bacteria was grown for 12 hours in LB + 50 μg/ml ampicillin (Sigm, St. Louis, MO). This culture was seeded onto NMG plates containing 25 μg/ml carbenicillin (Sigma, St. Louis, MO) and 1 mM Isopropyl-ß-D-thio-galactopyranoside (IPTG) (Research Products International Corporation, Mt. Prospect, IL). B0432.2 RNAi was induced overnight at room temperature. The following day five L3-L4 hermaphrodites were transferred onto the NGM plates. These nematodes were grown for 72 hours at 15°C for the RNAi to take effect. Single adults were then plated onto new individual NGM plates with additives and RNAi containing bacteria. Progeny of these adults were used in subsequent assays.

Thioflavin S histochemistry: *C. elegans* specimens treated with 25 M rotenone for 4 days were fixed overnight in 10% formalin at 4C. These specimens were then embedded in Histogel (Richard-Allan Scientific, Kalamazoo, MI) and further processed for paraffin

embedding. The resulting blocks were cut into 10 m sections. The paraffin-embedded sections were then rehydrated and autoclaved for 15 min at 121C. The slides were cooled to room temperature and washed for 5 minutes in PBS. The sections were then incubated with 0.5% thioflavin S for 8 minutes, washed three times in 80% ethanol for 5 minutes, washed once with dH_2O and mounted in Fluoromount-G (Electron Microscopy Sciences, Hatfield, PA).

Slot Blot Analysis: The non-tg and A53T -synuclein strains treated with rotenone were analyzed via slot blot for -synuclein aggregation. Samples were vacuumed through a slot blot apparatus onto nitrocellulose membrane. Recombinant aggregated -synuclein was used as a positive control. The nitrocellulose membrane were blocked and probed with the Syn303 antibody (1:500) as described previously in the Immunoblot Analysis section.

Statistical Analysis - Statistical analysis on the raw numbers was done using an unpaired t-test or ANOVA analysis followed by a Newman Keuls post hoc analysis (GBSTAT), when necessary. All results experiments were performed in triplicate.

Acknowledgements: We would like to thank Roger Horvitz (MIT) for providing the Ced3 knockout nematodes, and Virginia Lee (UPenn) for providing the Syn303 antibody. We would also like to thank Todd Lee (Northwestern University) for help with the statistical analysis. This work was supported by grants to BW from NINDS, USAMRC and NIA.

FIGURES:

Figure 1. Verification of α-synuclein expression and knockout of K08E3.7 in transgenic C. elegans strains. (A) PCR analysis of expressed wild type and A53T α-synuclein transgenes. 450 bp band is present in the wild type (WT) and A53T α-synuclein expressing lines (lanes 1 and 2) and co-migrates with a band amplified from α-synuclein cDNA (lane 4). The 450 bp α-synuclein-specific band is absent from the non-tg lane (lane 3). (B) Immunoblot probed with a monoclonal α-synuclein antibody. α-Synuclein protein expression (arrow, 19 kD band) is observed lysates from the wild type (WT, lane 2) and A53T α-synuclein strains (lane 3), but absent from the non-tg nematodes (lane 1). A non-specific band is present at ~50 kD in all lanes. (C) PCR of genomic DNA across the KO8E3.7 gene yields a 1.37 Kb band for non-tg nematodes (lane 1) and a 0.26 Kb band for the K08E3.7 KO strain (lane 2). (D) The amino acid sequence alignment of K08E3.7 and human parkin. Exact amino acid matches are indicated with the identical amino acid in between the K08E3.7 and human parkin sequences. The N-terminal ubiquitin-like domain (shaded box – upper right), RING finger domains (boxed), in-between RING domain (shaded box) are indicated. (E) Diagram of the full length K08E3.7 gene and the K08E3.7 gene containing the 1132 bp deletion from the K08E3.7 knockout.

Figure 2. Characterization of the K08E3.7 KO transgenic strain. (A) A life span curve shows that K08E3.7 KO (square) strain has life span that is 15.4% shorter than the non-tg (diamond), wild type (WT, triangle) and A53T (circle) α-synuclein expressing strains.

Mean life span for the non-tg, WT and A53T α-synuclein expressing strains was 18.5 ± 0.169, while the mean life span of the K08E3.7 KO strain was 15.65 ± 0.211. $p<0.01$ compared to the non-tg. (B) Immunoblot probed with monoclonal ubiquitin antibody showing higher levels of high molecular weight ubiquitin conjugates present in the non-tg (lane 1) strain than the K08E3.7 knockout (KO, lane 2) strain. (C) Longer exposure of immunoblot shows high molecular weight smears of ubiquitin conjugates in the stacking gel in the lysates from the non-tg strain. (D) Densitometric quantification of immunoblot from panel B blot; (*) $p<0.01$.

Figure 3. K08E3.7 KO, wild type and A53T α-synuclein expressing strains are selectively vulnerable to rotenone-induced toxicity. (A and B) No increase in sensitivity of the K08E3.7 KO, wild type or A53T α-synuclein expressing lines is observed following treatment with iron (II) (panel A), copper (II) (panel A), or paraquat (panel B) compared to the non-tg strain. (+) $p<0.01$ compared to untreated nemotodes of the same strain. (C) Both wild type and A53T α-synuclein are slightly protective against etoposide treatment, while K08E3.7 KO strain is slightly vulnerable compared to the non-tg strain. (*) $p<0.01$ compared to non-tg. (+) $p<0.01$ compared to untreated nematodes of the same strain. (D) K08E3.7 KO, wild type and A53T α-synuclein expressing strains show enhanced vulnerability after 4 days of rotenone treatment compared to the non-tg strain; (*) $p<0.01$. At 50 μM rotenone, the A53T α-synuclein expressing strain is also more vulnerable than the wild type α-synuclein strain; (#) $p<0.01$. (+) $p<0.01$ compared to untreated of the same strain. (E) Kill curve over a 24-hour treatment with azide. Shows

no of Neither the K08E3.7 KO, wild type nor A53T α-synuclein expressing strains show increased sensitivity to sodium azide compared to the non-tg strain; (+) $p<0.01$.

Figure 4. K08E3.7 KO, wild type and A53T α-synuclein expressing strains are also selectively vulnerable to other mitochondrial complex I inhibitors. (A-C) K08E3.7 KO, wild type and A53T α-synuclein expressing strains show enhanced toxicity after treatment for 4 days with fenperoximate, pyridaben, and stigmatellin compared to the non-tg strain; (*) $p<0.01$, (+) $p<0.01$ compared to untreated nematodes of the same strain.

Figure 5. Protection against rotenone-induced toxicity. (A) Co-treatment of the K08E3.7 KO and A53T α-synuclein expressing strains with rotenone and probucol yielded partial protection of the non-tg, K08E3.7 KO and A53T α-synuclein strains compared to untreated of the same strain; (+) $p<0.01$. (B & C) Co-treatment of the non-tg, K08E3.7 KO and A53T α-synuclein expressing strains with rotenone and DβHB (panel B) or TUDCA (panel C) fully protected the non-tg strain, but partially protected the K08E3.7 KO and A53T α-synuclein expressing strains compared to untreated nematodes of the same strain (+) $p<0.01$. Treatment with probucol, DβHB or TUDCA was unable to completely overcome the enhanced rotenone-induced toxicity of the transgenic strains as compared to the non-tg strain in any treatment group; (*) $p<0.01$.

Figure 6. Combined treatment using a mitochondrial complex II activator and a putative apoptotic inhibitor completely protects against rotenone-induced toxicity. (A) Both probucol and DβHB provided partial protection against rotenone for K08E3.7 KO and

A53T α-synuclein expressing strains, but did not show any additive benefit when combined together; (+) $p<0.01$ comparing the treatments, and (*) $p<0.01$ comparing the strains. (B) Probucol also did not show any additive benefit against rotenone toxicity when combined with TUDCA; (+) $p<0.01$ comparing the treatments, and (*) $p<0.01$ comparing the strains. (C) Combining DβHB and TUDCA fully protected against rotenone-induced toxicity in all the strains compared to untreated of the same strain; (+) $p<0.01$.

Figure 7. Analysis of the mechanisms of action of TUDCA and paraquat. (A) Treatment with TUDCA does not protect against rotenone-induced toxicity in the Ced-3 knockout worm compared to the untreated group; (+) $p<0.01$. The Ced-3 knockout worms was less vulnerable to rotenone toxicity than the non-tg strain, but addition of TUDCA did not provide any additional protection; (*) $p<0.01$. (B) Treatment with DβHB did not protect the non-tg, K08E3.7 KO or A53T α-synuclein expressing strain against paraquat induced toxicity. (+) $p<0.01$ compared to untreated of the same strain. (C) Treatment with probucol partially protects against paraquat induced toxicity in the non-tg, K08E3.7 KO and A53T α-synuclein expressing strains; (#) $p<0.01$ compared to paraquat treated of the same strain. (+) $p<0.01$ compared to untreated of the same strain.

Figure 8. Knockdown of DJ-1 increases vulnerability to rotenone and is rescued by DβHB and TUDCA. (A) Knockdown of DJ-1 increased the vulnerability to rotenone-induced toxicity; (*) $p<-.01$. (+) $p<0.01$ as compared to untreated of the same strain. (B) Treatment with DβHB and TUDCA fully protected both the non-tg strain and the DJ-

1 knockdown nematodes; (+) $p<0.01$ compared to untreated nematodes of the same strain. (*) $p<0.01$ as compared to non-tg of the same treatment group.

Supplemental Figure 1. Increased Fibrillogenisis in the A53T α-Synuclein Expressing Strain. (A) Slot blot analysis of non-tg and A53Tα-synculein expressing strain lysates using the Syn303 antibody that recognizes fibrillar α-synuclein. Row 1 – Recombinant aggregated α-synuclein (aged 1 month); Row 2 – non-tg strain; Row 3 – non-tg treated with rotenone (25 μM, 4 days); Row 4 – A53T α-synuclein expressing strain; Row 5 – A53T α-synuclein expressing strain treated with rotenone (25 μM, 4 days). Lysates were analyzed in triplicate. Aggregated α-synuclein was observed in the recombinant α-synuclein and in the A53T α-synuclein expressing strain treated with rotenone. (B) Quantification of slot blot analysis; (*) $p<0.01$ compared to non-tg. (C) Paraffin embedded sections from non-tg and A53T α-synuclein expressing strains were stained with thioflavin S. Staining with thioflavin S (arrows) was observed only in the A53T α-synuclein expressing strain following treatment with 25 μM rotenone for 4 days. Non-tg basal conditions (a), non-tg plus rotenone (b), A53T α-synuclein expressing strain basal (c), A53T α-synuclein expressing strain plus rotenone (c).

REFERENCES:

Auluck, P. K., Chan, H. Y., Trojanowski, J. Q., Lee, V. M., and Bonini, N. M. (2002). Chaperone suppression of alpha-synuclein toxicity in a Drosophila model for Parkinson's disease. Science *295*, 865-868.

Barnhart, R. L., Busch, S. J., and Jackson, R. L. (1989). Concentration-dependent antioxidant activity of probucol in low density lipoproteins in vitro: probucol degradation precedes lipoprotein oxidation. J Lipid Res *30*, 1703-1710.

Betarbet, R., Sherer, T. B., MacKenzie, G., Garcia-Osuna, M., Panov, A. V., and Greenamyre, J. T. (2000). Chronic systemic pesticide exposure reproduces features of Parkinson's disease. Nat Neurosci *3*, 1301-1306.

Bonifati, V., Rizzu, P., van Baren, M. J., Schaap, O., Breedveld, G. J., Krieger, E., Dekker, M. C., Squitieri, F., Ibanez, P., Joosse, M.*, et al.* (2003). Mutations in the DJ-1 gene associated with autosomal recessive early-onset parkinsonism. Science *299*, 256-259.

Chun, H. S., Gibson, G. E., DeGiorgio, L. A., Zhang, H., Kidd, V. J., and Son, J. H. (2001). Dopaminergic cell death induced by MPP(+), oxidant and specific neurotoxicants shares the common molecular mechanism. J Neurochem *76*, 1010-1021.

Conway, K., Harper, J., and Lansbury, P. (1998). Accelerated in vitro fibril formation by a mutant alpha-synuclein linked to early-onset Parkinson disease. Nature Med *4*, 1318-1320.

Conway, K., Rochet, J., Bieganski, R., and Lansbury, P. (2001). Kinetic Stabilization of the -Synuclein Protofibril by a Dopamine--Synuclein Adduct. Science *294*, 1346-1349.

Conway, K. A., Lee, S. J., Rochet, J. C., Ding, T. T., Williamson, R. E., and Lansbury, P. T., Jr. (2000). Acceleration of oligomerization, not fibrillization, is a shared property of both alpha-synuclein mutations linked to early-onset Parkinson's disease: Implications for pathogenesis and therapy. Proc Natl Acad Sci U S A *97*, 571-576.

Dauer, W., and Przedborski, S. (2003). Parkinson's disease: mechanisms and models. Neuron *39*, 889-909.

Dong, M. Q., Chase, D., Patikoglou, G. A., and Koelle, M. R. (2000). Multiple RGS proteins alter neural G protein signaling to allow C. elegans to rapidly change behavior when fed. Genes Dev *14*, 2003-2014.

Dragunow, M., Faull, R. L., Lawlor, P., Beilharz, E. J., Singleton, K., Walker, E. B., and Mee, E. (1995). In situ evidence for DNA fragmentation in Huntington's disease striatum and Alzheimer's disease temporal lobes. Neuroreport *6*, 1053-1057.

Feany, M. B., and Bender, W. W. (2000). A Drosophila model of Parkinson's disease. Nature *404*, 394-398.

Fraser, A. G., Kamath, R. S., Zipperlen, P., Martinez-Campos, M., Sohrmann, M., and Ahringer, J. (2000). Functional genomic analysis of C. elegans chromosome I by systematic RNA interference. Nature *408*, 325-330.

Giasson, B. I., Duda, J. E., Quinn, S. M., Zhang, B., Trojanowski, J. Q., and Lee, V. M. (2002). Neuronal alpha-synucleinopathy with severe movement disorder in mice expressing A53T human alpha-synuclein. Neuron *34*, 521-533.

Goldberg, M. S., Fleming, S. M., Palacino, J. J., Cepeda, C., Lam, H. A., Bhatnagar, A., Meloni, E. G., Wu, N., Ackerson, L. C., Klapstein, G. J.*, et al.* (2003). Parkin-deficient mice exhibit nigrostriatal deficits but not loss of dopaminergic neurons. J Biol Chem *278*, 43628-43635.

Greene, J. C., Whitworth, A. J., Kuo, I., Andrews, L. A., Feany, M. B., and Pallanck, L. J. (2003). Mitochondrial pathology and apoptotic muscle degeneration in Drosophila parkin mutants. Proc Natl Acad Sci U S A *100*, 4078-4083.

Hashimoto, M., LJ, H., Xia, Y., Takeda, A., Sisk, A., Sundsmo, M., and Masliah, E. (1999). Oxidative stress induces amyloid-like aggregate formation of NACP/α-synuclein *in vitro*. NeuroReport *10*, 717-721.

Hoglinger, G. U., Carrard, G., Michel, P. P., Medja, F., Lombes, A., Ruberg, M., Friguet, B., and Hirsch, E. C. (2003). Dysfunction of mitochondrial complex I and the proteasome: interactions between two biochemical deficits in a cellular model of Parkinson's disease. J Neurochem *86*, 1297-1307.

Kahle, P. J., Neumann, M., Ozmen, L., Muller, V., Jacobsen, H., Spooren, W., Fuss, B., Mallon, B., Macklin, W. B., Fujiwara, H.*, et al.* (2002). Hyperphosphorylation and insolubility of {alpha}-synuclein in transgenic mouse oligodendrocytes. EMBO Rep *3*, 583-588.

Kashiwaya, Y., Takeshima, T., Mori, N., Nakashima, K., Clarke, K., and Veech, R. L. (2000). D-beta-hydroxybutyrate protects neurons in models of Alzheimer's and Parkinson's disease. Proc Natl Acad Sci U S A *97*, 5440-5444.

Kayed, R., Head, E., Thompson, J. L., McIntire, T. M., Milton, S. C., Cotman, C. W., and Glabe, C. G. (2003). Common structure of soluble amyloid oligomers implies common mechanism of pathogenesis. Science *300*, 486-489.

Keene, C. D., Rodrigues, C. M., Eich, T., Chhabra, M. S., Steer, C. J., and Low, W. C. (2002). Tauroursodeoxycholic acid, a bile acid, is neuroprotective in a transgenic animal model of Huntington's disease. Proc Natl Acad Sci U S A *99*, 10671-10676.

Kitada, T., Asakawa, S., Hattori, N., Matsumine, H., Yamamura, Y., Minoshima, S., Yokochi, M., Mizuno, Y., and Shimizu, N. (1998). Mutations in the parkin gene cause autosomal recessive juvenile parkinsonism. Nature *392*, 605-608.

Kruger, R., Kuhn, W., Muller, T., Woitalla, D., Graeber, M., Kosel, S., Przuntek, H., Epplen, J., Schols, L., and Riess, O. (1998). Ala30Pro mutation in the gene encoding α-synuclein in Parkinson's disease. Nature Gen *18*, 106-108.

Lakso, M., Vartiainen, S., Moilanen, A. M., Sirvio, J., Thomas, J. H., Nass, R., Blakely, R. D., and Wong, G. (2003). Dopaminergic neuronal loss and motor deficits in Caenorhabditis elegans overexpressing human alpha-synuclein. J Neurochem *86*, 165-172.

Langston, J. (1998). Epidemiology versus genetics in Parkinson's disease: Progress in resolving an age-old debate. Ann Neurol *44*, S45-52.

Lee, M., Stirling, W., Xu, Y., Xu, X., Qui, D., Mandir, A., Dawson, T., Copeland, N., Jenkins, N., and Price, D. (2002). Human α-synuclein-harboring familial

Parkinson's disease-linked Ala-53 to Thr mutation causes neurodegenerative disease with α-synuclein aggregation in transgenic mice. PNAS *99*, 8968-8973.

Maraganore, D. M., Farrer, M. J., Hardy, J. A., Lincoln, S. J., McDonnell, S. K., and Rocca, W. A. (1999). Case-control study of the ubiquitin carboxy-terminal hydrolase L1 gene in Parkinson's disease. Neurology *53*, 1858-1860.

Mitsumoto, A., and Nakagawa, Y. (2001). DJ-1 is an indicator for endogenous reactive oxygen species elicited by endotoxin. Free Radic Res *35*, 885-893.

Mochizuki, H., Goto, K., Mori, H., and Mizuno, Y. (1996). Histochemical detection of apoptosis in Parkinson's disease. Journal of the Neurological Sciences *137*, 120-123.

Nagakubo, D., Taira, T., Kitaura, H., Ikeda, M., Tamai, K., Iguchi-Ariga, S. M., and Ariga, H. (1997). DJ-1, a novel oncogene which transforms mouse NIH3T3 cells in cooperation with ras. Biochem Biophys Res Commun *231*, 509-513.

Ostrerova, N., Petrucelli, L., Farrer, M., Mehta, N., Alexander, P., Choi, P., Palacino, J., Hardy, J., and Wolozin, B. (1999). α-Synuclein shares physical and functional homology with 14-3-3 proteins. J Neurosci *19*, 5782-5791.

Ostrerova-Golts, N., Petrucelli, L., Hardy, J., Lee, J., Farrer, M., and Wolozin, B. (2000). The A53T α-Synuclein Mutation Increases Iron-Dependent Aggregation and Toxicity. J Neuroscience *20*, 6048-6054.

Palacino, J. J., Sagi, D., Goldberg, M. S., Krauss, S., Motz, C., Klose, J., and Shen, J. (2004). Mitochondrial dysfunction and oxidative damage in Parkin-deficient mice. J Biol Chem.

Perez, R. G., Waymire, J. C., Lin, E., Liu, J. J., Guo, F., and Zigmond, M. J. (2002). A role for alpha-synuclein in the regulation of dopamine biosynthesis. J Neurosci *22*, 3090-3099.

Petrucelli, L., O'Farrell, C., Lockhart, P. J., Baptista, M., Kehoe, K., Vink, L., Choi, P., Wolozin, B., Farrer, M., Hardy, J., and Cookson, M. R. (2002). Parkin protects against the toxicity associated with mutant alpha-synuclein: proteasome dysfunction selectively affects catecholaminergic neurons. Neuron *36*, 1007-1019.

Polymeropoulos, M. H., Lavedan, C., Leroy, E., Ide, S. E., Dehejia, A., Dutra, A., Pike, B., Root, H., Rubenstein, J., Boyer, R.*, et al.* (1997). Mutation in the alpha-synuclein gene identified in families with Parkinson's disease. Science *276*, 2045-2047.

Ramsay, R., Krueger, M., Youngster, S., Gluck, M., Casida, J., and Singer, T. (1991). Interaction of 1-methyl-4-phenylpyridinium (MPP^+) and its analogs with the rotenone/piericidin binding site of NADH dehydrogenase. J Neurochem *56*, 1184-1190.

Rodrigues, C. M., Fan, G., Ma, X., Kren, B. T., and Steer, C. J. (1998a). A novel role for ursodeoxycholic acid in inhibiting apoptosis by modulating mitochondrial membrane perturbation. J Clin Invest *101*, 2790-2799.

Rodrigues, C. M., Fan, G., Wong, P. Y., Kren, B. T., and Steer, C. J. (1998b). Ursodeoxycholic acid may inhibit deoxycholic acid-induced apoptosis by modulating mitochondrial transmembrane potential and reactive oxygen species production. Mol Med *4*, 165-178.

Rodrigues, C. M., Sola, S., Nan, Z., Castro, R. E., Ribeiro, P. S., Low, W. C., and Steer, C. J. (2003a). Tauroursodeoxycholic acid reduces apoptosis and protects against

neurological injury after acute hemorrhagic stroke in rats. Proc Natl Acad Sci U S A *100*, 6087-6092.

Rodrigues, C. M., Sola, S., Sharpe, J. C., Moura, J. J., and Steer, C. J. (2003b). Tauroursodeoxycholic acid prevents Bax-induced membrane perturbation and cytochrome C release in isolated mitochondria. Biochemistry *42*, 3070-3080.

Scott, B. A., Avidan, M. S., and Crowder, C. M. (2002). Regulation of hypoxic death in C. elegans by the insulin/IGF receptor homolog DAF-2. Science *296*, 2388-2391.

Sharon, R., Goldberg, M. S., Bar-Josef, I., Betensky, R. A., Shen, J., and Selkoe, D. J. (2001). alpha -Synuclein occurs in lipid-rich high molecular weight complexes, binds fatty acids, and shows homology to the fatty acid-binding proteins. Proc Natl Acad Sci U S A *98*, 9110-9115.

Sherer, T. B., Betarbet, R., Stout, A. K., Lund, S., Baptista, M., Panov, A. V., Cookson, M. R., and Greenamyre, J. T. (2002). An in vitro model of Parkinson's disease: linking mitochondrial impairment to altered alpha-synuclein metabolism and oxidative damage. J Neurosci *22*, 7006-7015.

Sherer, T. B., Betarbet, R., Testa, C. M., Seo, B. B., Richardson, J. R., Kim, J. H., Miller, G. W., Yagi, T., Matsuno-Yagi, A., and Greenamyre, J. T. (2003). Mechanism of toxicity in rotenone models of Parkinson's disease. J Neurosci *23*, 10756-10764.

Shimura, H., Hattori, N., Kubo, S., Mizuno, Y., Asakawa, S., Minoshima, S., Shimizu, N., Iwai, K., Chiba, T., Tanaka, K., and Suzuki, T. (2000). Familial parkinson disease gene product, parkin, is a ubiquitin-protein ligase. Nat Genet *25*, 302-305.

Singleton, A. B., Farrer, M., Johnson, J., Singleton, A., Hague, S., Kachergus, J., Hulihan, M., Peuralinna, T., Dutra, A., Nussbaum, R.*, et al.* (2003). alpha-Synuclein locus triplication causes Parkinson's disease. Science *302*, 841.

Snyder, H., Mensah, K., Theisler, C., Lee, J., Matouschek, A., and Wolozin, B. (2003). Aggregated and monomeric alpha-synuclein bind to the S6' proteasomal protein and inhibit proteasomal function. J Biol Chem *278*, 11753-11759.

Souza, J. M., Giasson, B. I., Lee, V. M., and Ischiropoulos, H. (2000). Chaperone-like activity of synucleins. FEBS Lett *474*, 116-119.

Tieu, K., Perier, C., Caspersen, C., Teismann, P., Wu, D. C., Yan, S. D., Naini, A., Vila, M., Jackson-Lewis, V., Ramasamy, R., and Przedborski, S. (2003). D-beta-hydroxybutyrate rescues mitochondrial respiration and mitigates features of Parkinson disease. J Clin Invest *112*, 892-901.

Valente, E. M., Abou-Sleiman, P. M., Caputo, V., Muqit, M. M., Harvey, K., Gispert, S., Ali, Z., Del Turco, D., Bentivoglio, A. R., Healy, D. G.*, et al.* (2004). Hereditary Early-Onset Parkinson's Disease Caused by Mutations in PINK1. Science.

Vila, M., Jackson-Lewis, V., Vukosavic, S., Djaldetti, R., Liberatore, G., Offen, D., Korsmeyer, S. J., and Przedborski, S. (2001). Bax ablation prevents dopaminergic neurodegeneration in the 1-methyl- 4-phenyl-1,2,3,6-tetrahydropyridine mouse model of Parkinson's disease. Proc Natl Acad Sci U S A *98*, 2837-2842.

Yang, Y., Nishimura, I., Imai, Y., Takahashi, R., and Lu, B. (2003). Parkin suppresses dopaminergic neuron-selective neurotoxicity induced by Pael-R in Drosophila. Neuron *37*, 911-924.

Yokota, T., Sugawara, K., Ito, K., Takahashi, R., Ariga, H., and Mizusawa, H. (2003). Down regulation of DJ-1 enhances cell death by oxidative stress, ER stress, and proteasome inhibition. Biochem Biophys Res Commun *312*, 1342-1348.

Zarranz, J. J., Alegre, J., Gomez-Esteban, J. C., Lezcano, E., Ros, R., Ampuero, I., Vidal, L., Hoenicka, J., Rodriguez, O., Atares, B.*, et al.* (2004). The new mutation, E46K, of alpha-synuclein causes parkinson and Lewy body dementia. Ann Neurol *55*, 164-173.

Zhang, Y., Gao, J., Chung, K. K., Huang, H., Dawson, V. L., and Dawson, T. M. (2000). Parkin functions as an E2-dependent ubiquitin- protein ligase and promotes the degradation of the synaptic vesicle-associated protein, CDCrel-1. Proc Natl Acad Sci U S A *97*, 13354-13359.

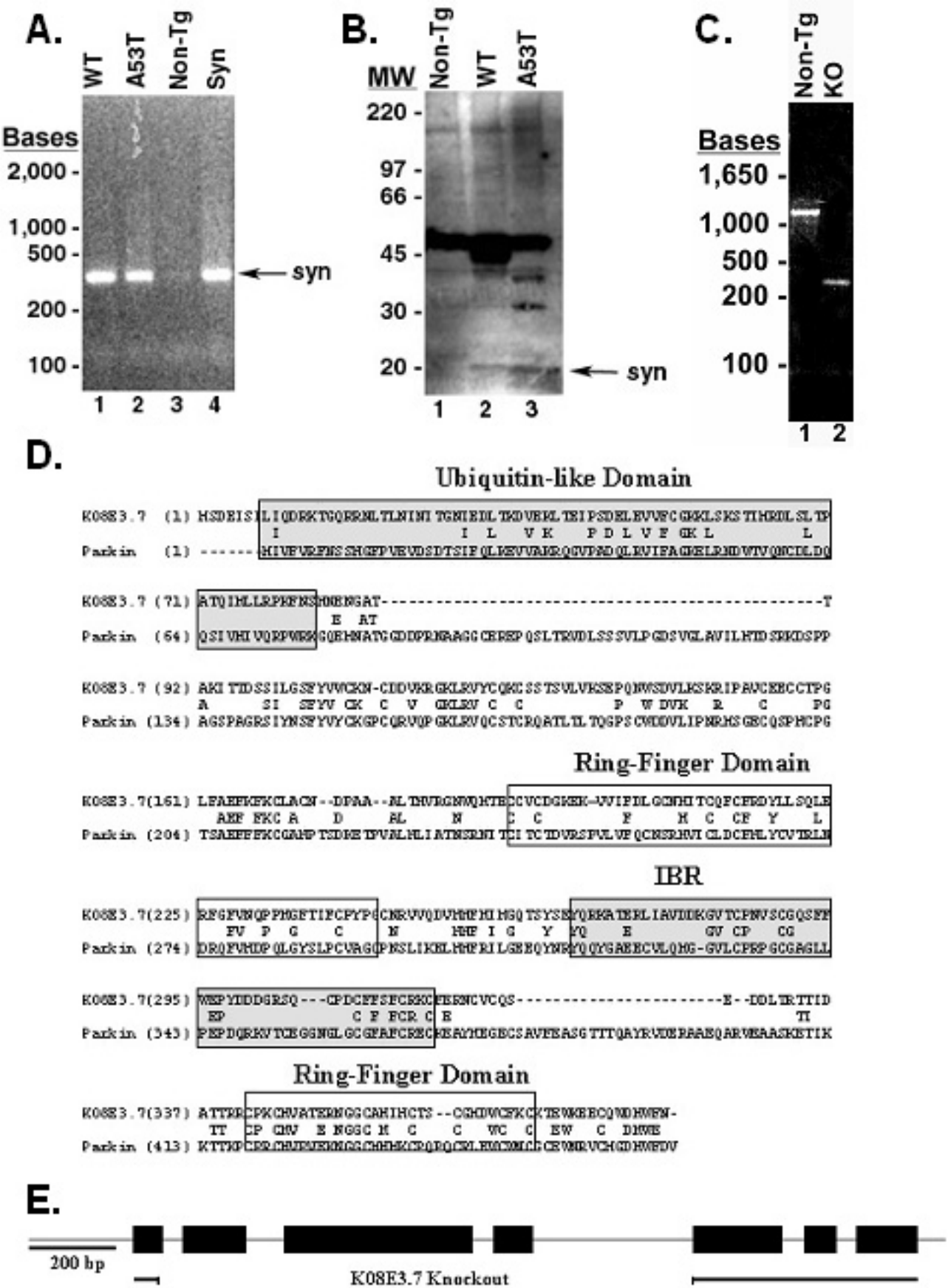
A.
WT
A53T
Non-Tg
Syn
Bases
2,000
1,000
500
200
100
syn
1 2 3 4
B.
MW
Non-Tg
WT
A53T
220
97
66
45
30
20
syn
1 2 3
C.
Non-Tg
KO
Bases
1,650
1,000
500
200
100
1 2
D.
Ubiquitin-like Domain
K08E3.7 (1) MSDEISILIQDEKTGQERMLTLNINITGNIEDLTKDVEKLTEIPSDELEVVFCGKKLSKSTIHEDLSLTF
Parkin (1) ------MIVFVRFNSSHGFPVEVDSDTSIFQLKEVVAKRQGVPADQLRVIFAGKELRNDVTVQNCDLDQ
K08E3.7 (71) ATQIHLLRPKFNSHNENGAT----------T
Parkin (64) QSIVHIVQRPWKKGQEHNATGGDDPRNAAGGCERSPQSLTRVDLSSSVLPGDSVGLAVILHTDSRKDSPP
K08E3.7 (92) AKITDSSILGSFYVVCKN-CDDVKRGKLRVYCQKCSSTSVLVKSSPQNWSDVLKSKRIPAVCEECCTPG
Parkin (134) AGSPAGRSIYNSFYVYCKGPCQRVQPGKLRVQCSTCRQATLTLTQGPSCWDDVLIPNRHSGECQSPHCPG
Ring-Finger Domain
K08E3.7(161) LPAEPKFKCLACN--DPAA--ALTNVRGNWQHTECCVCDGKEK-AVIPILGCNHITCQFCFDDYLLSQLE
Parkin (204) TSAEPFFKCGAWPTSDKETPVALHLIATESRHICIPCTDVRSPVLVFQCNSRHVICLDCFHLYCVTRLN
IBR
K08E3.7(225) RFGFVWQPPHGFTIPCPYPGCNRVVQDVHHFHIHGQTSYSEYQRKAIERLIAVDDKGVTCPNVSCGQSFF
Parkin (274) DRQFVHDPQLGYSLPCVRGQPNSLIKELHHFRILGEEQYWRYQQYGAEECVLQNG-GVLCPEPGCGAGLL
K08E3.7(295) WEPYDDDGRSQ---CPDCFFSFCRKCFEENCVCQS----------E--DDLTRTTID
Parkin (343) PEPDQRKVTCEGGNGLGCGFAFCREC-KEAYHEGECSAVFEASGTTTQAYRVDERAAEQARVEAASKETIK
Ring-Finger Domain
K08E3.7(337) ATTRPCPKCHVATERNGGCAHIHCTS--CGHDWCFKCKTEWKEECQNDHWFN-
Parkin (413) KTTKPCPRCHVPVEKNGGCMHMKCPQPQCKLHWCWMCGCEWNRVCHGDHWFDV
E.
200 bp
K08E3.7 Knockout

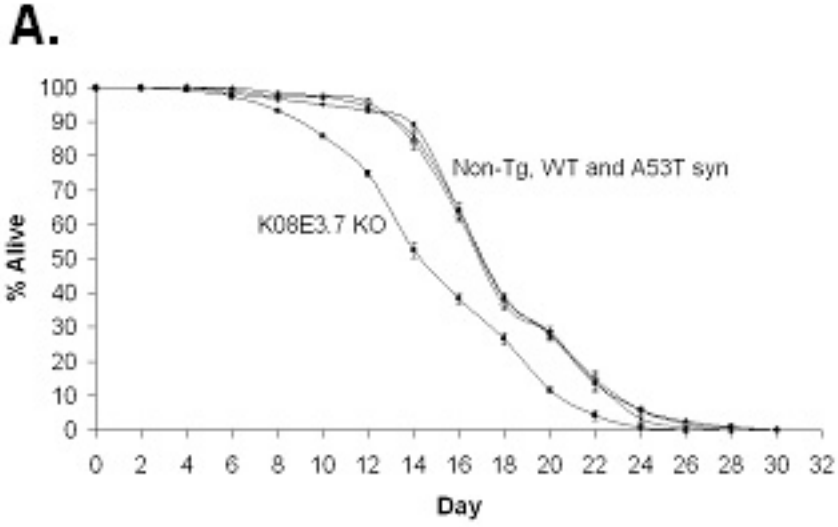
A.
100
90
80
70
60
50
40
30
20
10
0
% Alive
Non-Tg, WT and A53T syn
K08E3.7 KO
0 2 4 6 8 10 12 14 16 18 20 22 24 26 28 30 32
Day

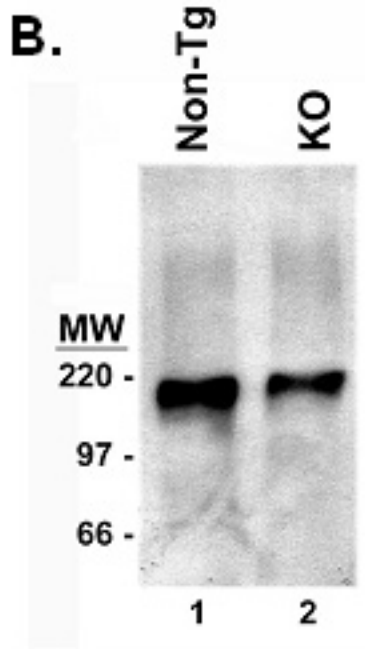
B.
Non-Tg
KO
MW
220 -
97 -
66 -
1
2

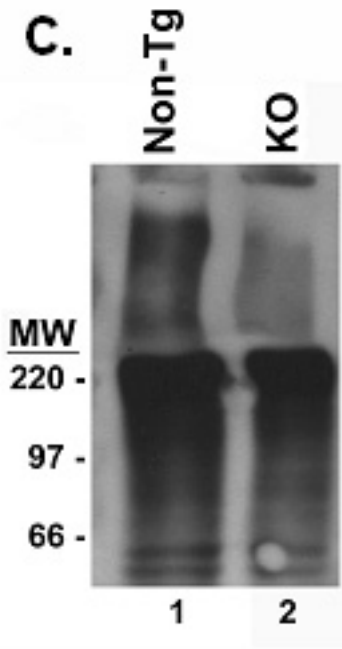
C.
Non-Tg
KO
MW
220 -
97 -
66 -
1
2

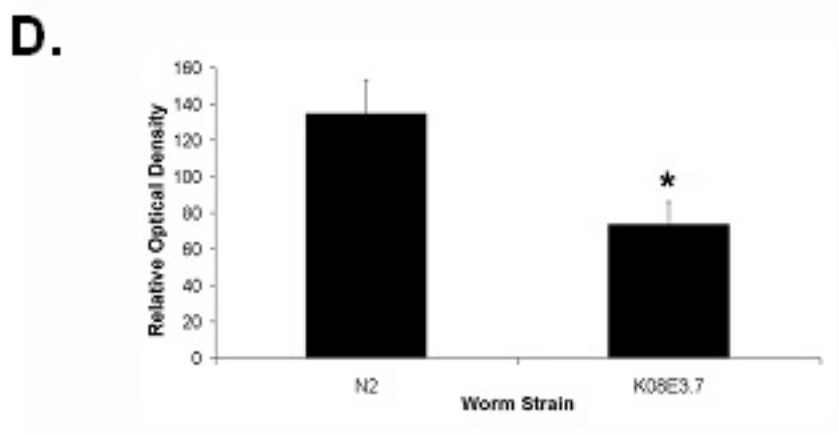
D.
160
140
120
100
80
60
40
20
0
Relative Optical Density
*
N2
K08E3.7
Worm Strain

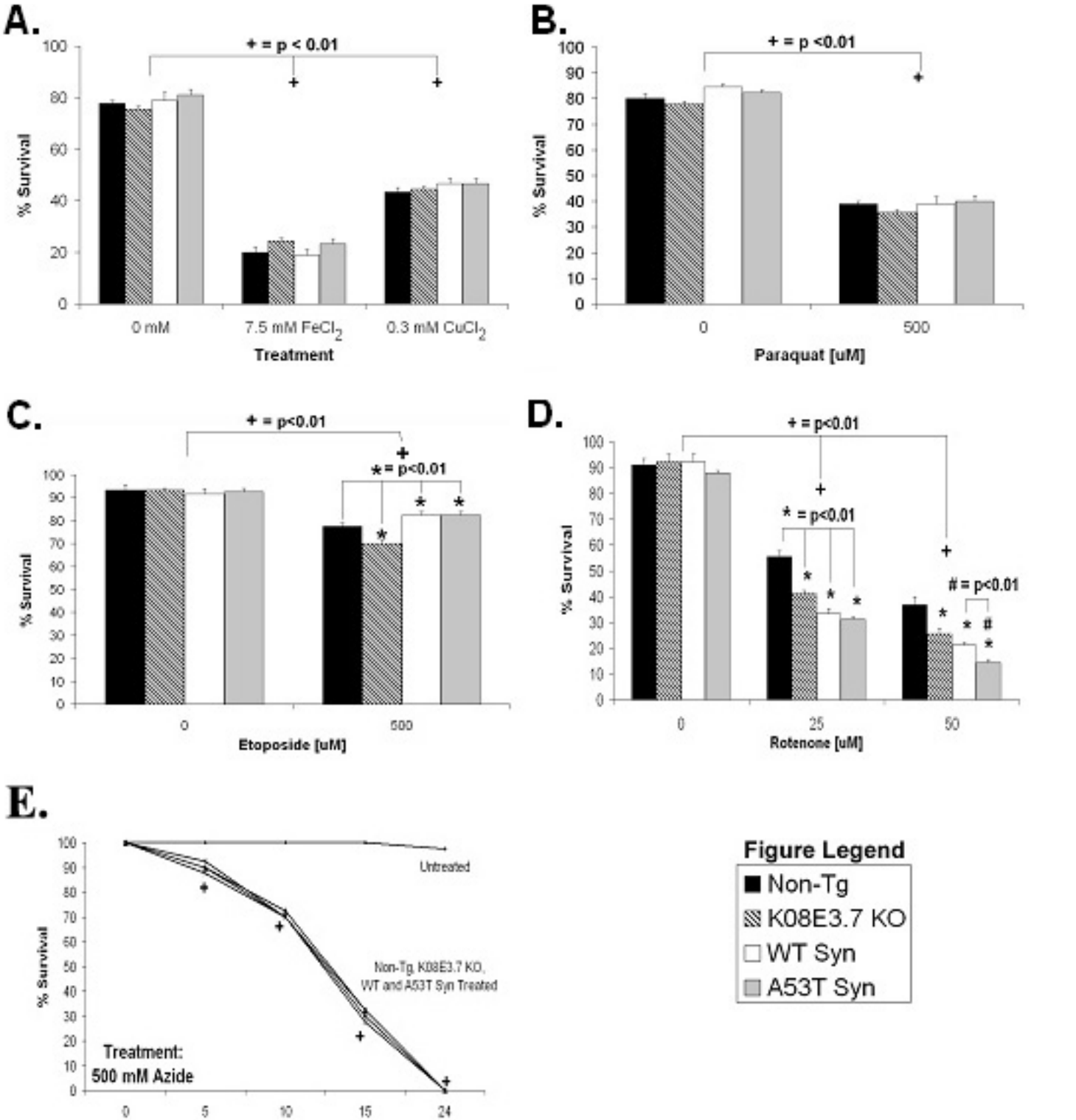
A.
+ = p < 0.01
% Survival
0 mM
7.5 mM FeCl2
0.3 mM CuCl2
Treatment
B.
+ = p <0.01
% Survival
0
500
Paraquat [uM]
C.
+ = p<0.01
* = p<0.01
% Survival
0
500
Etoposide [uM]
D.
+ = p<0.01
* = p<0.01
# = p<0.01
% Survival
0
25
50
Rotenone [uM]
E.
Untreated
Non-Tg, K08E3.7 KO,
WT and A53T Syn Treated
% Survival
Treatment:
500 mM Azide
0
5
10
15
24
Figure Legend
Non-Tg
K08E3.7 KO
WT Syn
A53T Syn

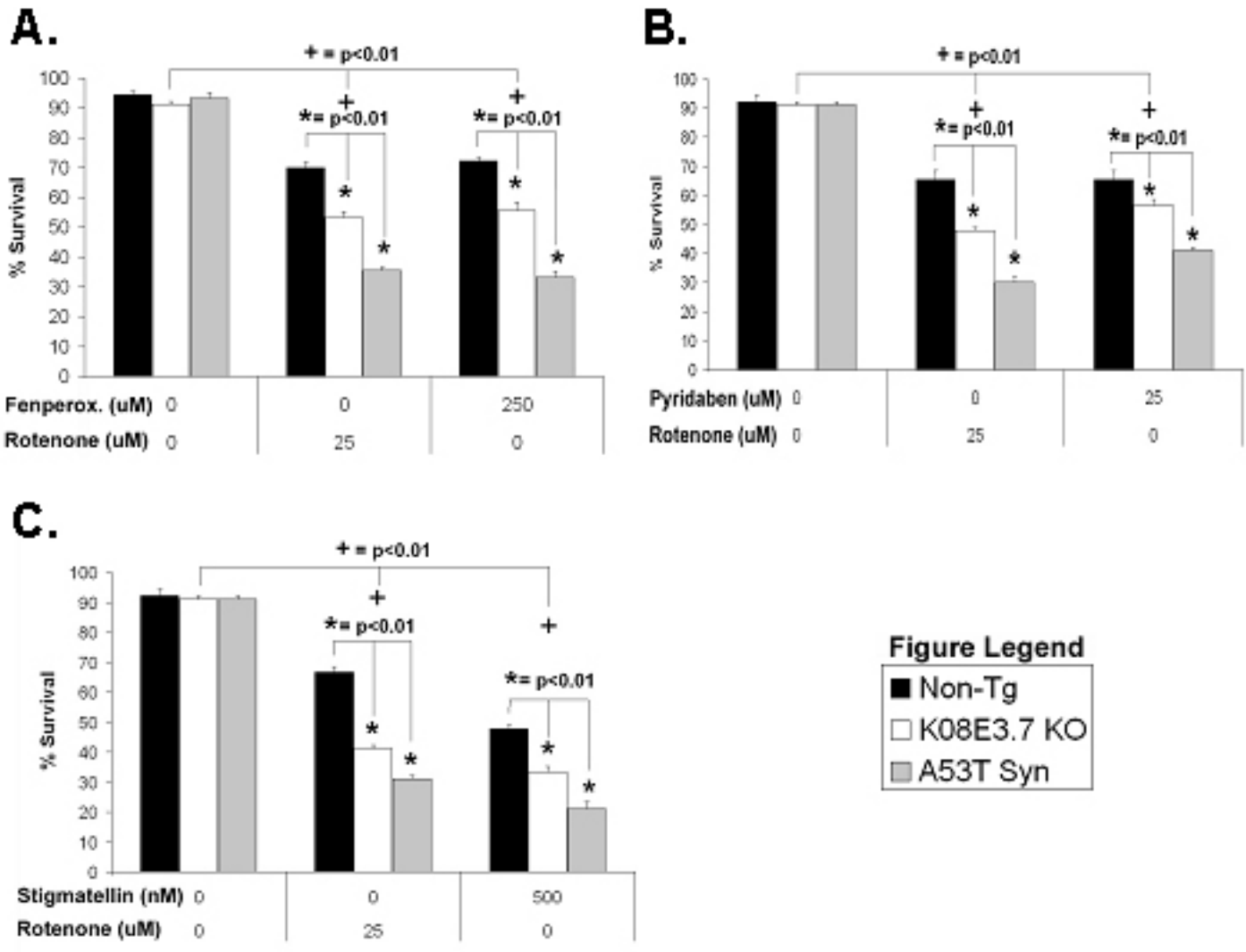
A.
+ = p<0.01
*= p<0.01
% Survival
Fenperox. (uM) 0 0 250
Rotenone (uM) 0 25 0
B.
+ = p<0.01
*= p<0.01
% Survival
Pyridaben (uM) 0 0 25
Rotenone (uM) 0 25 0
C.
+ = p<0.01
*= p<0.01
% Survival
Stigmatellin (nM) 0 0 500
Rotenone (uM) 0 25 0
Figure Legend
Non-Tg
K08E3.7 KO
A53T Syn

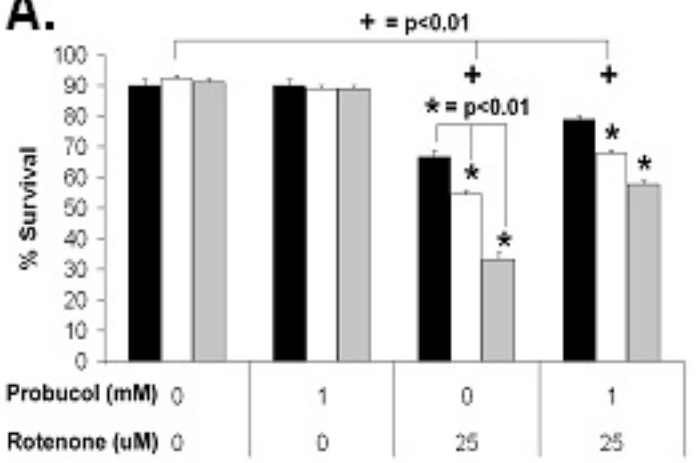

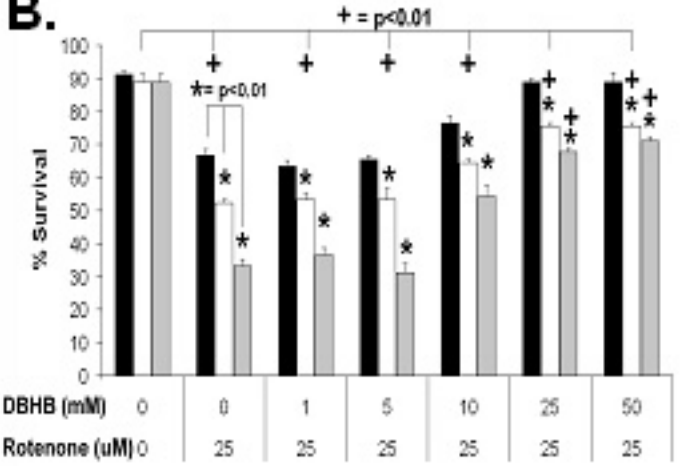

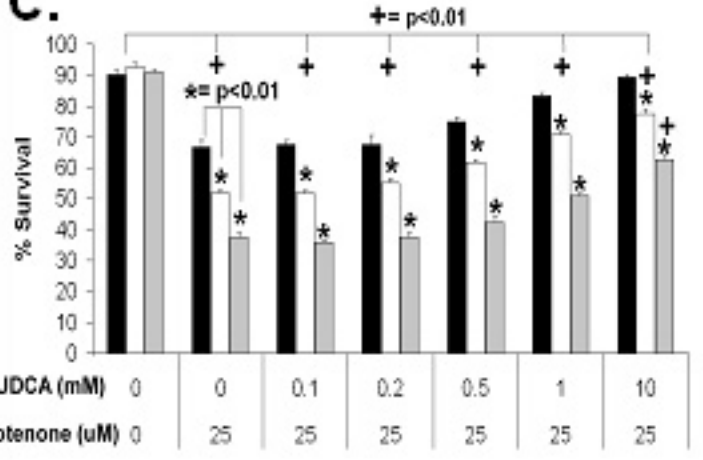

Figure Legend

- Non-Tg
- K08E3.7 KO
- A53T Syn

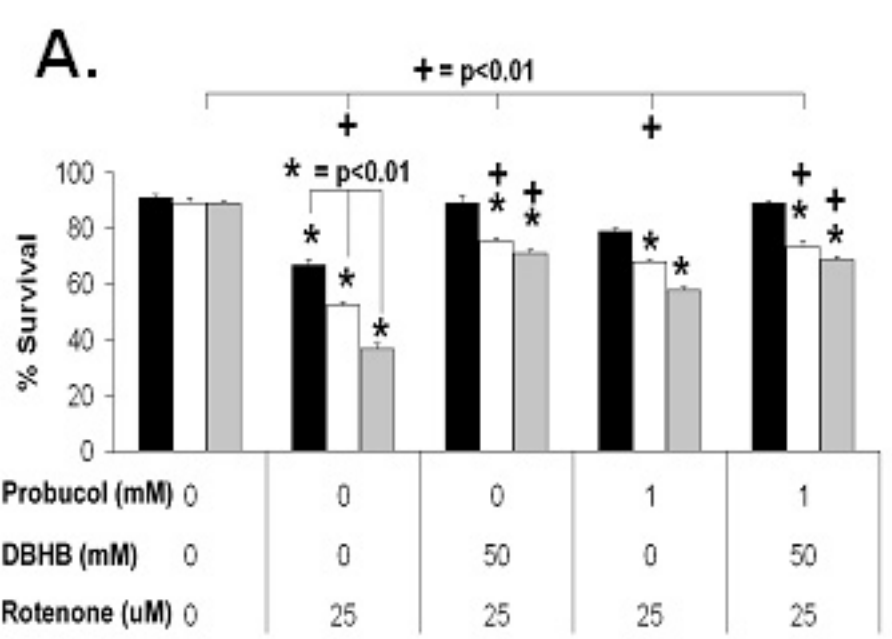

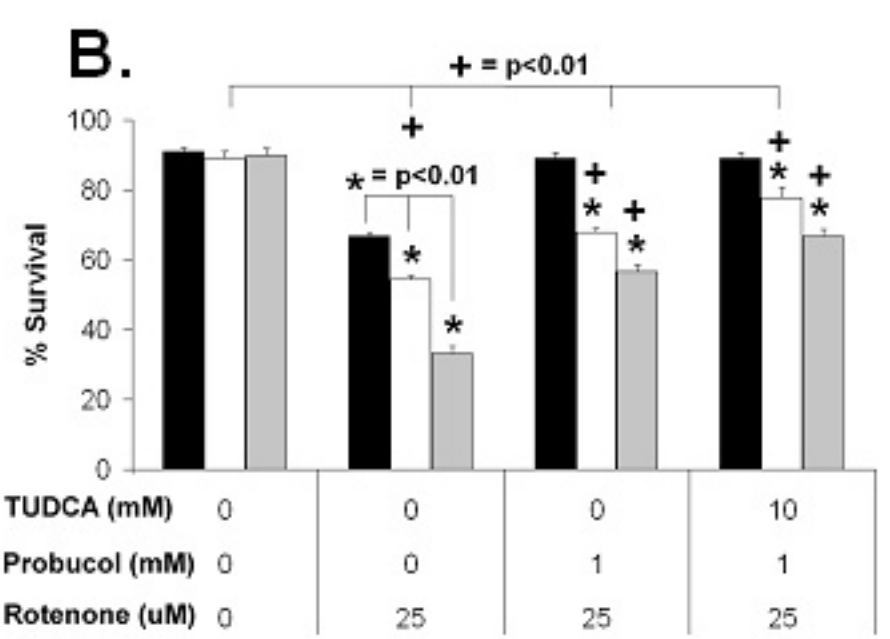

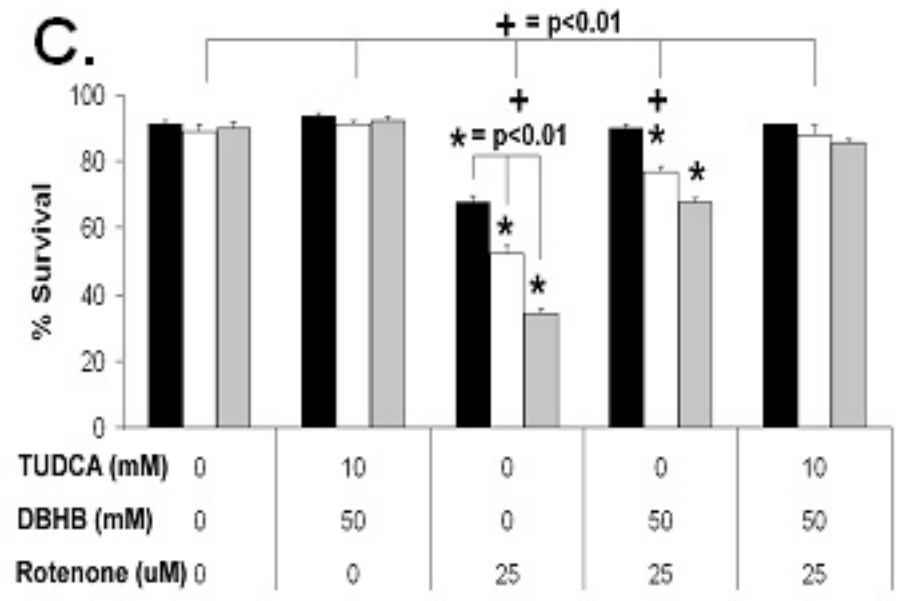

Figure Legend

- Non-Tg
- K08E3.7 KO
- A53T Syn

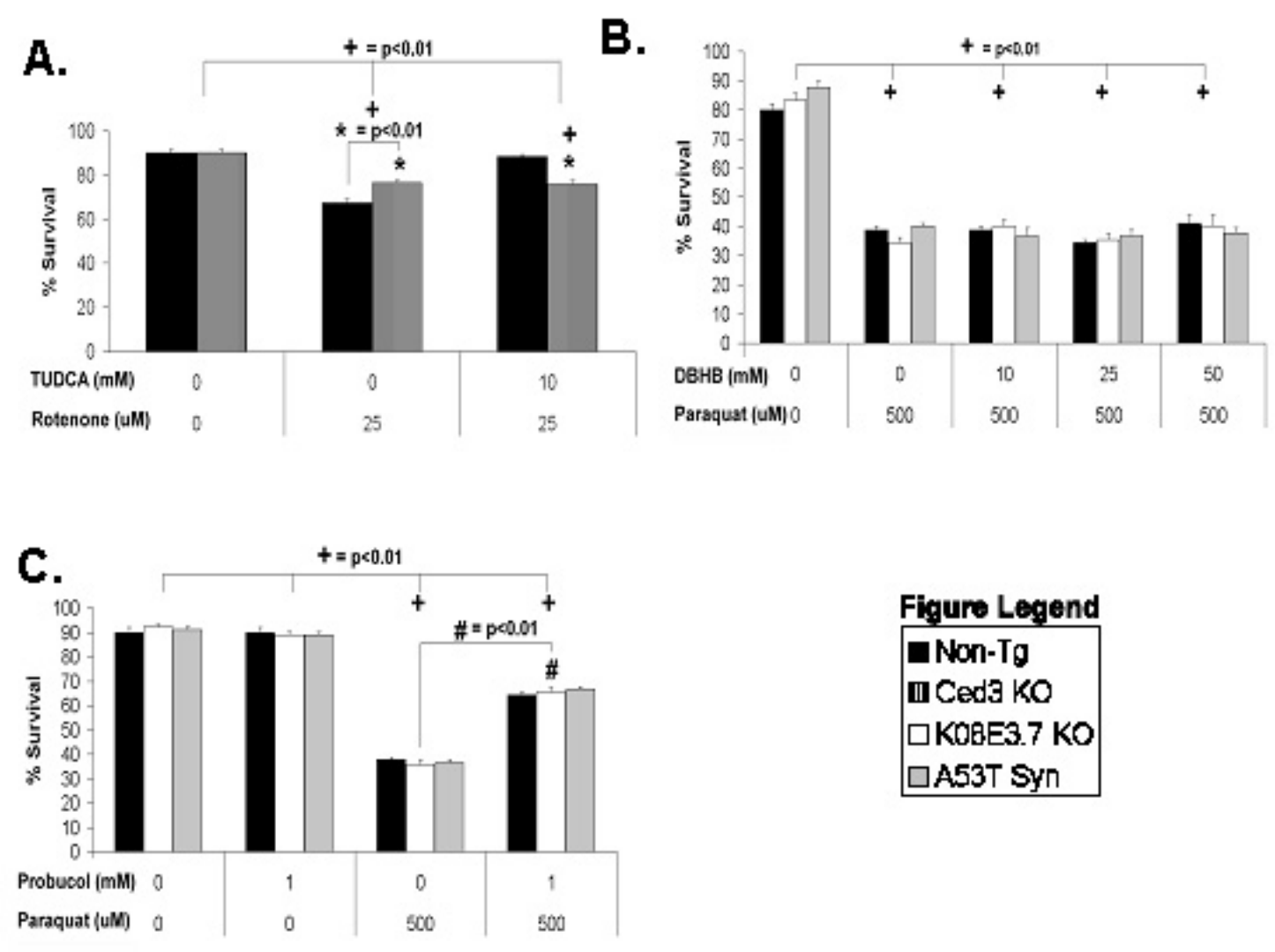
A.
+ = p<0.01
* = p<0.01
% Survival
TUDCA (mM) 0 0 10
Rotenone (uM) 0 25 25
B.
+ = p<0.01
% Survival
DBHB (mM) 0 0 10 25 50
Paraquat (uM) 0 500 500 500 500
C.
+ = p<0.01
# = p<0.01
% Survival
Probucol (mM) 0 1 0 1
Paraquat (uM) 0 0 500 500
Figure Legend
Non-Tg
Ced3 KO
K08E3.7 KO
A53T Syn

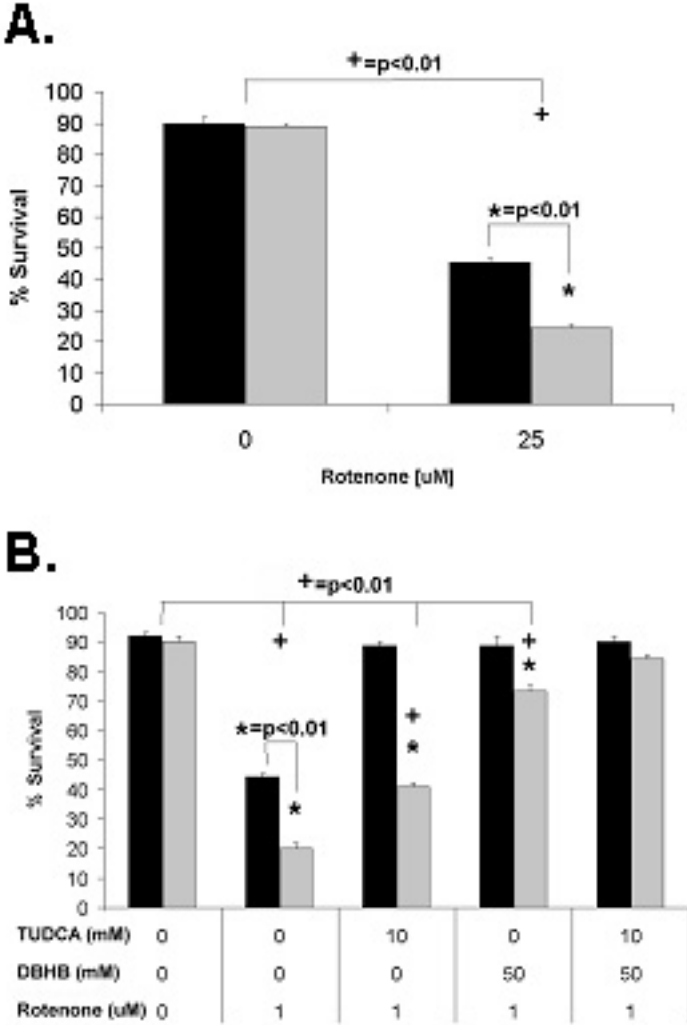

Figure Legend

■ Non-tg

□ DJ-1

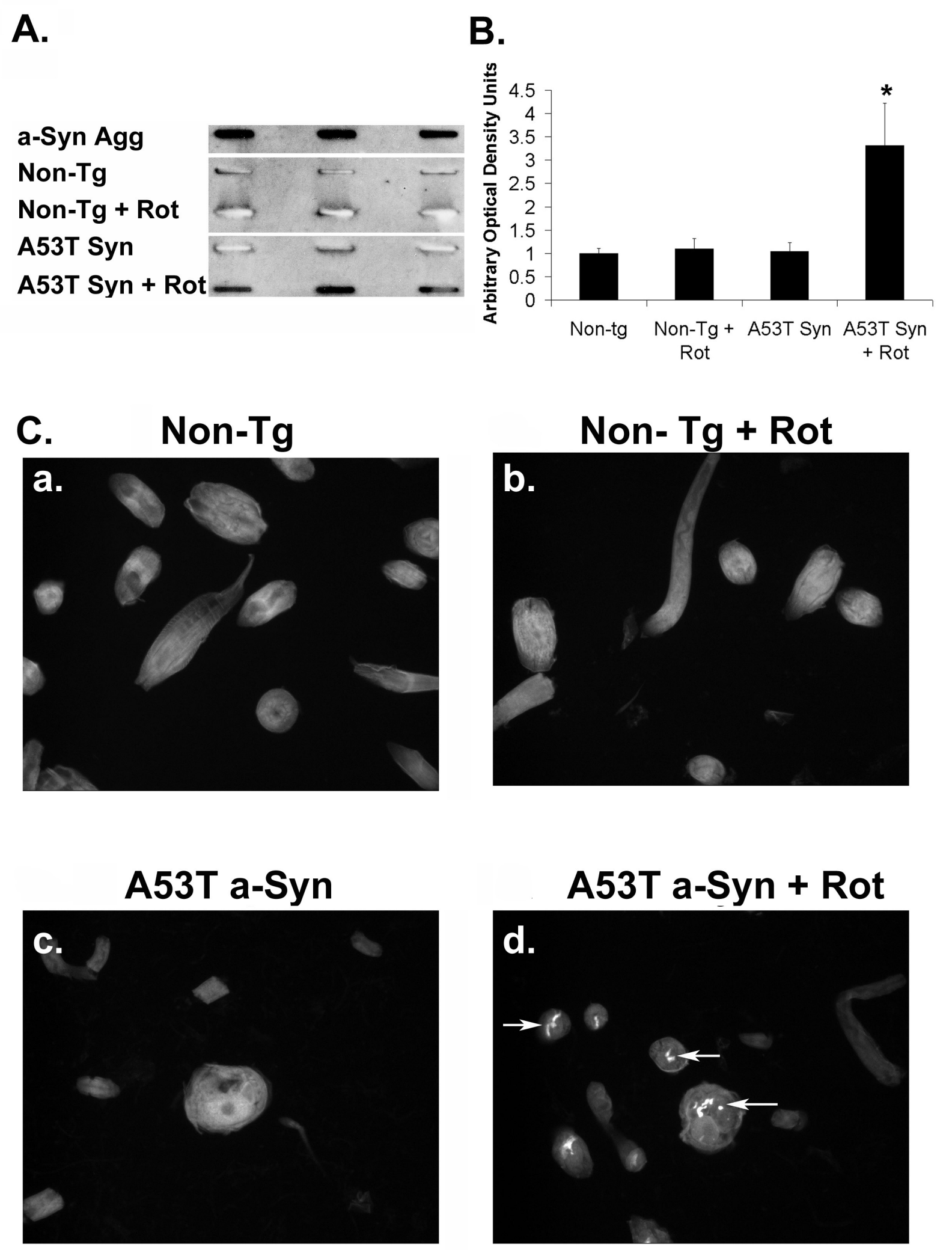
A.
a-Syn Agg
Non-Tg
Non-Tg + Rot
A53T Syn
A53T Syn + Rot
B.
Arbitrary Optical Density Units
4.5
4
3.5
3
2.5
2
1.5
1
0.5
0
*
Non-tg
Non-Tg + Rot
A53T Syn
A53T Syn + Rot
C.
Non-Tg
a.
Non- Tg + Rot
b.
A53T a-Syn
c.
A53T a-Syn + Rot
d.